Measuring on main kinetic parameters of molecular catalyst for olefin polymerization using high-pressure-type quenched flow reactor

Maria Maddalena Eleonora Ranieri

N° d'ordre: **84 - 2012** Année 2012

THESE DE L'UNIVERSITE DE LYON

UNIVERSITE CLAUDE BERNARD LYON 1

ECOLE DOCTORALE

DIPLOME DE DOCTORAT
(arrêté du 7 août 2006)
Spécialité CHIMIE GENIE DES PROCEDES

Présentée

par

Melle Maria Maddalena Eleonora RANIERI

MEASURING OF MAIN KINETIC PARAMETERS OF MOLECULAR CATALYST FOR OLEFIN POLYMERIZATION USING HIGH-PRESSURE-TYPE QUENCHED FLOW TECHNIQUE

Directeur de thèse : M. Christophe BOISSON

JURY : Prof. D. BIANCHI (Président)
Prof. R. DUCHATEAU (rapporteur)
Prof. R. CIPULLO (rapporteur)
Prof. C. PAULIK
M. C.BOISSON
M. T.F.L. McKENNA

UNIVERSITE CLAUDE BERNARD - LYON 1

Président de l'Université	**M. François-Noël GILLY**
Vice-président du Conseil d'Administration	M. le Professeur Hamda BEN HADID
Vice-président du Conseil des Etudes et de la Vie Universitaire	M. le Professeur Philippe LALLE
Vice-président du Conseil Scientifique	M. le Professeur Germain GILLET
Secrétaire Général	M. Alain HELLEU

COMPOSANTES SANTE

Faculté de Médecine Lyon Est – Claude Bernard	Directeur : M. le Professeur J. ETIENNE
Faculté de Médecine et de Maïeutique Lyon Sud – Charles Mérieux	Administrateur provisoire : M. le Professeur G. KIRKORIAN
UFR d'Odontologie	Directeur : M. le Professeur D. BOURGEOIS
Institut des Sciences Pharmaceutiques et Biologiques	Directeur : Mme la Professeure C. VINCIGUERRA.
Institut des Sciences et Techniques de la Réadaptation	Directeur : M. le Professeur Y. MATILLON
Département de formation et Centre de Recherche en Biologie Humaine	Directeur : M. le Professeur P. FARGE

COMPOSANTES ET DEPARTEMENTS DE SCIENCES ET TECHNOLOGIE

Faculté des Sciences et Technologies	Directeur : M. le Professeur F. De MARCHI
Département Biologie	Directeur : M. le Professeur F. FLEURY
Département Chimie Biochimie	Directeur : Mme le Professeur H. PARROT
Département GEP	Directeur : M. N. SIAUVE
Département Informatique	Directeur : M. le Professeur S. AKKOUCHE
Département Mathématiques	Directeur : M. le Professeur A. GOLDMAN
Département Mécanique	Directeur : M. le Professeur H. BEN HADID
Département Physique	Directeur : Mme S. FLECK
Département Sciences de la Terre	Directeur : Mme la Professeure I. DANIEL
UFR Sciences et Techniques des Activités Physiques et Sportives	Directeur : M. C. COLLIGNON
Observatoire de Lyon	Directeur : M. B. GUIDERDONI
Polytech Lyon	Directeur : M. P. FOURNIER
Ecole Supérieure de Chimie Physique Electronique	Directeur : M. G. PIGNAULT
Institut Universitaire de Technologie de Lyon 1	Directeur : M. C. VITON
Institut Universitaire de Formation des Maîtres	Directeur : M. R. BERNARD
Institut de Science Financière et d'Assurances	Directeur : Mme la Professeure V. MAUME-DESCHAMPS

This work is part of the Research program of the Dutch Polymer Institute, PO Box 902, 5600AX, Eindhoven, The Netherlands, project nr. # 635.

Non est quod timeas ne operam perdideris, si tibi didicisti

Lucio Seneca

Al professore Vincenzo Busico
che per primo ha creduto in me.

Aknowledgement/ Remerciements /Ringraziamenti

I would like to thank the members of jury: Prof. Bianchi, Prof. Duchateau, , Prof Cipullo and Prof Paulik for their contribution to this manuscript and for time.

I would like to thank the Dutch Polymer Institute for financing this thesis and Dr. Ian Stamhuis for his support during the oral presentation in DPI meeting.

I would like to thank Prof. V. Busico and Dr. F. Cutillo for the useful collaboration and interesting discussions.

Honnêtement cette thèse a été vraiment difficile et longue. Je n'aurais jamais parié de pouvoir finir et pourtant.. J'ai réussi surtout grâce à la patience et au soutien de mes directeurs de thèse Christophe et Tim. Je voudrais profiter de cet espace pour te remercier Christophe pour toutes les fois ou tu m'as accueillie dans ton bureau lors d'une crise de pleurs parce que le réacteur « ne marche pas » et pour les (énormes) efforts (de ne pas me mettre dehors) pour me convaincre que je pouvais faire de la recherche. Merci pour tous les moments de discussion sur les metallocenes je n'oublierai pas quand tu m'as expliqué l'hapticité dans la Circumvesuviana !

Merci Tim pour les heures que tu as dédié à la correction de mon anglais pourri et pour avoir géré mes moments de panique avec une patience Zen. Je te remercie vraiment beaucoup pour m'avoir donné des conseils inestimables et pour avoir tant de confiance en moi de m'avoir aidée pour la suite.

Mais cette thèse n'aura pas pu démarrer sans l'incomparable aide de Jean-Pierre Broyer qui a pris une italienne maladroite et l'a transformée dans une experte de stopped flow et d'argot. J'ai appris plein de chose avec toi et pas seulement de chimie.

Un merci particulier à Nathalie. Pour les bonbons qui remontent le moral et pour le temps et les mots gentils que tu trouve à chaque fois qu'on a besoin.

Merci Etienne d'être la première personne qui m'a montré amitié aussi hors du labo et pour être resté à l'hôpital avec moi lors de mon accident. Merci pour avoir démontré humanité quand d'autres ont démontré seulement indifférence…

Merci à Pierre-Yves pour les bons moments dans et hors du labo. Et surtout pour m'avoir prêté DMC.

Pendant ces 4 ans j'ai connu plein de gens, certains je ne vais jamais les oublier. Ana, ho passato dei momenti splendidi in tua compagnia, non dimenticherò mai le sere passate a guardare dei film e video comici né la nostra super estate e nemmeno i nostri pomeriggi a spasso per negozi. Sei stata una vera amica quasi sorella. Julien, merci pour tous, les cours, les déménagements, les soirées à jouer aux cartes en regardant la télé et les piques niques…Merci pour ta gentillesse et pour ton amitié.

Merci a tous ceux qui ont partagé le bureau avec moi. In particolare grazie Estevan per essere stata la mia parte d'Italia quotidiana e per aver diviso con me i viaggi e le "gioie" del DPI.

Merci Cédric surtout pour l'énorme patience que tu as eu dans les derniers 6 mois de ma thèse. T'as été un super camarade de bureau et un bon ami. N'oubliez pas d'arroser les plantes !!

Merci Vincent Monteil pour toutes les fois que tu m'as soutenu dans le présentations orales, pour toute la biblio que tu m'as passé (et que j'ai lu) et pour tous les moments de vie social pendant les congrès et meeting DPI. Je n'oublierai pas les pauses cafés de l'aprem.

A tous les autre permanents, Muriel, Frank (et ses shorts), Elodie, Bernadette et Olivier, merci pour votre aide et pour m'avoir accueilli au labo.

A tous les autres étudiants Edgard (merci pour ta gentillesse), Aurélie (merci pour les bons moments gossip) , Guilhem, Delphine, Arash, Benoit, Thomas, Quiao, Celine, Virginie, Isabel (merci pour les moments passés hors du labo), Xuiwei, Emilie.. c'était un plaisir de partager une partie de ma vie avec vous. Bonne chance pour la suite.

Infine voglio ringraziare i miei genitori per essere sempre presenti e per appoggiarmi in ogni cosa che faccio. Questa tesi di dottorato è anche merito vostro.

Un grazie di cuore a Xavier, per avermi dato un motivo per restare e finire la tesi, per avermi sopportato e voluto bene in un momento difficile della mia vita. TVB.

Abstract

Ziegler-Natta catalysts are generally obtained by the combination of a transition metal complex with an alkylaluminium compound and possibly another co-catalyst. For molecular Ziegler-Natta catalyst, generally, the active species is a cationic compound. However, in regards to the actives species, the olefin may compete in the polymerization medium with other metal alkyl, the solvent or the counteranion. Thus, it is not an easy task to determine the total active metal site fraction which remains an important challenge in the field of polyolefins. Several methods have been developed to perform this measurement. Among these the most reliable one is rely on the determination of number of macromolecules formed initially, and it requires working in initial controlled regime where the chain transfer reactions are very limited. It should be possible to achieve the controlled regime for molecular catalyst for time going from several milliseconds to fraction of second. This means that technically demanding fast kinetic techniques such as quenched flow technique are necessary for the investigation of kinetic parameters of olefin polymerization catalysts. Up to now this technique has been only implemented in very mild conditions. Recently a stopped flow reactor operating at high temperature and high pressure has been developed in Lyon. In the present study, the usefulness of this reactor for measuring the chain propagation rate constant kp and the fraction of metal active site [M*]/[M] is assessed.

In the first part of this work we have focused on the investigation of some metallocene-based catalysts. In particular, we have observed how these catalysts behave at initial stage of polymerization, when they are activated with different co-catalyst and in some case a kinetic description was also possible.

The last part of this work was dedicated to kinetic study of some post-metallocene catalysts such as amine bisphenolate and (bis phenoxy-imine) -Zr and -Ti based complexes activated with MAO in a large range of polymerization temperatures. A successful kinetic investigation of Bis(cumyl)[ONNO]ZrBz_2 complex activated with MAO/*t*Bu_2-PhOH has been performed which allowed the determination of [M*]/[M], k_p and activation parameters such as $\Delta H^{\ddagger}$ and $\Delta S^{\ddagger}$. In the case of [*N*-(3-*tert*-butylsalicylidene)-2,3,4,5,6 pentafluoroanilinato] titanium dichloride activated with MAO an original changing in kinetic regime is reported by increasing the polymerization temperature.

Résumé

Ce travail de thèse traite de l'étude de l'influence des paramètres expérimentaux, comme les conditions de polymérisation ou les effets du co-catalyseur sur la cinétique des premiers instants de polymérisation avec des catalyseurs metallocene et post-metallocene en utilisant la technique du « quenched flow ».

Afin de mieux comprendre la cinétique de polymérisation l'un des objectifs est la détermination de la concentration de sites actifs des catalyseurs moléculaires ainsi que des constants cinétiques (k_p, k_t). Les catalyseurs Ziegler-Natta sont obtenus en combinant un complexe de métal de transition avec un alkylaluminium ou d'autre co-catalyseur. L'espèce active d'un catalyseur moléculaire Ziegler-Natta est généralement cationique. Cependant, l'oléfine est en compétition avec l'alkylaluminium, le solvant ou le contre-anion pour la coordination sur l'espèce active. De plus, l'équation exprimant la vitesse de propagation de chaine est loin d'être triviale.

$$R_p = \frac{-d[Mon]}{dt} = k_p([M^*]/[M])[mon]^{a(\approx 1)} \quad (1)$$

La principale difficulté dans la résolution de cette équation est l'indentification du k_p et de [M*]/[[M] même dans des conditions bien définies. Ce problème est dû à la complexité des réactions chimiques impliquées dans la formation des sites actifs ainsi que la croissance et la terminaison de la chaîne de polymère. Il est reconnu que l'espèce active est un complexe métallique cationique qui est stabilisé par un anion de faible coordination. Mais la fraction active des centres métalliques est mal connue ce qui mène à des modélisations erronées. Jusqu'à maintenant l'un des principaux challenges du domaine d'étude des polyoléfines est la détermination du nombre des sites actifs pour la famille des catalyseurs Ziegler-Natta, qui inclut les systèmes hétérogènes, les metallocenes et les post-metallocenes.

Considérant l'importance de la mesure de la constante cinétique et de la concentration de sites actifs un nombre conséquent de travaux a été consacré à l'identification de ces paramètres. Ainsi de nombreuses méthodes de détermination des sites actifs ont été proposées, comme les méthodes basées sur le « radio-tagging » donnant cependant de résultats erronées. En effet, la chimie impliquée n'a pas été suffisamment mis au point. Parmi ces méthodes l'une des plus fiables est basée sur la détermination cinétique du nombre des chaînes macromoléculaires. Cette méthode a été développée par Natta comme alternative aux autres méthodes. La méthode de détermination du nombre de macromolécules est basée sur la relation entre le degré de polymérisation et la concentration des sites actifs. Si on se place dans des conditions

ou P_n augmente avec le temps de polymérisation c'est-à-dire dans les tous premiers instants de réaction avant que les réactions de transfert de chaîne devient significatives, on peut, alors, déterminer k_p en utilisant l'équation ci-dessous.

$$\frac{1}{P_n} = \frac{1}{k_p\,[mon]t} + \frac{\sum_{i=1}^{n} k_{tr}[X]^i\,t}{k_p\,[mon]t} \qquad (2)$$

Si on suppose que R_p est indépendant du temps et que les seules réactions de terminaison de chaîne sont les réactions de transferts, alors le graphique de l'inverse du degré de polymérisation ($1/P_n$) en fonction de l'inverse du temps (1/t) sera linéaire. La pente de la droite donnera la valeur de k_p et l'interception sur l'axe des ordonnes la valeur de la fréquence de transfert de la chaîne. Si k_p et [mon] sont indépendant du temps, et que tous les sites sont actifs instantanément le rendement de polymérisation Y (mol/mol_{met}) est donné par la relation suivant :

$$Y = k_p\,[mon]\frac{[M^*]}{[M]}t \qquad (3)$$

L'équation est valide que pour des conversions très faibles (inferieures à 10%). Si les conditions sont remplies on peut calculer la valeur de [M*]/[M] en utilisant le droite du rendement de polymérisation en fonction du temps et en introduisant le valeur de k_p trouvé avec l'équation (2).

Comme on l'a indiqué ci-dessus, afin d'obtenir des résultats représentatifs, un certain nombre des conditions doivent être remplies. Premièrement, afin d'obtenir des valeurs fiables de [M*]/[M] il est nécessaire de se placer dans un régime où les transferts de chaines sont limités. Dans ce cas, sur chaque site actif il y a une chaîne qui grandit. Ce régime est communément appelé *régime initial contrôlé.* Lors du régime contrôle une augmentation linéaire de la masse molaire avec le temps est observée. Si on adapte nos conditions expérimentales de manière à ce que l'on soit dans un régime contrôlé au moment où on stoppe la chaîne en croissance alors le comptage des chaîne donne accès au nombre d'espèces actives. Ceci implique l'utilisation de techniques de polymérisation pemettent temps des réactions très courts comme la technique du Quenched Flow (QF). Ce type de technique permet de polymériser les oléfines avec des temps de séjour très courts. Ces temps des séjours très courts sont obtenus en mélangeant instantanément deux solutions, une solution avec le complexe métallique et le co-catalyseur et une autre avec le monomère, et en stoppant brutalement la réaction. Les temps de séjours devraient être plus courts que le temps de vie moyen de croissance des chaines de polymère. L'idée d'utiliser la technique du « Quenched flow » est de réaliser des conditions différentes de conditions conventionnelles où les temps de séjours sont de 1-3h. Dans ces conditions l'activité d'un catalyseur varie avec le temps à

cause de plusieurs réactions secondaires comme les phénomènes de désactivation ou réactions de transfert ou de terminaison de chaînes.
Le réacteur utilisé dans notre étude est un réacteur « Quenched Flow » à haute pression qui réalise des temps de séjours très courts (80 ms) dans une gamme de températures de 25°C à 80°C et à des pressions en monomère jusqu'à 13 bars. Ce réacteur permet l'étude de l'influence de la température et surtout de la concentration du monomère sur la cinétique des catalyseurs moléculaires.

Le chapitre II détaille l'utilisation de ce réacteur, ainsi que les caractéristiques et les exigences techniques. Afin d'obtenir des résultats significatifs, le temps de formation des sites actifs doivent être sensiblement plus faibles que le temps de polymérisation. Une section du chapitre II est dédiée à la description des différentes modifications réalisées sur le réacteur pour que ce dernier soit mieux adapté à notre étude. A l'origine ce réacteur avait été conçu pour des études de morphologie pour les catalyseurs hétérogènes Ziegler-Natta et il n'était pas parfaitement adapté aux études cinétiques. Apres un certain nombre de modifications il a été possible d'obtenir une reproductibilité satisfaisante.

Dans cette optique, la cinétique et l'influence des activateurs sur la polymérisation de l'éthylène ont été étudiées dans le chapitre III en utilisant des catalyseurs metallocene. Les catalyseurs étudiés sont le dichloro *rac*-Me_2Si(2-méthyl-4-phényl-1-indényl)$_2$ zirconium (FESBIZrCl_2), le dichloro diphénylméthylidène-cyclopentadiènyl-fluorenylzirconium ((CPh_2)CpFluZrCl_2) et le dichloro bis(pentaméthyl-cyclopentadiènyl) zirconium dichloride (Cp*$_2$ZrCl_2). Le comportement de ces catalyseurs dans les premiers instants de polymérisation a été étudié lors de l'activation avec différents co-catalyseurs.
Dans la première section du chapitre III le complexe FESBIZrCl_2 activé avec du MAO et par *i*Bu_3Al/[$HNMe_2$Ph][B(C_6H_5)$_4$] a été étudié. L'absence d'une période d'induction en fait un bon candidat pour débuter notre étude.
L'activation du complexe (CPh_2)CpFluZrCl_2 a été étudiée sur des temps très courts. Le MAO, Le MAO modifié avec un phénol ainsi que le *i*Bu_3Al/[$HNMe_2$Ph][B(C_6H_5)$_4$] ont été utilisés comme activateurs. Plusieurs paramètres expérimentaux, comme la concentration du monomère, le rapport Al/Zr ainsi que le rapport B/Zr ont été considérés.
Dans la dernière section du chapitre III l'étude cinétique de Cp*$_2$ZrCl_2 a été effectuée à trois températures (60°C, 40°C et 25°C) en utilisant une même concentration en monomère. La détermination de principaux paramètres expérimentaux, k_p et [M*]/[Zr], a été réalisée.

L'étude cinétique de deux principaux catalyseurs post-métallocène est l'objet du chapitre IV. Le premier post-métallocène étudié est un complexe à base de Zr supporté par un ligand [ONNO] tétradentate. Les principaux paramètres cinétiques ont été calculés sur une large plage de températures (-23°C à 60°C). A basse température le complexe Bis(cumyl)[ONNO]$ZrBz_2$ activé par MAO et *t*Bu_2-PhOH est capable de polymériser l'éthylène de façon contrôlé sur des temps longs. A hautes températures (>25°C) le catalyseur Bis(cumyl)[ONNO]$ZrBz_2$/MAO/*t*Bu_2-PhOH polymérise l'éthylène de façon contrôlée pour des temps de réactions de l'ordre de la second ou pour fractions des secondes. Le réacteur quenched Flow s'est avéré être est un outils tres adapté pour l'étude cinétique du catalyseur Bis(cumyl)[ONNO]$ZrBz_2$/MAO/*t*Bu_2-PhOH à 40°C et 60°C.

La dernier partie du chapitre IV est dédiée à l'étude des catalyseurs a base de zirconium et titane supportés deux ligands phenoxy-imine. Une étude comparative de l'activation du complexe bis (phenoxy-imine) à base de Zr a été réalisée en utilisant respectivement le MAO et un mélange $[HNMe_2Ph][B(C_6H_5)_4]$ AlR_3 comme activateurs.

Finalement le complexe bis(phenoxy-imine) à base de titane été étudié en utilisant le MAO comme activateur. Les valeurs de k_p et [M*]/[M] ont été calculées pour trois températures (25°C, 40°C et 55°C).

Table of contents

Introduction

Introduction

This Ph.D. dissertation focuses on the study of the influence of experimental parameters such as the polymerization conditions or the effect of co-catalyst on the kinetics of some classical metallocene and post-metallocene catalyst systems in the first instant of polymerization using the quenched flow technique.

One of first goal of this Ph.D. was the determination of possible concentration of active sites for molecular catalysts in order to better understand the kinetic of polymerization. Ziegler-Natta catalysts are obtained by the combination of a transition metal complex with an alkylaluminium compound and, possibly, other co-catalysts. For molecular Ziegler-Natta catalysts, in general, the active species is a cationic compound. However, in regards to the actives species, the olefin may compete in the polymerization medium with other metal alkyl, the solvent or the counteranion. Indeed, several theoretical and practical difficulties complicate the not-so trivial rate equation linking the rate of polymerization R_p to the concentration of monomer, the active site concentration C*[M] via a propagation rate constant k_p:

$$R_p = \frac{-d[Mon]}{dt} = k_p(C*[M])[mon]^{a(\approx 1)} \quad (1)$$

The major difficulty associated with the use of this equation is the independent identification of k_p and C*[M], even under well-defined conditions. This is due to the complexity of chemical reactions involved in forming the active site, growing and terminating polymer chain. For instance, in the case of metallocene catalyst, it is now well accepted that the active species in olefin polymerization is a cationic metal alkyl complex $[L_2M—R]^+$ which is stabilized by a weakly coordinating anion but this species is only one of complex that can be formed so it is not clear what fraction of metal atoms act as active sites and an incorrect estimation of number of active sites can lead to erroneous modelling. Up to now one of the major challenges in polyolefins fields was the determination of amount of active sites for all family of Ziegler-Natta catalysts, including heterogeneous systems, metallocene and post metallocene.

Given the importance of knowing the rate constants and the active site concentrations, it should not be surprising that a significant amount of experimental work has been done for

identifying these parameters. Indeed several methods have been suggested for counting active sites such as based on the radio-tagging methods (e.g., reaction of M-P bonds with ^{14}CO or CH_3OT) which yield doubtful results, because the chemistry involved has not been fully worked out. Among these methods one of most reliable is that based on kinetic determination of number of macromolecules which was first devised by Natta as valid alternative to method based on the insertion of a chain-stopping agent. The method based on number of macromolecules is relied on the relationship between the degree of polymerization, P_n defined as (moles of monomer which react at time t)/(number of polymer chain formed at time t), and the concentration of active sites. If P_n increases with polymerization time during the very early stages of reaction before the first transfer reaction occur, it is possible to determine k_p using the equation below.

$$\frac{1}{P_n} = \frac{1}{k_p\,[mon]t} + \frac{\sum_{i=1}^{n} k_{tr}[X]^i\, t}{k_p\,[mon]t} \qquad (2)$$

If it can assume that the R_p are time independent and that the chain termination reactions are the only kind of chain transfer process then a graph of the reciprocal of degree of polymerization ($1/P_n$) as a function of reciprocal of time (1/t) will be a straight line with a slope of $1/(k_p[mon])$ and an intercept that gives us the value of frequency of chain transfer. Further if k_p and [mon] are time independent, and all of the sites are activated instantaneously to the same level of activity, the polymerization yield, Y, expressed in moles of monomer polymerized per mole of transition metal can be given by equation (2):

$$Y = k_p\,[mon]\frac{[M^*]}{[M]}t \qquad (3)$$

This equation is valid at low conversion (preferably much less than 10%). If this condition is satisfied the fraction of active sites, [M*]/[[M] (where C* = [M*]/[M]), can be found using the plot of polymer yield as function of time and introducing the k_p found from Eq. (2).

In order to extract meaningful data using this approach several requirements must be satisfied. First of all in order to obtain reliable value of [M*]/[[M] it is necessary to work in a regime where the chain transfer reactions are very limited. In this case, all the active sites have a chain growing on them and there are few dead chains in the system - this is often referred as controlled regime. If they are in controlled regime catalyst systems show a linear increment of molar mass with the time in the first instant of polymerization. If we can adapt our experimental conditions in such a way that this happens we can “capture” the chain before the

transfer reactions becomes important, it should be a straight forward exercise to count the sites. This means that technically demanding fast kinetic methods such as *Quenched Flow technique* are necessary for this study. Strictly speaking the quenched-flow or stopped-flow technique is designed to provide a reactor with a short, very well-defined residence time; usually obtained by provoking almost instaneous mixing followed by an instantaneous "stopping" of the reaction. This residence time should be less than the average lifetime of the growing polymer chains if it is to be used for analyzing rate constants and active site concentrations (as we will do in this work). The idea is to create conditions different from convention laboratory or commercial reactors where the average residence is on the order of 1-3h, during which the catalytic activity varies with time according to various side-reaction such as secondary activation, deactivation, chain-transfer or termination reactions.

The quenched flow device used in this work is a high-pressure-type quenched flow reactor which allows working in at very short reaction time (the minimum residence time is 80ms) and in a range of temperature from 25°C to 80°C and pressure up to 13 bar. The originality of this device is its suitability for investigation of influence of temperature and in particular of the monomer concentration on the kinetic of molecular catalysts such as metallocene and post metallocene catalysts.

In chapter II a very detailed description of the device is given. All the technical characteristics and the requirements are reported. One of most important is that the time required for the formation of the active sites at the beginning of the polymerization must be negligible compared with the polymerisation time. A section of chapter II is relative to the description of changes on the reactor made in order to fit it to our kinetic investigations. Originally the high-pressure-type quenched flow reactor was designed for morphogenesis studies of supported Ziegler-Natta catalyst systems, meaning that the reactor was not ideally configured for very precise studies such as the kinetic investigations. We therefore made several modifications and finally we were able to perform tests with satisfactory reproducibility, despite the delicacy of the technique.

Thus, in chapter III we have investigated the kinetic and the influence of activator of some major metallocene catalysts for **ethylene polymerization** such as *rac*-Me_2Si(2-methyl-4-

phenyl-1-indenyl)$_2$zirconium dichloride (FESBIZrCl$_2$), diphenylmethylidene-cyclopentadienyl-fluorenyl zirconium dichloride ((CPh$_2$)CpFluZrCl$_2$), and bis(pentamethyl-cyclopentadienyl) zirconium dichloride (Cp*$_2$ZrCl$_2$). We have observed how these catalysts behave at initial stage of polymerization, when they are activated with different co-catalyst and in some case a kinetic description was also possible.

The study of FESBIZrCl$_2$ activated with MAO and *i*Bu$_3$Al/[HNMe$_2$Ph][B(C$_6$F$_5$)$_4$] has been reported in first section of chapter III. In particular the absence of induction period observed in mild conditions and the high activity make the FESBIZrCl$_2$/MAO catalyst a good candidate for start our investigation.

The activation of (CPh$_2$)CpFluZrCl$_2$ complex was studied at very short reaction times (from 0.1 s to 3.5 s). The MAO, the MAO modified with the addition of phenol, the *i*Bu$_3$Al/[HNMe$_2$Ph][B(C$_6$F$_5$)$_4$] were used as activator. Several experimental parameters such as monomer concentration, Al/Zr ratio, B/Zr ratio have also been screened.

A full investigation of Cp*$_2$ZrCl$_2$ activated by MAO at three temperatures (60°C, 40°C and 25°C) and similar monomer concentration was assessed. In particular, for set of run at 25°C the calculation of main kinetic parameter of k_p and [M*]/[Zr] has been made.

In chapter IV, a kinetic study of two major post-metallocene catalysts at similar time scales is shown. The first post-metallocene investigated is a Zr-based complex bearing the tetradentate [ONNO] ligand. The main kinetic parameters were calculated for a wide range of temperatures (-23°C to 60°C). At low temperature the Bis(cumyl)[ONNO]ZrBz$_2$ activated with MAO and *t*Bu$_2$-PhOH polymerizes ethylene in controlled fashion for time on the order of minutes. At temperature up to 25°C the catalyst system polymerizes ethylene in controlled regime for reaction times on the order of seconds or fraction of seconds. Thus the quenched flow reactor presented in this work is well-adapted to do a kinetic investigation at T= 40°C and 60°C.

We focused also on the behavior of Zr- and Ti-based catalyst supported by two phenoxy-imine ligands. The bis(phenoxy-imine) Zr-based complex was activated with MAO and with [HNMe$_2$Ph][B(C$_6$F$_5$)$_4$] compound using as alkylating agent *i*Bu$_3$Al and H*i*Bu$_2$Al in order to compare the catalyst system in term of activity and polyethylene properties.

Last, we have investigated the mechanism of activation of bis(phenoxy-imine) Ti-based complex using the main kinetic parameters obtained at three temperatures 25°C, 40°C and 55°C at [ethylene] = 0.5 mol$*$L^{-1} which in the best of our knowledge is one of first example in this fields.

Chapter I

Literature Review

Chapter I: Literature Review

I. Polyolefins: the story so far

1. Plastics: historyfrom 1862

The first studies on polymers were made in the middle of 19th century on material derived from cellulose and natural rubber. In 1861 T. Graham introduced the concept of colloids (from Greek = *kolla*) to explainhigh solution viscosities. In the beginning of the 20th century Harries concluded that natural rubber was formed by combination of cyclic dimers, and in 1920 Staudinger introduce the concept of high molecular weight macromolecules. This laid the foundations of modern macromolecular science and led to development of a new generation of polymers that could replace natural materials: e.g. polyvinyl chloride (PVC), used in the manufacture of pipes, vinyl coatings and insulation of electric wire; polyethylene resins (PE) that played a key role during World War II for military applications like radar insulation; polytetrafluoroethylene (Teflon) which offers a great resistance to both corrosion and heat; and polyamide (Nylon) which was the first high performance engineering plastic.
After World War II, the Plastics Industry became a strong and innovative sector of commercial activity, and there is probably no comparable industrial sector which has grown so rapidly over the last half century. The result is that plastics are now an essential part of our everyday existence, and it is probably no exaggeration to state that they have revolutionized modern life - indeed it is difficult to think of any modern product or innovation that could have been possible without plastics.

2. Development of polyolefins activities

The history of the development of polyolefins (POs) begins in 1894 with the synthesis of the first polymer with a "polymethylene" structure by Von Pechmann from the decomposition of diazomethane. Between 1897 and 1938, numerous reports of the synthesis of similar linear crystalline PE products appeared in the literature, but no commercial use was made of these. Since then the history of POs as commercial plastics has known four milestones:

i. In the early 1930s, involved the development of commercially viable technologies to make low density polyethylene (LDPE). The polymerization reaction proceeds by a free-radical mechanism in supercritical ethylene at

high pressures around 60-350 MPa and temperatures of 200-350°C. This process was first developed in 1933 by Fawcett and Gibson, at Imperial Chemical Industries (ICI). Theresidues they scraped from the inner surface of anautoclave were identified as polyethylene which had been produced by a trace of oxygen that had leaked into the reaction vessel.

ii. In the late 1940s, the discoveries of a catalyst for ethylene polymerization by a mechanism of coordination insertion were made by Hogan and Bank at Phillips Petroleum Company. They discovered that ethylene could be catalytically polymerized into a solid plastic under milder conditions than for the free-radical process (a pressure of 364 kPa and temperature of 70-100°C) with a catalyst containing chromium oxide on an alumina and/or silica support (also called Phillips catalysts). Today hundreds of different grades of high density polyethylene (HDPE) are manufactured by several different commercial processes worldwide.

iii. In 1953-54 during an experiment carried out atthe Max Planck institute Karl Ziegler discovered that the catalyst made by combination with between $AlEt_3$ and $TiCl_4$ was able to polymerize ethylene. The linear polyethylene obtaineddisplayed high molar masses. In the same period (1954) Giulio Natta at Politecnico di Milano obtained with similar catalysts the polymerization of propylene with high degree of crystallinity and introduced the concept of “isotacticity”.These two shared the Nobel Prize for Chemistry in 1963.

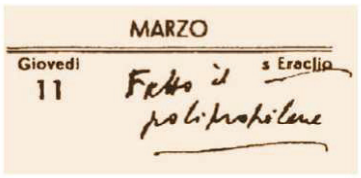

Figure 1. From Natta’s personal diary "I made Polypropylene" (Pasquon 2004)

The first plant to produceisotactic polypropylene (*i*PP) was built in Ferrara by Montecatini in 1957: it was the beginning of industrial development of polypropylenes.Several generations of Ziegler-Natta catalysts have been developed and are used nowadays for the production of HDPE, LLDPE and the vast majority of *i*PP.

iv. In the late 70s Sinn and Kaminsky discovered that metallocene complexespolymerized olefin with high activities when activated by MAO (methylaluminoxane). Subsequent research revealed that subtle variations of the metallocene molecular architecture dramatically change both the catalyst performance and the polymer characteristics. This type of catalyst therefore has the ability to truly tailor polymer architecture.This great advantage opens up new ways of making specific polymers with targeted characteristics and performances. Henceforth it should be possible to synthesize almost all kinds of stereoregular and partially regular homopolymers and copolymers in order to meet the demand for upgrading and diversification of existing polymers, and to provide solutions for modern technologies.

3. Polyethylene

Polyethylene, the most widely produced polymer in the world, is an inexpensive and versatile polymer with several applications. The control of the macromolecularstructure and subsequent control of density lead to different types of PE. Polyethylenecan be:

- linear (high-density and ultrahigh-molecular-weight polyethylene; HDPE and UHMWPE, respectively);
- branched to a greater or lesser degree (low-density and linear low-density polyethylene; LDPE and LLDPE, respectively).

Branched polyethylenes have similar structural characteristics (e.g., low crystalline content), properties (high flexibility), and uses (packaging film, plastic bags, mulch, insulation, squeeze bottles, toys, and housewares). HDPE has a dense, highly crystalline structure of high strength and moderate stiffness; uses include beverage bottles, liquid detergent jugs, crates, barrels, and luggage. UHMWPE has molar masses 6 to 12 times higher than HDPE; it can be spun and stretched into stiff, highly crystalline fibers with a tensile strength many times that of steel; uses include bulletproof vests.

4. Polypropylene

Polypropylene is classified on the base of the orientation of each methyl group relative to the methyl group of the neighbouring monomer unit. Different orientations strongly influence the crystallization properties of polymer. Four families of PP are reported below:

- Isotactic Polypropylene (*i*PP): the methyl group are consistently on one side. The polymer shows a high crystallinity degree. This polymer is produced at large scale using Ziegler-Natta catalysts (50 MT/years).
- SyndiotacticPolypropylene: alternate pendant methyl groups are on opposite site of polymer back-bone with exactly opposite configuration relative to polymer chain.
- Atactic Polypropylene: the methyl groups are arranged randomly along the polymer chain, rendering the polymer amorphous.
- Hemiisotactic Polypropylene: in this configuration most pendant methyl group are in the same side of PP chain, as in isotactic PP. However other methyl group are inserted at regular interval on the opposite side of chain.

One of main copolymer of ethylene and propylene is the ***EPDM*** rubber aterpolymer of ethylene, propylene and a diene-component. Dienes currently used in the manufacture of EPDM rubbers are dicyclopentadiene (DCPD), ethylidenenorbornene (ENB), and vinyl norbornene (VNB). EPDM rubber is used in seals glass-run channels, radiators, garden and appliance hose, tubing, pond liners, washers, belts, electrical insulation, vibrators and vehicles.

In order to manufacture these products various catalytic system are employed using different processes. This will be described briefly in the following paragraph.

5. Polymerization processes

Until the 1950's the only type of polyethylene produced was the low density polyethylene (LDPE). Low density polyethylene is produced at relatively high pressures and temperatures. This *high-pressure free radical polymerization* produces polyethylene with many branches due to intermolecular and intramolecular chain transfer during polymerization. The reactors used for high pressure processes are stirred autoclave or tubular reactor types. For stirred autoclaves the temperature varied from 180°C to 240°C while in tubular reactor the temperatures are in the range 140°C to 190°C when oxygen is used as radical initiator.

Other types of polyethylene are synthesized via catalytic polymerization, which is also the only way to produce polypropylene. Three main types of processes for the catalyzed production of polyolefins can be distinguished of the phase of continuous medium: solution (only polyethylene), slurry or gas phase.

Solution polymerization (liquid phase) is typically carried out in a continuous stirred reactor (although small plug flow reactors are used as pre-polymerizes in some processes) at temperatures in a range of 130°C-250°C in order to maintain the polymer in solution. The polymer obtained is made with a molecular catalyst.

Gas phase polymerization processes produce polymers with density in a range of 0.91-0.97 g/cm^{3}using temperatures in a range of 70-120°C and pressures of 20-30 bars. The reactors used for this type of polymerization are fluidized bed reactor (FBR), stirred tank reactor (CSTR), or horizontal stirred bed reactor (HSBR).

Slurry phase polymerization process leads to polyethylene with a density in the range 0.93-0.97 g/cm^3 in loop or stirred reactors. The first loop reactor system was developed in 1970 by Phillips Petroleum for polymerization of ethylene with chromium catalysts, and these reactors are used in the production of over 50% of polyolefins today.

In general three families of catalysts are used in industry to produce polyethylene: Phillips, Ziegler Natta and more recently single sites catalysts.

I. *Phillips catalysts*(Cr catalysts) are mainly used to produce HDPE and some LLDPE. The 40-50% of all HDPE produced, generally used for tanks or other type of

containers, is made by Phillips catalysts, which produce polymer with the broadest molecular weight distribution (MWD). The Phillips catalysts are usually made by impregnating a chromium compound onto porous, high surface area silicate carrier [1]. The support is calcinated under dry air at 500-900°C, which removes much of the excess hydroxyl group population and the Cr is grafted on the support. The active species is formed by reduction of Cr(VI) toCr(II) or Cr(III) by ethylene. Commercial catalyst usually contains 0.5-1% in weight of Cr but only a small fraction of this metal is active for polymerization. In 1956 the first Phillips plant became operational, sales were very slow during the first year but with the invention of the Hula-Hoop, a toy that became extremely popular in USA, the Phillips business was safe.

II. A Ziegler-Natta (Z-N) catalyst is a complex formed by reaction of a transition metal compound (alkoxide, alkyl, aryl derivative or most frequently a halide) of groups4 to 8 transition metals (e.g. Ti, V, Cr, and Zr) with alkyl or alkyl halide of main group metals(also called co-catalyst or activator).In first generation catalysts other alkylaluminium compound were used instead of Et_3Al. However the low activities of the catalysts required them to be present in high concentration. Removal of catalyst residues from polymer by washing with HCl was also necessary. The second-generation catalysts incorporating solid $TiCl_3$ and alkylaluminium were much more active than first generation. The third generation catalysts were produced commercially by supporting the titanium compound on $MgCl_2$, SiO_2, or Al_2O_3 to increase the amount of active titanium from 0.1% to 5%. The fourth generation of Z/N catalysts are produced by milling $MgCl_2$ with about 5% of $TiCl_4$ and $Al(C_2H_5)_3$ as co-catalyst. Only a small fraction of titanium (1-20%) is active for polymerization. However the catalysts are so productive that the residue can be left in the processed product.

Both Phillips and Z/N catalysts have some points that could be improve:

- The fraction of titanium or chromium forming active sites in the catalysts is low, only 1-20%;
- When $MgCl_2/TiCl_4$ catalyst is used 5-50 ppm of chlorine remains in process and can eventually be responsible for corrosion problems;

- Copolymerization with some α-olefins is possible but only in a small range;
- It is difficult to control the polymer microstructure.

Thus there is a strong interest in new kinds of catalysts such as metallocene that can show high activities and produce a wide range of copolymer products.

II. Metallocene catalysts

The work presented in the current thesis focused on the investigation of molecular catalysts which are represented by metallocene and post-metallocene catalyst precursors. Since the mechanisms that govern the activation of metallocene have been deeply studied in last two decades and the activation pathways of metallocene are similar to post-metallocene precursors, we will focus essentially on the investigation of metallocene catalyst precursorsin this chapter.

1. Introduction

The development of homogeneous catalysts for olefin polymerization was an important stage in the evolution of Ziegler-Natta catalysts. In 1950 Wilkinson[2]identified the structure of the ferroceneCp_2Fe. In the same decade bis(cyclopentadienyl) titanium dichloride (Cp_2TiCl_2) was activated with alkyl aluminium chloride (AlR_2Cl) for ethylene polymerization. A classical metallocene catalyst of group 4 shows a typically sandwich structure in which the transition metal (Ti, Zr or Hf)is linked to two cyclopentadienyl ligands carbon atoms and 2 other groups, often alkyl or chlorine (see Figure 2).

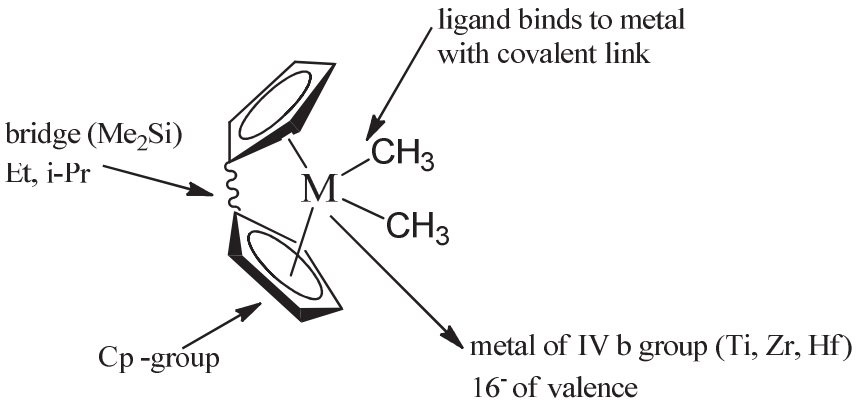

Figure 2.Metallocene catalyst

For a long time metallocenes did not have a big impact on industrial scale applications. In the late 1950s, soon after the Ziegler and Natta discovery, the metallocenes were used[3, 4] in combination with alkyl aluminium compounds, such as triethyl aluminium (TEA) or diethyl aluminium chloride (DEAC) for olefin polymerization as soluble model of Ziegler-Natta catalysts. Furthermore the activities shown by metallocene were poor and lower than activities shown by Ziegler-Natta catalysts, thus they were used mainly for mechanistic studies. Indeed it has been confirmed[5-10] that the active species in olefin polymerization catalyzed by electron deficient early-transition-metal complexes is the cationic metal alkyl $[L_2M—R]^+$, highly electophilic hard Lewis acid (e.g. in Figure 3).

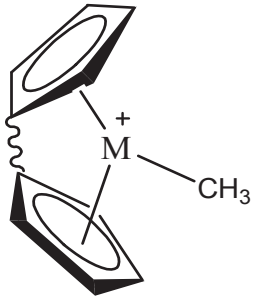

Figure 3. Active site for metallocene catalyst

Non-bridgemetallocene catalysts are generally non-sterospecific producing only atactic polypropylene because of the symmetric feature of active centres. Modified metallocenes containing stereorigid ligand systems were found suitable for stereospecific olefin polymerization. Among the modified metallocene, the *ansa*-metallocenes, in which the cyclopentadienyl group is linked by a short bridging group, are very important. The

modification of catalysts, by variation of the ligands surrounding the active centre, allows correlation of catalyst structure with catalytic activity and stereo specificity (see Figure 4).

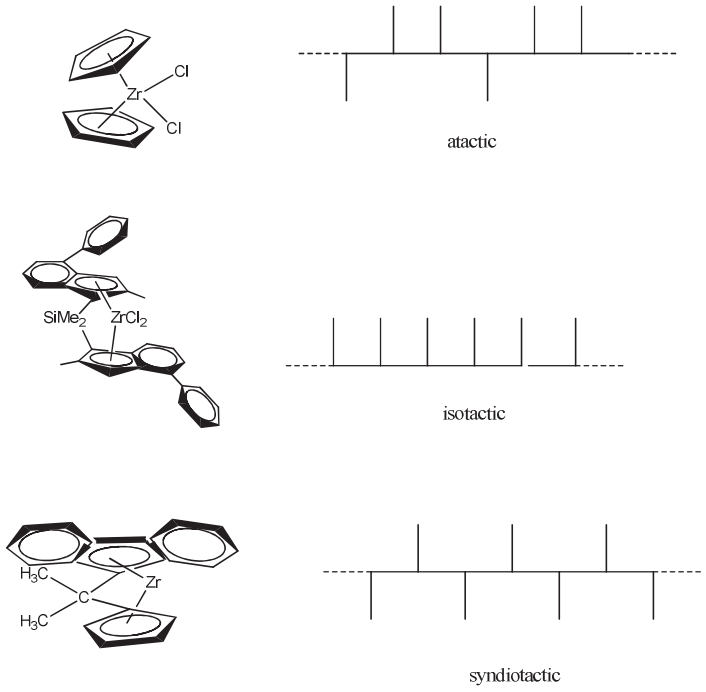

Figure 4. Main metallocene catalysts and resulting PP structure

The development of 'half-metallocene' or constrained geometry catalyst CGC (e.g. in Figure 5),bearing a silylene-bridged cyclopentadienyl–amido ligand, was another significant event in the story of evolution of Z/N catalysts. New families of ethylene and α-olefin copolymers have been prepared using these catalyst systems by Dow under the trade name 'INSITE'.

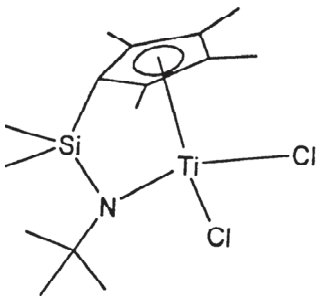

Figure 5. Constrained Geometry Complex

2. Activators of single site catalyst precursors.

Several methods exist for generating cationic active catalyst according to the model reported in Figure3. Among the activators, Methylaluminumoxane (MAO) is one of the most common co-catalysts employed in industrial production, but it shows several disadvantages such as its evolution with time and high costs. Alternatives to MAO have been developed, among these the use of boranes or borate salts, generally in combination with an alkylaluminium. A description of main characteristics of these activators is reported below.

2.1 Alkylaluminiumcompound

Although alkylaluminium compounds are not efficient activators for metallocene complexes for the negligible activity showed[4], several investigations with various alkyl groups and investigation of kinetics have helped to define the nature of active centres of some homogeneous catalysts, to establish the mechanism of interaction of olefins with active centres and to explain some elementary mechanistic steps. In particular many efforts have been made in order to identify the active species. Breslow et al.[3] pointed out that polymerization takes place mainly when titanocene exists as Ti(IV). From NMR studies it was observed that the rate of polymerization decreases when Ti changes oxidation state from Ti(IV) to Ti(III)[11].As early as 1960 from spectroscopic and chemical studies[12] of Cp_2TiCl_2/AlR_nCl_{3-n},titanium alkyl species **I** reported in Figure 6was proposed as a possible active species.

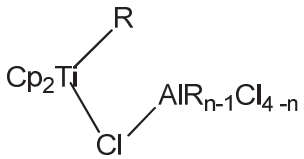

I

Figure 6.Active site proposed by Long et al.[12]

Dyachkovskii et al.[13] suggested that the reaction between $Cp_2Ti(R)Cl$ and $AlRCl_2$ leads to Cp_2Ti^+-R centre, generated by Cl^- abstraction, where ethylene can be polymerized, as shown inFigure 7:

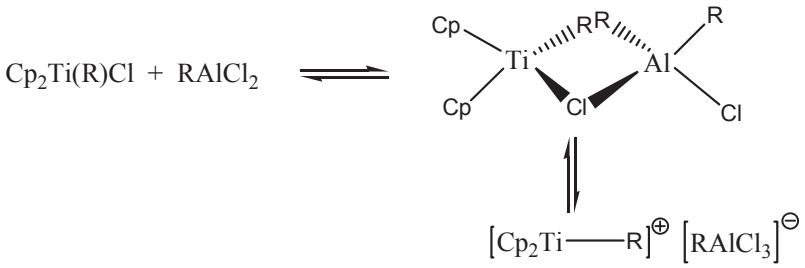

Figure 7.Active species for ethylene polymerization suggested by Dyachkovskii et al.[13]

In early 80s,Eisch[14] isolated the cationic complex II (see Figure 8) in the early stages of silylacetylene insertion. They have proposed that the active component is the cationic species Cp_2TiMe^+.

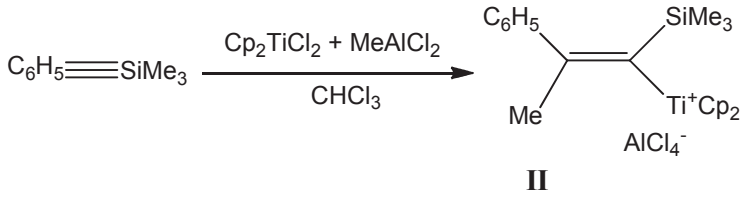

Figure 8.Cationic species isolated by Eisch et al.[14]

Overall the low activities shown by metallocene activated by alkylaluminium halides for propylene polymerization in particular, and olefin polymerization in general, have limited their use.

2.2 MAO

Many efforts have been made in order to improve the performance of metallocenes activated by alkylaluminium halides to polymerizeα-olefins. Among these the effect of water addition on the polymerization activity has been observed[15] for the system $Cp_2TiEtCl/AlEtCl_2$. Further investigation of the system $Cp_2TiCl_2/AlMe_2Cl$[16]suggested that the formation of a dimeric aluminoxane, ClMeAl-O-AlMeCl, a stronger Lewis acid, is responsible for increasing ethylene polymerization activity. In early 70s Sinn and Kaminsky observed an unusual

increase of activity for ethylene polymerization with the addition of water to polymerization inactive $Cp_2ZrMe_2/AlMe_3$ catalyst system[17]. The species formed from the reaction with $AlMe_3$ an H_2O able to increase the polymerization activity is the methylaluminoxane $(-AlMe-O-)_n$ in which $5<n<20$. MAO was initially formed directly *in situ* in early 80s from partial hydrolysis of TMA according to simplified reaction[18]:

$$4Al(CH_3)_3 + 3H_2O \rightarrow Al_4O_3(CH_3)_6 + 6CH_4$$

Note that TMA is produced according to the reactionbelow[19]:

$$(CH_3)_3Al_2Cl_3 + 3Na \rightarrow (CH_3)_3Al + 3NaCl + Al$$

Furthermore the hydrolysis is more complicated than expected. An alkyl aluminum–water complex is formed, which subsequently eliminates methane to provide a dimethylaluminum hydroxide complex. This compound rapidly associates to give dimers or larger oligomers in solution.

Several methods based on metal hydrates salts, such as $CuSO_4$, $Al_2(SO_4)_3$, $FeSO_4$, or rely on the use of water vapor[20] have been investigated. In general the use of salts achieves a good control of hydrolysis, but the MAO conversion is not complete and the unreacted TMA remains in solution in "association" with MAO or such "free" TMA. Non-hydrolytic methods have also been investigated in order to avoid the dangerous use of water. The most common are based on the reaction between TMA andphenylboronicacid[21] or trialkylboroxine[22]. The production of MAO by thermal treatment of TMA with organic compounds such as benzoic acid or carbon dioxide, has also reported[23].

MAO can be defined as a species in which aluminum and oxygen atoms are positioned alternately and free valences are saturated by methyl groups, but the structure is likely more complicated than this definition suggests. Up to now several structures have been proposed for MAO. The earlier structures proposed were mono-dimensional linear chain or rings (structure **A** and **B**in Figure 9) which suggest tri-coordinated aluminum, which could be considered to be highly Lewis acid. From DFT studies[24] a 3-dimensional cage structure was shown to be more stable than cyclic ones.

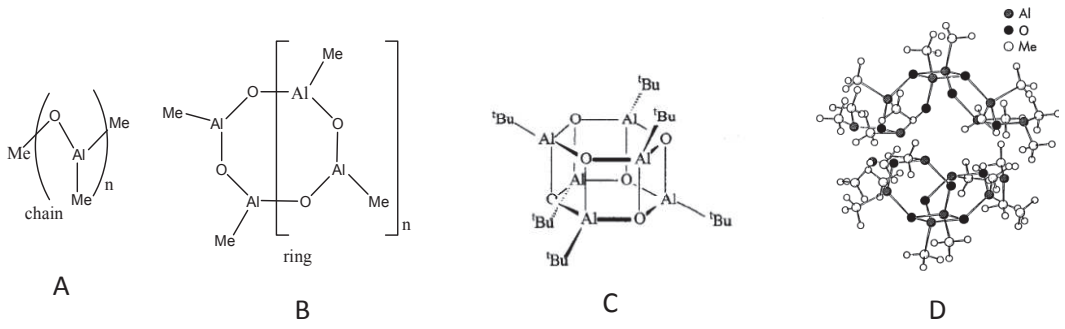

Figure 9.Possible structures of MAO[25, 26]

From studies of Barron et al.[25] on tert-butylaluminoxanes, structure **C**, Sinn[26] proposed structure **D** as possible structure for MAO. MAO plays an important role for olefin polymerization, indeed high activities (10^6 $g \cdot g_{Zr}^{-1} \cdot h^{-1} \cdot bar^{-1}$) were obtained when it was used as an activator for Cp_2ZrMe_2[27].Using the more stable chloro-derivate, Cp_2ZrCl_2, the activity measured was five times higher than the activity obtained with dimethylated metallocene[28]. Despite the high activity in metallocene olefin polymerization, MAO shows several disadvantages such as the very low solubility in aliphatic solvents, and poor storage stability in solution. For these reasons, other more soluble aluminoxanes such as ethylaluminoxane and isobutylaluminoxane have been tested[29]. However these aluminoxanes do not provide the same level of activity with metallocene as MAO. Other disadvantages of MAOincludes the large quantities required to obtain useful activities with different metallocene complexes[30], as well as poor control of morphology when metallocene are supported, and finally the poorly understood activation process and the nature of active species formed by the reaction between MAO and metallocene.

In summary, MAO is composed of a mixture of oligomers with free TMA. Only a low fraction of Al is involved in reaction. In addition MAO can evolve with time; it is for this reason that MAO must be stored at low temperature .Consequently, new co-catalysts have been developed in order to provide equivalent or grater activities and also could allow to isolation and characterization of active species formed.

2.3 Boron-based activators

Other co-catalysts have been investigated with the aim of finding effective activators which do not show the same disadvantages of MAO but are able to form active species capable of being isolated and characterized. It was observed that the use of organoboranes such as $B(C_6F_5)_3$ or borate salts $[B(C_6F_5)_4]X$, where X= CPh_3, $HNMe_2Ph$, leads to highly active cationic metallocene catalysts[31].

Borate salts

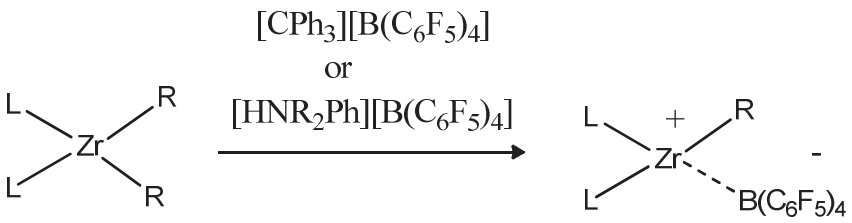

These activators offer several advantageous properties, including improved solubility, thermal stability and the resulting cationic complexes are easily to be isolated and characterized. Jordan et al.[5] isolated the cationic species of a zirconocene $[Cp_2MR]^+$. They prepared the complex $[Cp_2Zr(CH_3)(THF)][BPh_4]$ by reacting $Cp_2Zr(CH_3)_2$ with $AgBPh_4$ in CH_3CN followed by re-crystallization in THF. From X-Ray diffraction analysis found that Zr-CH_3 bonds and the average Zr-Cp distance were shorter than corresponding distances in $Cp_2Zr(CH_3)_2$ implying that there is a greater Lewis acidity of the metal centre in this cationic compound. Further they found a significant π-component in Zr-O bond meaning that Cp_2ZrR is a complex lacking aπ donor ligand. In addition Bochmann and co-workers[32]presented a reaction using Cp_2TiMe_2 and $NH_4^+X^-$ (where X^- = PF_6^-or ClO_4^-) at room temperature in THF as solvent. Later on, the synthesis of $[Cp'_2ThMe][BPh_4]$ from the Th-based metallocene and $[HNR_3][BPh_4]$ was also reported[33]. Hlatky and co-workers[10]observed the formation of the zwitterionic complex $[Cp'_2ZrC_6H_4][BPh_4]$via Zr-Me bond protonolysis followed by subsequent BPh_4^- aryl C-H bond activation. Thus, in order to avoid the C-H activation to limit the stability of the ion pair, the dimethylaluminiun salt of noncoordinating anion such as $B^-(C_6F_5)_4$,was developed[34].

Borane

In early 90s,Yang et al.[35, 36]observed that activating metallocene Zr-based Cp_2ZrMe_2 with tris(pentafluorophenyl)borane $B(C_6F_5)_3$ provided activities comparable with those obtained with MAO as co-catalyst.$B(C_6F_5)_3$ is a strong Lewis acid that promotes highly efficient olefin polymerization. Though tris(pentafluorophenyl)borane, $B(C_6F_5)_3$, was synthesized in early 60's, it was employed in combination with group 4 metallocene for olefin polymerization only in early 90s.

The $B(C_6F_5)_4^-$ anion in combination with Ph_3C^+, a powerful alkide and hydride abstraction reagent, has shown to form a dissociated ion pair with a metallocene pre-catalyst that is highly effective for olefin polymerization[37]. Further ammonium $HNRR'_2^+$ in combination with non- or weakly coordinating borate has also been used[38] as effective co-catalyst for activating metallocene or related metal alkyls. Metallocenes activated by borate salts show high activity. Indeed catalysts formed by the reaction between *rac*-$Et(Ind)_2ZrMe_2$and $[Ph_3C][B(C_6F_5)_4]$ are 6 times more active in propylene polymerization than those activated by MAO[37]. The tendency of an anion to bind a Lewis acid metal centre is decreased by delocalisation of charge over a large volume[39]. In order to decrease the nucleophilicity of the anion multiply-encumbered perfluorarylboranes, as well as bifunctionalboranes, have been developed[40, 41].

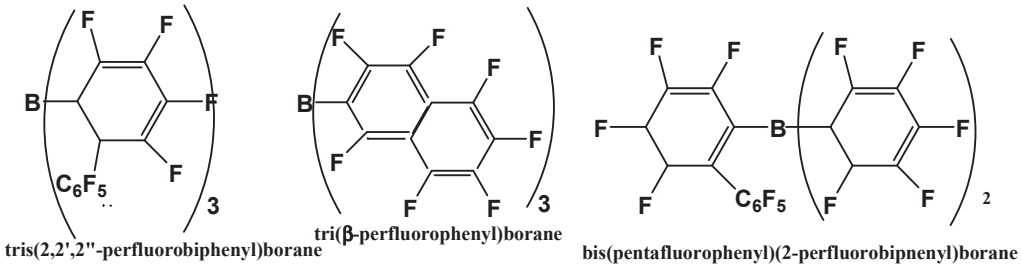

Figure 10.Encumberedperfluoarylboranes

A great advantage of boron-based activators is that the ratio of B/Metal is about 1:1 rather than 1000-5000 to 1 as in the case of MAO. On the other hand dichlorozirconocenes do not react with boron derivates to generate the active species, and the synthesis and storage of analogue dialkylcomplex is difficult because of their highly sensitive to air moisture and light.

Further resulting catalyst are highly sensitive to poisons and decomposition and must be stabilized by addition of aluminium alkyls such as Al*i*Bu$_3$; in this case the necessary ratio of Al:Metal is 100-500 to 1.

3. Mechanism of polymerization

3.1 Introduction to polymerization mechanism

The simplest scheme for polymerization reaction consists of three steps:

A. Formation of catalytic centres and monomer insertion;

B. Chain growth reaction

C. Transfer reactions

In the following paragraphs we will investigate in detail these steps beginning with what appears to be the most complicated step: activation.

A. Activation

If it is accepted that the active species in olefin polymerization catalyzed by metallocene complexes is the cationic metal alkyl complex $[Cp_2M—R]^+$ (see Figure 3), a highly electrophilic hard Lewis acid, the formation of this complex is not as straightforward as expected. Nevertheless, in general the activation process is resumed in these two steps:

- Alkylation of M-X bonds in the precursor, making at least one M-R bond;
- Development of coordinative and electronic un-saturation at metal centre.

3.1.1 Alkylation

Generally, the first step in the formation of catalyst is the alkylation of the catalyst precursor using an organometallic complex of a main group metal. Depending on the alkylating agent used different complexes are obtained. The alkylating agent for metallocene precursor are typically aluminium alkylsor MAO.

3.1.1.1 Alkylaluminium compoundas alkylating agent

The most common alkylating agents are triisobutylaluminium (TIBA),triethylaluliminium (TEA) and trimethylaluminium (TMA) (e.g. in Figure 11).

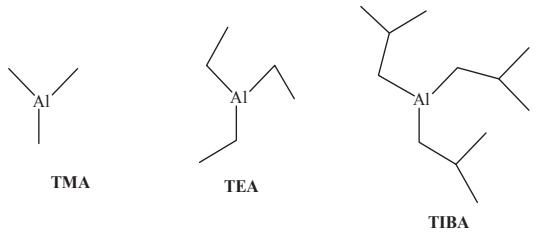

Figure 11.Structures of main alkylating agent

TEA

Early studies[42]on the alkylation step showed that the reaction between dichlorozirconocene and TEA formed different species depending on the Al/Zr ratio. Indeed when one equivalent of TEA is employed in C_6D_6, complex **Ia (**see Figure 12**)**, which is in equilibrium with **Ib**, is detected. Increasing the number of equivalents of TEA leads to formation of complex **II** together with ethane. At higher Al/Zr ratio, 3:1, complex **III** and **IV** are formed by C-H activation reaction.

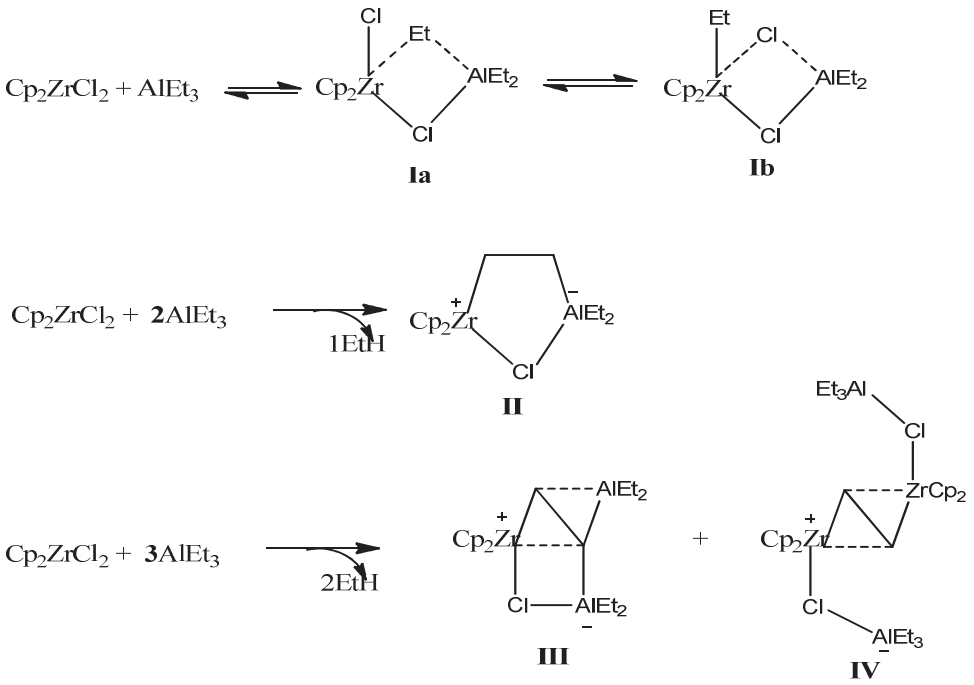

Figure 12.Transient species formed during alkylating step by alkyl aluminium

TMA

It was observed that using TMA as an alkylating agent leads to the formation ofonly monoalkylated species, even at high excesses of alkylating agent[43]. It was also observed that the rate of formation of monoalkylating species depended strongly on the metallocene structure and its ligands. They introduced the concept of steric and electronic contributions that could affect the position of such exchange equilibrium. Increasing number of alkyl or silylsubstituents on Cp-ligand increase the electron density at Zr centre and monolakylation reaction is not favored. Decreasing the electron density at Zr centre of Cp_2ZrCl_2 complex thus appears to favor uptake of methyl group. Some deviations from expected electron density trend might be explains by steric effect.

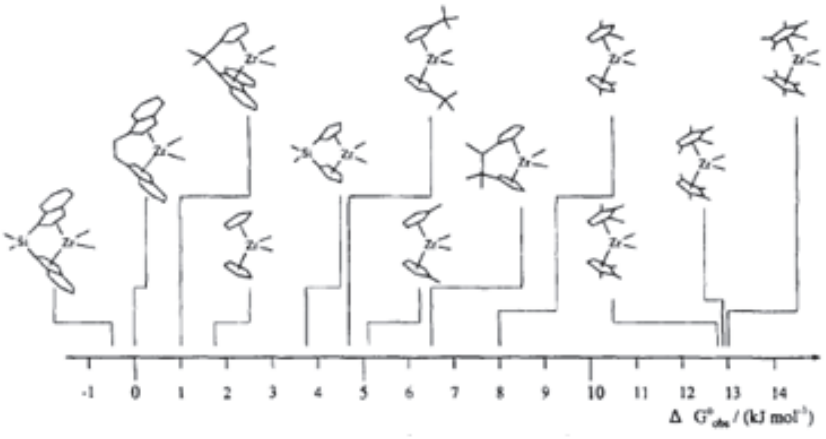

Figure 13. Free enthalpy changes, ΔG_{obs}, for methyl transfer from TMA to different zirconocene dichloride complexes. (Reprinted from *InorganicaChimicaActa*, Copyright 1998 with permission of Elsevier**).**

Brintzinger and Bech[43]observed also a different behavior when TEA is used rather than TMA. By measuring of electronic density it was also observed the reaction between Cp_2ZrCl_2 and TEA in C_6D_6 is ten times more efficient than alkyl exchange with TMA. The less favorable formation of heterobimetallic species contributes to this observation. Indeed, when the ratio is increased from 2:1 to 4:1 the ^1H NMR spectra indicate the evolution of ethane and formation of additional Zr species which could correspond to species **II**, **III** and **IV** proposed by Sinn and Kaminsky (see Figure 12).

TIBA

Studies carried out with TIBA as an alkylating agent have also been carried out. The reaction of *rac*-$Me_2Si(Ind)_2ZrCl_2$(SBIZrCl_2)with Al^iBu_3 at room temperature in Al/Zr ratio of 2:1 in toluene leads to a mixture of (SBI)ZrCl_2 and (SBI)Zr*i*Bu. By adding up to 5 equivalents of TIBA,90% of conversion to (SBI)ZrCl^iBu was observed (c.f. Figure 14).

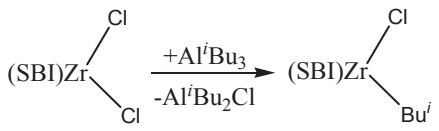

Figure 14.Themonoalkylated species formed with TIBA

The formation of monobutylating species was also observed in case of reaction between $Ph_2C(CpFlu)ZrCl_2$ and TIBA[44]. In this case the Al/Zr ratio has a strong influence on the conversion of monoalkylated complex; in fact more than 10 equivalents of TIBA are required for total conversion. With a surplus of 10 equivalents of TIBA or higher, a single species is formed. Even with 50-fold excess of alkylating agent no further reaction to dialkyl complex is observed. The type of product formed also depends on the ligand of metallocene. With Cp_2ZrCl_2 more than 2 equivalents of TIBA are required for total conversion of pre-catalyst in alkylated complex. When 10 equivalents of TIBA were added it was observed that dimericmetallocene$[Cp_2ZrH_2{\cdot}Al\textit{i}Bu_3]_2$ containing Zr-H-Zr and Zr-H-Al bridges was formed (see Figure 15). It can be assumed that $[Cp_2ZrH_2Al\textit{i}Bu_3]_2$ is the intermediate obtained via the formation of $Cp_2Zr\textit{i}Bu_2$followed byβ–H elimination which leads to formation of isobutene.

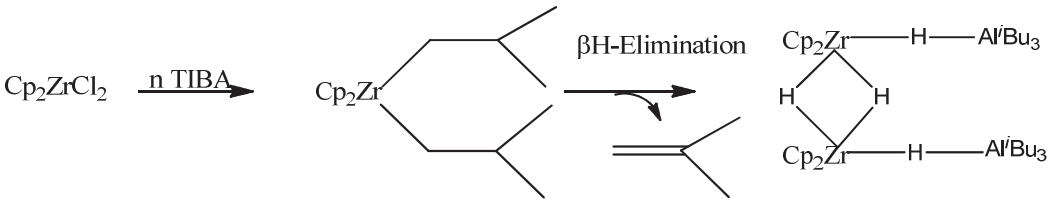

Figure 15.Hetero-bimetallic complex formed by reaction of Cp_2ZrCl_2 with an excess of TIBA

3.1.1.2 Methylaluminoxane (MAO)as alkylating agent

At the current time the mechanism by which the methylation occurs for metallocene activated by MAOis unclear because of role played by $Al(CH_3)_3$. For example in the case of the Cp_2ZrCl_2/MAO catalytic system, spectroscopy studies[45]suggested that the alkylating agent was the TMA present in MAO. On the other hand, using $Cp_2TiMeCl$ it was shown[46] that MAO was more important than TMA in the formation of Cp_2TiMe_2. Other UV/visible investigations [47-49] with Cp_2ZrCl_2 showed that the first monomethylated agent was MAO. Further studies[50, 51] at different concentrations of TMA for a fixed Al/Zr ratio showed that free TMA is not indispensable for this methylating step. However at high TMA concentrations, a bimetallic compound known as “dormant” species, for olefin polymerization, has been detected for both Cp_2ZrMe_2/MAO and Cp_2ZrCl_2/MAO systems (see species **II** in Figure 16).

NMR studies have revealed that if the ratio Al/Zr increases predominant species become species **I** and **II**. Further at high Al/Zr ratio(>500) the ratio **I**:**II** is 1:4 but this ratio strongly depends on the content of "free" TMA in MAO.

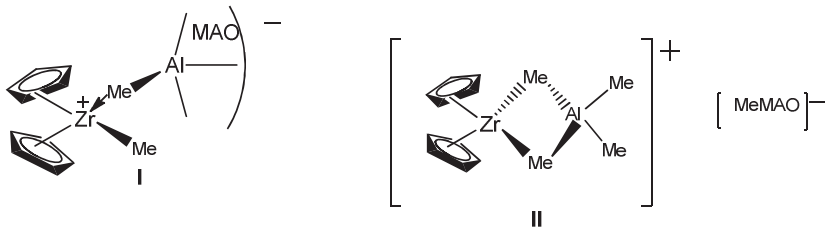

Figure 16.Species formed in Cp_2ZrCl_2/MAO system: dormant species II is formed by « free » TMA

If the Al/Zr ratio increases, species **II** tends to dissociate. A possible explication is that at high Al/Zr ratios, the strongest Lewis acidic sites of MAO abstract Me^- and form Me^--Al≡MAO of species **I**.

3.1.2 Formation of ion pair

The second step for activation of a metallocene complex after the alkylation is the formation of a coordination site for monomer coordination. This proceeded via formation of a cationic metal species that is stabilized by a weakly coordinating anion. If the weakly coordinating anion is already part of structure of activator the cation formation proceeds via:

1. Abstractive cleavage of M-X (X= R or Cl) bonds

- byone electron oxidant such as Ag^+ Na^+ or $(C_5H_4R)_2Fe^+$. If a Lewis base is present it stabilized the cationic species. Jordan et al.[5-7] isolates the cationic metallocene complex by reacting Cp_2ZrMe_2 with $Ag^+BPh_4^-$ in CH_3CN as reported in scheme below.

$$Cp_2Zr(CH_3)_2 + Ag^+BPh_4^- \xrightarrow{CH_3CN} [Cp_2Zr(CH_3)(CH_3CN)][Ph_4B] + C_2H_6 + Ag^0$$

In this case the isolation of a stable salt requires the use of relatively non-coordinating, non-reactive counterions such as $B(C_6H_5)_4^-$.

- By Lewis acid cations such as Ph_3C^{+}[37]or R_2Al^{+} stabilized by weakly coordinating anions[52](Figure 17) .

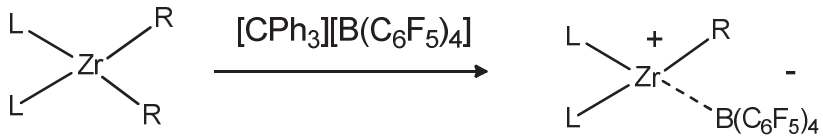

Figure 17.Abstractive cleavage by Lewis acid cations

2. Protonolysis of M-R bonds by a strong Brønsted acid which leads to the formation of a cation and methane.

When investigating an alternative route to MAO,Bochmann[53]observed that neutral amine coordinate to the cationic metal centre when a$[HNMe_2Ph][B(C_6H_5)_4]$complex is employed in protonolytic activation process. According to Bochmann[53] the product of the reaction between zirconocene with $[HNR_2Ph][B(C_6F_5)_4]$ is an aniline complex as reported in Figure 18:

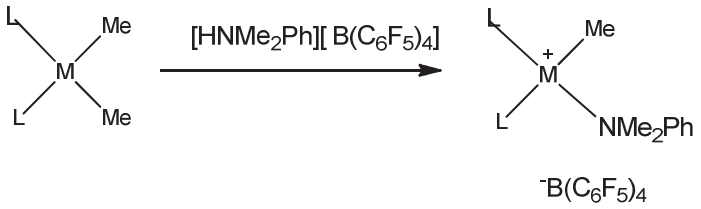

Figure 18.Activation of dialkylmetallocene center by $[HNMe_2Ph][B(C_6F_5)_4]$

This aniline complex should be considered as a dormant site for catalyst since the aniline must be displaced by the olefin to form the active species.

When the weakly coordinating anion is formed during the reaction, the formation of ion pair isobtained via alkyl or chloride abstraction from alkylated metal complex by a strong Lewis acid (e.gFigure 19).

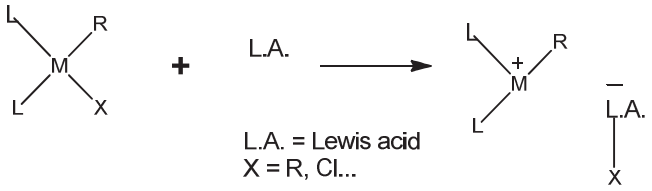

Figure 19.Simplified scheme of formation of active species using a strong Lewis acid

This abstraction is performed by a strong Lewis acid site, which is the Al centre present in MAO or by a neutral strong Lewis acid such as tris(pentafluorophenyl)borane or $Al(C_6F_5)_3$. In the following paragraphs we will illustrate how MAO, boranes and borates are employed to form an active catalyst.

3.1.2.1 MAO as active species generator

As in case of methylation step the role of TMA is not clear in the ionization step.It was first proposed that TMA is the actual cation generator[54], whereas the polymerization activities for Cp_2ZrMe_2/TMA and Cp_2ZrPh_2/TMA systems are much lower than polymerizations using MAO. For other metallocenes such as *rac*-Et$(Ind)_2ZrCl_2$ and *i*Pr(Cp)(Flu)$ZrCl_2$, activated with TMA only the methylation of Zr was observed[47]. From NMR studies[46, 55-57]it has been observed that various species are formed by interaction of the metallocene with MAO as shown in scheme in Figure 20:

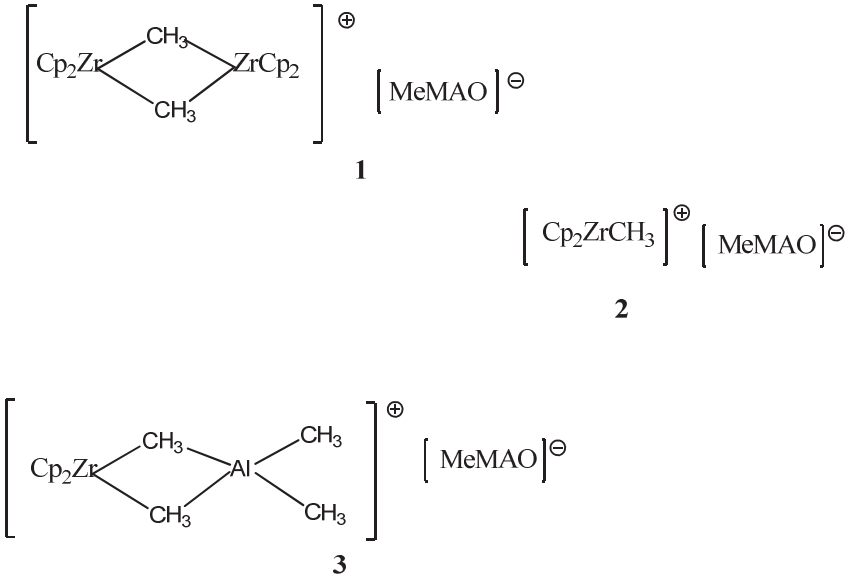

Figure 20. "Dormant" species formed with MAO as activator

Tritto et al.[55] used Cp_2ZrMe_2 as precursor that reacts with MAO to form the binuclear μ-methyl complex **I** and the monomeric complex **II (**c.f. Figure 20).Complex **III** was also detected at higher Al/Zr ratios. The same proposal was made by Bochmann et al.[58] who also

observed the formation of the cationic species **III**, $[Cp_2Zr(\mu\text{-}Me)_2AlMe_2]$, from reaction between Cp_2ZrMe_2 and $[Ph_3C]^+[B(C_6F_5)_4]^-$ in presence of MAO which is the "dormant" species.

3.1.2.2 Borate and aluminate salts as active species generator

These complexes are often used in combination with a trialkylaluminium compound. Mixtures of $CPh_3^+X^-$ salts with alkylaluminium, such as $AlMe_3$, or TIBA which is more effective have been employed. Indeed it is convenient to replace preformed metal alkyls by the corresponding metal chlorides which are easier to store and less sensitive to poison. The trialkylaluminium (in excess) act as alkylating agent in situ and also as scavenger for impurities that could partially poison the catalyst.

Bochmann et al.[59] investigated the ternary system $Cp_2MR_2/[CPh_3][B(C_6F_5)_4]/AlR_3$and obtained very high initial activities and then a significant decrease or decay in activity with time[60]. It was first observed that the reaction between $[CPh_3][B(C_6F_5)_4]$ and aluminium alkyl AlR_3 at elevated temperature forms $AlMe_{3-x}(C_6F_5)_x$ and BR_3 compounds via the formation of the highly electrophilic transient AlR_2^+ species(e.g. Figure 21**);** this reaction is much slower if R is a methyl group rather than isobutyl group.

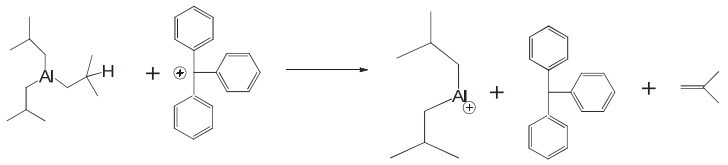

Figure 21.Formation of AlR_2^+ specie from reaction between TiBA and trytilderivates

Further the transient species $[Al(^iBu)_2]^+$[61] was also observed in the reaction between $[PhNMe_2H][B(C_6F_5)_4]^-$and Al*i*$Bu_3$ which leads to complete degradation of $[B(C_6F_5)_4]^-$.The formation of intermediate species which could influence the effectiveness of these ternary catalytic systems has been observed, and depends on the Al/Zr ratio. For the ternary system (SBI)$ZrCl_2$/Al*i*Bu_3/$[CPh_3][B(C_6F_5)_4]$, where SBI=*rac*-$Me_2Si(Ind)_2$, NMR studies[62]have shown that the cationic zirconium species which are present and can be predominant at different amount of aluminium alkyls. The complex **I** in Figure 22was predominant at low Al/Zr ratios (<10).

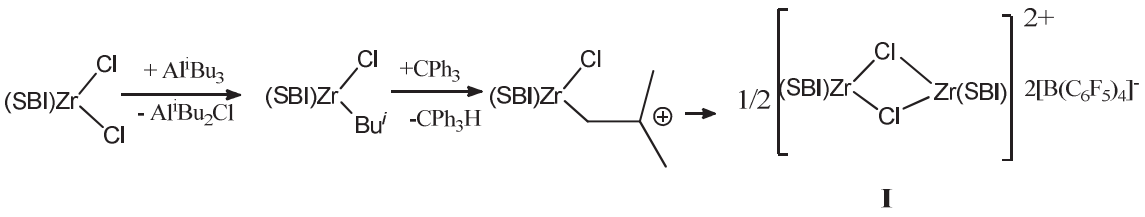

Figure 22.Dormant species formed in the (SBI)$ZrCl_2$/Al*i*Bu_3/[CPh_3][$B(C_6F_5)_4$] ternary system

An increment of Al/Zr ratio (>20) leads to formation of species **II** in Figure 23**.**

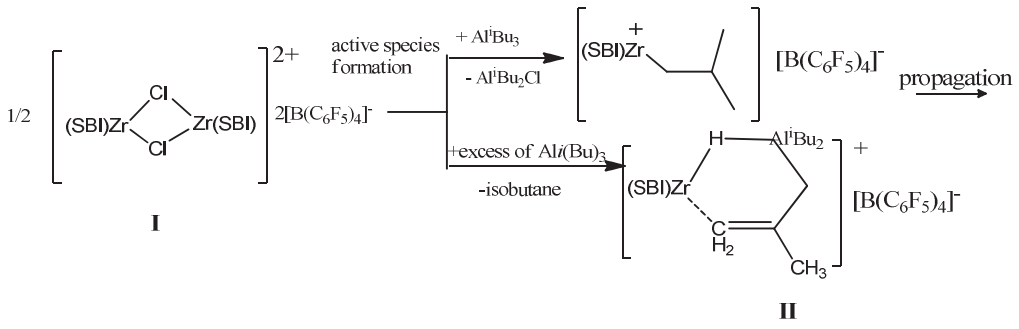

Figure 23. Another dormant species formed in (SBI)$ZrCl_2$/Al*i*Bu_3/[CPh_3][$B(C_6F_5)_4$] ternary system

The influence of Al/Zr ratio was also studied for the catalytic systemPh_2C(CpFlu)$ZrCl_2$/[$PhNMe_2H$][$B(C_6F_5)_4$]/TIBA. At Al/Zr ratios lower than 50,two species were detected, and atAl:Zr ratio of 1:100 the dinuclear complex [Ph_2C(CpFlu)Zr*i*Bu•Al*i*Bu_3] can be formed; with the loss of isobutene, this complex can rearrange to form [Ph_2C(CpFlu)Zr-μ-H-μ-(C_4H_7)Al*i*Bu_2][$B(C_6F_5)_4$].For Cp_2ZrCl_2 at least three species were found, meaning that the structure of the metallocene precursor starting to influence the formation of active sites[63] and that activation using borate in combination with AlR_3 is not a simple process.

In addition, it is expected that when a metallocene complex is activated in the presence of ethylene different complexes can be generated. In summary an active species should display a metal-C bond and a vacant site in cis-positive as shown in model studies using a dimethyl metallocene (Cp_2ZrMe_2) in combination with borate activator [X][$B(C_6F_5)_4$]. However during polymerization a range of complex can be formed in particular in presence of AlR_3 as illustrated above.

3.1.2.3 More about the ion pair

Up to now we have widely discussed about the formation of active species, we have seen different dormant species and other phenomena which occurs during the first instant of polymerization, furthermore we have focus only on the cationic metal alkyl $[L_2M—R]^+$species without a great consideration of counterion. In fact, the ion pair generated, $[L_2M—R]^+X^-$ is by far considered the main resting state of polymerization process and, in particular, the anion position could influence strongly the polymerization. The counterion X^- strongly affects the catalyst activity and stability, the stereoregularity and the molecular weight distribution [64, 65]. More, in case of slurry polymerization it is also important to consider the effect of solvent. An ion pair in which no solvent molecule interposes between the two ions is called a contact or tight ion pair, but it is possible to find also a solvent separated or loose ion pair.

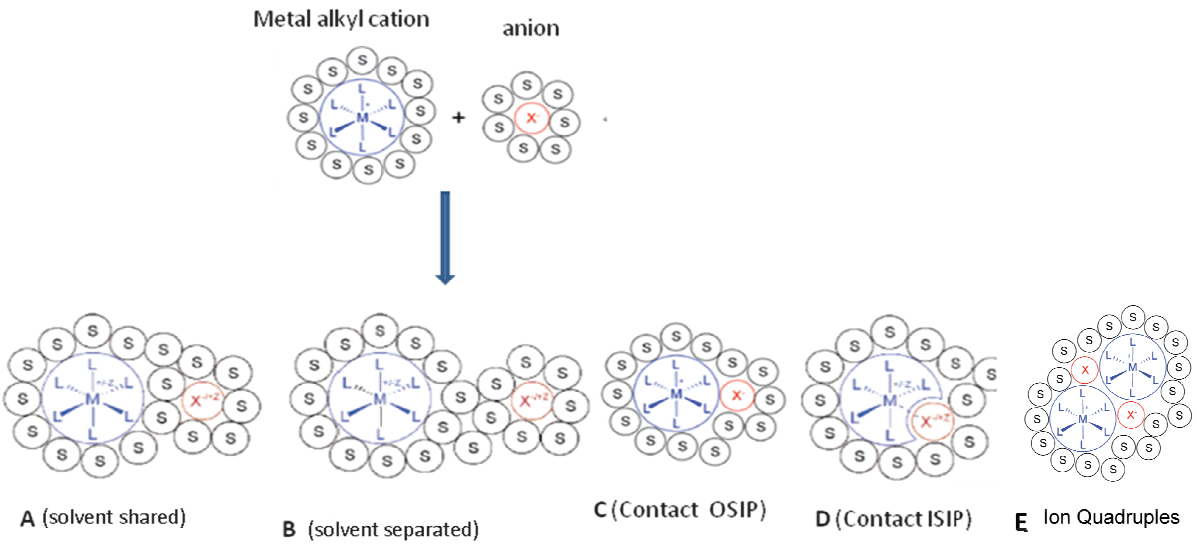

Figure 24.Transition metal complex ion pairs.

In the case of transition metal it is possible to find a solvent shared ion pair which is a variation of solvent separated ion pair but only a shell of solvent is interpose between the anion and cation species. Furthermore, the possibility of finding these species becomes smaller. It is easier to find the contact-type ion pair. In transition metal ion pair it is possible to define the two contact ion pairs as outer-sphere ion pairs (**OSIP**s) and inner-sphere ion

pairs (**ISIP**s), which are respectively the species **C** and **D** of Figure 24. They are contact ion pairs in which the counterion is in the first coordination sphere of the metal-containing moiety [66]. Considering the strong unsaturation of metal of species $[L_2M—R]^+$ it could be hypothesized that X^- occupies one of coordination sites in this case the contact ion pair formed is an ISIP type. In fact it would be more correct to consider the $L_2M^+R\cdots X^-$ as a Lewis acid-base adduct or zwitterion[67].For this reason one of the main critical points to clarify is if the initial contact ion pair with an anion in the first coordination sphere converts into a contact ion pair with the anion in the second coordinating sphere leaving a coordination site "free" with a successive reaction with olefin, or if a purely associative transition state has to be considered. The situation becomes more complicated when the monomer molecule approaches to ion pair. The olefin coordination that occurs with displacement of counterion X^- from $L_2M^+R\cdots X^-$ leads to formation of $[L_2MR(monomer)]X$ where the counterion stays in the second coordination sphere of the metal. In this case the $[L_2MR(monomer)]X$ complex becomes an OSIP contact ion pair. Up to now these complexes have been never observed in a catalytic system due to their thermodynamic instability, which is due to weak olefin coordination in the absence of metal-olefin back donation, and because of their reactivity leading to alkyl migration into coordinated olefin. In some cases the situation is more complicated, in low polarity solvents such as benzene or toluene the ion pairs are present in aggregate form, such as ion quadruples (species **E** in Figure 24) and even higher aggregates[68]. In fact $[L_2MRL']X$ OSIP shows a marked tendency to aggregate[69 70, 71] at concentration higher than 0.5 $mmolL^{-1}$. Maybe this is due to an increment of dipole moment, due to reduction of ion-pairing strength, which favors the formation of ion quadruples or higher aggregates.

B. Chain propagation

After the activation step the active site is typically depicted as having a coordination vacancy that attracts theπ electrons of the olefin. Coordination is followed by insertion into the polymer chain and re-establishment of a coordination vacancy for further monomer insertion. The first mechanism which tried to explain the insertion and propagation stage was proposed by Cossee[72, 73] and applied to conventional Ziegler-Natta catalysts. Cossee's mechanism, also called the mechanism of monometallic centres, has been widely accepted, even though this

model does not take into consideration the presence of an activator or products formed from it in Ziegler-Natta polymerization systems. The bimetallic mechanism proposed by Rodriguez and van Looy[74-76] on the base of Cossee's mechanism explains the role of activators. The monometallic mechanism seems to be inherently simpler than the bimetallic mechanism except for the need of migration step.

Despite the many uncertainties, it is generally accepted that the first step in chain growth is the complexation of the olefins with the transition metal (c.f. Figure 25).

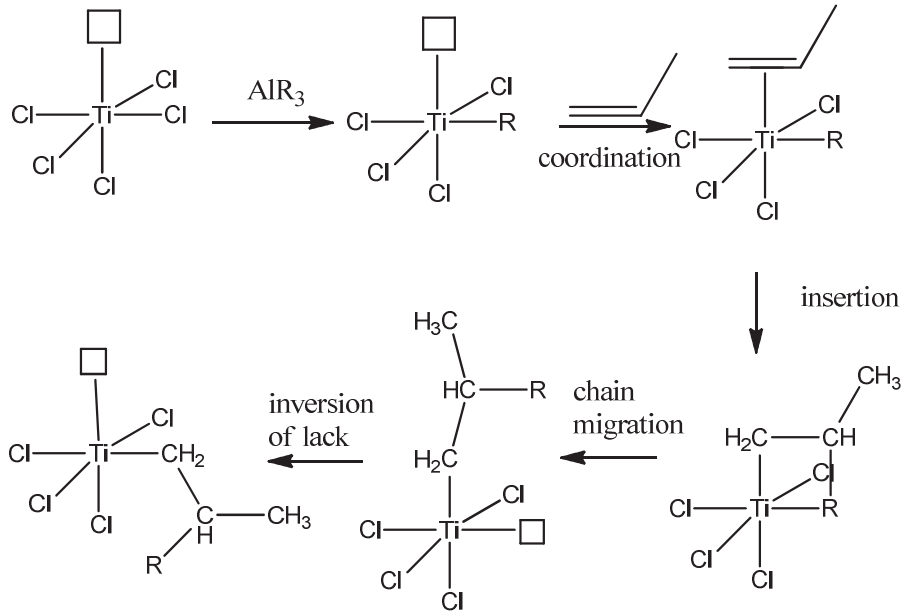

Figure 25.Cossee'smechanism for propylene insertion[72, 73]

The monomer is coordinated to the vacant orbital of the octahedral transition metal complex and then inserted into the polymer chain at transition metal-carbon bond; this results in regeneration of the vacant orbital with an orientation different from original. In the case of propylene if propagation continued with this species, the result would be syndiotactic polymerization. Isotactic polymerization requires the migration of polymer chain to its original site with regeneration of the original vacant orbital.

Farina[77]proposed a mechanism (c.f. Figure 26) for insertion and propagation in the case of metallocene which is based on Cossee's mechanism.

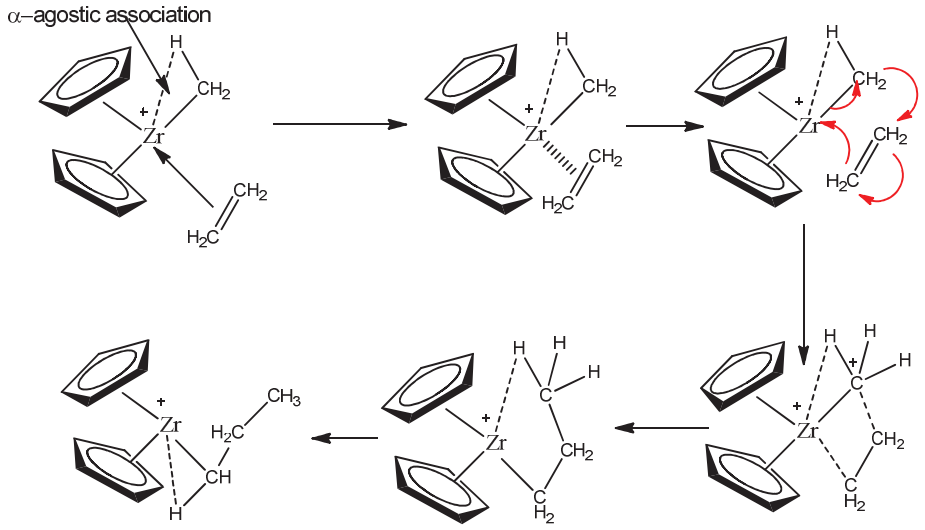

Figure 26. Farina's mechanism formetallocene catalysts[77]

In this mechanism, the positively charged metal atom Zr is stabilized because of a α-agostic association of the methyl ligand. The electrons from the carbon-hydrogen bond are shared with Zr. The monomer is inserted at the electron vacant site on Zr and the atoms then rearrange themselves to form a slightly different structure. In the end Zr shows an electron vacancy but the α-agostic association is with C-H bond of ethylene unit. Further ethylene insertion proceeds according to the same mechanism.

C. Transfer reactions

Hydrogen is a very effective chain-transfer agent in olefin polymerization reactions with Ti-based Ziegler-Natta catalysts. In fact$H_2$is introduced during the reaction for controlling the molar masses. For metallocene catalysts, H_2can be also added as transfer agent but the main transfer and termination reaction is β-H elimination assisted or not by the monomer. In the case of polymerization of propylene theβ-Me elimination is also reported. Other chain transfer reactions are those to monomer and to aluminum (AlR_3 is also a transfer agent). In the figure below all transfer mechanism are shown in details (c.f. Figure 27).

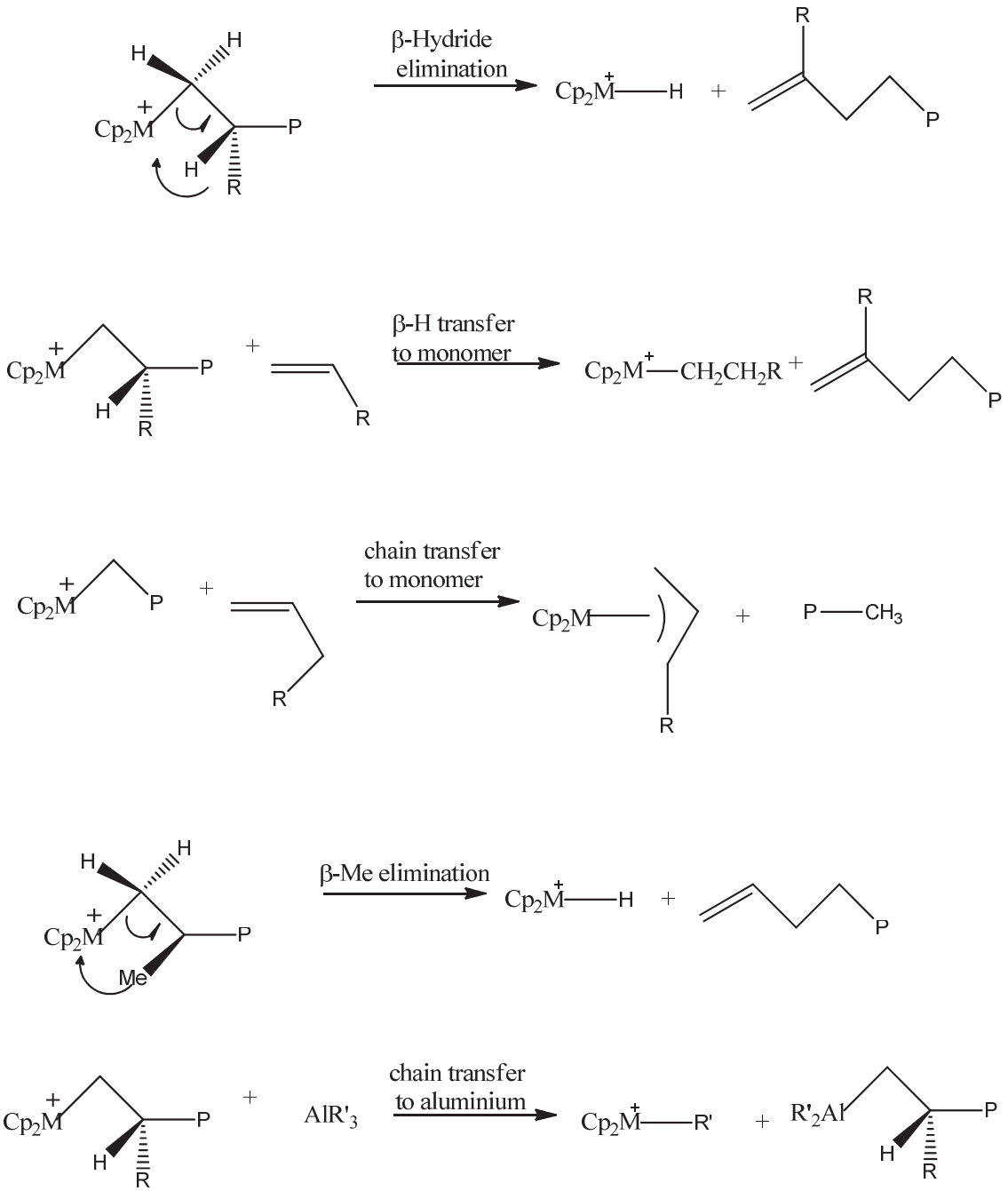

Figure 27.Scheme for chain transfer reactions

Transfer reactions are the key events in catalytic polymerization since they influence the lifetime of chain growth and consequently the molar masses. Further the chain transfer reactions also affect the measure of active site concentration since, when the transfer reaction occurs the active site is re-generated. This phenomenon could give an overestimation of measure of active centers.

3.2 More on the activation of metallocene catalysts: an overview

As discussed above, the active catalytic species is part of a complex set of equilibria where the monomer, may compete for the coordination vacancy with the solvent, other metal alkyl species or the counter-anion. In order to have a complete picture of all the equilibria involved a tentative mechanistic scheme for catalytic olefin polymerization in homogeneous phase was proposed by Bochmann[71]and shown in Figure 28.

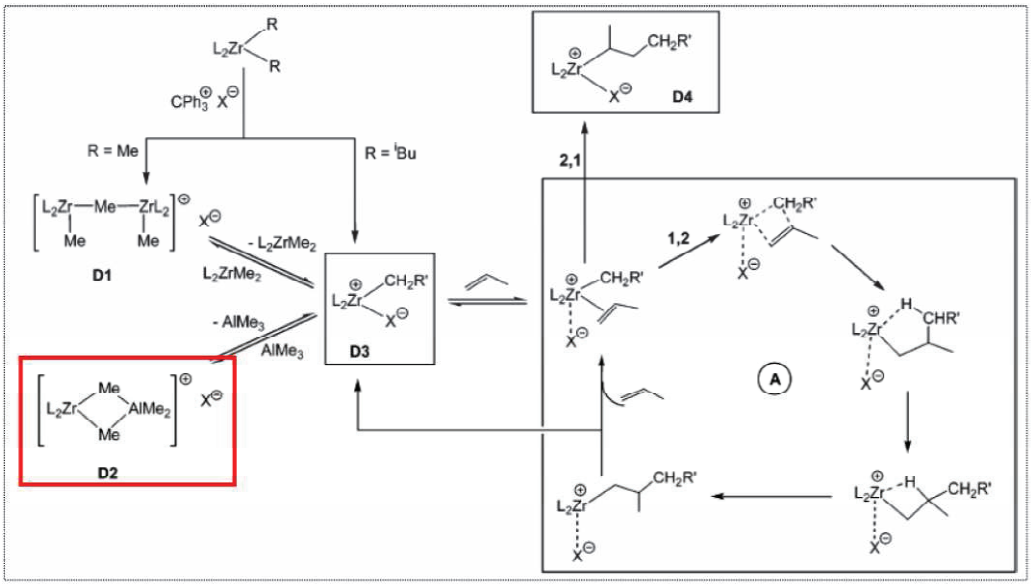

Figure 28.Bochmann'smechanistic scheme[71]

The reaction of metallocene dimethyl compound with $[CPh_3][B(C_6F_5)_3]$leads to primarily homo-binuclear complexes $[(L_2ZrMe)_2(\mu\text{-}Me)][B(C_6F_5)_3]$which in some cases are sufficiently stable to allow isolation and structural characterization[41]. Conversion of complexes $[(L_2ZrMe)_2(\mu\text{-}Me)][B(C_6F_5)_3]$ into mononuclear ion pair complexes $[L_2M^+Me\text{----}B^-(C_6F_5)_3]$ is slow.

When metallocene dimethyl compound reacts with MAO, the $AlMe_3$, which is present in commercial MAO in equilibrium with MAO, leads the formation of the heterobimetallic cations$[L_2M(\mu\text{-}Me)_2AlMe_2]^+$ which are more stable than homobimetallic complexes.

Since the contact ion pairs, complexes **D3** in Figure 28, are likely to be the dominant resting state, the both species**D1** and **D2** are the so called **dormant species**.

Further it has been proposed that the first step in the formation of a catalytically active metallocene species is the monomer association/dissociation pre-equilibrium with an electron-deficient metallocene species[78-80]. This multiplicity of states constitutes the "active species" involved in the chain growth process. On the other hand, investigations of the reaction kinetics of metallocene catalysts, to elucidate chemistry involved in Ziegler-Natta catalysts, suggested that polymerization could be explained by a series of equilibria. Fink proposed[81-84] the "intermittent" chain growth model which seems typical of most metallocene catalysts.

In conclusion as we showed above the activation step is not fully understood, and the insertion mechanism is not completely clear, in particular in so far as the insertion of first molecule is concerned. Clearly all of these events depend not only on the activator, but also on metallocene precursor. Thus we expected different types of active sites to behave differently. Also the active species is only one of complex that can be formed so it is not clear what fraction of metal atoms act as active sites. Up to now one of the major challenges in polyolefins fields was the determination of amount of active sites for all family of Ziegler-Natta catalysts, including heterogeneous systems, metallocene and post metallocene catalyst.

4. Introduction: Counts of active sites

The kinetics of Ziegler-Natta[85] and related[86] α-olefin polymerization is still a matter of debate.Indeed several theoretical and practical difficulties complicate the interpretation of the (not so) simple equation:

(1) $$R_p = \frac{-d[Mon]}{dt} = kp\frac{[M^*]}{[M]}[Mon]^{a(\approx 1)}$$

First of all, in the case of homogeneous catalyst, even if we have only one type of active site, (i.e. unique value for k_p) it is unclear how to calculate the value of [M*]/[M], the concentration of active metal for reasons we saw in first part of this chapter. This situation is further complicated in the event that the catalyst precursor is supported. It is well know that interaction between $TiCl_4$ and the commonly used support $MgCl_2$ lead to a multiplicity of

active sites. This can also happen when metallocenes are supported on silica. In either case the observable R_p is normally an apparent rate averaged on a population of active sites widely differing in reactivity[85, 86]. In addition, non integer pseudo reaction orders in the range $0<a<1$ have also been reported[85, 87].

In the rest of this manuscript we will focus to a discussion of processes where the catalyst precursors are in solution and not supported in the form of heterogeneous particles. As mentioned above the major challenge associated with the use of equation (1) in the case of solution processes is the independent identification of k_p and [M*]/[M], even under well-defined conditions. Given the importance of understanding it, it should not be surprising that a significant amount of experimental work has been done to identify these parameters. In particular, as we will show in next paragraphs, counts of active sites based in radio-tagging techniques can be heavily affected by occurrence of side reactions[88].

4.1 Methods for counting active sites

Indeed several methods have been suggested for the "counting" of active site and it is difficult to devise a unified and simple classification. We focused only on tagging methods which are based identification of a suitable tag that could be incorporated into the polymer. This can be done[88]:

a. by labelling an organometallic component and monitoring an initiating group in the polymer;
b. by labelling a growing chain based on:
    i. Determination of the number of macromolecules using M_n data;
    ii. Determination of the number of metal-polymer bonds (MPB);
    iii. Selective tagging of growing chain;

For the first case, method a) includes methods in which the chain is labelled in the initiation step; method b) includes all methods based on labelling of the chain during the growth stage. In particular the three sub-groups can be characterized conveniently using an example of idealized "living" Z/N polymerization catalysts with a single type of active site.

4.2 Methods based on labelling of Macromolecules

4.2.1 Labelling of Macromolecules by radioactive organometals

In this case the labelling of polymer chain occurs during the activation step, when the active site is generated by alkylating reaction between pre-catalyst and transition metal compounds by organometals, co-catalyst. Thus the labelled alkyl becomes an end group of growing chain. Natta was the first to use this technique[89]. He used $TiCl_3$ that was activated by a ^{14}C-labelled alkylaluminium compound, which was then used to obtain radioactive polypropylene.

(1)

Figure 29.Mechanism for labelling active site with radioactive alkylating agent

The R group, is present in the catalytic complex at start of polymerization, thus the total number of R groups found in the polymer should be the same of number of active centres. The determination of number of ethyl groups present as chain ends was a direct measure of active site concentration, which was about 1 mol per 100 moles of $TiCl_3$ in $Al(C_2H_5)_3/\alpha$-$TiCl_3$ system. Subsequent studies[90-93]showed that this method leads to an overestimation of [M*]/[M] due to the decomposition of the transition metal-alkyl group that can lead to the formation of alkene and to its incorporation into a polymer.

4.2.2 Labelling a growing chain

4.2.2.1 Determination of the number of metal-polymer bonds (MPB)

The growing chain can be labelled making use of either splitting (2) or insertion (3) reactions with a suitable quencher agent according to reactions in Figure 30:

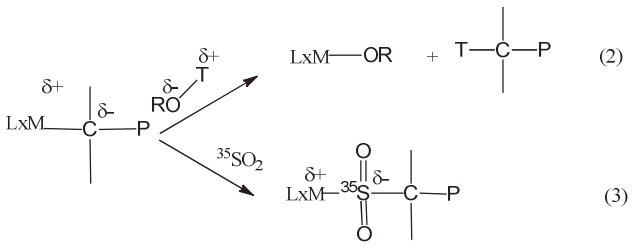

Figure 30.Mechanism for labelling growing chain

A general disadvantage of methods based on MPB-determination is linked to impossibility to quench just a part of active centres without influencing the whole catalyst system.

In next paragraphs we will give a short overview of these methods and their relative shortcomings.

<u>Determination of (MPB) with tritiated alcohols</u>

Labelling of MPB using a tritiated alcohol such as EtOT[94] or MeOT[95], prepared by reaction of MeO^-Na^+ with T_2O, where T=^{3}H= tritium, was originally developed by Feldman and Perry[96]. The kinetic procedure for calculating [M*]/[M] from the concentration of metal polymer bonds, [MPB], is done using equation (2):

$$(2)[MPB] = Cp + \frac{k_{tr}^{A}\, Y}{kp\,[Mon]}\left(\frac{K_A[A]}{1+K_A}\right)$$

Where Cp = initial concentration of MPB→ $[MPB]_0 = k\left(\frac{K_A[A]}{1+K_A}\right)$

Y = polymer yield

[A] = concentration of alkyl aluminium

K_A= adsorption constant

k^A_{tr}= transfer constant to aluminium

Indeed the most common feature, which is also one of disadvantages shown by this method, is that the quencher reacts not only with the growing chain, but also with non-propagative metal polymer bonds formed via transfer reaction to aluminium (see Figure 31):

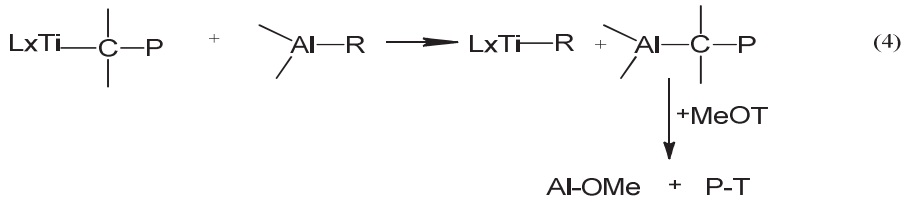

Figure 31.Insertion of MeOT in non propagative chain

Using tritiated ethanol as quencher of $MgCl_2/TiCl_4$/diether, Yaluma and co-workers [97] observed not only the Ti-bond chains, and therefore [M*]/[M], but also the rate of formation of Al-bond chain via chain transfer to $AlEt_3$. They concluded that the incidence of chain transfer to aluminium in polymerization at 50°C was in the range of 2-6 chain transfer reactions per million monomer insertions, significantly less than the rate of chain transfer to monomer. Other commonly considered transfer reactions (with monomer, solvent, hydrogen) do not result in the formation of metal polymer bond.

The kinetic isotope effect is another substantial disadvantage of methods based on stopping the polymerization by tritium labelled Brønsted acids. The Kinetic Isotope Effect (KIE) is the ratio of reaction rates of two different isotopically labeled molecules in a chemical reaction. An isotopic substitution can greatly modify the reaction rate when the isotopic replacement is in a chemical bond that is broken or formed in the rate-limiting step. In such a case, the change is termed a **primary isotope effect**. When the substitution is not involved in the bond that is breaking or forming, a smaller rate change, termed a **secondary isotope effect** is observed. In this case it is referred to MeOH and MeOT thus KIE= k_H/k_T. The variability of isotope effect even within the same catalyst system was mainly due to changes in ratios of various metal carbon bonds (active centers, non propagative metal polymer bonds, metal-alkyl bonds) when changing experimental conditions. If each species exhibited its own isotope effect, the overall effect varied. An indirect method to determine the KIE is the slow and fast

addition of the quencher. The slow addition should assure a quantitative reaction of both protiated and tritiated quencher with a metal polymer bond, the fast addition of the quencher should assure its immediate excess over metal polymer bonds and the isotope effect can develop. Furthermore the slow addition of quencher can easily change the number and/or nature of active sites. Furthermore, other species can react with the quencher and false conclusion can be drawn. A method without the risk of modification of the catalyst by a slow addition of the quencher was suggested by Chien and Kuo[98]. The method is based on varying of total amount of ROH/ROT mixture. If the amount of quencher is just equivalent to all metal carbon bonds, it should react quantitatively and the isotope effect should not develop. When higher amounts of the quencher are used, the isotope effect should be observed. Values of k_H/k_T can be calculated from ratio of MPB found at equivalent and higher-than-equivalent amounts of the quencher.

Determination of the number of metal-polymer bonds (MPB) with SO_2

Another method of determination of [M*]/[M] based on an insertion of $^{35}SO_2$ into a metal polymer bond was suggested by Zakharov[99] et al. Mejzlik et al.[100] employed non radioactive SO_2 as quencher for $TiCl_3/AlEt_2Cl$ catalyst system for propylene polymerization. One of the main conditions of using SO_2 as a quenching agent is that the polymerization stops upon addition of the amount of SO_2 equivalent to $AlEt_2Cl$ present in the catalytic system

The application of non-isotopic SO_2 as a quenching agent offers the following advantages in comparison with tritiated alcohols:

- ✓ Kinetic isotope effect would be excluded;
- ✓ A fairly simple trace sulphur analysis might be employed instead of the rather troublesome handling of tritium-labelled acids and the analysis of the labelled polymer.

Nevertheless, a high extent of side reaction of SO2 with the main polymer chain makes the application of this method very difficult for polymerization catalyzed by $TiCl_3$-based system[100].

4.2.2.2 Selective labelling of growing chain

The tagging of growing chain with carbon monoxide, CO, was developed at first by a group of authors at Novosibirsk Institute of Catalyst[101]. The CO tag inserts into propagative transition metal carbon bonds. The reactions involved are supposed to proceed as the sequence reported in Figure 32.

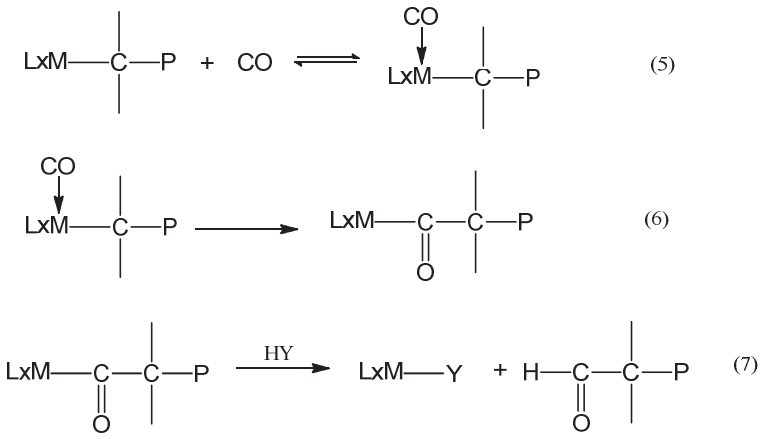

Figure 32.Proposed mechanism of CO insertion

Reaction (7) shows the addition of a strong quencher (Brønsted acid HY) to get the functionalised chain end. However this step has not been studied in depth. Carbon monoxide can be identified in the polymer in the form of carbonyl group. On the other hand, if the corresponding ^{14}C-labelling compound is used, it can be more easily detected. Furthermore the use of CO method shows several disadvantages.

First of all the insertion of CO is fast but not instantaneous so it requires a few minutes to complete. Furthermore an increase of number of tags incorporated into the chain has been detected during the prolonged contact between polymer and CO due to side reactions, such as copolymerization of CO with the olefin and chain transfer reaction to Al as shown in Figure 33**.** In a number of cases, a rather large excess of CO must be used to inhibit the polymerization.

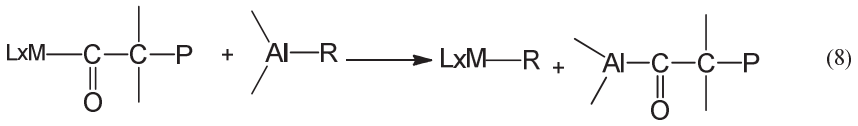

Figure 33.Proposed mechanism of CO insertion in non propagative polymer chain

It also appears that the active centres of $MgCl_2$-supported catalyst do not react with the poison in the initial stages of propylene polymerization, whereas those present in the more advanced stages of polymerization do [98, 102]. This is an example of the "non-universality" of the method.

Furthermore the CO reacts with some catalyst systems rather unexpectedly. It might lead to the generation of methane, formaldehyde, diketene or contribute to a change in a valence state of Ti changes during the treatment of $Cp_2TiCl_2/AlMe_2Cl$ with CO; in other words since CO can change drastically the catalytic species it is difficult to be sure that the number of tagging sites corresponds closely to the number of active sites and it is one of pitfalls of method.

In general there is a large gap between results reported in literature due to different interpretation of data obtained. Data published by Novosibirsk group [103, 104] were compared with those obtained by Warzelhan et al[105]using similar catalyst systems. The Novosibirsk group claimed that the correct value of[M*]/[M] and k_p are obtained at short contact times (always on a scale of several minutes) and they concluded that the increase of number of tags as due to side reactions describe above. When conditions are unfavourable for side reactions (absence of the monomer and organometal compound in the reaction mixture) the whole amount of selective stopper incorporated into polymer can be assigned to the active centres. Thus the k_p values found for $TiCl_3/AlEt_2Cl$ catalyst system by Warzhelhan et al.[105] seems to be in the range of 20 L mol^{-1} s^{-1} for isotactic PPs which are much lower than values found by Novosibirsk authors who performed short contact times. The picture is even more complicated for metallocene systems activated by MAO. Tait et al.[106]) used ^{14}CO method and reported that 100% of the zirconium atoms were active for polymerization of ethylene using the catalyst system Cp_2ZrCl_2/MAO. This is unlikely, and Chien et al.[107] reported a value of about 10% for polymerization in similar conditions. The difference may arise from different $AlMe_3$ contents of commercial MAO samples that were used.

The choice of selective tag which can label the growing chain is not limited to CO; other candidates are CO_2 and CS_2.

The CO_2 as tag is believed to be a more suitable agent for one component catalysts (e.g. $TiCl_3$) because the tag does not accumulate in the polymer[103]. Furthermore CO_2 is much more effective than CO in the ethylene polymerization catalyzed by $Zr(C_3H_5)_4/Al_2O_3$, $Zr(C_3H_5)_4/SiO_2$ and $TiBz_4/Al_2O_3$ system [108]. On the other hand CO_2 is not suitable for system containing AlR_3 because it reacts easily with Al-C bond[109]. It was observed[110-112] that CO_2 is

much less efficient than CO in propylene polymerization catalyzed by $TiCl_3/AlEt_2Cl$ system, and inert in ethylene polymerization catalysed by $Cp_2TiEtCl/AlEtCl_2$ system.

According to Vozka[113], CS_2 should react only with the centres where a growing chain and a vacancy coexist, thus giving similar results obtained with ^{14}CO method, and trace sulphur analysis can be used to monitor labelled chains. However CS_2 is not a suitable tag for a number of catalyst systems. As shown by Tait[95] for the case of the Cp_2ZrCl_2/MAO, CS_2 is not able to completely stop the polymerization but does so in the case of the $MgCl_2/TiCl_4$-$AlEt_3$ catalyst system. This might mean that either the adsorption of CS_2 is reversible and so the consumption of ethylene is reduced but not stopped by presence of poison, or that copolymerization with ethylene took place.

4.2.3 Number of macromolecules

The method for counting active sites based on **kinetic** determination of number of macromolecules was first devised by Natta[89] as valid alternative to radiochemical method. In fact, in addition to the shortcoming showed in paragraph 1.1.1, the method based on radiochemical labelling of active centres for α-$TiCl_3/Al(C_2H_5)_3$ used by Natta only applies to those centres present on $TiCl_3$ surface after treatment with triethylaluminium and repeated washing the solvent prior to polymerization. These centres do not necessarily correspond to the centres present during the steady-state polymerization. In fact, depending on the size of $TiCl_3$ crystals, the polymerization may show an initial setting period, during which there is a variation of surface area of $TiCl_3$, and consequently in the number of accessible active centres. The method based on number of macromolecules relies on relationship between the degree of polymerization, P_n, and the concentration of active sites. P_n is defined as the ratio of (moles of molecules of monomer which react at time t)/(number of polymer chain formed at time t) which can be expressed by equation (3):

(3) $$Pn = \frac{\int_0^t Rp\, dt}{M^* + \int_0^t \sum_{r=1}^{n} R_r dt}$$

Where R_p is rate of propagation of growing chain and $\sum_{r=1}^{n} R_r$ is the termination rate of growing chain**.**

If P_n increases with polymerization time (in the controlled regime) it is possible to determine k_p and [M*]/[M] (see below). The main shortcoming of this method based of number of macromolecules was the determination of P_n due to not completely availability of firsts GPC-HT devices. At the time this method was developed, the number average molecular weight,M_n, was obtained from viscosity data according to relationship $P_n = K[\eta]$. The constant K was calculated from the plot of intrinsic viscosity vs moles of $–C_2H_5$chain ends. It was found that the two methods, radiochemical and kinetic method, led to values of same order of magnitude, which were less than 1% of moles of $–C_2H_5$/moles of $TiCl_3$, meaning that not all active centres taking part in polymerization.

If chain transfer reactions are negligible, then the number of macromolecules present during the *living* regime of a polymerisation is equal to the number of active sites in the reactor. This means that we can rewrite equation (3) as follows:

(4) $$P_n = k_p\,[\mathrm{Mon}]\,t$$

If only a low fraction of chains has undergone a chain transfer reaction which corresponds to the initial controlled regime then equation (4) can be rewritten as:

$$Pn = \frac{Y}{M^* + M^* \sum_{i=1}^{n} k_{tr}\,[X]^i\,t} \Leftrightarrow \frac{1}{Pn} = \frac{M^* + M^* \sum_{i=1}^{n} k_{tr}\,[X]^i\,t}{Y} \Leftrightarrow$$

$$\Leftrightarrow \frac{1}{Pn} = \frac{M^*}{M^* k_p\,[mon]t} + \frac{M^* \sum_{i=1}^{n} k_{tr}\,[X]^i\,t}{M^* k_p\,[mon]t}$$

(5) $$\Leftrightarrow \frac{1}{Pn} = \frac{1}{k_p\,[mon]t} + \frac{\sum_{i=1}^{n} k_{tr}[X]^i\,t}{k_p\,[mon]t}$$

The equation (5) is the equation for the approach developed by Natta.

If we impose the following boundary conditions:

- R_p and R_t are time independent;
- Chain-terminating reactions are the only kind of chain transfer process;

we obtain a straight line from plot of reciprocal of average degree of polymerization ($1/P_n$) as function of reciprocal of time (1/t); the slope is $1/k_p$[Mon] and the intercept gives us the value of frequency of chain transfer.

Further, the yield of polymerization, Y, expressed in mol of monomer polymerized per mol of transition metal is given by equation (6).

(6) $$Y = \int_0^t k_p \frac{[M^*]}{[M]} [mon] dt$$

We assume that k_p and [mon] are time-independent the equation (6) becomes equation (7).

(7) $$Y = k_p [mon] \int_0^t \frac{[M^*]}{[M]} dt$$

The equation (7) can be applied if very low conversions are reached (conventionally less than 10% of conversions) otherwise the changes of monomer concentration need to be accounted for. If this condition is assessed we can calculate the [M*]/[M]value using the plot of polymer yield as function of time and introducing the k_p value obtained by equation (5) in equation (7).

The k_p value found by this method is a real kinetic value because is based on the effective number of metal sites which are effectively active and involved in polymerization. Thus the value of k_p obtained by this method is generally much higher than the k_{papp} obtained by yield using equation (1) and considering the initial amount of active metal.

Of course the key condition of being able to use this method is the ability to accurately measureM_n. It appears that [M*]/[M] obtained by this method is generally lower than value obtained with labeling methods. This difference in the kinetic parameters must be attributable to differences between the polymerization stages studied in each method. For instance the method based on number of macromolecules gives information on the active sites at the beginning of polymerization, while other methods, based on labeling of growing chain using radio tagging agents, deal with the later stage of polymerization where catalyst deactivation, various type of chain transfer reaction and fragmentation of catalyst particles occurs alongside reaction. The kinetic parameters obtained by other methods are given by superimposing the individual factors generated during the polymerization. In contrast, methods based on counting the number of macromolecules seem to be most reliable and useful for elucidating what happens on the active sites just after their formation at initial stage of polymerization.

In order to extract meaningful data using equation (5) several requirements must be satisfied.

First of all in order to obtain a reliable value of [M*]/[M] it is necessary to work in a regime where the chain transfer reactions, such as transfer to monomer or aluminum, and the chain transfer termination are negligible. This is a typical behavior of living polymerization [114, 115]. Several metallocene catalyst systems show a living behavior in specifically experimental conditions. For example Fukui et al.[116] showed that Cp_2ZrMe_2 activated by $B(C_6F_5)_3$ was capable of living polymerization of propylene at -78°C. Shiono et al.[117] demonstrated that CGC-based system activated by MAO-free TMA produce syndiotactic propylene in living fashion at 0°C. We should assume that metallocene catalyst systems show a linear increment of molecular weight distribution with time in first instants of polymerization, where we can observe the production of only the first generation of polymer chains.

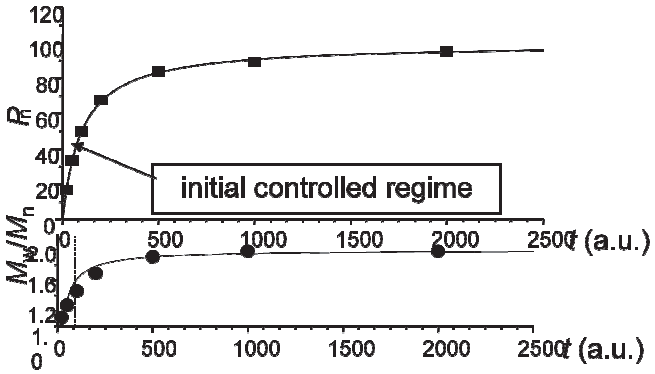

Figure 34.Montecarlo simulation of build up of MWD

As shown in Figure 34 the degree of polymerization increases with time in early stages of polymerization, and then can stabilize at plateau value. During the initial regime the increment of molar masses is linear and corresponds to polydispersity index that is less than 2, the value characteristic of Schultz-Flory regime.

It should be possible to polymerize olefins using metallocene catalytic systems in this transient controlled regime if the reactor can be run for times going from fraction of seconds to a few seconds. This means that technically demanding fast kinetic methods such as *stopped/quenched flow technique* are necessary for the study.

4.3 The stopped/quenched flow technique

The stopped-flow technique, originally developed by Chance in the early 1940s for studying fast enzyme reactions (references in [118]) and is quite useful for this purpose. This technique consists of the rapidly mixing of two or more reactive components and then instantaneously quenching of the reaction after predetermined time by changing the reaction environment (e.g. in Figure 35).

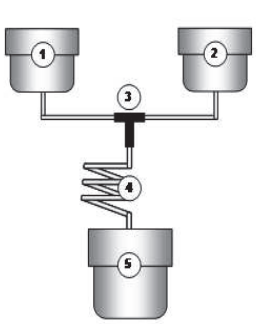

Figure 35. The polymerization occurs in a Teflon tube from point 3 to point 4 where the polymerization reaction is quenched by rapid mixing with the vessel 5 solution

This technique, associated with a specific on-line recording spectroscopic detector (e.g. UV/visible absorbance, light scattering, fluorescence, FTIR, etc.), has proven to be a powerful means for elucidating kinetic mechanisms and obtaining real-time information concerning active species, reaction intermediates and other kinetic parameters for heterogeneous catalysts[119-121]and for homogeneous catalysis[71, 122, 123]. However these studies employed devices operating in mild conditions at low temperature and pressure. It is therefore desirable to apply this method (if is possible) at higher temperatures and pressures in order to understand how changes in reactor conditions influence the kinetic parameters and in particular the [M*]/[M].

It is not common to confuse stopped flow and quenched flow reactors. In general these two techniques are similar in so far as they both require rapid mixing and very well-defined reaction times. The difference consists in the final part. In the *stopped flow* technique the resulting flow is abruptly stopped by use of suitable stopper and in general a suitable detection system completes the basic device. The quenched-flow apparatus is a variation of stopped

flow device. It offers the same steps of rapid mixing and ageing in delay line, but the reaction is chemically stopped when exposed to a quenching agent. Analyses are then performed off-line after sufficient quenched aged-mixture was collected. The *quenched-flow* method was mainly applied to reactions which cannot be monitored optically, but produced stable and quantifiable intermediates when the reaction was stopped under suitable conditions

The block diagrams of both the stopped-flow and the quenched-flow techniques showed in Figure 36illustrate these differences.

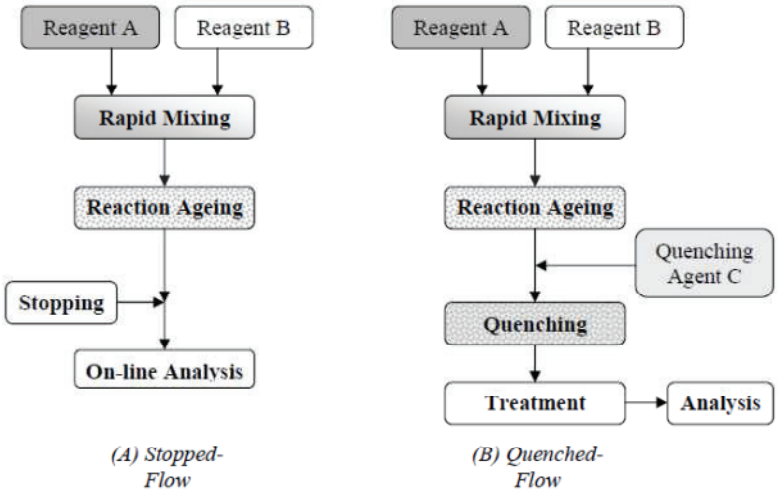

Figure 36.Diagrams of both stopped flow (A) and quenched flow (B) techniques

4.3.1 Heterogeneous polymerization using stopped flow technique

The stopped flow techniques were widely employed to investigate various kinds of polymerization reactions such as cationic polymerization[124, 125], anionic polymerization[126], and group transfer polymerization[127]. For Ziegler-Natta catalyzed olefin polymerization, the quenched flow technique was first employed by Keii and Terano in 1987[128, 129] to study the slurry polymerization of propylene and ethylene with $MgCl_2$-supported Ziegler catalyst. They were also able to satisfy the basic requirements of stopped flow method. Their device, show in Figure 37, was composed by two special glass vessel (A and B in Figure 37) equipped with water jacket.

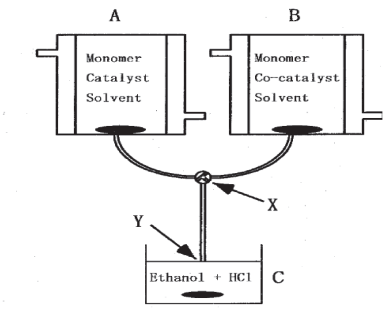

Figure 37. Schematic illustration of a stopped flow polymerization set up. A and B are special glass vessels containing catalyst and co-catalyst solution. C is flask containing a quenching agent. X is the mixing point of catalyst slurry and co-catalyst solution resulting in the formation of the active sites and initiation of the polymerization. Y is the end point at which the polymerization is terminated by contact with quenching agent. The polymerization occurs in Teflon tube from point x to Y. *Reprinted and adapted by* [117] *By permission of John Wiley & Sons Inc.*

Catalyst slurry and co-catalyst solution saturated with monomer are placed in vessels A and B respectively. C is a flask containing a solution of Alcohol/HCl. After the contents of the upstream vessels reach the desired conditions they are forced to flow simultaneously through a Teflon tube from vessels A and B into flask C under an over pressure of nitrogen; Polymerization occurs in tube form point X to Y points. The polymerization is quenched at point Y. The effectiveness of this technique allow investigating many aspects of polymerization such as the nature of active sites, the determination of kinetic parameters, the effect of hydrogen, the effect of catalyst preparation and etc. The rate constants of propagation k_p and transfer k_{tr} and the concentration of polymerization centres were determined using the following relation:

(8) $$M_n = M_0 * \frac{k_p[mon]t}{1 + k_{tr} + t}$$

Where M_0 is the molar weight of monomer. Considering that the average degree of polymerization is given by number average molar weight of polymer and molar weight of monomer ratio, $vizP_n = \frac{M_n}{M_0}$, the equation (8) could be turned in equation (5) proposed by Natta. From tangent and intercept of a plot of 1/Pn vs 1/t Mori et al. obtained a value of k_p= 1230 $L{\cdot}mol^{-1}{\cdot}s^{-1}$anc C* 6.4% for polypropylene polymerization in slurry phase with heptane at 20°C[120].

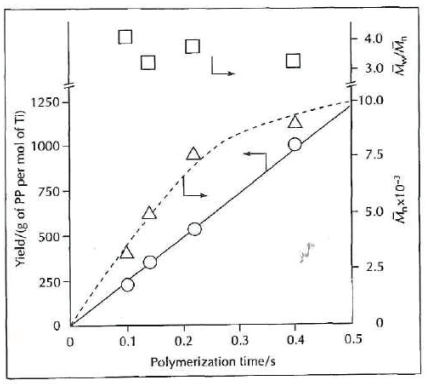

Figure 38. Dependence on polymerization time of polymer yield (O), number average molar weight ($M_n\Delta$) and molecular weight distribution ($M_w/M_n\square$) of polypropylene obtained with $MgCl_2$-supported Z-N catalyst in presence of $Al(C_2H_5)_3$ at 20°C; 0.002 bar. *Reprinted and adapted by*[120] *by permission of John Wiley & Sons Inc.*

As shown in Figure 38 the MWD expressed by PDI value (3.2-4) is rather broad. The authors observed that polypropylenes obtained at times of 0.2s had a similar value of MWD as polypropylenes obtained after 10 s when the chain transfer is considered to start in competition with propagation reaction. The same authors also studied[119] the effect of co-catalyst and the hydrogen always on the polymerization of propylene and concluded that increasing the concentration of TEA led an increment of active sites but the sites were still the same in terms of kinetics. The effect of treatment of the co-catalyst precursor with TEA on the rate profile and particle morphology (e;g; in Figure 39) was also studied by Di Martino et al.[130,131] who used a high pressure quenched flow reactor at temperatures up to 90°C and pressure up 20 bar similar to that proposed by Mori[121].

Di Martino et al. polymerized ethylene with $MgCl_2$-supported Z-N catalysts and found that the number average molecular weight reaches a plateau value quite suddenly whereas the weight average molecular weight value increases with reaction time. This means that at very short reaction times many small chains are produced, while longer chains are produced afterwards. The authors concluded that this was an indication that the active sites evolved with reaction time.

4.3.2 Homogeneous polymerization using stopped flow technique

The idea that metallocenes are single site catalysts has led to the wide-spread belief that all metal centres are active and that all these sites are active at the same time. Thus, up to now, we found only a few studies on metallocene kinetics and in general the constants of rate propagation found are apparent values or educated guess. Nevertheless the few investigations effectuated on kinetic of metallocene catalysts have allowed elucidating important phenomena.

In fact, in the 70's and 80's, investigation of the reaction kinetics of metallocene catalysts was used extensively to elucidate elementary mechanistic step in Z/N polymerizations. Fink and co-workers[81-84]pioneered this practice and used quenched flow and ^{13}C NMR labelling techniques to study ethylene oligomerization catalyzed by Cp_2TiRCl/AlR_2Cl (R= Me, Et), which is a relative slow catalyst system to determine of the relative rate of first, second and subsequent ethylene insertions into the Ti-Me bond. The authors were able to show that the slowest insertion step is the first one.

Another investigation of Cp_2TiCl_2using stopped/quenched flow technique was made by Shiono and coworkers[132] who studied the activation of this metallocene-based precursor using MAO for ethylene polymerization. Using a basic model of the stopped flow device[128] they performed a series of 4 runs at 20°C under atmospheric pressure. The interest of this work consists in the detection of induction period at very short reaction time, (30 ms realized with a 5 cm tubular reactor.) that can be seen in Figure 39 (plot (a)).They observed a non-linear increases of both M_n and polymer yield at very short reaction times. At longer reaction times they observed that M_n and polymer yield increased linearly with time as shown in Figure 39 (plot (b)).

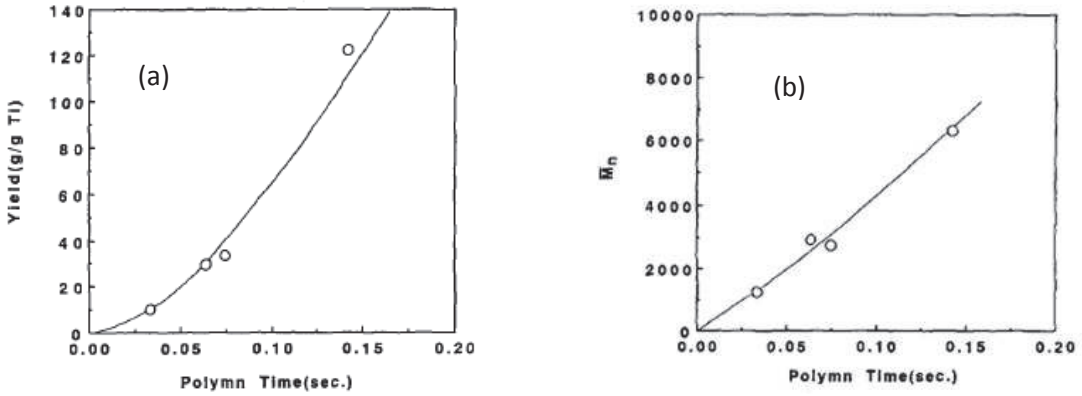

Figure 39.Plot of polymer yield vs time (a) and M_n vs time (b) of series of tests realised by Shiono et al. ; in plot (a) the induction period is more evident due to poor linearity of polymer yield at very short reaction time. *Reprinted from Polymer, 35, T.Shiono,M. Ohgizawa,K. Soga, 187, Copyright (1994), with permission from Elsevier*

They supposed that polymerization during the induction period should be treated as a slowly initiated system without any chain transfer and termination reaction using a modified equation rather than the basic version of Natta. For calculating the right value of main kinetic parameters they inserted a term relative to induction period in equations (5) and (7):

(9) $$Y = \langle f_p \rangle C_{st}^{*} \left\{ t + \frac{1}{\langle f_i \rangle} [\exp(\langle f_i \rangle t - 1] \right\}$$

(10) $$\frac{1}{Pn} = \frac{\langle f_t \rangle}{\langle f_p \rangle} + \frac{1 - \exp(\langle f_i \rangle t - 1}{t + \frac{1}{\langle f_i \rangle}[\exp(\langle f_i \rangle t - 1] \langle f_p \rangle}$$

Where $\langle f_p \rangle = \langle k_p \rangle [mon]^a$; is the average turnover frequency of monomer insertion; $\langle f_t \rangle = \sum_{i=1}^{n} \langle k_{tr\,i} \rangle [X]^i$ is the average turnover frequency of chain transfer: $\langle f_i \rangle$ is the average frequency of an initiation process for induction period; C_{st}^{*} is the stationary value of C* reached once the induction period is over. Using this equation they found a value of $14 s^{-1}$ for *fi* and a value of 19000 $L \cdot mol^{-1} \cdot s^{-1}$ for k_p, which was on the same order of magnitude of k_p found ($5 \times 10^4 L \cdot mol^{-1} \cdot s^{-1}$) for $MgCl_2$-supported $TiCl_4$ catalyst system[133134].

Busico et al.[122]adopted the quenched flow method for the study of the homogeneous catalyst system rac-Me_2Si(2-Methyl-4-phenyl-1-indenyl)$_2ZrCl_2$/MAO for ethylene and propylene polymerization. They used a basic stopped flow device composed of two vessels, one of which contained a catalyst solution and MAO in toluene under N_2 and the other a solution of MAO in toluene saturated with monomer at same temperature. The two solutions are driven to

flow along PTFE tubes. This device allowed authors to do polymerization at different temperatures and lower monomer concentrations that corresponded to ethylene pressures of about 0.5bar over atmospheric pressure. The reactions were quenched with a solution of methanol/HCl. They found different results for ethylene and propylene:

-*Polyethylene*: the value of [M*]/[M] found was relatively low 5-25% of initial concentration of Zr is active in polymerization. This showed that, like for conventional Ziegler-Natta catalysts the transition metal not all of sites are active. Another important result was that the R_p measured under stopped flow was at least 10^2 orders of magnitude higher than result obtained in conventional experiments [135] and the predominant chain transfer process showed by ^{1}HNMR analysis transfer to $AlMe_3$. No induction period was detected at 3 temperatures investigated (20, 40, 60°C).

-*Polypropylene*: for this monomer the only one series of test, conducted at 40°C and a pressure slightly higher than 0,5bar, showed an induction period, in spite of the long pre-contact period between catalyst and co-catalyst. Applying the modified equation proposed by Shiono et al.[132]they found the value of$\langle k_p \rangle$, which in this case is an apparent kinetic constant of chain propagation for propylene since is actually an average on all possible monomer insertion modes. In fact the $\langle k_p \rangle = \frac{\langle k_{pp} \rangle}{2}$ where $\langle k_{pp} \rangle$ is the constant of 1,2 primary enchainment of monomer. Further they found that the $\langle k_{pp} \rangle$ value was 10^2 lower than $\langle k_p \rangle$found for ethylene meaning that there is a difference in reactivity of two monomers. In addition they observed a lower chain transfer for propylene than ethylene.

The induction period, was also observed by Landis et al.[136, 137] during the polymerization of 1-hexene using stopped flow polymerization. They developed a similar polymerization mechanism leading to the rate law of equation (11).

$$-\frac{d[mon]}{dt} = k_p[mon]\,[C_0]\,(1 - exp(k_i[mon]_0 t)) \quad (11)$$

This equation is different from the basic law rate equation for a pre-exponential factor; but in general the difference is small being due to only the amount of monomer consumed in the initiation step.

Another interesting work using quenched flow device for homogeneous catalyst system was reported by Bochmann andSong[71]. Using a more sophisticated reactor system they performed

reactions varying the monomer concentrations. Propylene concentration, in fact, was varied by diluting a toluene solution saturated with propylene under 1 bar at 25°C with additional toluene to obtain monomer concentrations from 0.15-0.59 mol·L^{-1}. With this apparatus they were able to investigate the kinetic behavior of (SBI)$ZrMe_2$/Al*i*Bu_3/[Ph_3C][CN{$B(C_6F_5)_3$}$_2$] (1:100:1) (where SBI = rac-$Me_2Si(Ind)_2$) at different monomer and catalyst concentration continuously, but also at low monomer pressure and small experimental volume.

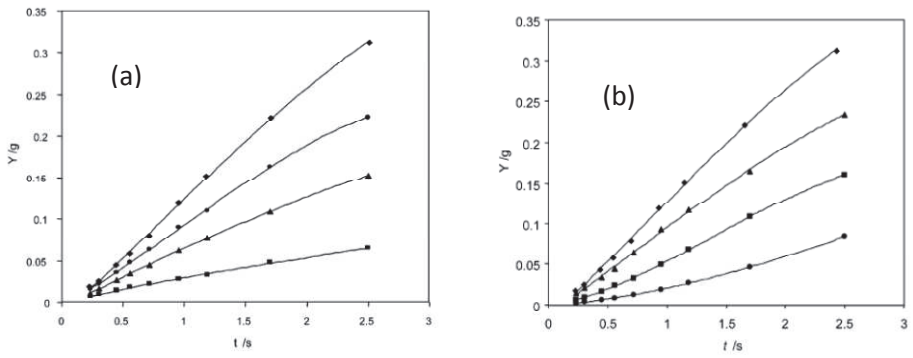

Figure 40.Time dependence of polymer yield for different initial monomer concentration at [Zr]= 9.52x10^{-5}mol·L^{-1} (a) and for different catalyst concentration at [mon]= 0.59 mol·L^{-1}(b). *Reprinted with permission from [71]. Copyright 2003 American Chemical Society."*

They reported the evolution of polymer yield, Y, as function of time at constant monomer concentration [mon]= 0.59 mol L^{-1}(plot (b) in Figure 40)and at constant catalyst concentration [Zr]= 9.52x10^{-5}mol L^{-1} (plot (a) in Figure 40). In both cases they noted a non-linear dependence of yield during reaction times, particularly at long reaction times over 1.5s, where the negative curvature corresponds to a decreasing monomer concentration, while positive curvature, in the initial stage of polymerization suggests the presence of an induction period. They supposed that the anion remains within the ion pair solvent cage and that the induction period detected was strictly due to the displacement of counterion X^-. They supposed that when the catalyst precursor SBI$ZrMe_2$reactswith AliBu_3/[Ph_3C][CN{$B(C_6F_5)_3$}$_2$]co-catalyst system gives a zirconocenes isobutyl species (species **I** in Figure 41). The species **I**, according to displacement of counterion X^- either could give a solvent-stabilized ion pair (species **IIa** in Figure 41) which reacts rapidly with monomer or a tighter ion pair (species **IIb** in Figure 41) which however could give propagation.

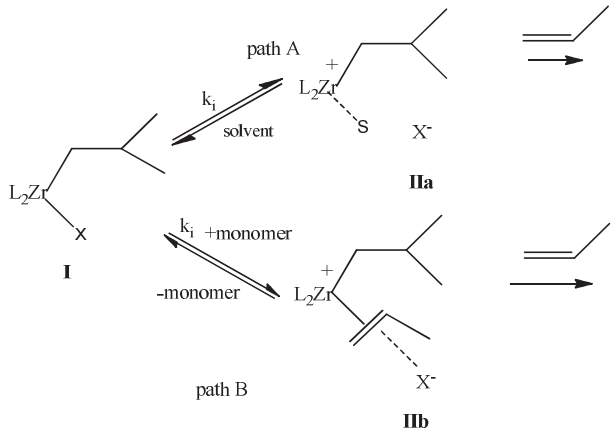

Figure 39: Possible formation and structure of active states as result of changes in anion coordination

Considering the non-living behavior as indicated by not-exactly straight lines reported in plot (b) of Figure 40, they calculated the value of k_p fitting to Natta's equation only for M_n data which are predominantly within range 50-90% of limiting value. Then, from polymer yield, considering the total concentration of metal site which correspond to the initial analytical concentration of Zr used for the polymerization, they obtained a value of k_p which should be considered an *apparent* value, k_{papp}. The k_{papp} found was generally lower than one order of magnitude of k_p from M_n. Naturally, if the Natta's equation should not applied to whole data set, the [M*]/[M] should be calculate from k_{papp}/k_p ratio. In case of $SBIZrCl_2$ activated both tritylborate and MAO the [M*]/[M] found was 8%.

5. Conclusion and introduction of experimental work

As shown through this literature review the count of active sites for molecular catalysts used for olefin polymerization is one of the big issues of this field. Understanding how a catalyst is activated, and how it evolves allows us to improve its effectiveness, but this is not always possible due to the difficultyof precisely knowing the number of active sites. The radio-tagging methods are not reliable methods due to several shortcomings detailed above. The method based on kinetic investigation such as the method of counting macromolecules could be a universal method because they are based on the effective measure of chain produced by metal site. Originally,one of most important shortcoming of this technique was the

unavailability of M_n. Nowadays the improvement of GPC-HT devices has allowedobtainingreliable values for molar masses of polyolefins.

The techniques used for measuring active site concentration applying number of macromolecules methods are in general the Stopped or Quenched Flow; and as shown here these techniques have been used for both homogeneous and heterogeneous olefin polymerization catalysts. Many parameters that influence the formation of active sites have been investigated such as the reaction temperature or the co-catalyst concentration or monomer. For instance the number of active sites of FESBI$ZrCl_2$/MAO for the ethylene polymerization increaseswith temperature, but an induction period has been observed for propylene polymerization. At different monomer concentrations, the induction period was also observed for another bis-indenyl based catalyst, (SBI)$ZrCl_2$, when activated byboth MAO and trityl borate systems..

However an important parameter which influences the formation of active site is also the monomer concentration. Measurements of polymer yield Y versus reaction time t for propyleneconcentrations ([mon]=0.15-0.59 $mol*L^{-1}$) and zirconocene concentrations in the range ([Zr]=2.38-9.52x$10^{-5}$$mol*L^{-1}$) for the (SBI)$ZrMe_2$/Al*i*$Bu_3$/[$Ph_3C$][$CN\{B(C_6F_5)_3\}_2$] system showed first-order dependence on [mon] and [Zr]. Furthermore these tests have been performed in continuously, far from industrial conditions, on small volume of toluene and same temperature (T = 25°C) on a time scale from 0.230s to 5 min, which is too high for a stopped flow reaction time. Another method for the investigation of monomer concentrations is the use of high pressure-type stopped flow reactor, which allows varying the monomer concentration varying directly the monomer pressure. Up to now the high pressure stopped flow has been used for morphogenesis or copolymerization studies and not for kinetic investigations which are prerogative of basic atmospheric pressure device.

The topic of this thesis was the investigation of the influence of monomer concentration on the formation of active sites and its concentration using polymerization tests obtained in quenched flow device in line with conventional tests.

References

1. Clark, A.; ; Hogan, J. P.; Banks, R. L.; Lanning, W. C. *Industrial and Engineering Chemistry* **1956,** 48, 1152-5.
2. Wilkinson, G.; Birmingham, I. *JACS* **1954,** 76, 4281.
3. Breslow, B. S.; Newburg, N. R. *JACS* **1957**79, 5072.
4. Natta, G.; Pino, P.; Corradini, P.; Danusso, F.; Mantica, E.; Mazzantini, G.; Moraglio, G. *JACS* **1955,** 77, 1708.
5. Jordan, R. F.; Bajgur, C. S.; Willett, R.; Scott, B. *Journal of the American Chemical Society* **1986,** 108, (23), 7410-7411.
6. Jordan, R. F.; Dasher, W. E.; Echols, S. F. *Journal of the American Chemical Society* **1986,** 108, (7), 1718-1719.
7. Jordan, R. F.; LaPointe, R. E.; Bajgur, C. S.; Echols, S. F.; Willett, R. *Journal of the American Chemical Society* **1987,** 109, (13), 4111-4113.
8. Bochmann, M.; Jaggar, A. J. *Journal of Organometallic Chemistry* **1992,** 424, (2), C5-C7.
9. Bochmann, M.; Lancaster, S. J. *Journal of Organometallic Chemistry* **1992,** 434, (1), C1-C5.
10. Hlatky, G. G.; Turner, H. W.; Eckman, R. R. *Journal of the American Chemical Society* **1989,** 111, (7), 2728-2729.
11. Henrici-Olivè, G.; Olivè, S. *Journal of Organometallic Chemistry* **1969,** 16, (2), 339-341.
12. Long, W. P.; Breslow, D. S. *Journal of the American Chemical Society* **1960,** 82, (8), 1953-1957.
13. Dyachkovskii, F. S.; Shilova, A. K.; Shilov, A. E. *Journal of Polymer Science Part C: Polymer Symposia* **1967,** 16, (4), 2333-2339.
14. Eisch, J. J.; Piotrowski, A. M.; Brownstein, S. K.; Gabe, E. J.; Lee, F. L. *Journal of the American Chemical Society* **1985,** 107, (24), 7219-7221.
15. Reichert, K. H.; Meyer, K. R. *Die Makromolekulare Chemie* **1973,** 169, (1), 163-176.
16. Long, G. S.; Breslow, B. S. *Justus Liebigs Annalen der Chemie* **1975,** 3, 463.
17. Sinn, H.; Kaminsky, W. 1976.
18. Kaminsky, W. *Advances in Catalysis* **2001,** 46, 89-159.
19. Howie, M. S. *Metcon'93 Proceedings, Catalyst Consulting, Inc., Spring House, PA USA* **1993**.
20. Winter, H.; Schnuchel, W.; Sinn, H. *Macromolecular Symposia* **1995,** 97, (1), 119-125.
21. Geerts, R. L.; Hill, T. G.; Co., P. P. 1995.
22. Welborn, H. C. 1990.
23. Smith, G. M.; Palmaka, J. S.; Malpass, D. B. 1998.
24. Zakharov, I. I.; Zakharov, V. A.; Potapov, A. G.; Zhidomirov, G. M. *Macromolecular Theory and Simulations* **1999,** 8, (3), 272-278.
25. Mason, M. R.; Smith, J. M.; Bott, S. G.; Barron, A. R. *Journal of the American Chemical Society* **1993,** 115, (12), 4971-4984.
26. Sinn, H. *Macromolecular Symposia* **1995,** 97, (1), 27-52.
27. Sinn, H.; Kaminsky, W.; Vollmer, H.-J.; Woldt, R. *Angewandte Chemie International Edition in English* **1980,** 19, (5), 390-392.
28. Kaminsky, W.; Schlobohm, M. *Makromolekulare Chemie. Macromolecular Symposia* **1986,** 4, (1), 103-118.
29. Kaminsky, W.; Steiger, R. *Polyhedron* **1988,** 7, (22-23), 2375-2381.
30. Ribeiro, M. R.; Deffieux, A.; Portela, M. F. *Industrial & Engineering Chemistry Research* **1997,** 36, (4), 1224-1237.
31. Zambelli, A.; Longo, P.; Grassi, A. *Macromolecules* **1989,** 22, (5), 2186-2189.
32. Bochmann, M.; Wilson, L. M.; Hursthouse, M. B.; Short, R. L. *Organometallics* **1987,** 6, (12), 2556-2563.

33. Lin, Z.; Marechal, L.; Francois, J.; Sabat, M.; Marks, T. J. *Journal of the American Chemical Society* **1987,** 109, (13), 4127-4129.
34. Chen, E. Y.-X.; Marks, T. J. *Chemical Reviews* **2000,** 100, (4), 1391-1434.
35. Yang, X.; Stern, C. L.; Marks, T. J. *Journal of the American Chemical Society* **1991,** 113, (9), 3623-3625.
36. Yang, X.; Stern, C. L.; Marks, T. J. *Journal of the American Chemical Society* **1994,** 116, (22), 10015-10031.
37. Chien, J. C. W.; Tsai, W. M.; Rausch, M. D. *Journal of the American Chemical Society* **1991,** 113, (22), 8570-8571.
38. Yang, X.; Stern, C.; Marks, T. J. *Organometallics* **1991,** 10, (4), 840-842.
39. Wilson, P. A.; Hannant, M. H.; Wright, J. A.; Cannon, R. D.; Bochmann, M. *Macromolecular Symposia* **2006,** 236, (1), 100-110.
40. Li, L.; Marks, T. J. *Organometallics* **1998,** 17, (18), 3996-4003.
41. Chen, Y.-X.; Stern, C. L.; Yang, S.; Marks, T. J. *Journal of the American Chemical Society* **1996,** 118, (49), 12451-12452.
42. Sinn, H.; Kaminsky, W. *Justus Liebigs Annalen der Chemie* **1975,** 3, 424.
43. Beck, S.; Brintzinger, H. H. *Inorganica Chimica Acta* **1998,** 270, (1-2), 376-381.
44. Götz, C.; Luft, G.; Rau, A.; Schmitz, S. *Chemical Engineering & Technology* **1998,** 21, (12), 954-958.
45. Cam, D.; Giannini, U. *Die Makromolekulare Chemie* **1992,** 193, (5), 1049-1055.
46. Tritto, I.; Sacchi, M. C.; Li, S. *Macromolecular Rapid Communications* **1994,** 15, (3), 217-223.
47. Pédeutour, J.-N.; Coevoet, D.; Cramail, H.; Deffieux, A. *Macromolecular Chemistry and Physics* **1999,** 200, (5), 1215-1221.
48. Coevoet, D.; Cramail, H.; Deffieux, A. *Macromolecular Chemistry and Physics* **1998,** 199, (7), 1451-1457.
49. Coevoet, D.; Cramail, H.; Deffieux, A. *Macromolecular Chemistry and Physics* **1998,** 199, (7), 1459-1464.
50. Pédeutour, J.-N. l.; Cramail, H.; Deffieux, A. *Journal of Molecular Catalysis A: Chemical* **2001,** 176, (1-2), 87-94.
51. Pédeutour, J.-N. l.; Cramail, H.; Deffieux, A. *Journal of Molecular Catalysis A: Chemical* **2001,** 174, (1-2), 81-87.
52. Kim, K.-C.; Reed, C. A.; Long, G. S.; Sen, A. *Journal of the American Chemical Society* **2002,** 124, (26), 7662-7663.
53. Bochmann, M. *Organometallics* **2010,** 29.
54. Resconi, L.; Bossi, S.; Abis, L. *Macromolecules* **1990,** 23, (20), 4489-4491.
55. Tritto, I.; Donetti, R.; Sacchi, M. C.; Locatelli, P.; Zannoni, G. *Macromolecules* **1997,** 30, (5), 1247-1252.
56. Tritto, I.; Li, S.; Sacchi, M. C.; Zannoni, G. *Macromolecules* **1993,** 26, (26), 7111-7115.
57. Tritto, I.; Li, S. X.; Sacchi, M. C.; Locatelli, P.; Zannoni, G. *Macromolecules* **1995,** 28, (15), 5358-5362.
58. Bochmann, M.; Lancaster, S. J. *Angewandte Chemie* **1994,** 106, (15-16), 1715-1718.
59. Bochmann; Sarsfield, M. J. *Organometallics* **1998,** 17, (26), 5908-5912.
60. Chien, J. C. W.; Xu, B. *Die Makromolekulare Chemie, Rapid Communications* **1993,** 14, (2), 109-114.
61. Götz, C.; Rau, A.; Luft, G. *Journal of Molecular Catalysis A: Chemical* **2002,** 184, (1-2), 95-110.
62. Bryliakov, K. P.; Talsi, E. P.; Semikolenova, N. V.; Zakharov, V. A.; Brand, J. r.; Alonso-Moreno, C.; Bochmann, M. *Journal of Organometallic Chemistry* **2007,** 692, (4), 859-868.
63. Götz, C.; Luft, G.; Rau, A.; Schmitz, S. *Chemie Ingenieur Technik* **1998,** 70, (11), 1424-1427.
64. Fusco, R.; Longo, L.; Proto, A.; Masi, F.; Garbassi, F. *Macromolecular Rapid Communications* **1998,** 19, (5), 257-262.

65. Rappé, A. K.; Skiff, W. M.; Casewit, C. J. *Chemical Reviews* **2000,** 100, (4), 1435-1456.
66. Macchioni, A. *Chemical Reviews* **2005,** 105, (6), 2039-2074.
67. Braga, D.; Grepioni, F.; Tedesco, E.; Calhorda, M. J. *Zeitschrift für anorganische und allgemeine Chemie* **2000,** 626, (2), 462-470.
68. Beck, S.; Lieber, S.; Schaper, F.; Geyer, A.; Brintzinger, H.-H. *Journal of the American Chemical Society* **2001,** 123, (7), 1483-1489.
69. Zuccaccia, C.; Stahl, N. G.; Macchioni, A.; Chen, M.-C.; Roberts, J. A.; Marks, T. J. *Journal of the American Chemical Society* **2004,** 126, (5), 1448-1464.
70. Babushkin, D. E.; Brintzinger, H.-H. *Journal of the American Chemical Society* **2002,** 124, (43), 12869-12873.
71. Song, F.; Cannon, R. D.; Bochmann, M. *Journal of the American Chemical Society* **2003,** 125, (25), 7641-7653.
72. Arlman, E. J.; Cossee, P. *Journal of Catalysis* **1964,** 3, (1), 99-104.
73. Cossee, P. *Journal of Catalysis* **1964,** 3, (1), 80-88.
74. Rodriguez, L. A. M.; van Looy, H. M. *Journal of Polymer Science Part A-1: Polymer Chemistry* **1966,** 4, (8), 1951-1969.
75. Rodriguez, L. A. M.; van Looy, H. M.; Gabant, J. A. *Journal of Polymer Science Part A-1: Polymer Chemistry* **1966,** 4, (8), 1917-1926.
76. Rodriguez, L. A. M.; van Looy, H. M.; Gabant, J. A. *Journal of Polymer Science Part A-1: Polymer Chemistry* **1966,** 4, (8), 1905-1916.
77. Farina, M.; Di Silvestro, G.; Terragni, A. *Macromolecular Chemistry and Physics* **1995,** 196, (1), 353-367.
78. Casey, C. P.; Carpenetti, D. W., II; ; Sakurai, H. *JACS* **1999,** 121, 9483.
79. Wu, Z.; Jordan, R. F.; Petersen, J. L. *Journal of the American Chemical Society* **1995,** 117, (21), 5867-5868.
80. Casey, C. P.; Hallenbeck, S. L.; Pollock, D. W.; Landis, C. R. J. *JACS* **1995,** 117, 9770.
81. Fink, G.; Rottler, R.; Schnell, D.; Zoller, W. *Journal of Applied Polymer Science* **1976,** 20, (10), 2779-2790.
82. Fink, G.; Schnell, D. *Die Angewandte Makromolekulare Chemie* **1982,** 105, (1), 31-38.
83. Fink, G.; Zoller, W. *Die Makromolekulare Chemie* **1981,** 182, (11), 3265-3278.
84. Fink, G.; Fenzl, W.; Mynott, R. *Zeitschrift fuer Naturforschung* **1985,** (2), 158.
85. Kissin, Y. V. *Springer-Verlag, New York, chapter 1* **1985**.
86. Brintzinger, H. H.; Fischer, D.; Mülhaupt, R.; Rieger, B.; Waymouth, R. M. *Angewandte Chemie International Edition in English* **1995,** 34, (11), 1143-1170.
87. Martin, Y. *Journal of Catalysis* **1991,** 129, (2), 383-401.
88. Mejzlik, J.; Lesna, M.; Kratochvila, J. *presented in part at 7th Intern. Symp. on Cationic Polym. and Related Processes, Jena, GDR,* **1985**.
89. Natta, G. *Journal of Polymer Science* **1959,** 34, 21-48.
90. Atarashi, Y. *Journal of Polymer Science Part A-1: Polymer Chemistry* **1970,** 8, (11), 3359-3366.
91. Ayrey, G.; Mazza, R. J. *Die Makromolekulare Chemie* **1975,** 176, (11), 3353-3370.
92. Burfield, D. R. *Journal of Polymer Science: Polymer Chemistry Edition* **1978,** 16, (12), 3301-3305.
93. Ketley, A. D.; Moyer, J. D. *Journal of Polymer Science Part A: General Papers* **1963,** 1, (7), 2467-2476.
94. Yaluma, A. K.; Chadwick, J. C.; Tait, P. J. T. *Macromolecular Symposia* **2007,** 260, (1), 15-20.
95. Marques, M. M.; Tait, P. J. T.; Mejzlík, J.; Dias, A. R. *Journal of Polymer Science Part A: Polymer Chemistry* **1998,** 36, (4), 573-585.
96. Feldman, C. F.; Perry, E. *Journal of Polymer Science* **1960,** 46, (147), 217-231.
97. Yaluma, A. K.; Tait, P. J. T.; Chadwick, J. C. *Journal of Polymer Science Part A: Polymer Chemistry* **2006,** 44, (5), 1635-1647.

98. Chien, J. C. W.; Kuo, C.-I. *Journal of Polymer Science: Polymer Chemistry Edition* **1985,** 23, (3), 761-786.
99. Zakharov, V. A.; Bukatov, G. D.; Dudchenko, V. K.; Ermakov, Y. I. *Kinetika i Kataliz* **1975,** 16, (2), 417-24.
100. Mejzlík, J.; Lesná, M.; Majer, J. *Die Makromolekulare Chemie* **1983,** 184, (10), 1975-1985.
101. Zakharov, V. A.; Bukatov, G. D.; Ermakov, Y. I. *Kinetika i Kataliz* **1971,** 12, (1), 263.
102. Chien, J. C. W.; Kuo, C.-I. *Journal of Polymer Science: Polymer Chemistry Edition* **1985,** 23, (3), 731-760.
103. Bukatov, G. D.; Zakharov, V. A.; Yermakov, Y. I. *Die Makromolekulare Chemie* **1978,** 179, (8), 2097-2101.
104. Zakharov, V. A.; Bukatov, G. D.; Chumaevskii, N. B.; Ermakov, Y. I. *Reaction Kinetics and Catalysis Letters* **1974,** 1, (2), 247-52.
105. Warzelhan, V.; Burger, T. F.; Stein, D. J. *Die Makromolekulare Chemie* **1982,** 183, (2), 489-504.
106. Tait, P. J. T.; Booth, B. L.; Jejelowo, M. O. *Die Makromolekulare Chemie, Rapid Communications* **1988,** 9, (6), 393-398.
107. Chien, J. C. W.; Wang, B.-P. *Journal of Polymer Science Part A: Polymer Chemistry* **1989,** 27, (5), 1539-1557.
108. Zakharov, V. A.; Bukatov, G. D.; Dudchenko, V. K.; Minkov, A. I.; Yermakov, Y. I. *Die Makromolekulare Chemie* **1974,** 175, (10), 3035-3040.
109. Ziegler, K.; Krupp, F.; Weyer, K.; Larbig, W. *Justus Liebigs Annalen der Chemie* **1960,** 629, (1), 251-256.
110. Lesnà, M.; Mejzlík, J. *Reaction Kinetics and Catalysis Letters* **1978,** 9, (1), 99-103.
111. Lesnà, M.; Mejzlík, J. *Collection of Czechoslovak Chemical Communications* **1980,** 45, (5), 1346-50.
112. Mejzlík, J.; Lesná, M. *Die Makromolekulare Chemie* **1977,** 178, (1), 261-266.
113. Vozka, P.; Mejzlík, J. *Die Makromolekulare Chemie* **1990,** 191, (7), 1519-1528.
114. Coates, G. W.; Hustad, P. D.; Reinartz, S. *Angewandte Chemie International Edition* **2002,** 41, (13), 2236-2257.
115. Matyjaszewsky, K.; Müllerb, A. H. E. NAMING OF CONTROLLED, LIVING AND "LIVING" POLYMERIZATIONS. http://www.polyacs.org/725.html
116. Fukui, Y.; Murata, M.; Soga, K. *Macromolecular Rapid Communications* **1999,** 20, (12), 637-640.
117. Hasan, T.; Ioku, A.; Nishii, K.; Shiono, T.; Ikeda, T. *Macromolecules* **2001,** 34, (10), 3142-3145.
118. Gomez-Hens, A.; Perez-Bendito, D. *Analytica Chimica Acta* **1991,** 242, (0), 147-177.
119. Liu, B.; Matsuoka, H.; Terano, M. *Macromolecular Rapid Communications* **2001,** 22, (1), 1-24.
120. Mori, H.; Terano, M. *Trends in Polymer Science (Cambridge, United Kingdom)* **1997,** 5, (10), 314-321.
121. Mori, H.; Yamahiro, M.; Prokhorov, V. V.; Nitta, K.-h.; Terano, M. *Macromolecules* **1999,** 32, (19), 6008-6018.
122. Busico, V.; Cipullo, R.; Esposito, V. *Macromolecular Rapid Communications* **1999,** 20, (3), 116-121.
123. Shiono, T.; Ohgizawa, M.; Soga, K. *Polymer* **1994,** 35, (1), 187-192.
124. Pepper, D. C. *Journal of Polymer Science, Polymer Symposia* **1976,** 56.
125. Sawamoto, M.; Higashimura, T. *Macromolecules* **1979,** 12, (4), 581-585.
126. Warzelhan, V.; Löhr, G.; Höcker, H.; Schulz, G. V. *Die Makromolekulare Chemie* **1978,** 179, (9), 2211-2219.
127. Brittain, W. J.; Aquino, E. C.; Dicker, I. B.; Brunelle, D. J. *Die Makromolekulare Chemie* **1993,** 194, (5), 1249-1272.
128. Keii, T.; Terano, M.; Kimura, K.; Ishii, K. *Die Makromolekulare Chemie, Rapid Communications* **1987,** 8, (11), 583-587.

129. Keii, T.; Terano, M.; Kimura, K.; Ishii, K. *Transition Met. Organomet. Catal. Olefin Polym., [Proc. Int. Symp.]* **1988**, 3-12.
130. Di Martino, A.; Weickert, G.; McKenna, T. F. L. *Macromolecular Reaction Engineering* **2007,** 1, (1), 165-184.
131. Di Martino, A.; Weickert, G.; McKenna, T. F. L. *Macromolecular Reaction Engineering* **2007,** 1, (2), 229-242.
132. Shiono, T.; Ohgizawa, M.; Soga, K. *Polymer* **1994,** 35, (1), 187-192.
133. Soga, K.; Ohgizawa, M.; Shiono, T.; Lee, D. H. *Macromolecules* **1991,** 24, (7), 1699-1700.
134. Soga, K.; Ohgizawa, M.-a.; Shiono, T. *Die Makromolekulare Chemie* **1993,** 194, (8), 2173-2181.
135. Kaminsky, W. *Macromolecular Chemistry and Physics* **1996,** 197, (12), 3907-3945.
136. Liu, Z.; Somsook, E.; White, C. B.; Rosaaen, K. A.; Landis, C. R. *Journal of the American Chemical Society* **2001,** 123, (45), 11193-11207.
137. Liu, Z.; Somsook, E.; Landis, C. R. *Journal of the American Chemical Society* **2001,** 123, (12), 2915-2916.

Chapter II

Quenched Flow Reactor: Groundwork and general experimental protocols.

Chapter II: Groundwork and general experimental protocol

1. Introduction

Keii and Terano[1] were the first researchers to use the stopped/quenched flow technique to study olefin polymerisation. They used this "simple and elegant technique" to study the kinetic mechanism of olefin polymerization with heterogeneous Ziegler-Natta catalysts. Strictly speaking the quenched-flow or stopped-flow technique is designed to provide a reactor with a short, very well-defined residence time; usually obtained by provoking the quasi-instantaneous mixing of the reactants followed a very specific time later by an instantaneous "stopping" of the reactor. In the context of the present work, this time should be less than the average lifetime of the growing polymer chains if it is to be used for analyzing rate constants and active site concentrations. The idea is to create conditions different from convention laboratory or commercial reactors where the average residence of the particles in on the order of 1-3h, during which the catalytic activity varies with time according to various side-reaction such as secondary activation, deactivation, chain-transfer or termination reactions. As we will discuss below, it might be possible to use the stopped-flow technique to work with constant active site concentrations or the occurrence of side reactions.

Note that others have used stopped flow (or quenched flow) reactors to study particle fragmentation and morphology using $MgCl_2$-supported catalysts[2] and silica supported catalysts[3], and to look at heat transfer in gas phase reactors[4]. While all of these authors occasionally used the reactor for times of a fraction of a second, they also used the reactors under conditions that were not conducive to the study of active site concentrations (one could still consider the reactors to be stopped or quenched flow nonetheless.)

2. Requirements in methods

In order to use this technique for the precise study of polymerisation kinetics, Liu et al.[5] proposed that the following requirements be met:

1) The time required for the formation of the active sites at the beginning of the polymerization must be negligible compared with the polymerisation time;
2) The monomer must be highly soluble in the solvent used in the polymerisation in order to obtain an appropriate and relatively high monomer concentration;

3) The mixing of the catalyst slurry in the reactor should be efficient in order to avoid temperature and concentration gradients;
4) The flow velocity must be constant during the polymerisation to avoid deviation of the polymerization time within one run;
5) The monomer conversion must be kept below ca. 10% in order to avoid significant changes in monomer concentration and polymerisation temperature of the polymerization mixture in the delay line;
6) The polymerization must be stopped immediately and completely in order to avoid deviation in polymerization time;
7) Sufficient amounts of polymer must be obtained to perform all analytical measurements required.

Note that point (1) is the most relevant to the interpretation of the kinetic date, the rest are more related to the need to obtain "device-independent" results. As we shall see in the following chapters, this condition is occasionally difficult to satisfy.
The stopped flow reactor should also be able to work under similar reaction conditions of T and P encountered at a longer time scale in order to understand if/how the reaction, rate constants, active sites, M_n evolve. If they do not evolve with time, we should be able to identify comparable values for different time scales; if they do evolve, then we should be able to identify how and (hopefully) why.

2.1 Low pressure stopped flow devices

The stopped-flow apparatus conceived by Keii and Terano[1] to study the homo-polymerization of propylene and of ethylene using heterogeneous Ziegler-Natta catalysts is shown Figure 1**.** Their polymerization procedure was as follows: a catalyst suspension (a few grams) in 200 cm^3 heptane (A) and 200 cm^3 of an AlR_3 solution in heptane (B), both saturated with monomer at 20°C under atmospheric pressure were placed in 250 cm^3 flasks [1]. At about 1 bar of monomer and 20°C, the solubility of ethylene (C2) and propylene (C3) in toluene are 0.12 $mol \cdot L^{-1}$ and 0.70 $mol \cdot L^{-1}$ respectively. The solutions were agitated using small stirrer chips to maintain a homogeneous state. After the solutions reached the desired conditions, an overpressure of nitrogen was applied to cause the two solutions to flow through short tubes to a T-mixer (X in Figure 1). It was assumed that mixing was very rapid and that the

polymerization began instantaneously starting at the T-mixer. The polymerizing solution then flowed through tubular reactor into a 1 dm^3 flask (Y in Figure 1) containing at least400 $cm^3$of acidified ethanol or methanol as quenching agents. The polymer was then washed, separated by filtration and dried in a vacuum before being analyzed. Special pressure-resistant vessels (e.g. stainless steel autoclaves) can be used when higher working pressures were needed [6]. The use of various length of reaction tube and/or the modifying of the solution flow rate allows sweeping the reaction ageing from a few milliseconds to several second. By way of illustration, Keii et al.[1] varied the polymerization time from 0.1 to 1 s via the use of a Teflon tube of 2 mm inner diameter and with a length between 20-200 cm. The residence, t_r, time is calculated using the following equation:

$$t_r = (t_m \cdot L \cdot D^2)/(8 \cdot V) \quad (1)$$

Where t_m is the time needed to elute the volume 2V, L is the tube length, and D is the inner diameter of tubular reactor.

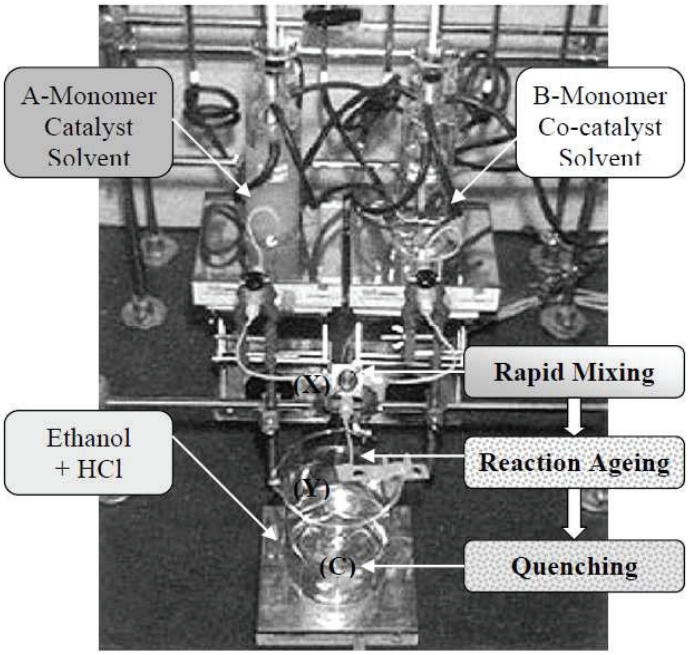

Figure 1. Illustration of basic stopped flow apparatus (low pressure type)for propylene or ethylene homopolymerization. (A) and (B) are special glass vessels equipped with water jackets containing catalyst slurry and cocatalyst solution. (C) is a flask with a quenching agent. (X) indicates the mixing point and (Y) corresponds to the end of the polymerization tube . *Reproduced and adapted from[5] by permission of John Wiley & Sons Inc.*

The stopped flow device used by Busico et al.[7], for kinetic investigations of ethylene and propylene homo-polymerization catalyzed by metallocene catalyst systems, was similar to one showed above. Since the catalyst system was a metallocene-based precursor activated by MAO, the main difference with the Keii device was in the experimental procedure. The vessel

(A) was filled with a solution of catalyst and MAO under N_2 while vessel (B) was filled with a solution of toluene and MAO, which in this case was the scavenger, saturated with the monomer. The reactor employed was a PTFE tube with outer diameter of 6 mm and the inner diameter of 4 mm. The L values of 0.05-1.5 m resulted in t values of 0.05 to 1.5 s.

2.2 High pressure devices

Up to now the quenched/stopped flow technique which allow to work at pressures greater than one bar was principally used for investigating olefin block copolymer with a well-defined structure and properties[6], or morphogenesis studies of nascent polymer[8, 9]. In both case the authors used $MgCl_2$ supported Ziegler Natta catalysts.

The system used by Mori et al.[6] allowed the authors to work with three special vessels. In the first one the aluminium alkyl solution of toluene and pressurized with propylene, the second vessel was filled with a slurry of catalyst in toluene and pressurized with propylene, and the third one was filled with ethylene-saturated toluene. The monomer concentration was controlled with a mass-flow meter. The maximum of pressure was set to 6 bars and the control of flow rate was assessed by using a pressure regulator valve in combination with a digital pressure gauge. With this set up it was possible to achieve reaction times as short as 0.1 s[6].

A detailed study on the influence of monomer concentration on the activation of metallocene catalysts was carried out by Bochmann and co-workers[10], who set up a quenched flow reactor that allowed them to work at propylene concentrations ranging from 0.15 to 0.59 mol L^{-1} by diluting a toluene solution saturated with propylene (under 1 bar of propylene at 25°C = 0.68 mol·L^{-1}) with additional propylene for this reason it should not called high pressure-type quenched flow. The device used by authors had 2 reservoirs, the first one only filled with toluene and the second one filled with a solution of toluene and propylene, both connected to a syringe. In this manner the syringe could be either purged with neat toluene or be filled with a monomer solution. The syringe fed a mixing chamber with small positive pressure. The pre-catalyst and co-catalyst solutions are mixed in a “pre-chamber”, then the catalyst solution was also driven into mixing chamber where it met the monomer solution and caused the polymerisation to start. This very sophisticated device worked only on very small volume, 100ml, and the lowest reaction time was 250 ms.

The main objective of this thesis is to find a reliable method for the experimental determination of a set of active site concentrations ([M*]/[M]) and values of the average kinetic constant of chain propagation (k_p) for molecular catalysts in ethylene polymerizations using a high-pressure-type quenched flow reactor. The basic reactor set-up at the beginning of this work was described in detail by Di Martino et al.[8,11], and used for understanding of mechanism of particle growth and the associated processes governing the development of the particle morphology.

3. Equipment

The quenched flow device that was initially used for this work, shown Figure 2 and Figure 3, comprised[8]:

1) Two special pressure-resistant flat-bottomed cylindrical tanks (A) and (B) (0.5 L, 7 cm inner diameters) manufactured in 360 stainless steel to resist against corrosion. Each tank is equipped with heating jackets. Holes through the lid allow us to pass a mixing shaft and impeller (only one shared motor but two driving belts), two side taps (one to feed the tank in monomer and the other for the pressure sensor and to make the internal pressure equal if need be), a thermometer pocket, a vent nozzle, an outflow tube (the orifice of the tube is placed very close to the impeller at the bottom of the tank), and a load tap with a larger internal diameter.
2) The quench reactor (C) is a simple 1L 360 stainless steel vessel (10 cm inner diameter), the top of which is equipped with a load tap, a sampling tube, a vent nozzle connected with the over-flow valve, a central hole for the reaction tube, a CO_2 sparger, a pressure measurement tap, and a thermometer pocket.
3) The reactor is a 4 mm inner diameter (6 mm outer diameter) tube made of Polyamide-11,12 (Manuril/Tecalan®). The maximum service pressure is 23 bar at 20°C and 11bar at 80°C (bursting pressure: 100 bar at 20°C and 45 bar at 80°C).
4) The temperature in the quench and upstream reservoirs is monitored with a standard Type K cladded thermocouple and the pressure via a 0-25 bar sensor (accuracy: 0.25%; maximum pressure: 75 bar; service temperature: 0-70°C; with a 4-20 mA (2wires) output).

5) The gas storage tanks are equipped with dual stage regulators: e.g. ethylene feedstock: first stage 0-300 bar, second stage 0-80 bar; or single stage regulator: e.g.argon feedstock: only one stage 0-25 bar (accuracy: 2.5 %).
6) The upstream – downstream pressure difference is controlled via the use of an overflow pressure-regulating valve. The device used here is a special model designed to meet our specifications of wide working pressure range (0-24 bar) with adequate sensitivity. A 35 mm diameter Viton membrane, a 7 mm long spring and a 1 mm diameter vent passage are combined to this end. Silicon seals allow us to work over a broad range of temperature: usually -40°C to 80°C continuously and down to -70°C for short periods.

The reasoning behind these choices are outlined in[8].

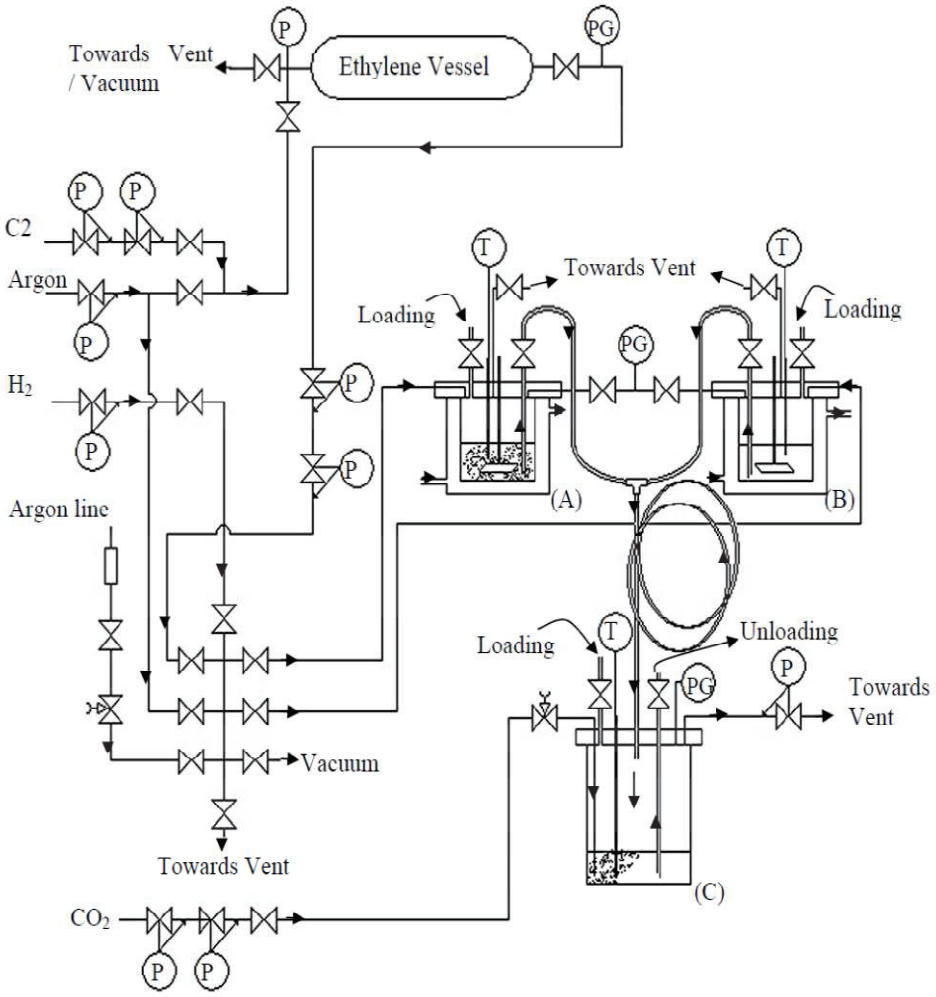

Figure 2. Schematic illustration of high pressure quenched flow reactor. (P) is pressure regulator; (PG) Pressure gauge; (T) temperature sensor. *Reproduced and adapted from[8] by permission of John Wiley & Sons Inc*

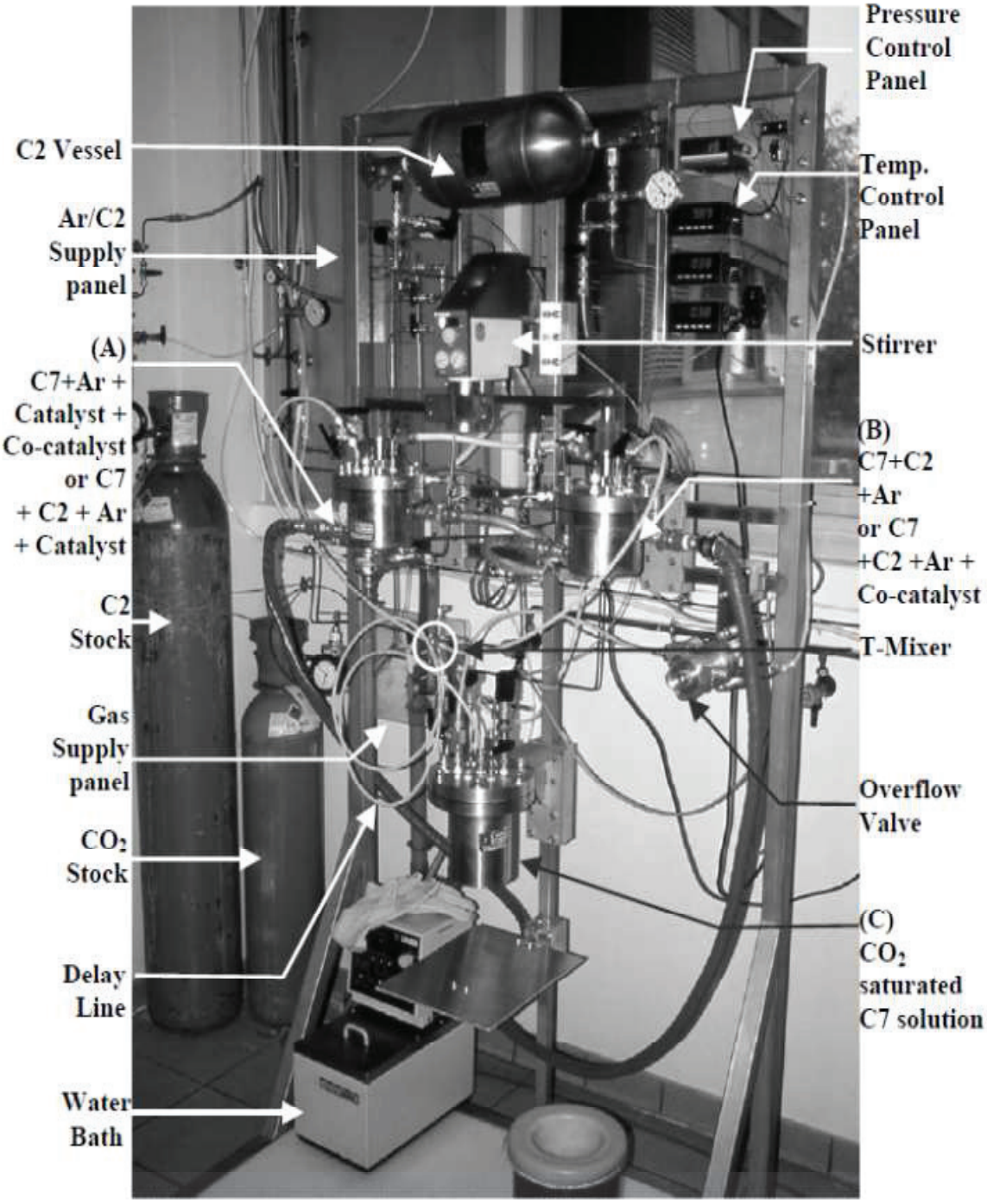

Figure 3. Picture of quenched flow apparatus: it is possible to use it for a wide range of monomer concentrations, total pressure, temperatures, residence times, poisoning conditions, etc...

3.1 Setup

A very though description of the device is available[8] in the literature, so here we will only focus on key points that are fundamental to understanding how the device works, and discuss some changes that we have made to the original device in order to improve it and fit it for our kinetic investigations.

3.1.1. Mixer

The mixer is the heart of this reactor: it had to be designed to shorten the mixing time and mixing distance, i.e. to shorten the dead time and to localize mixing in time and space. It is well known that operation at high volumetric flows is expected to guarantee a short mixing due to the creation of turbulence induced by direct collision of the two reactant streams. The T-mixer used for this reactor (where the two reagent streams meet at 90° to each other) can produce high degrees of uniformity and minimize mixing time [12-14].

3.1.2 Delay line and flow regulation

After the mixing step, the delay line allows reaction ageing from few milliseconds to several seconds by modifying the solution flow rate and or the delay line volume. In fact, in a conventional Quenched Flow reactor the residence time is controlled by varying the volume of reaction tube by varying its length. When operating at pressures above one atmosphere, it is possible to control the flow and thus the residence time by varying the pressure drop between the upstream tanks and the downstream quenching tank. In fact, by applying a pressure difference it is possible to overcome the drop in pressure of the assembly (viscous loss due to the flow of fluid in tube, accident of flow, geometric change of flow and gravity) and to ensure the fixed flow. For morphogenesis studies, the monomer or argon pressure acts as a piston to force the flow of co-catalyst (in vessel A) and slurry (in vessel B). In case of kinetic studies of metallocene catalyst system the co-catalyst and metallocene precursor were filled in the same vessel (in general vessel B) under argon, so if we use the monomer pressure as piston for both vessels we will promote the reaction directly in vessel B, rather than reactor

tube. On the other hand, if we use argon pressure as piston for both vessels, then the total concentration of monomer in vessel A will result. Even when this last strategy was attempted, we observed the pressures were never quite equalized between vessels A and B, as shown from test 1 in Table 1. All these observations led us to modify the feed system in such a way that they two upstream reservoirs operate independently.

Table. 1 Flow measurement for vessel A and vessel B

Tests	Pressure (bar)	Vessel A ($ml \cdot s^{-1}$)	Vessel B ($ml \cdot s^{-1}$)	Vessel A/Vessel B
1	0.86	63.2	55.8	1.12
2	0.86	60.9	60.0	1.01

To do this, a 5 L gas vessel was placed between the vessel B and the Ar storage tank. In addition, each of the ethylene and argon storage tanks were equipped with dual stage regulators: first stage 0-300 bar, second stage 0-16 bar (accuracy: 2.5%) rather than a second stage of 0-25 bar. The use of the dual stage regulator allowed us to impose a constant working pressure since the element (membrane and/or spring) is sensitive and reactive enough. Later on, we eliminated the pressure regulator which was placed between the 5L ethylene vessel and vessel B in order to avoid possible drop in pressure. By using the force of two gas vessels the delay between the flow of vessel A and vessel B was minimized as shown from test 2 in Table 1.

An overflow valve was installed on the quench vessel in order to avoid the increase of internal pressure due to the reactant inflow in the quenching reactor an overflow valve. The required relief rate changes constantly as the tank fills, so the valve was designed to keep the pressure in quench vessel (vessel C in Figure 2) constant during the filling period. The upstream-downstream pressure difference was found by solving the macroscopic mechanical energy balance of our system. A compressed air cleaning system was built between the vent tube and the overflow valve, in order to avoid the accumulation of polymer or other impurities on the membrane which could influence or delay the rate of the response of the valve.

With the hardware modifications, and by varying the length of the reaction tube (4 mm inner diameter; length: 0.5, 1, 2 and 4m), and a pressure drops on the order of 1-6 bars are enough to reach a broad range of residence times as shown in Figures 4 and 5.

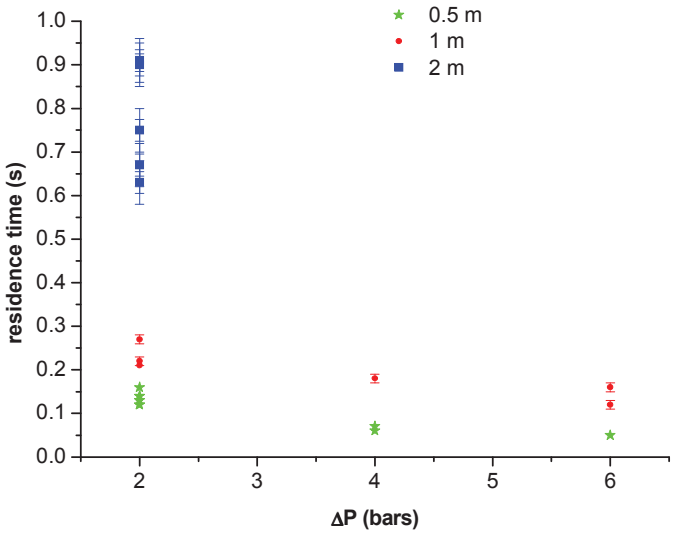

Figure 4. Residence times we can easily reach according to the upstream-downstream pressure (ΔP) we imposed for 3 lengths of reaction tube (0.5,1 and 2 m) each points is an individual run.

The tests reported in Figure 5 have been carried out using three tube lengths (0.5, 1, 2 m) by applying a difference in pressure of 2, 4, 6 bar employing in upstream a pressure from 8 bar to 2 bar. These tests have been carried out at variable volume of solvent and this could explain the variability from test to test.

The minimum of residence times that we can accurately handle is 0.08 s with a ΔP of 2 when the downstream was composed by a glass vessel of 2 L as quench vessel under atmospheric pressure and the pressure in upstream was 2 bar_{rel}.

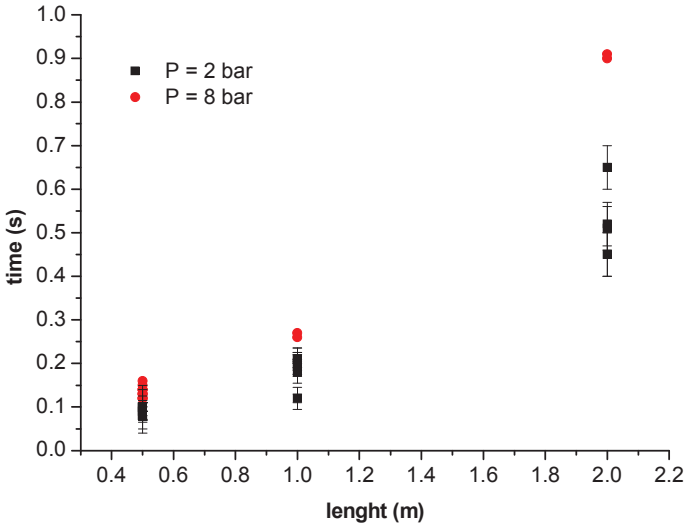

Figure 5. Residence times for 3 tube lengths at ΔP = 2 bar and different monomer pressure

In fact, the shortest reaction times were obtained for pressure in upstream of 2 bar and $\Delta P = 2$ and this, at least in part, could be due to the fact that, for this tests, the overflow valve was not employed (see Figure 5).

Note that, the polymerization times were systematically measured for all polymerization tests by applying the Eq. (1) considering as volume the one that effectively passed through the reactor tube. It is obtained by a volume balance on the initial volumes which are filled in the two vessels and the amount of solutions which remains after the reaction in the vessels, and in the reaction tube (in case of reaction tubes longer than 50 cm).

3.1.3 Installation of reaction tube

The reaction tube is connected to "T-mixer" and the quench vessel. For morphological studies the temperature of quench vessel was settled at -20°C in order to avoid the formation of temperature gradient the reaction tube ended just below the lid of the quench vessel. The time that it takes for the incoming particles to fall into the quench is negligible and estimated at about 4ms.In order to further minimize this delay for kinetic investigation we have placed the reaction tube at 5 cm below the lid of quench vessel. This 6 cm steel tube is inserted through the quench vessel and it is connected with the Teflon tube reactor by a valve. The length of reactor is calculated taking in account the 12 cm resulting by the sum of this quench tube and the valve length. The function of valve was to isolate the reaction tube from the quench vessel. In this way it was possible to recover the solution that might remain the tube more easily. The reason for this is to obtain a more precise material balance. Another option is to install the reactor tube directly at the level of the surface of quench solution, but we have noticed that the when the quench vessel is under pressure the quench solution tends to rise in the reaction tube and this could have a negative influence on the reaction.

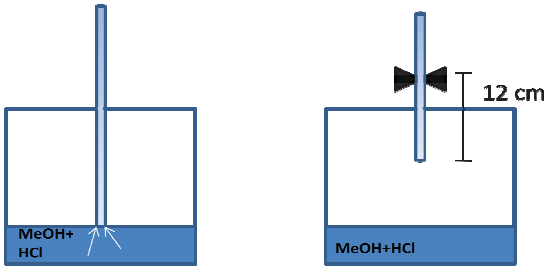

Figure 6. Installation of reaction tube

3.1.4 Quench vessel

The original protocol employed a CO_2 saturated heptane solution as the quench solution. The suspension fell from reactor tube into solution and where it was assumed that they were rapidly quenched. CO_2 is useful when the objective is to recover the particles with an intact morphology but it was not optimal for kinetic investigation. We therefore chose to use the same solution as the authors cited above and replaced the CO_2-saturated solution with one of 10% w/w HCl in methanol. In order to minimize the effect of HCl on the steel vessel, a glass liner was inserted into the original quench vessel. For reactions carried out at higher pressures, the quench vessel was pressurized with argon via the use of a sparger, in order to assure the settled ΔP. Note that for the series of tests at 2 bars gauge, reported in sections 2 and 4 of chapter III, we used a 2L glass beaker as quench vessel. In this case was unnecessary to use a pressurized steel quench vessel. The agitation of solution was assured with a 10 cm magnetic stirrer.

3.1.5 Temperature profiles.

One important question concerns the evolution of the temperature in the reactor. The equation below was used to prove that the adiabatic temperature rise is lower than 1°C (ΔT = 0.1-0.5°C), even in case of monomer consumption higher than 10%.

$$\Delta T = (Q \cdot Mw)/(C_p \cdot \rho \cdot V) \quad (2)$$

Where

Cp is given by eq. $Cp= C_1+C_2T +C_3T^2$ whit C_1 = 140140 C_2=-152.3 C_3=0.695 for toluene[15]

ρ is the toluene density = 0.87 $g \cdot ml^{-1}$;

V is the volume which was passed through the Teflon tube;

Mw is the molar weight of toluene = 92.14 $g \cdot mol^{-1}$;

The released heat, Q, is given by the product between ΔH of polymerization and the mol of monomer consumed. The value of ΔH[16] of polymerization is 25 kcal·mol^{-1}.

A series of tests were carried out where we measured the temperature in tubular reactor in order to evaluate the difference temperature between in and out. Two type K thermocouples were used to measure the ΔT during the ethylene polymerization using FESBIZrCl$_2$/MAO catalyst system (which is shown in detail in Chapter III). The first thermocouple was positioned in point **3** (see Figure 8), replacing the T-mixer with a cross-mixer; the second one was placed in point **5** at the end of tubular reactor. The temperature profiles in Figure 7 are relative to runs 277 and 278 carried out using tubular reactor of 2m and run 270 carried out using tubular reactor of 0.5 m (for more details see Table 3 chapter III) which corresponds to residence times of 0.51, 0.7 and 0.09 s respectively, and ethylene consumption up to 6%.

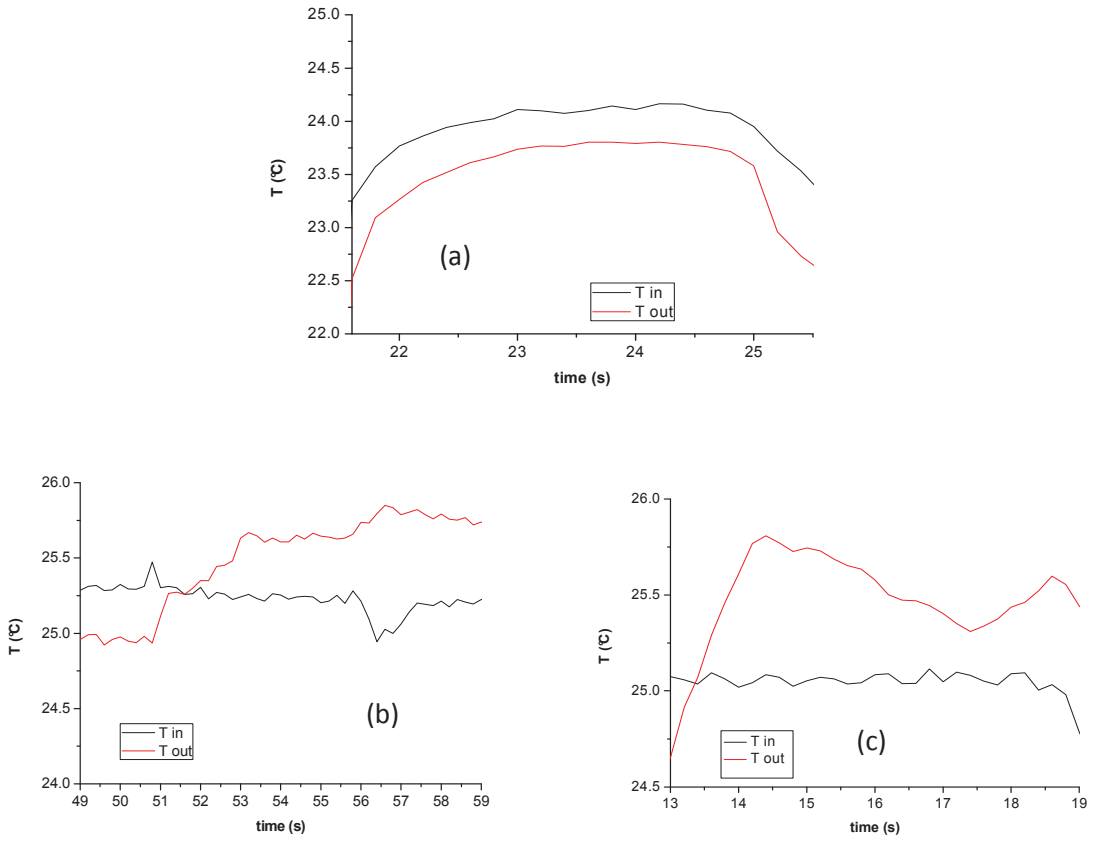

Figure 7. Temperature profiles of (a) run 270, (b) run 277, (c) run 278

For tests at short reaction times, the ΔT measured was lower than 0.5°C, furthermore for reactions carried out at long reaction time we observed a maximum of 1°C, which means that even for long reaction time the heat release during the polymerization is negligible.

4. Conclusions

The quenched flow reactor used for the kinetic studies for measuring the active sites concentration of molecular catalyst at variable temperature and pressure was originally devised for morphogenesis studies of $MgCl_2$-supported Ziegler Natta catalysts. The first runs that we carried out using the original hardware showed a broad molecular weight distribution and also a very poor reproducibility, meaning that the reactor was not ideally configured for very precise studies such as the kinetic investigations. We therefore made two major types of modifications:

Mechanical: we separated upstream part of the device into two distinct zones with the insertion of two gas storage tanks, one for ethylene and one for argon. We have also improved the pressure regulators for gas distribution in order to minimize the delay that we have observed in gas flow in upstream. A better overflow valve was installed in order to minimize the pressure fluctuations. A glass insert was added to the quench vessel in order to minimize the effect of hydrochloridric acid on the steel of quench vessel. The device was kept under vacuum at 80°C over night in order to limit the air and moisture infiltrations;

Chemical: a strong quencher consisting of a solution of HCl in MeOH was employed rather than the CO_2 saturated heptane solution. In order to minimize the presence of impurities a solvent and monomer purification systems were introduced (see section 5-*Materials* for further details).

At the end we were able to perform tests with satisfactory reproducibility, despite the delicacy of the technique as shown in Table 2.

Table 2. Reproducibility tests for $Cp^*_2ZrCl_2$/MAO at 25°C and P=2bar$_{abs}$

run[a]	time (s)	Y (mg)	activity ($kgPE \cdot mol_{Zr}^{-1} \cdot h^{-1} \cdot [C_2H_4]^{-1}$)
140	0.08	10.7	$3.5x10^6$
141	0.08	10.5	$3.4x10^6$
142	0.08	10.8	$3.5x10^6$
245	0.08	11.0	$3.6x10^6$
266	0.10	12.0	$3.1x10^6$
170	0.10	12.8	$3.3x10^6$

a. $[Cp^*_2ZrCl_2] = 2.5\mu mol \cdot L^{-1}$; $[C_2H_4] = 0.11\ mol \cdot L^{-1}$; Al/Zr = 1000; T=25°C; in toluene

5. Experimental procedure

In this section a description of experimental protocol is given, which could be considered as reference for better understand the polymerization procedure applied in chapter III and IV.

Each of upstream feed vessels was filled with a known quantity (about 250 ml per vessel) of toluene solutions, both previously prepared at room temperature. In general, in the vessel **1** (see Figure 7) was filled with a solution of scavenger such as MAO or iBu$_3$Al (1 $mmol \cdot L^{-1}$) in toluene under ethylene. The ethylene concentration in the liquid phase is calculated according to the following equation[17]:

$$[C_2H_4] = p(C_2H_4) \cdot 1{,}15 \cdot 10^{-3} \cdot e^{2700/RT}$$

The vessel **2** (see Figure 8) was typically was filled with a solution of the metallocene precursor and the co-catalyst, in order to promote the formation of active species under argon. After the two solutions reachedthe desired pressure and temperature (this usually takes approximately10 minute), they were forced to flow simultaneously through a reaction tube of various length. When both solutions met at point **3** (in Figure 8) at T-mixer the polymerization started, instantaneously and occurs in the Teflon tube (indicated by point **4** in Figure 8) until the poison step (point **5**). The polymerization was quenched in 300 ml of MeOH/HCl (10% in weight) solution under argon. The mixture was degassed and the polymer (on the order of 2 to 100 mg) was recovered by using a filtration device, and then analyzed.

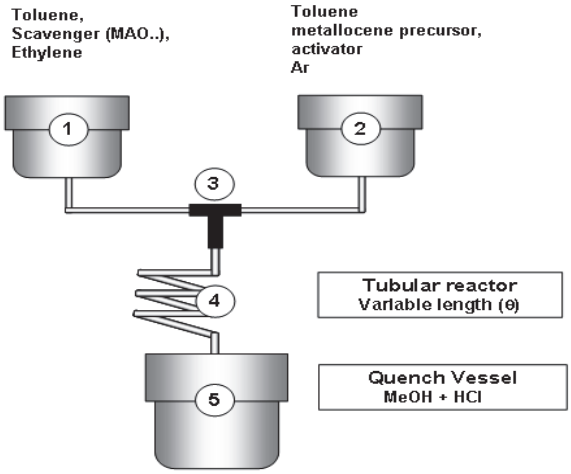

Figure 8. Experimental protocol

During the kinetic investigation several experimental protocols have been employed in order to improve the activation of metal sites. A schematic description is given below:

Protocol 1: this experimental protocol was assured, for tests using FESBIZrCl_2/MAO and Cp•$_2$ZrCl_2/MAO and (Ph_2C)CpFluZrCl_2/MAO catalysts systems and The bis(phenoxy-imine) Ti- and Zr based complexes

Vessel 1: solution of MAO as scavenger (1 mmol·L^{-1}) in 250 ml of toluene prepared at room temperature was filled and pressurized with ethylene at desired T and P.

Vessel 2: a solution of MAO as co-catalyst and metallocene precursor in about 250 ml of toluene prepared at room temperature in 500 ml glass flask. The precontact is assured for 10 minutes at desired temperature under argon pressure.

Protocol 2: this *modus operandi* was followed for the Bis(cumyl)[ONNO]ZrBz_2 /MAO/*t*Bu_2-PhOH and (Ph_2C)CpFluZrCl_2/MAO/*t*Bu_2-PhOHcatalyst systems.

Vessel 1: solution of MAO as scavenger and *t*Bu_2-PhOH in 250 ml of toluene prepared at room temperature was filled and pressurized with ethylene at desired T and P.

Vessel 2: a solution of MAO with *t*Bu_2-PhOH in about 250 ml of toluene was prepared at room temperature in 500 ml glass flask. The contact was assured for 30 minutes at room temperature. After, the solution was filled in steel reactor. After, 15 minutes at desired T and

P, the catalyst precursor in 10 ml of toluene was added and the pre-contact was assured for further 15 minutes at desired T and P.

Protocol 3: this experimental protocol was followed when the *i*Bu_3Al/$[PhNMe_2H][B(C_6F_5)_4]$ complex was used as co-catalyst.

Vessel 1: solution of *i*Bu_3Al (1 mmol·L^{-1}) in 250 ml of toluene prepared at room temperature was filled and pressurized with ethylene at desired T and P.

Vessel 2: a solution of *i*Bu_3Al and $[PhNMe_2H][B(C_6F_5)_4]$ and catalyst precursor in about 250 ml of toluene was prepared at room temperature in 500 ml glass flask and after injected in steel vessel. In several cases the three components have been combined in different way in order to improve the activation, as it will explained in deeply in next chapters.

Filtration: In order to recover the polymer in the end of polymerization, a solvent filtration system under vacuum by Millipore has been employed. The membrane for filtration used was a PVDF with a pore diameter of 0.45µm. The filtration duration was on the order of 5-10 hours. When the polymer was recovered it was dried under vacuum at 80°C over night.

Materials:the FESBI$ZrCl_2$ and $(Ph_2C)CpFluZrCl_2$ and $Cp•_2ZrCl_2$ metallocene complexes were supplied by Sigma Aldrich. The Bis(cumyl)[ONNO]$ZrBz_2$ was supplied by U-Naples laboratories. The bis(phenoxy-imine) Ti- and Zr based complexes were synthesized in this laboratory using protocols described in the literature (see appendix B for experimental protocol). The MAO 10% in weight in toluene, the *i*Bu_3Al, the *t*Bu_2-PhOH were supplied by Sigma Aldrich, the MAO 30% in weight in toluene was supplied by Albermarle. The $[PhNMe_2H][B(C_6F_5)_4]$ was supplied by Strem Chemical. The toluene (Carlo Erba pure synthesis) was purified by passing it through a mixed-bed activated-Cu/A4-molecular-sieves column in an MBraun SPS-5 unit (final concentration of O_2 and H_2O < 1 ppm). Ethylene (polymerization grade) was purchased from Air Liquide and used after purification through 3 columns set with oxidized BASFR3-11 catalyst, Selixorb® COS catalyst and 3Å molecular sieves.

References

1. Keii, T.; Terano, M.; Kimura, K.; Ishii, K. *Die Makromolekulare Chemie, Rapid Communications* **1987,** 8, (11), 583-587.
2. Di Martino, A.; Weickert, G.; McKenna, T. F. L. *Macromolecular Reaction Engineering* **2007,** 1, (1), 165-184.
3. Silva, F. M.; Broyer, J. P.; Novat, C.; Lima, E. L.; Pinto, J. C.; McKenna, T. F. *Macromolecular Rapid Communications* **2005,** 26, (23), 1846-1853.
4. Tioni, E.; Spitz, R.; Broyer, J. P.; Monteil, V.; McKenna, T. *AIChE Journal* 58, (1), 256-267.
5. Liu, B.; Matsuoka, H.; Terano, M. *Macromolecular Rapid Communications* **2001,** 22, (1), 1-24.
6. Mori, H.; Yamahiro, M.; Prokhorov, V. V.; Nitta, K.-h.; Terano, M. *Macromolecules* **1999,** 32, (19), 6008-6018.
7. Busico, V.; Cipullo, R.; Esposito, V. *Macromolecular Rapid Communications* **1999,** 20, (3), 116-121.
8. Di Martino, A.; Broyer, J.-P.; Schweich, D.; de Bellefon, C.; Weickert, G.; McKenna, T. F. L. *Macromolecular Reaction Engineering* **2007,** 1, (2), 284-294.
9. Di Martino, A.; Weickert, G.; McKenna, T. F. L. *Macromolecular Reaction Engineering* **2007,** 1, (2), 229-242.
10. Song, F.; Cannon, R. D.; Bochmann, M. *Journal of the American Chemical Society* **2003,** 125, (25), 7641-7653.
11. Di Martino, A.; Broyer, J. P.; Spitz, R.; Weickert, G.; McKenna, T. F. *Macromolecular Rapid Communications* **2005,** 26, (4), 215-220.
12. Schwarzer, H., C.;; Manhart, M.; Peukert, W. *11th European Conference on Mixing.* **14-17 October 2003** Bamberg Germany.
13. Engler, M.; Kockmann, N.; Kiefer, T.; Woias, P. *Chemical Engineering Journal* **2004,** 101, 315-322.
14. Wong, S. H.; Ward, M. C. L.; Wharton, C. W. *Sensors and Actuators B: Chemical* **2004,** 100, (3), 359-379.
15. Perry, R. H.; Green, D. W., *Perry's Chemical Engineers' Handbook (7th Edition)*. McGraw-Hill 1997.
16. Hutchinson, R. A.; Chen, C. M.; Ray, W. H. *Journal of Applied Polymer Science* **1992,** 44, 1389-1414.
17. Kissin, Y. V. *Springer-Verlag, New York, chapter 1* **1985**.

Chapter III

Investigation of Metallocene Catalyst Systems

Chapter III: Investigation of metallocene catalyst systems

1. Introduction to the chapter

In this chapter we will focus on the investigation of the polymerization kinetics of three different metallocene catalyst precursors: *rac*-Me_2Si(2-methyl-4-phenyl-1-indenyl)$_2$ zirconium dichloride (FESBIZrCl_2), diphenylmethylidene-cyclopentadienyl-fluorenyl zirconium dichloride ((CPh_2)CpFluZrCl_2), and bis(pentamethyl-cyclopentadienyl) zirconium dichloride (Cp*$_2$ZrCl_2).

As seen in Chapter I, the activation of a metal species can be quite complex and influenced by many parameters, including the co-catalyst, temperature and the monomer concentration. In this chapter we will use the high pressure quenched flow reactor described earlier to investigate the influence of these parameters on active site formation at very short reaction times, under conditions where chain growth is predominant and other reactions, such as transfer/termination reactions, can be considered negligible. The quenched flow reactor could be use also for investigating the activation of catalyst precursor using different co-catalysts, in order to detect possible induction period or different behaviour.

Since the investigation of influence of temperature for the complex FESBIZrCl_2 activated by methylaluminoxane (MAO) has been already reported in literature[1]using a quenched flow reactor (QFR) under low monomer concentration ([C_2H_4] = 0.081 mol·L^{-1}) we have investigated the influence of monomer concentration on this catalyst system by examining the impact of two class of activators: MAO and borate salts. Then we have investigated the behaviour of complex (CPh_2)CpFluZrCl_2 activated by various co-catalyst systems and finally the behaviour of metallocene Cp*$_2$ZrCl_2 activated with MAO.

In order to compare the results obtained in the stopped flow reactor at very short times with the behaviour under conventional polymerization time, reference polymerization tests were carried out under similar conditions in 500 mL glass reactor for several minutes for each set of temperature and pressure. Where not indicated the GPC values were obtained by universal calibration using PS standards.

2. *The rac*-Me_2Si(2-methyl-4-phenyl-1-indenyl)$_2$zirconium dichloride metallocene precursor: a comparative study.

The *rac*-Me_2Si(2-methyl-4-phenyl-1-indenyl)$_2$ zirconium dichloride (FESBIZrCl_2)is a bridge chiral zirconocene which exhibits a C_2-symmetry.

Figure 1: The rac-Me_2Si(2-methyl-4-phenyl-1-indenyl)$_2$ zirconium dichloride

In general this metallocene complex is used for its high isotacticity in propylene polymerization induced by its symmetry combined with high rigidity and favorable electronic and steric characteristic imposed by silicon bridge[2]. Further the alkyl and phenyl substitution on the bis-indenyl moieties promotes the formation of higher molecular weight polymers than analogous alkyl substituted cyclopentadienyl structure[3,4]. In fact the homopolymerization of ethylene using the complexFESBIZr$Cl_2$when activated with MAO (Al/Zr = 200) displayed a high molar mass[5](7,3x10^5 g·mol^{-1}).

Two characteristics make the FESBIZrCl_2 a good candidate for our investigation:

1. its high activity might allow us to recover enough of polymer to perform the necessary analyses, even for short reactions;

2. previous results in mild conditions suggest that the activation of the complex is rapid, and without an induction period (in particular for ethylene homopolymerization). In addition, the data reported in literature[1] can be compared with the results presented here at higher ethylene concentrations.

The stopped flow reactor used by Busico et al.[1] was composed of two glass flasks, each containing an equal volume of solutions of FESBIZrCl_2 and MAO in toluene under N_2 and of

MAO and ethylene in toluene (as scavenger) at the same temperature. Polymerizations were performed in PTFE tube of different lengths, and were stopped in a 5 liter beaker containing 2 liters of acidic methanol (MeOH/HCl solution). The authors calculated the relative propagation rate constant, and the concentration of active sites (see Table 1) for ethylene polymerization at three temperatures (20°, 40° and 60°C) using FESBIZrCl$_2$/MAO catalyst system at monomer pressure of 0.5 bar.

Table 1. Best fit value of k_p and [M*]/[Zr] for ethylene polymerization at 20°C and [C_2H_4] = 0.081 mol·L^{-1} reported by Busico[1]

T (°C)	**[C_2H_4]** (mol·L^{-1})	**k_p** (L·mol^{-1}·s^{-1})	**[M*]/[Zr]** (mol·mol$_{Zr}^{-1}$)
20	0.081	2.6±0.3 x10^5	0.046±0.007
40	0.059	1.1±0.1 x10^6	0.10±0.01
60	0.045	2.8±0.5 x10^6	0.23±0.04

The active site concentration and the constant of rate propagation k_p increase with the temperature. It is quite impressive that at 25°C only a 5% of metal sites are active. All these tests have been carried out at very low monomer concentration. In next paragraphs we have investigated the influence of slightly higher monomer concentration on the kinetic behavior of the same catalyst system at the same temperature using QFR.

2.1 The rac-Me$_2$Si(2-methyl-4-phenyl-1-indenyl)$_2$ZrCl$_2$ /MAO catalyst system

Ethylene was first polymerized using the complexFESBIZrCl$_2$ activated with MAO in a conventional glass reactor. The experimental protocol used for this investigation was as follows. A solution of MAO (0.8-1mmol·L^{-1}) in toluene was put in the glass reactor which was then pressurized with ethylene at 1.5 bar$_{abs}$. After 10 minutes, the time necessary to reach the desired temperature, a solution of FESBIZrCl$_2$ in toluene was added to the reaction medium through a small injection port. This catalyst system provoked a significant exotherm: after 1 min of polymerization the reaction temperature increased by 20°C from 25.3°C to 44.8°C. In order to minimize the exothermic effect the polymerizations were carried out at the

lowest catalyst and co-catalyst concentrations that we can accurately handle. The reference test for comparison to quenched flow time scale is reported in Table 2.

Table 2. Ethylene polymerization in conventional glass reactor with $FESBIZrCl_2$/MAO catalyst system.

Run[a]	T (°C)	[$FESBIZrCl_2$] ($\mu mol \cdot L^{-1}$)	Time (min)	Yield (g)	Activity ($kgPE \cdot mol_{Zr}^{-1} \cdot h^{-1} \cdot [C_2H_4]^{-1}$)	M_n[c] ($kg \cdot mol^{-1}$)	PDI
ERC11_11	25	0.8	2	1.48	13.8×10^5 13.7×10^{3b}	115	1.8
ERC48_10	40	1	2	5.9	44.2×10^5 44.1×10^{3b}	86	2.2

a. Al/Zr = 1000; $[C_2H_4]$ = 0.16 $mol \cdot L^{-1}$; in 250 mL toluene; **b.**$molPE \cdot mol_{Zr}^{-1} \cdot s^{-1} \cdot [C_2H_4]^{-1}$**c.** GPC values obtained by PE relative calibration

Two tests have been carried out using the conventional batch reactor for the investigation of influence of temperature and monomer pressure for $FESBIZrCl_2$/MAO catalyst system. As expected, an increase in activity (by factor 3) together with a decrease of M_n was observed when the polymerization temperature increased at same monomer concentration.

The experimental protocol used for tests carried out in the quenched flow reactor was already reported in chapter II. In vessel 1 about 250 mL of toluene were introduced pressurized under ethylene (3 bar_{abs}). A solution containing MAO (1.5-2.5 $mmol \cdot L^{-1}$) and $FESBIZrCl_2$ in toluene was added to a second vessel that was also pressurized under argon (3 bar_{abs}). The reaction was performed when both solutions reached the set temperature after 10 minutes. The quench vessel, in this case is a glass container of 2 L, contained 300 mL of MeOH/HCl (10% HCl in volume) under atmospheric pressure. The results of the polymerizations are reported in Table 3.

In order to find the best experimental conditions and avoid overheating, we did preliminary tests at 1.5, 2 and 2.5 $\mu mol \cdot L^{-1}$ of Zr and found that we needed 2.5 $\mu mol \cdot L^{-1}$ in order to get enough polymer.

Table 3. Results of ethylene polymerization under QFR condition for FESBIZrCl$_2$/MAO complex at 25°C

Run[a]	Time (s)	Yield (mg)	Activity	Mn (kg/mol)	PDI	n_{chain}/n_{Zr}	Y (mol/mol$_{Zr}$)	Monomer consumption(%)
270	0.09	7	14.6 x10^5[b] 14.5 x10^3[c]	83	1.8	0.06	204	0.32
274	0.10	9	16.8 x10^5[b] 16.7 x10^3[c]	95	1.8	0.07	263	0.40
275	0.21	19	17.4 x10^5[b] 17.3 x10^3[c]	111	1.9	0.14	570	0.86
277	0.51	81	31.3 x10^5[b] 31.1 x10^3[c]	124	1.9	0.57	2494	4.09
278	0.70	114	32.1 x10^5[b] 31.9 x10^3[c]	131	2.0	0.76	3511	5.74

a.[Zr] = 2.4-2.6 µmol·L^{-1}; Al/Zr = 1000; [C_2H_4] = 0.16 mol·L^{-1}; T = 25°C; in 500±20 mL toluene **b**. kgPE·mol$_{Zr}^{-1}$·h^{-1}·[C_2H_4]$^{-1}$ **c**. molPE·mol$_{Zr}^{-1}$·s^{-1}·[C_2H_4]$^{-1}$

As explained in Chapter II one of main requirements of the stopped flow method is to keep the monomer conversion below ca. 10% in order to avoid significant changes in concentration and temperature in the delay line. From Table 3 it is possible to observe that the monomer consumption was always less than 10% and, in particular for tests performed at shorter reaction time (runs 270 and 274), the monomer consumption was even lower than 1%.

From the trend of polymer yield as function of time, shown in Figure 2 and in Table 3, it is possible to observe a linear increment with time. As expected we do not observe an induction period.

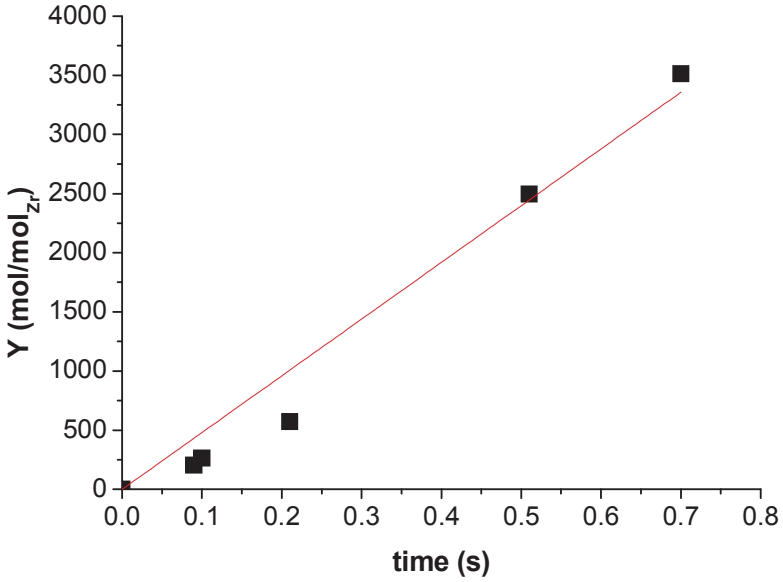

Figure 2. Dependence of polymerization yield from time for FESBIZrCl$_2$/MAO catalyst system at 25°C

Another important observation is that the activities obtained, in particular for tests at shorter reaction times in QFR (14-29 x10^5 kgPE·mol$_{Zr}^{-1}$·h^{-1} ·[C_2H_4]$^{-1}$) are in agreement with the activity obtained in batch reactor (14 x10^5 kgPE·mol$_{Zr}^{-1}$·h^{-1} ·[C_2H_4]$^{-1}$).

Concerning the molar masses we could observe two regimes:

1. For tests at short reaction times (270 and 275 in Table 3, less than 200 ms) it is possible to observe an increment of M_n with time, we could consider these tests in controlled regime.
2. After a certain polymerization time, M_n reaches a limit value (≈ 130kg·mol^{-1}) and the polydispersity index increased to around 1.9. The plateau value is comparable with the M_n value (115 kg·mol^{-1}) observed for test at long reaction time (see Table 2) meaning that this catalyst system is out of controlled regime for times longer than 200 ms

In particular for at short reaction times, in terms of the fraction of Zr molecules that are active (i.e. that have been used to form a chain) that can be obtained from the number of chain per Zr at shorter polymerization time, we observed that this was 6-7%, which is in good agreement with 5% of active sites found by Busico with the same catalyst system at lower ethylene concentrations and 20°C.

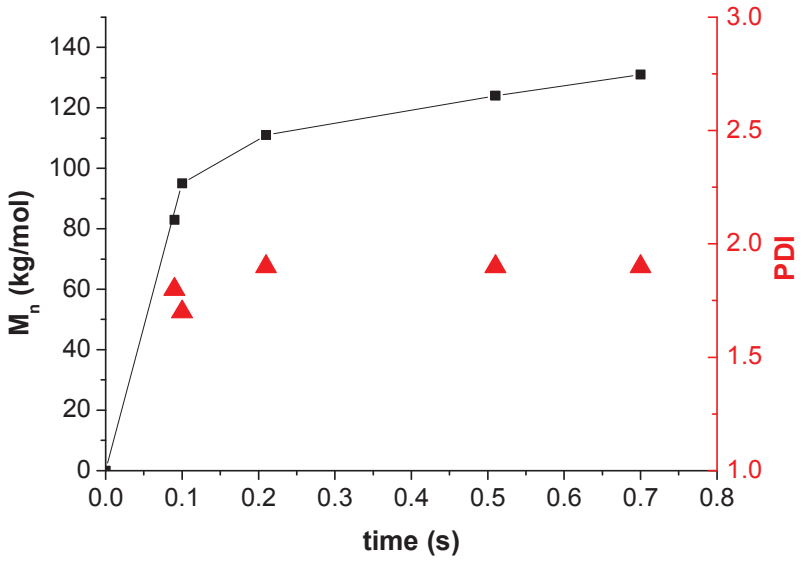

Figure 3:(■)Dependence of M_n from time for FESBIZrCl$_2$/MAO system at 25°C; (▲) Trend of PDI as function of time

Since the MWD does not increase linearly with the time, Natta's equation (see chapter I), not apply in the case of FESBIZrCl$_2$/MAO catalyst system.

However we could estimate the k_p value using the tests at shorter reaction times (runs 270 and 274). If the activities values, given in molPE·mol$_{Zr}^{-1}$·s^{-1}·[C_2H_4]$^{-1}$, are divided for the fraction of active sites expressed as n_{chain}/n_{Zr} and that is respectively 0.06 and 0.07 mol·mol$_{Zr}^{-1}$ we found in both case that k_p is 2.4x10^5 L·mol^{-1}·s^{-1} which is in good agreement with results reported in literature (see Table 1). This is further evidence that the first tests are in the controlled regime.

The fact that the results agree well on the basis of tests run in different laboratories, with different reactors and material suppliers, give us confidence in the quality of our reactor, and the reproducibility of our operating procedures.

Considering that in batch reactor we have found the same value of activity than in QFR we could assume that the two series of tests, in batch and in QF reactor have the same fraction of active metal sites. Thus using the value of [M*]/[Zr] = 0.06 mol·mol$_{Zr}^{-1}$ we found that k_p for reaction in batch reactor at 25°C is 2.4x10^5 L·mol^{-1}·s^{-1}.This means that the QFR is able to reproduce the reaction conditions encountered at a longer time scale and the reactor works reasonably well, we know that the experiments are reproducible, and this gives us confidence when we go to interpret our results on less well-characterized catalyst systems

2.2 The rac-Me$_2$Si(2-methyl-4-phenyl-1-indenyl)$_2$ZrCl$_2$/AliBu$_3$/[HNMe$_2$Ph][B(C$_6$H$_5$)$_4$] system

We saw in the previous section that it is difficult to perform experiments in the controlled regime with the complex FESBIZrCl$_2$when it is activated with MAO, even at T = 25°C and [C_2H_4] = 0.16 mol·L^{-1} because of its high activity. There seemed to be no point pursuing an evaluation of the kinetic parameters of that catalyst system at higher temperatures using the quenched flow device. We therefore investigated other activation pathways using a combination of *i*Bu$_3$Al as alkylating agent and N,N-dimethylaniliniumtetra(pentafluorophenyl)borate, [HNMe$_2$Ph][B(C$_6$F$_5$)$_4$], as an activator.

Table 4. Ethylene polymerization in conventional glass reactor with FESBIZrCl$_2$/Al*i*Bu$_3$/[HNMe$_2$Ph][B(C$_6$H$_5$)$_4$] system.

Run[a]	T (°C)	Time (min)	Yield (g)	Activity (kgPE·mol$_{Zr}^{-1}$·h^{-1}·[C$_2$H$_4$]$^{-1}$)	M$_n$[b] (kg·mol^{-1})	PDI
ERC49_10	25	5	4.1	15.7x10^5	60	2.07

a. [FESBIZrCl$_2$] = 0.8µmol·L^{-1}; [*i*Bu$_3$Al] = 4mmol·L^{-1}; [[HNMe$_2$Ph][B(C$_6$F$_5$)$_4$]] = 1.6µmol·L^{-1} ; [C$_2$H$_4$] = 0.16 mol·L^{-1}; in 250 mL toluene.
b. GPC obtained using light scattering detector coupled with refractometer detector.

The experimental protocol used for the 5 minutes test in the glass reactor was different from one used for the tests in Table 2 since in this case a ternary system has been investigated. The [HNMe$_2$Ph][B(C$_6$F$_5$)$_4$] compound was added to a solution of *i*Bu$_3$Al (1mmol in 250 mL) in toluene. Then the solution was introduced into the batch reactor, which was then pressurized with ethylene (1.5 bar$_{abs}$) and the medium was stirred until the temperature reached the desired value. 10 mL of a solution of FESBIZrCl$_2$ in toluene was added through the small injection port at the top of reactor to start the polymerization.

The 5-minute activity of FESBIZrCl$_2$ activated by *i*Bu$_3$Al/[HNMe$_2$Ph][B(C$_6$F$_5$)$_4$] is on the same order of magnitude as that found for the FESBIZrCl$_2$/MAO system under the same experimental conditions (15.7x10^5 rather than 14x10^5 kgPE·mol$_{Zr}^{-1}$·h^{-1}·[C$_2$H$_4$]$^{-1}$). However, in spite of the activity shown by the FESBIZrCl$_2$/*i*Bu$_3$Al/[HNMe$_2$Ph][B(C$_6$F$_5$)$_4$] system in batch reactor we observed no activity for reaction times from 0 to 500 ms in the quenched flow reactor. Note that in the QFR all of the catalyst components are contacted in the same reactor under argon.

It was not possible to produce any measurable quantity of polymer even if the amount of catalyst precursor was increased from 4 µmol·L^{-1} to 16 µmol·L^{-1}, the temperature increased from 25°C to 60°C, or the B/Zr ratio increased from 2 eq. to 4 eq. In an attempt to overcome this limitation, different activation protocols were also assessed:

- Several tests were performed by adding the Zr complex to a solution of *i*Bu$_3$Al and [HNMe$_2$Ph][B(C$_6$F$_5$)$_4$]compound in toluene. It was expected that the activation of catalyst precursor could be improved after contacting the alkylating agent and the salt [HNMe$_2$Ph][B(C$_6$F$_5$)$_4$].

- In other tests, carried out for times up to 560 ms, the FESBIZrCl$_2$ complex was first added to a solution of *i*Bu$_3$Al in toluene in order to pre-form an alkylated species, FESBIZrCl(*i*Bu). The salt [HNMe$_2$Ph][B(C$_6$F$_5$)$_4$]was then added in a second step.

Once again no polymer was formed with either of these protocols, indicating that the formation of active species in presence of ethylene requires more than 500 ms. Bochmann[6] observed an induction period for propylene polymerization with the ethylene bis-indenyl based catalyst, SBIZrMe$_2$ (where SBI = rac-Me$_2$Si(Ind)$_2$) activated by a bulky co-catalyst such as [Ph$_3$C][CN{B(C$_6$F$_5$)$_3$}$_2$]. They postulated that zirconocene isobutyl (species **I** in Figure 4**)** generated by the system SBIZrMe$_2$/Al*i*Bu$_3$/[Ph$_3$C][CN{B(C$_6$F$_5$)$_3$}$_2$] leads to the formation of the active species by changing the anion coordination.

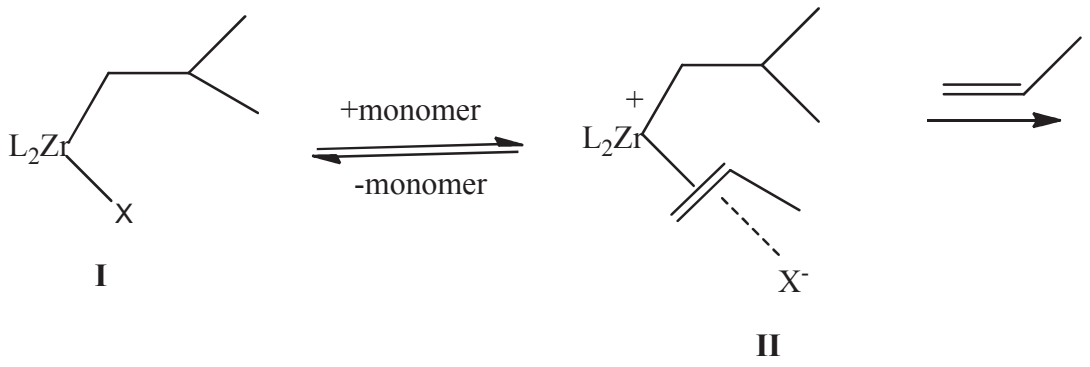

Figure 4. Possible formation of active states II as result of changes in anion coordination as proposed by Bochmann[6]

In the case of the FESBIZrCl$_2$/*i*Bu$_3$Al/[HNMe$_2$Ph][B(C$_6$F$_5$)$_4$] ternary system it appears that the species [FESBIZr(*i*Bu)][B(C$_6$F$_5$)$_4$], analogous to species **I** in Figure 4**,** was formed. The dissociation of the ion pair seems to be more complicated than that of the pair formed with MAO, and does not allow a fast initiation of polymerization – at least during the first fractions of a second, or possibly the first seconds of reaction. In this particular case the dissociation of this ion pair is a long event not suitable for the time scale of quenched flow. To see if the catalyst formed in the presence of ethylene might allow us to avoid the induction period, a solution of *i*Bu$_3$Al/[HNMe$_2$Ph][B(C$_6$F$_5$)$_4$] and one of FESBIZrCl$_2$ could be both pressurized in separate vessels with monomer. However the separation of the metallocene precursor from its co-catalyst should not lead in itself to a fast activation at time scale of QFR.

Another explanation for the observed induction period could be linked to the fact that in the QFR experiments, the Zr is contacted with *i*Bu$_3$Al and [HNMe$_2$Ph][B(C$_6$F$_5$)$_4$] in absence of ethylene. The implications of this will be discussed more deeply in the section of ((CPh$_2$)CpFluZrCl$_2$).

2.3 Conclusions

From these series of tests we have observed two limiting situations with the same catalyst precursor. When the metallocene FESBIZrCl$_2$ is activated by MAO the resulting complex is immediately active for ethylene polymerization. However, it is difficult to operate in a controlled regime for more than a fraction of a second. For times longer than 200 ms, the polymerization shows activities and molecular weight distributions typical of a Shultz-Flory regime even in mild conditions (T=25°C and P=1.5bar). Clearly if we wanted to investigate this polymerization catalyst under more realistic conditions it would be necessary to have a reactor that allowed us to obtain very short reaction times on the order of 10^{-1} to 10^{0} ms. Nevertheless, the results obtained at 25°C are in agreement with results already reported in literature[1] using a different device and large excess of MAO, meaning that the QFR developed in the current work is able to give very reproducible results.

On the other hand, using the FESBIZrCl$_2$/*i*Bu$_3$Al/[HNMe$_2$Ph][B(C$_6$F$_5$)$_4$] ternary system to activate the catalyst leads to creation of an induction period that lasts for at least 0.5 seconds, even if we increase the temperature of the reaction to 60°C. In this case we would need a device able to offer us longer reaction times, e.g. in the range of several seconds, in order to avoid this problem (providing of course that all of the active sites are activated simultaneously). One possible solution could be the use of a methylated metallocene precursor, FESBIZrMe$_2$, which could improve the efficiency of catalyst system.

From these series of tests we could conclude that in order to investigate the activation of FESBIZrCl$_2$ it is necessary to stretch the window of residence times beyond what is possible with our quenched flow device.

3. The diphenylmethylidene(cyclopentadienyl)(fluorenyl) zirconium dichloride catalyst precursor

Diphenylmethylidene-cyclopentadienyl-fluorenyl zirconium dichloride ($(CPh_2)CpFluZrCl_2$) is a C_s-symmetric *ansa*-metallocene catalyst precursor, sterically open and it is well known to produce syndiotactic polypropylene[7].

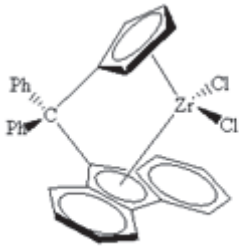

Figure 5. Diphenylmethylidene-cyclopentadienyl-fluorenyl zirconium dichloride

It was also used for synthesis of copolymers of ethylene with propylene, hexene or higher α-olefins[8].

When activated with MAO, $(CPh_2)CpFluZrCl_2$ shows an activity of 3×10^3 $kgPE\cdot mol_{Zr}^{-1}\cdot h^{-1}\cdot[C_2H_4]^{-1}$, somewhat lower than activity of $FESBIZrCl_2$/MAO catalyst system ($16x10^3$ $kgPE\cdot mol_{Zr}^{-1}\cdot h^{-1}\cdot[C_2H_4]^{-1}$) under similar experimental conditions (30°C P=2.5 bars Al/Zr= 250). In addition, the $(CPh_2)CpFluZrCl_2$ system allows to obtain a high value of the molecular weight ($M\eta= 630x10^{-3} g\cdot mol^{-1}$) [5].

At high temperatures 130°C, and high pressure, 25 bar, the catalyst system $(CPh_2)CpFluZrCl_2/iBu_3Al/[PhNMe_2H][B(C_6F_5)_4]$ shows a higher activity ($13.2x10^3$ $kgPE\cdot mol_{Zr}^{-1}\cdot h^{-1}\cdot[C_2H_4]^{-1}$) and broad molecular weight distribution (M_n = $40x10^3$ $g\cdot mol^{-1}$ and PDI = 2.9)[9].

In order to determine the best experimental conditions to evaluate the desired kinetic parameters, preliminary tests were performed using the catalyst system $(CPh_2)CpFluZrCl_2$/MAO/tBu_2-PhOH (described in detail in section 3.2). For practical reasons the homopolymerization of ethylene using $(CPh_2)CpFluZrCl_2$ with different co-catalyst systems was assessed at temperature of 60°C(the quenched flow device was not able to work

at temperatures higher than 80°C). As shown in Table 5, high activity (one order of magnitude than activity at 40°C) and molar mass were obtained at 60°C.

Table 5.Dependence of activity from temperature for (CPh_2)CpFluZrCl_2/MAO/*t*Bu_2-PhOH in batch reactor

Run[a]	T (°C)	[(CPh_2)CpFluZrCl_2] ($\mu mol \cdot L^{-1}$)	Time (min)	Y (g)	Activity[b]	M_n[c] ($kg \cdot mol^{-1}$)	PDI
ERC37_10	40	2	10	0.098	$4.1x10^3$	92	1.5
ERC35_10	60	2	10	1.5	$62x10^3$	208	2.0

a. Al/Zr = 2000; *t*Bu_2-PhOH/Al = 0.5;[C_2H_4] = 0.29 $mol \cdot L^{-1}$; in 250 mL of toluene; **b.** $kgPE \cdot mol_{Zr}^{-1} \cdot h^{-1} \cdot [C_2H_4]^{-1}$ **c.** GPC obtained using PE relative calibration.

The activation of (CPh_2)CpFluZrCl_2 complex with different co-catalyst systems was assessed; MAO, MAO with the addition of *t*Bu_2-PhOH, Al*i*Bu_3 in combination with [Me_2PhNH][$B(C_6F_5)_4$] complex, were used as activators.

3.1 The CpFluZrCl₂/MAO system

The first activator used for the investigation of (CPh_2)CpFluZrCl_2 complex was MAO. The yield, average activity, M_n and PDI for ethylene polymerization using this metallocene complex activated by MAO in a glass batch reactor are reported in Table 6. The polymerization was performed by injecting the zirconium complex in a 250 mL of solution of MAO (2 $mmol \cdot L^{-1}$) in toluene into the reactor under 2 bar_{abs} of ethylene.

Table 6.Ethylene polymerization by (CPh_2)CpFluZrCl_2/MAO system in batch reactor.

Run[a]	Time (min)	Yield (mg)	Activity ($kgPE \cdot mol_{Zr}^{-1} \cdot h^{-1} \cdot [C_2H_4]^{-1}$)	M_n[b] ($kg \cdot mol^{-1}$)	PDI
ERC16_10	10	75	$13x10^3$	48	2.27

a. [(CPh_2)CpFluZrCl_2] = 1$\mu mol \cdot L^{-1}$; Al/Zr = 2000; [C_2H_4] = 0.13 $mol \cdot L^{-1}$; T = 60°C in 250 mL toluene; **b.** GPC obtained using PE relative calibration.

The activity measured for this test is two orders of magnitude lower than activity observed for the FESBIZrCl_2/MAO at 25°C and 40°C ($14x10^5$ and $44x10^5$ $kgPE \cdot mol_{Zr}^{-1} \cdot h^{-1} \cdot [C_2H_4]^{-1}$ respectively, as reported in Table 2), which is a general indication of inherent slowness of this metallocene-based catalyst.

However using quenched flow reactor it was possible to recover a measurable amount of polymer in only one of the tests (run 253), carried out at the longest possible reaction time (1.03 seconds) and at higher monomer concentrations than usual (0.37 $mol{\cdot}L^{-1}$ vs 0.13 $mol{\cdot}L^{-1}$ of test ERC16_10), and with more metallocene than in the test batch (12 $\mu mol{\cdot}L^{-1}$ instead of 2.5 $\mu mol{\cdot}L^{-1}$). In this case, the measured activity ($4.7x10^3$ $kgPE{\cdot}mol_{Zr}^{-1}{\cdot}h^{-1}{\cdot}[C_2H_4]^{-1}$) was lower than that measured in the batch reaction. And even so, only 3 mg of PE was recovered which is not sufficient for further characterization.

The fact that we can make polymer in the batch reactor, but not in the QFR suggests that there is an induction period. It is well know that the presence of "free" TMA in commercial MAO can lead the formation of hetero-bimetallic species, the so-called dormant sites, leading to a decreasing of the concentration of active species. As reported in the literature[10], the addition of 2,6 di-*ter*-butylphenol in MAO can greatly improve the performance of catalysts. For this reason a series of tests have been carried out in order to investigate the whether or not the combination of MAO/2,6 di-*ter*-butylphenol as activator of $(CPh_2)CpFluZrCl_2$ complex could help reduce or eliminate this induction period.

3.2 The $(CPh_2)CpFluZrCl_2$/MAO/tBu_2-PhOH system

The 2,6 di-*ter*-butylphenol (tBu_2-PhOH) was added to MAO in an attempt to enhance the activation of the catalyst. As explained above, the "free" trimethylaluminium (TMA), invariably present in commercial methylaluminoxane, is responsible for formation of a hetero-bimetallic adduct (species **I** in Figure 6) which is a dormant site and reduces the efficacy of catalysts since it is not involved in chain propagation.

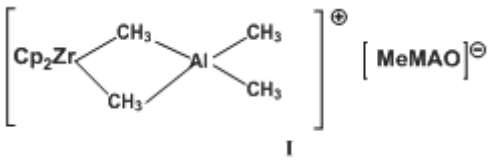

Figure 6.Dormant site species formed by reaction of metallocene precursor and MAO

When the phenol reacts with the "free" TMA, in a ratio of 2:1, the MeAl-(O-Ph(tBu)$_2$)$_2$ complex is formed[10]. These Al-compounds are described as non-interacting scrubbing agents

for metallocene precursors in combination with boron-based compounds because they do not (in principle) interact with the catalyst. Particular attention was paid to tBu$_2$-PhOH/Al ratio because it has been shown that optimal experimental conditions are obtained when a little bit of more than 2 eq. of phenol is used per "free" TMA. Since in commercial MAO the free TMA content is in the range of 20 mol% to 40 mol%, a ratio of tBu$_2$-PhOH/Al of 0.5 to 0.9 was used. The amount of "free" TMA content in MAO was determined by ^{1}H NMR. The NMR analyses on the batch of MAO used for these series of tests showed that the "free" TMA was about 22 mol% (see appendix C).

A series of tests was carried out in a batch reactor in order to find the best experimental conditions to apply for quenched flow investigations. In particular we focused on the influence of tBu$_2$-Ph-OH/Al ratio on activity, so two polymerization tests with ratio of tBu$_2$-Ph-OH/Al of 0.5 and 0.9 were performed.

Table 7. Influence of tBu$_2$-Ph-OH/Al ratio on the activity and MWD of (CPh$_2$)CpFluZrCl$_2$/MAO/tBu$_2$-PhOH system

Run[a]	**[(CPh$_2$)CpFluZrCl$_2$]** (μmol·L^{-1})	**Time** (min)	**tBu$_2$-PhOH/Al**	**Yield** (g)	**Activity**[b]	**M$_n$**[c] (kg·mol^{-1})	**PDI**
ERC13_10	1	10	0.9	0.53	40x10^3	714	1.8
ERC35_10	2	10	0.5	1.5	60x10^3	208	2.0

a.Al/Zr = 2000; [C_2H_4] = 0.29 mol·L^{-1}; T = 60°C; in 250 mL of toluene; **b**. kgPE·mol$_{Zr}^{-1}$·h^{-1}·[C_2H_4]$^{-1}$**c**. GPG value obtained using light scattering detector coupled with refractometer detector.

In our case a slightly more than 2 equivalents of tBu$_2$-PhOH, which corresponds to tBu$_2$-PhOH/Al = 0.5 ratio are enough to trap the free TMA. We could conclude that when the content of TMA is around 20% a tBu$_2$-PhOH/Al = 0.5 is a suitable value for the runs. The activity obtained using a combination of MAO and phenol is higher than the activity observed for (CPh$_2$)CpFluZrCl$_2$/MAO catalyst system. Even the molar masses found were one order of magnitude higher than ones found by using only MAO as co-catalyst.

Series of tests in quenched flow reactor

Tests in the quenched flow reactor were performed at 60°C and [C_2H_4] = 0.37 mol·L^{-1}, with a ratio of tBu$_2$-PhOH/Al = 0.5. The tBu$_2$-PhOH was added to a solution of MAO (3 mmol·L^{-1}) in toluene used as a scavenger, and to a solution of MAO (17 mmol·L^{-1}) in toluene used as the activator. Both solutions were stirred for 30 minutes at room temperature, and then introduced into the QFR feed reservoirs, one of which was pressurized with ethylene and the second with

argon (both to 11bar$_{abs}$). When the solutions reached the desired temperature (this took about 15 minutes) a solution of (CPh_2)CpFluZrCl_2 complex in toluene was added to vessel 2. The pre-contact time is particularly important in order to promote the reaction between the phenol and "free" TMA. The tests in Table 8 were carried out following this experimental protocol.

Table 8. Ethylene polymerization by (CPh_2)CpFluZrCl_2/MAO/*t*Bu_2-PhOH system in quenched flow reactor

Run[a]	**Time** (s)	**Yield** (mg)	**Activity** kgPE·mol$_{Zr}^{-1}$·h^{-1}·[C_2H_4]$^{-1}$	**M_n**[b] (kg·mol^{-1})	**PDI**	**n_{chain}/n_{Zr}**	**Monomer consumption**(%)
259	0.20	-	-	-	-	-	-
255	0.51	6	$22x10^3$	64	2.4	0.01	0.12
254	0.8	13	$31x10^3$	68	2.9	0.03	0.24
252	0.93	19	$39x10^3$	69	1.8	0.05	0.75

a.[(CPh_2)CpFluZrCl_2] = 10µmol·L^{-1}; Al/Zr = 2000; *t*Bu_2-PhOH/Al = 0.5; T = 60°C; [C_2H_4] = 0.37mol·L^{-1} in 500 ml of toluene **b.**GPC obtained using universal PS calibration

At the shortest reaction time no polymer was recovered. The activities obtained with the QFR were lower than the activity measured in batch reactor. In addition the number of chains per mol of zirconium was very low, and the polymers exhibited a high polydispersity index. In fact GPC chromatogram of run 254 and 255 showed a bimodal profile (see Figure 7).

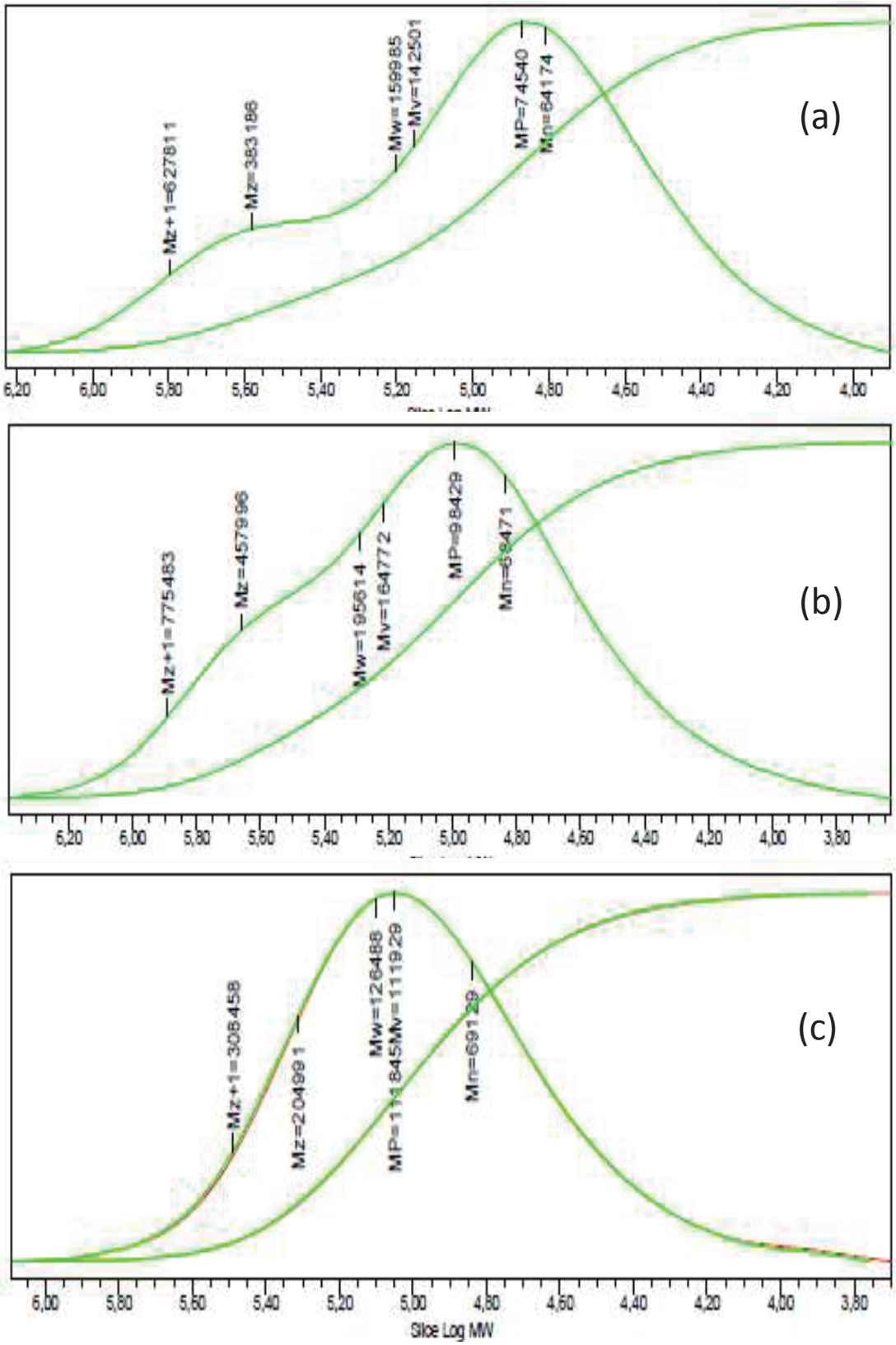

Figure 7. GPC profiles of test 255 (a), test 254 (b) and test 252 (c)

The bimodal profile of MWD suggests the presence of (at least) two different active sites. It appears that the fraction of high molar mass is less important at long polymerization times. However, the number of polymer chains per mol of Zr is indicative of very low concentration of active species, and the fact that no polymer was recovered below 500 ms is indicative of an induction period. While the induction period is short with respect to the residence time of a commercial reaction, it is still noticeable at the scale of the QFR. In addition, the fact that the PDI was broad suggests that the metallic sites active slowly and perhaps to form different active species at the time scale of these experiments.

Considering that both MAO and MAO with phenol both led to relatively low activities and slowly activating catalysts on the QFR time scale leads us to conclude that MAO is not a suitable activator for this metallocene complex. In next session the use of borate salt as activator is investigated.

3.3 The $(CPh_2)CpFluZrCl_2/iBu_3Al/[PhNMe_2H][B(C_6F_5)_4]$ system

The previous results have shown that reaction between MAO and $(CPh_2)CpFluZrCl_2$ leads to system which is not immediately active in the presence of monomer on the time scale of the quenched flow reactor. We tried to improve the performance of MAO with the addition of phenol, having initially postulated that free TMA was at the origin of the problem. As shown in the previous section the $(CPh_2)CpFluZrCl_2$/MAO/tBu$_2$-PhOH did not show significant improvements with respect to MAO alone, thereby leading us to conclude that the problem is not (only) free TMA.

In order to find a more suitable co-catalyst system we tried to activate $(CPh_2)CpFluZrCl_2$ using boron-based compounds. The activation of $(CPh_2)CpFluZrCl_2$ with borate salts has been reported in literature [8, 11]. It was observed that the strong Lewis acid $B(C_6F_5)_3$ was not useful for a CpFlu-based complex[12], while activators such as MAO or $[R][B(C_6F_5)_4]$ (where R = Me_2PhNH, Ph_3C) in combination with AlR_3 showed good results, even at elevated temperatures.

An initial reaction was carried out in the batch reactor using the anilinium-based salt $[Me_2PhNH][B(C_6F_5)_4]$. A solution of iBu$_3$Al (1 mmol per 250 mL) and the

$[Me_2PhNH][B(C_6F_5)_4]$ (4 $\mu mol \cdot L^{-1}$), in toluene was filled in the reactor and pressurized with ethylene up to 4 bar_{abs}. When the temperature reached 60°C a solution of Zr in toluene was injected through the injection module on the top of reactor. The results are reported in Table 9.

Table 9. Ethylene polymerization using $(CPh_2)CpFluZrCl_2/iBu_3Al/[Me_2PhNH][B(C_6F_5)_4]$ catalyst system

Run[a]	Time (min)	Yield (g)	Activity ($kgPE \cdot mol_{Zr}^{-1} \cdot h^{-1} \cdot [C_2H_4]^{-1}$)	M_n[b] ($kg \cdot mol^{-1}$)	PDI
ERC44_10	14	3.67	108 x10^3	156	2.04

a.$[(CPh_2)CpFluZrCl_2]$ = 2$\mu mol \cdot L^{-1}$; Al/Zr = 2000; B/Zr = 2; $[C_2H_4]$ = 0.29$mol \cdot L^{-1}$ in toluene; **b.**GPC obtained with the light scattering detector coupled with refractometer detector.

As shown in Table 9, although the molar mass is slightly lower than the molar mass found for the $(CPh_2)CpFluZrCl_2$/MAO/*t*Bu_2-PhOH system, the activity is higher than ones found using the other co-catalysts. This was encouraging for tests in QFR.

Other reactions were carried out by first mixing the $(CPh_2)CpFluZrCl_2$ with the alkylating agent and, afterwards, the borate salts in order to form the monobutylated species and then the ion pair. However this strategy displayed poor activity. This further underlines that it is of high importance to contact first the $[Me_2PhNH][B(C_6F_5)_4]$ compound withAl*i*Bu_3in order to form an aluminium salt[13]

Surprisingly, the tests in QFR did not shown reliable results. We have changed the experimental parameters such as: Zr concentration (increasing from 10 to 20 $\mu mol \cdot L^{-1}$); the Al/Zr ratio (increasing from 100 to 200 eq.); the use of $[CPh_3][B(C_6F_5)_4]$ in place of $[Me_2PhNH][B(C_6F_5)_4]$ (test 261).Even the sequence of addition of the three components of system was also varied. We have investigated the behavior of catalyst system when the Zr-complex is added only when the contact between Al*i*Bu_3 (0.5$mmol \cdot L^{-1}$) in toluene the $[Me_2PhNH][B(C_6F_5)_4]$ compound is already occurred, and when the Zr-complex was added to a solution of *i*Bu_3Al (0.5$mmol \cdot L^{-1}$) in toluene before the addition of $[Me_2PhNH][B(C_6F_5)_4]$ compound.

2 mg of polymer were obtained for the test at [Zr] = 20 $\mu mol \cdot L^{-1}$ with a reaction time of 3.34 seconds, which is the longest time that we can manage in the QFR; no polymer was obtained at shorter times, or for lower catalyst concentrations.

It is important to note that QFR investigations require mixing the precatalyst and the co-catalyst in absence of ethylene. Considering that, one possible explication of lack of activity for quenched flow experiments could be due to formation of non active species or species which require an activation period when the zirconium complex is combined with *i*Bu_3Al and $[Me_2PhNH][B(C_6F_5)_4]$ in absence of ethylene. Götz et al.[11] investigated the system $(CPh_2)CpFluZrCl_2$/*i*Bu_3Al/$[Me_2PhNH][B(C_6F_5)_4]$ by NMR and showed that in the presence of large excess of *i*Bu_3Al the formation of a hetero-bimetallic complex $[(CPh_2)CpFluZriBu•iBu_3Al]^+$ which can evolve to form the compound [(CPh_2)CpFluZr-μ-H-μ-*i*Bu_2Al] (see Figure 8) via loss of isobutene. These species have been detected in absence of monomer. It appears that the coordination of ethylene on later bimetallic species can certainly be a rate limiting step because of the coordination of the vinyl unit of the Al moiety on the Zr center.

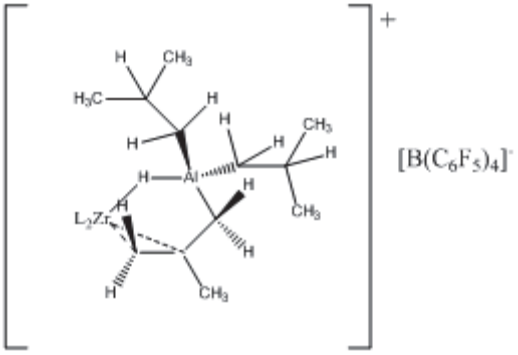

Figure 8. Species formed by reaction between $(CPh_2)CpFluZrCl_2$ and *i*Bu_3Al/$[Me_2PhNH][B(C_6F_5)_4]$

In order to see if we could avoid the induction period a series of tests were performed in presence of 1-hexene.

3.4 The $(CPh_2)CpFluZrCl_2$vs the activator: addition of α-olefins for improving the activation.

An important effect observed for conventional Ziegler Natta copolymerization is the increased ethylene consumption in the presence of α-olefins. The same effect has been observed also for metallocene-based catalysts depending on their structure. How the α-olefin acts is not fully understood. It has been suggested that with the introduction of the α-olefin, the ion pair

formed between catalyst precursor and the activator might be more dissociated than in absence of co-monomer.

We therefore decided to add 1-hexene in the reaction medium in an attempt to eliminate the induction period showed by the (CPh_2)CpFluZrCl_2/*i*Bu_3Al/[Me_2PhNH][B(C_6F_5)$_4$].

A test was carried out in the batch reactor adding 1-hexene (% of 1-hexene respect to ethylene = 33%) to a solution of MAO/*t*Bu_2-PhOH. As usual 10 mL solution of toluene and (CPh_2)CpFluZrCl_2 was filled through the small injection cartridge on the top of reactor. The results are shown in Table 10.

Table 10. Ethylene/1-hexene copolymerization using (CPh_2)CpFluZrCl_2/MAO/ *t*Bu_2-PhOH system in batch reactor

Run[a]	**Time** (min)	**Yield** (g)	**Activity** (kgPE·mol_{Zr}^{-1}·h^{-1}·$[C_2H_4]^{-1}$)	**M_n**[b] (kg/mol)	**PDI**
ERC41_10	10	2.2	$91x10^3$	92	1.7

a.[(CPh_2)CpFluZrCl_2] = 2μmol·L^{-1}; Al/Zr = 1000; *t*Bu_2-PhOH/Al = 0.5; [C_2H_4] = 0.29 mol·L^{-1};[C_6H_{12}] = 0. 037 mol; in 250 mL of toluene; **b**.GPC obtained with the light scattering detector coupled with refractometer detector.

A slightly increase in the activity is observed with respect to the same system without the hexene, and the observed rate is close to what we obtained with borate salt as co-catalyst.

The influence of addition of 1-hexene has been investigated on different systems in the quenched flow reactor. For (CPh_2)CpFluZrCl_2/*i*Bu_3Al/[$PhNMe_2$H][B(C_6F_5)$_4$] catalyst system the 1-hexene was added in a solution of *i*Bu_3Alanilinium borate in toluene before the addition of a solution of metallocene. In another test the 1-hexene was added to (CPh_2)CpFluZrCl_2/*i*Bu_3Al/[$PhNMe_2$H][B(C_6F_5)$_4$] catalyst solution in toluene.No polymer was recovered in either case for polymerisations lasting up to 1.5 seconds. Some polymer (7 mg) was obtained using the (CPh_2)CpFluZrCl_2/MAO catalyst system at a reaction time of 1.35s. Here the 1-hexene was added after the pre-contact between metallocene precursor and activator. The 7 mg of polymer recovered were used to perform the DSC analysis shown in Figure 9**.** The polymer obtained is a highly crystalline (77%) PE with a low amount of inserted hexene.

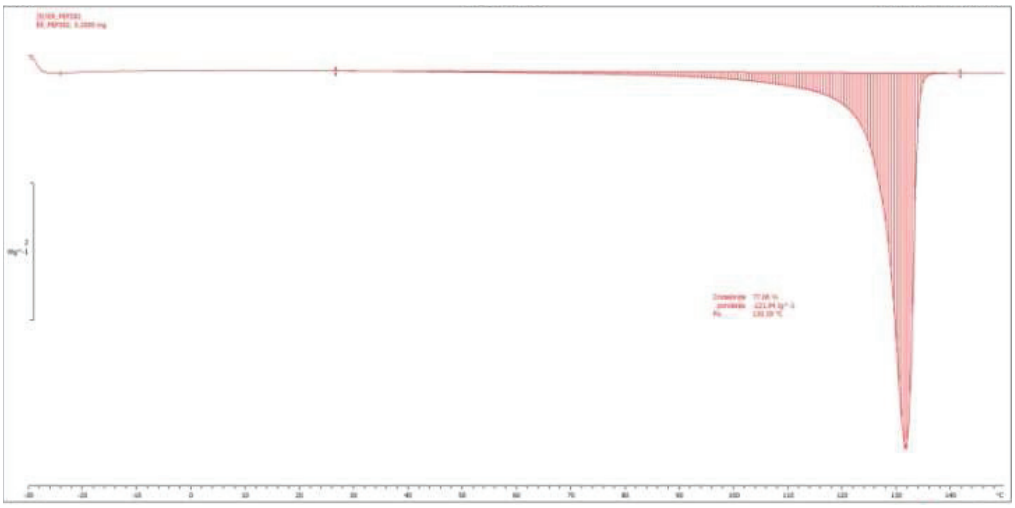

Figure 9.DSC thermogram of test 282

However the activity with the $(CPh_2)CpFluZrCl_2$/MAO catalyst was only $7x10^3$ $kgPE \cdot mol_{Zr}^{-1} \cdot h^{-1} \cdot [C_2H_4]^{-1}$, which is lower than that obtained without the addition of 1-hexene.

3.5 Conclusions

In this section both the first instants of polymerization of ethylene using $(CPh_2)CpFluZrCl_2$ complex, as well as longer time polymerizations have been investigated. The metallocene complex was activated by MAO, MAO modified via the addition of tBu$_2$-PhOH, and by the combination of$i$Bu$_3$Al with borate salt. In every case measurable polymerization activities were found in the batch reactor, but they were lower than the other metallocene catalysts that we investigated.

When the polymerization was done in the QFR, induction periods on the order of the time scale of the reactor residence times were observed. Activation parameters have been varied in order to solve these problems: the monomer concentration and the complex concentration have been increased, the Al/Zr ratio has been varied, and longer reaction times, in time scale of quenched flow, have been implemented. Even the addition of α-olefins in order to increase the activity has been investigated. In most cases little or no polymer was recovered. In experiments that lasted a (relatively) long time, small amounts of polymer were produced. However the polymers obtained had either a very broad, or bimodal MWD, or less than 5% of

Zr atoms (mol of PE per number of Zr = 0.05) introduced in the reactor were found to be active.

The initial induction period was found to be longer than one second in the case of (CPh_2)CpFluZrCl_2/MAO and (CPh_2)CpFluZrCl_2/MAO/*t*Bu_2-PhOH catalysts system, and longer than 2 seconds in the case of (CPh_2)CpFluZrCl_2/Al*i*Bu_3/[Me_2PhNH][B(C_6F_5)$_4$] catalyst system. In a conventional time scale this induction period is negligible but not in the quenched flow experiments. The QFR allows us to see that these catalysts activate in a very different manner than the FESBIZrCl_2, and that in certain cases there are at least 2 families of sites active (again perhaps only on the time scale of the QFR experiments).

Different explanations might be offered for the induction period. In the case of polymerization in conventional reactor the Zr catalyst precursor is injected in a solution saturated with ethylene containing the activator. In the case of QF system which requires instantaneous formation of active species the Zr complex is combined with the activator in the same vessel under Ar atmosphere to form first the expected cationic active species. In the case of catalyst based on (CPh_2)CpFluZrCl_2 it is possible that this reaction must be performed in presence of ethylene in order to form efficient active sites.

Another explication could be related to structure of the bridged cyclopentadienylfluorenyl structure.In fact the fluorenyl moieties have shown a facile slippage of central metal-bound five member ring from $\eta^5 \rightarrow \eta^3 \rightarrow \eta^1$ coordination which could also be a factor in their instability[14,15]. Evidently during the alkylation step this complex mighty change in its bonding hapticity, and the induction period might be explained as a rearrangement in the fluorenyl ligand.

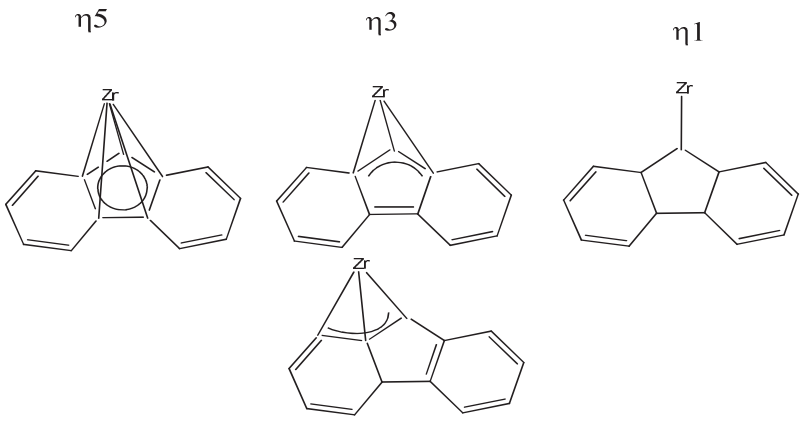

Figure 10. Changing in bonding hapticity

In conclusion the current design of the stopped flow reactor is not suitable for the determination of k_p and [M*]/[Zr] for this type of metallocene. However, we did learn that there is an induction period, and that (at least for the time scale of the QFR) some of the catalyst systems have at least 2 families of active sites. In the rare cases where we did make polymer the very broad MWD leads us to conclude that the activation of the metal atoms takes place progressively and not instantaneously as it did with FESBIZrCl$_2$

4. The bis(pentamethylcyclopentadienyl)zirconium dichloride precursor.

The sterically hindered bis(pentamethylcyclopentadienyl)zirconium dichloride Cp*$_2$ZrCl$_2$, where Cp*=C$_5$Me$_5$ is the last metallocene precursor candidate used for our study.

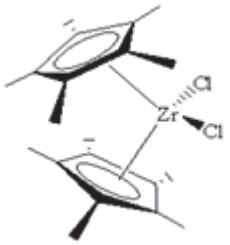

Figure 11.The (η^5-Cp*)$_2$ZrCl$_2$

The Cp*$_2$ZrCl$_2$ complex has been chosen because of its low tendency to form hetero-bimetallicadducts[6]. In fact, both of the cyclopentadienyl ligands are encumbered by 5 methyl groups, and the repulsion between these groups leads to a Cp-Zr-Cp bond angle of 134°. At low Al/Zr ratio this catalyst has shown quite low activity (1300 kgPE·molZr^{-1}·h^{-1}·[C$_2$H$_4$]$^{-1}$ at 30°C, 2.5bar of ethylene and Al/Zr=200) for ethylene homopolymerization, but on the other hand it has provided a polymer with high Mη(=1500x10^3 g·mol^{-1})[5].

As reported in literature the Cp*$_2$ZrCl$_2$/MAO catalyst system is also able to show a living behavior, under certain conditions. For example, at very low Al/Zr ratio (=12) it showed living behavior for ethylene polymerization[16], even at a temperature of 60°C, for several minutes (from 5 to 20 minutes). It remained in the pseudo-living regime[16] represented by a low value of polydispersity index (PDI = 1.7 after 20 minutes of polymerization) while M_n

was lower than 5000 g·mol^{-1}. We suspect that, at low Al/Zr ratio, a very peculiar polymerization system is formed which is hardly comparable the one obtained using more conventional experimental conditions.

In the next paragraphs we have investigated the activation of $Cp^*_2ZrCl_2$ with MAO (Al/Zr = 1000) at three temperature, 25°C, 40°C and 60°C under one bar of ethylene pressure. Unless otherwise indicated the GPC chromatograms have been obtained with universal calibration using PS standards.

4.1 The $Cp^*_2ZrCl_2$ in a batch reactor

The dependence of $Cp^*_2ZrCl_2$/MAO system on temperature is shown in Table 11. In order to find the best experimental conditions which allow us to work in quenched flow reactor we have tested in batch reactor this catalyst system at three different temperatures 25°C, 40°C and 60°C under the same monomer pressure.

Table 11. The $Cp^*_2ZrCl_2$/MAO at different temperatures and at same monomer pressure, 1 bar, in batch reactor

run[a]	T (°C)	[$Cp^*_2ZrCl_2$] (μmol·L^{-1})	[C_2H_4] (mol·L^{-1})	Time (min)	Y (g)	activity[b]	M_n (kg·mol^{-1})	PDI
ERC11_24	25	2	0.11	8	2.56	3.5 x10^5	760	1.66
ERC05_10	40	0.8	0.09	15	2.43	5.4 x10^5	362	1.63
ERC11_13	60	2	0.07	10	1.94	3.3x10^5	57	1.84

a.Al/Zr = 1000 in 250 mL of toluene; **b.**kgPE·molZr^{-1}·h^{-1}·[C_2H_4]$^{-1}$

The reactions, reported in Table 11, were carried out according the following experimental procedure: a 250 mL solution of MAO in toluene has been filled in 500 mL of glass batch reactor, and saturated with 1 bar of ethylene and 1 bar of argon. When the set point conditions are reached, the solution of catalyst precursor in toluene has been added via the injection module on the top of the reactor.

As shown in Table 11 the activity of $Cp^*_2ZrCl_2$/MAO showed a maximum at 40°C. This catalyst system appears to deactivate slightly at higher temperatures. This catalyst system has, generally, an activity lower than activity of $FESBIZrCl_2$/MAO at same temperatures

(FESBIZrCl$_2$/MAO has an activity of 44x10^5 kgPE·mol$_{Zr}^{-1}$·h^{-1}·[C$_2$H$_4$]$^{-1}$ under the same conditions).

4.2 The Cp*$_2$ZrCl$_2$/MAO system at 60°C in QFR

A series of tests was performed using Cp*$_2$ZrCl$_2$ activated with MAO at 60°C. All tests reported here and in next paragraphs were carried out at 3bar$_a$ meaning that 1 bar was argon and 2 bar were ethylene, with a ΔP of 2 bar. A solution of MAO as scavenger (0.5 mmol in 250 mL) in toluene was placed in the first vessel and pressurized with ethylene. Another solution contained MAO (0.75 mmol in 250 mL) in toluene and the metallocene complex was placed in the second feed vessel and pressurized with argon. The reaction was performed when the two solutions reached the desired pressure and temperature (10 minutes). The quench vessel, in this case was a glass vessel of 2L contained 300 mL of MeOH/HCl (10% in weight) at atmospheric pressure. The results obtained are reported in Table 12.

Table 12.Ethylene polymerization using Cp*$_2$ZrCl$_2$/MAO catalyst system using quenched flow reactor

run[a]	Time (s)	Y (mg)	activity	M_n (kg·mol^{-1})	PDI	n_{chain}/n_{Zr}	Y (mol/mol$_{Zr}$)	Monomer consumption(%)
166	0.08	10	5.6x10^6	74	1.9	0.11	308	1.02
165	0.1	12	6.5x10^6	51	1.9	0.24	443	1.44
163	0.18	25	6.3x10^6	90	2.0	0.24	783	2.90
153	0.45	27	2.8x10^6	85	2.2	0.29	877	2.55
154	0.45	33	3.7x10^6	95	1.8	0.34	1158	3.20

a.[Cp*$_2$ZrCl$_2$] = 1.90-2.44 µmol·L^{-1}; [C$_2$H$_4$] = 0.07 mol·L^{-1}; Al/Zr = 1000 T = 60°C in 570±40 mL of toluene; **b.** kgPE·mol$_{Zr}^{-1}$·h^{-1}·[C$_2$H$_4$]$^{-1}$

The catalyst displayed very high activity similar to the activity observed for the FESBIZrCl$_2$/MAO catalyst in both batch and QF reactor. The activity found is one order of magnitude higher than one observed in the batch reactor, which indicates that the catalyst Cp*$_2$ZrCl$_2$/MAO behave differently during the first instants of polymerization. In spite of this very high activity, the consumption of monomer was always lower than 5%. From plot of polymer yield according to time reported in Figure 12 it is possible to exclude the presence of

initial induction period, but the positive final curvature could be due to deactivation phenomena.

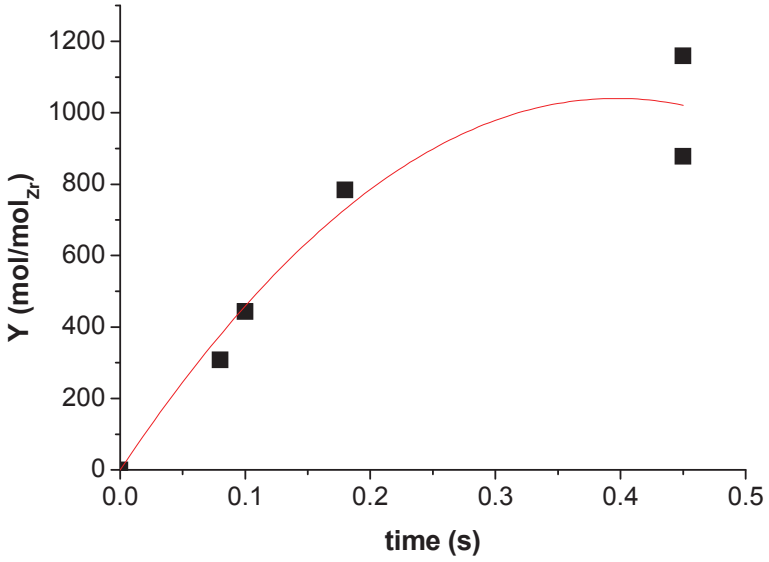

Figure 12. Dependence of polymerization yield according time for $Cp^*_2ZrCl_2$/MAO catalyst system at 60°C

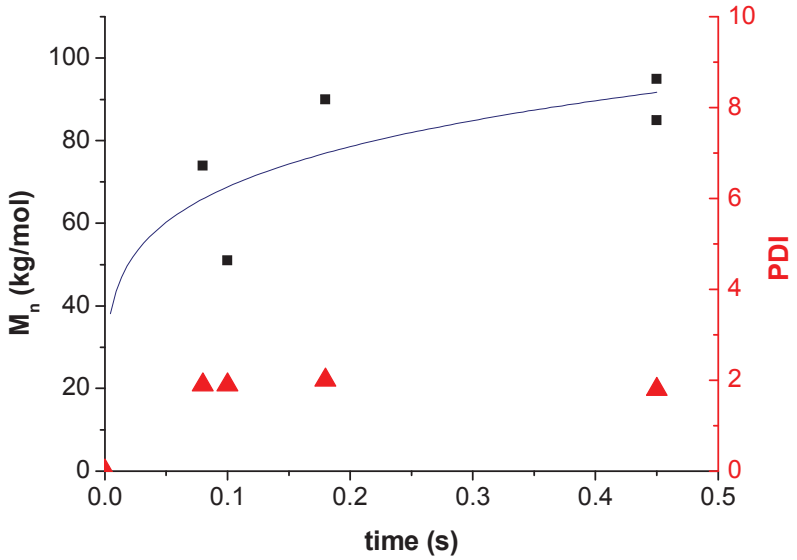

Figure 13.Dependence of M_n(■)according time; PDI evolution (▲)for $Cp^*_2ZrCl_2$/MAO catalyst system at 60°C

Furthermore as shown in Figure 13 the $Cp^*_2ZrCl_2$/MAO system at 60°C did not polymerize in living fashion even in this experimental conditions (low pressure). In fact the M_n value is

close to plateau value even at short reaction time 80 ms. Further the PDI values are typical of Schultz-Flory regime (1.8-1.9). The M_n value obtained in batch reactor, in the same experimental is slightly lower than ones obtained using quenched flow reactor (62 $kg{\cdot}mol^{-1}$ rather than average value of 80 $kg{\cdot}mol^{-1}$).

In conclusion the plateau values reached by molar masses at short reaction time suggest that this catalyst is out of initial controlled regime. In addition the non-linear increment of yield according to reaction time, which is also shown by decrement in activity after 0.45s seems to indicate that the behavior of catalyst change after the formation of the first polymer chains. This can be describing with a decreasing of the number of active sites or a change in the structure of the metal active sites. This is also related to the fact that at large time scale in batch reactor a lower activity was obtained.

This last investigation is a further proof that for very fast catalyst system the current design of quenched flow reactor is not a suitable for kinetic investigation which should be carried out at very short reaction time (probably in the order of ms).

4.3 The $Cp^*_2ZrCl_2$/MAO system at 40°C in QFR

Since k_p is function of temperature the polymerization temperature was decreased in order to get more convenient conditions for the investigation of this catalyst system. The M_n values obtained at 40°C (M_n = 285 $kg{\cdot}mol^{-1}$ see Table 11) are much higher than M_n obtained at 60°C meaning that at lower temperature the rates of chain transfer and termination reactions are decreased.

Table 13. The $Cp^*_2ZrCl_2$/MAO system at 40°C in quenched flow reactor.

run[a]	Time (s)	Y (mg)	activity	M_n ($kg{\cdot}mol^{-1}$)	PDI	n_{chain}/n_{Zr}	Y (mol/mol_{Zr})	Monomer consumption(%)
150	0.08	10	4.5×10^6	109	1.6	0.08	319	0.85
151	0.21	36	6.3×10^6	276	1.8	0.10	1170	3.05
157	0.22	40	6.7×10^6	275	2.1	0.11	1300	3.90
152	0.52	55	3.9×10^6	313	1.9	0.14	1856	4.55

a.$[Cp^*_2ZrCl_2]$ = 2.08-2.55$\mu mol{\cdot}L^{-1}$; $[C_2H_4]$ = 0.09 $mol{\cdot}L^{-1}$; Al/Zr = 1000 T = 40°C in 550±35 mL of toluene; **b**. $kgPE{\cdot}mol_{Zr}^{-1}{\cdot}h^{-1}{\cdot}[C_2H_4]^{-1}$

In terms of activity, the values shown in Table 15 are one order of magnitude higher than the ones measured in the batch reactor. However, the monomer consumption is always lower than 10%, and in some case lower than 1%. Concerning the molar masses, in spite of the increment of zirconium concentration in quenched flow reactor, the M_n values obtained are the same order of magnitude as obtained for polymerizations in the batch reactor.

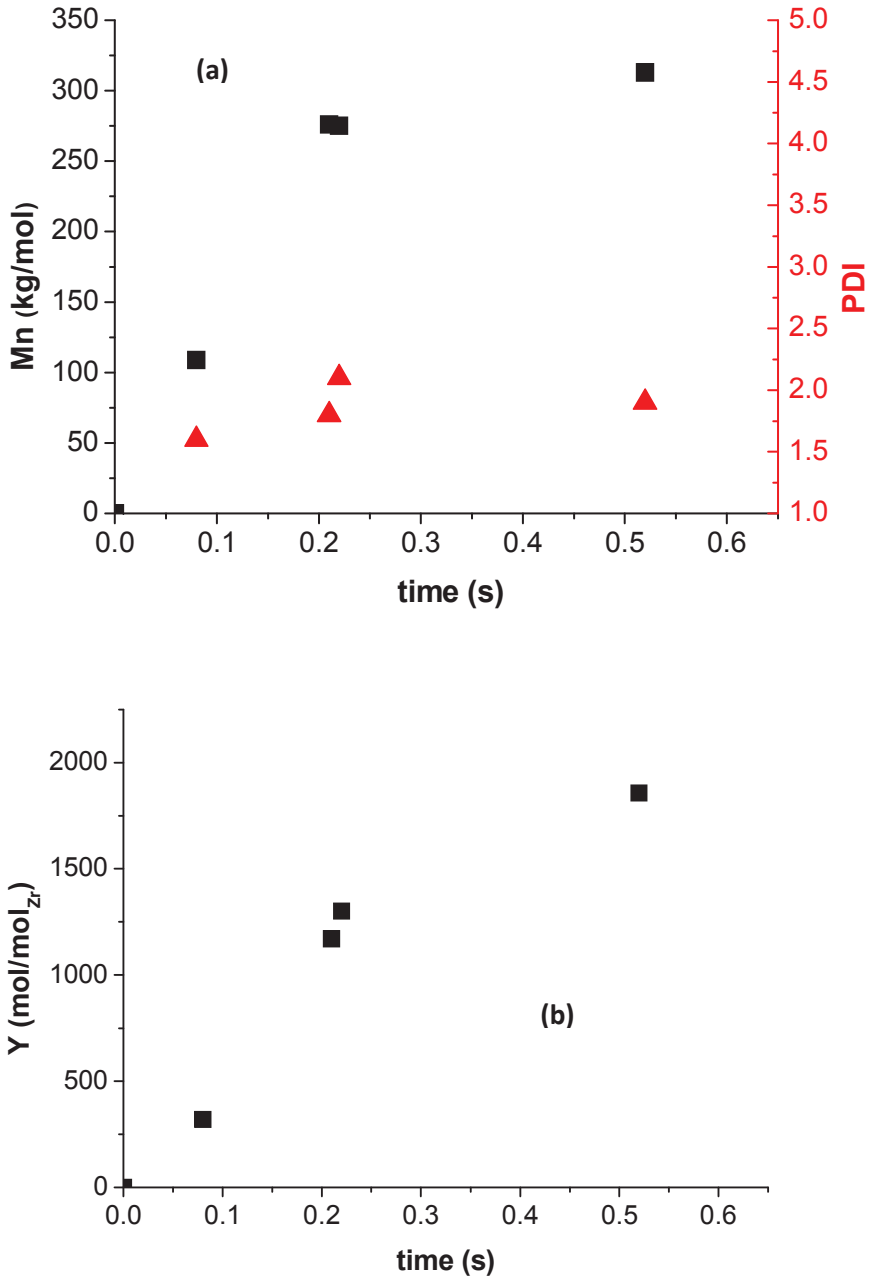

Figure 14.(a) Dependence of molar masses (■) and PDI evolution (▲) according to time; polymer yield (b) as function of time.

Focusing on the two plots in Figure 14, we can observe that at 40°C the $Cp^*_2ZrCl_2$/MAO worked in two regimes. For times below 200ms:

- M_n increased quite linearly with reaction time from 109 to 259 $kg{\cdot}mol^{-1}$ with surprisingly high Mw/M_n values (1.6-1.9);
- Polymerization yield increase linear with time.

These two trends are typical of initial controlled regime. While increasing the reaction times, over 200 ms:

- M_n reached a plateau with values of 300 $kg{\cdot}mol^{-1}$ which are comparable to results obtained in batch reactor, 290 $kg{\cdot}mol^{-1}$, and PDI values are typical of Schultz-Flory regime (2.0-2.2)
- Polymerization yield took a negative curvature.

These last results show that up to 200ms it was possible to keep in the initial controlled regime. Increasing the reaction times the $Cp^*_2ZrCl_2$/MAO catalyst system polymerized ethylene in Shultz-Flory fashion. Probably a further decrement of temperature could allow a better control of reaction. In order to validate this hypothesis a series of test at 25°C has been carried out.

4.4 The $Cp^*_2ZrCl_2$/MAO system at 25°C in QFR

As shown in previous paragraphs the $Cp^*_2ZrCl_2$/MAO catalyst system is strongly influenced by polymerization temperature. In fact at 60°C even at short reaction times (80-100 ms) it was impossible to keep the system in controlled regime. At 40°C the controlled regime was observed only at short reaction time, thus further decrease of polymerization temperature should insure a controlled regime for completely time scale permitted by quenched flow reactor. The experimental protocol followed has been described in section 4.2 and results are reported in Table 14.

Table 14. The $Cp^*_2ZrCl_2$/MAO system at 25°C in quenched flow reactor.

run[a]	Time (s)	Y (mg)	activity	M_n ($kg \cdot mol^{-1}$)	PDI	n_{chain}/n_{Zr}	Y ($mol \cdot mol_{Zr}^{-1}$)	Monomer consumption(%)
245	0.08	11	3.9×10^6	60	2.1	0.16	344	0.73
266	0.10	12	3.4×10^6	73	1.6	0.14	391	0.78
143	0.18	16	3.2×10^6	110	2.0	0.16	617	1.26
115	0.22	30	3.7×10^6	130	2.0	0.23	877	1.50
144	0.35	50	4.1×10^6	184	1.9	0.19	1557	3.52
155	0.65	97	4.2×10^6	362	2.3	0.23	2967	6.70

a.$[Cp^*_2ZrCl_2]$ = 1.8- 2.5µmol·L^{-1}; $[C_2H_4]$ = 0.11 mol·L^{-1}; Al/Zr = 1000; T = 25°C; in 550±45 mL toluene; **b.** $kgPE \cdot mol_{Zr}^{-1} \cdot h^{-1} \cdot [C_2H_4]^{-1}$

Form Table 14 we can observe a very good reproducibility in terms of the activity, and as shown in Figure 15 the productivity increase linearly with time and we did not observe for this temperature a decreasing in activity for long reaction time as seen for tests at 40°C and 60°C. Furthermore as observed also for tests at 60°C and 40°C the activity measured in QFR in one order of magnitude higher than activity observed in batch reactor.

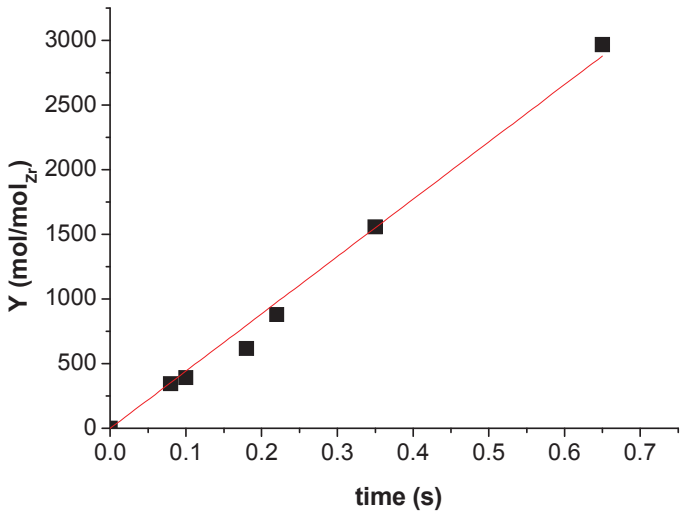

Figure 15. The dependence of yield as function of time for $Cp^*_2ZrCl_2$/MAO catalyst system at 25°C

Figure 16 shows that the number average molecular weight increased linearly with time for the range of polymerization times studied here**.** Despite this linear increase of M_n, we also

observed that the polydispersity index increased to around 2 (as discussed in Chapter I, we would expect PDI of around 1 if the experiments are truly in the controlled regime).

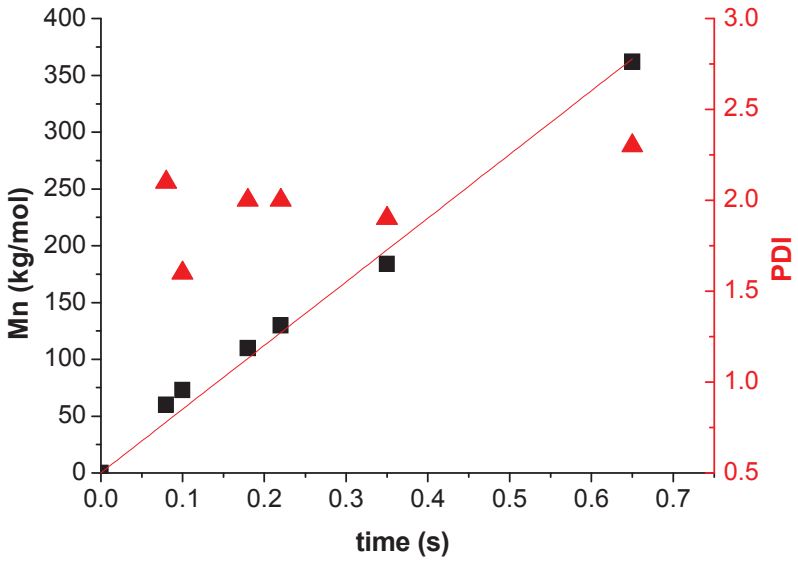

Figure 16. Dependence of molar masses (■) and PDI evolution (▲) according to time for $Cp^*_2ZrCl_2$/MAO catalyst system at 25°C

Since M_n shows a good linearity according to the polymerization time we could calculate the value of k_p using the plot in Figure 17 where the reciprocal of degree of polymerization is function of reciprocal of time.

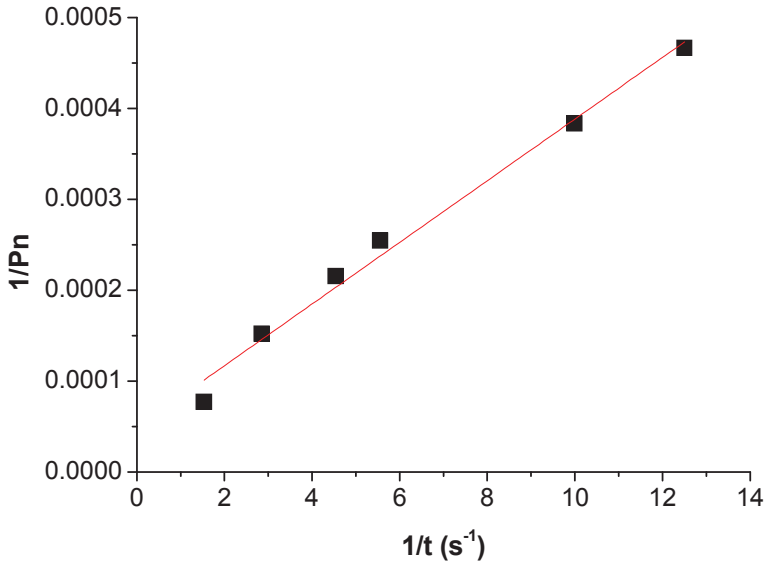

Figure17. The reciprocal of avarege degrre of polymerization as function of reciprocal of timefor $Cp^*_2ZrCl_2$/MAO catalyst system at 25°C

Applying Natta's equation (see chapter I) we could calculate k_p and the [M*]/[Zr], for $Cp^*_2ZrCl_2$/MAO system and the results are reported in Table 15.

Table 15. Main kinetic parameters for $Cp^*_2ZrCl_2$/MAO at 25°C

T (°C)	**k_p** ($L \cdot mol^{-1} \cdot s^{-1}$)	**[M*]/[Zr]** ($mol \cdot mol_{Zr}^{-1}$)	**f_t** (s^{-1})
25	$2.7 \pm 0.2 \times 10^5$	0.14±0.01	1.4±0.3

The k_p value is comparable as order of magnitude with k_p reported by Busico and coworkers [1] for FESBIZrCl$_2$/MAO, however it is more important to focus on the value of frequency of chain transfer reaction, f_t, which is extremely low (1.4 s^{-1}), meaning that the chain transfer reactions are negligible at this first instants of polymerization. Since the chain transfer reaction are not involved in this polymerization, and assuming that the actual design of reactor and the GPC device allow to obtain polymer with a very narrow molecular weight distribution (as shown in chapter 3) the phenomena that could explain the broad MWD found for some tests are:

- That the initiation of $Cp^*_2ZrCl_2$/MAO at 25°C could be lower than propagation rate
- The active site formed at first instant of polymerization could be different from the sites of second or generation of polymer chains, this could explain the broad MWD and also the fact that in batch we have observed a lower activity of one order of magnitude than that in QFR.

5. General conclusions

Results reported in this chapter have shown that the metallocene activation is a very complicated process, and the phenomena that occur during the first instant of polymerization are far from being well understood. With this study we have investigated three different kinds of catalyst precursors using different co-catalysts, and found a "long" (on the scale of time characteristic of QFR experiments) induction period, for (CPh_2)CpFluZrCl$_2$ and for FESBIZrCl$_2$ when they are activated by borate salt. The results also suggest that there is a progressive activation of the metal atoms. Even if this is for a period of a few seconds it is not necessarily expected.

Further during the study of $Cp^*_2ZrCl_2$ we have observed that this catalyst is much faster than expected. In fact at 60°C the catalyst system was out of controlled regime after 80 ms which is objectively a very short reaction time, decreasing temperature we have observed that the catalyst system followed a controlled trend only for residence times below 200 ms a medium reaction time for this kind of device. Only in mild condition of temperature and monomer pressure we were able to give a kinetic description of a catalyst system giving a real value to k_p and [M*]/[M]. However the catalyst is much less active after a longer polymerization time. The reason of the decrease in activity is still unclear but either is due to deactivation or a change in the catalyst structure after the formation of the first polymer chain.

In order to continue the study of influence of monomer concentration on activation processes in next chapter we have investigated other type of catalyst precursors such as post metallocene complexes for a better comparison with results obtained with metallocenes.

References

1. Busico, V.; Cipullo, R.; Esposito, V. *Macromolecular Rapid Communications* **1999,** 20, (3), 116-121.
2. Herrmann, W. A.; Rohrmann, J.; Herdtweck, E.; Spaleck, W.; Winter, A. *Angewandte Chemie* **1989,** 101, (11), 1536-1538.
3. Spaleck, W.; Kueber, F.; Winter, A.; Rohrmann, J.; Bachmann, B.; Antberg, M.; Dolle, V.; Paulus, E. F. *Organometallics* **1994,** 13, (3), 954-963.
4. Spaleck, W.; Antberg, M.; Rohrmann, J.; Winter, A.; Bachmann, B.; Kiprof, P.; Behm, J.; Herrmann, W. A. *Angewandte Chemie* **1992,** 104, (10), 1373-1376.
5. Kaminsky, W. *Advances in Catalysis* **2001,** 46, 89-159.
6. Song, F.; Cannon, R. D.; Bochmann, M. *Journal of the American Chemical Society* **2003,** 125, (25), 7641-7653.
7. Ewen, J. A.; Jones, R. L.; Razavi, A.; Ferrara, J. D. *Journal of the American Chemical Society* **1988,** 110, (18), 6255-6256.
8. Yano, A.; Hasegawa, S.; Yamada, S.; Akimoto, A. *Journal of Molecular Catalysis A: Chemical* **1999,** 148, (1-2), 77-86.
9. Brito de Oliveira, O.; Brandao, S. T.; Duarte de Freitas; John;, A.; Pires da Silva; Eleny; Meneghetti; Plentz;, S. M.; Meneghetti, M. R. *Polymer International* 57, (8), 1012-1016.
10. Busico, V.; Cipullo, R.; Cutillo, F.; Friederichs, N.; Ronca, S.; Wang, B. *Journal of the American Chemical Society* **2003,** 125, (41), 12402-12403.
11. Gotz, C.; Rau, A.; Luft, G. *Journal of Molecular Catalysis A: Chemical* **2002,** 184, (1-2), 95-110.
12. Ewen, J. A.; Elder, M. J. *Makromolekulare Chemie. Macromolecular Symposia* **1993,** 66, (1), 179-190.
13. Bochmann, M. *Organometallics* **2010,** 29, 4711-4740.
14. Razavi, A.; Ferrara, J. *Journal of Organometallic Chemistry* **1992,** 435, (3), 299-310.
15. Alt, H.; Samuel, E. *Chemical Society Reviews* **1998,** 27, (5)1205-1222.
16. di Lena, F.; Chen, P. *Helvetica Chimica Acta* **2009,** 92, (5), 890-896.

Chapter IV

Kinetic Investigation of Post-metallocene Catalysts

Chapter IV: Kinetic Investigation of Post-metallocene Catalysts

1. Introduction to chapter

An investigation of the kinetics of metallocene-based catalysts during the first instants of polymerization has been presented in the previous chapter. In this chapter we will present the results of a kinetic study of two major post-metallocene catalysts at similar time scales. A brief introduction on these complexes is presented in section II.

The first post-metallocene investigated is a Zr-based complex bearing the tetradentate [ONNO] ligand.

We focused also on the behavior of Zr- and Ti-based catalyst supported by two phenoxy-imine ligands.

All the experimental tests have been carried out in a conventional batch reactor in order to find the best experimental conditions and in quenched flow reactor for kinetic investigations.

2. The evolution of new generation single site Ziegler-Natta polymerization catalysts.

In the last 20 years a great interest has been shown in the development of new single site catalysts, also known as post-metallocene catalysts, capable of providing novel olefin-based materials, as well as higher catalyst productivity than conventional metallocenes. Increasing interest has been directed toward the new class of catalysts, involving complexes of transition metals throughout the periodic table[1]. Examples of successful new of highly active non-metallocene catalysts include late-transition metal systems such as the Brookhart's Ni and Pd diimine catalysts, and Fe bis(imino)pyridyl catalysts[2], and group 4 metal bis(phenoxyimine) catalysts[3]. Since the work presented here focused on Ti- and Zr-based post-metallocene complexes, we will describe briefly only post-metallocene catalysts based on the group 4 metals.

In the late 1980's, the development of half metallocenes containing dialkylsilyl-bridged alkylimido Cp ligands, such as constrained geometry (CGC) catalysts[4, 5], was an important event in story of evolution of Ziegler-Natta catalysts (e.g. in Figure 1).

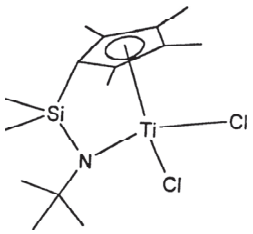

Figure 1. Constrained geometry catalyst CGC

In 1995 various sterically hindered chelating phenoxide complexes of titanium and zirconium were used as olefin polymerization catalysts[6]. Depending on the R substituent, in particular when R= MeO group (species **A** in Figure 2), these complexes have been shown to give high activity in ethylene polymerization. Using ethylene-bridged bis(phenoxide) complexes, it was also possible to copolymerize easily ethylene with styrene(species **B** in Figure 2)[7, 8]. Further it was observed that titanium alkoxides in combination with MAO are highly active catalysts for ethylene polymerization[9,10]; these catalysts are also highly active for ethylene/styrene copolymerization[11].

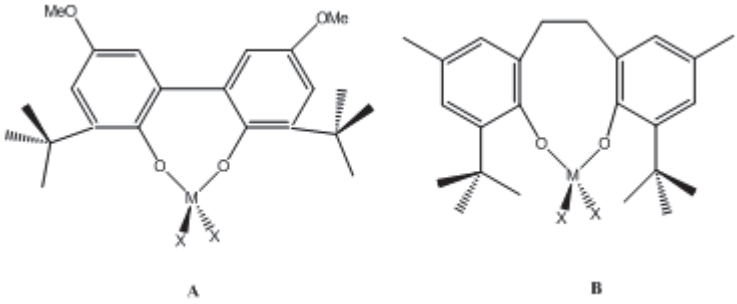

Figure 2. Examples of sterically hindered chelating phenoxide complexes

Bochmann and coworkers[12] and Horton et al.[13] synthesized chelating diamide complexes that have given moderate activity in the polymerization of ethylene. McConville et al.[14, 15]synthesized several chelating diamide complexes [2,6-$iPr_2C_6H_3N(CH_2)_3NC_6H_3$(2,6-)$iPr_2$]-$TiR_2$ (where R= Me; CH_2Ph) that, when activated with $B(C_6F_5)_3$, catalyze the polymerization of α-olefins at room temperature in a living fashion.

In 1999 a new family of a group 4 complexes bearing amine bis(phenolate) [ONO]- and [ONNO]- type ligands was introduced by Kol and co-workers[16]. They observed that complexes bearing the tridentate [ONO]-ligand (species **A** in Figure 3) displayed low activity in 1-hexene polymerization producing only 1-hexene oligomers. On the other hand, when Zr-complexes are supported by the tetradentate [ONNO] ligand (species **B** in Figure 3) and activated by $B(C_6F_5)_3$ at room temperature, they show a living nature for 1-hexene polymerization. Indeed they observed a linear increment of M_n with time (M_n up to 12 kg·mol^{-1}) and a very narrow molar masses distribution (PDI =1.11-1.15) [17] which are characteristic of living polymerization.

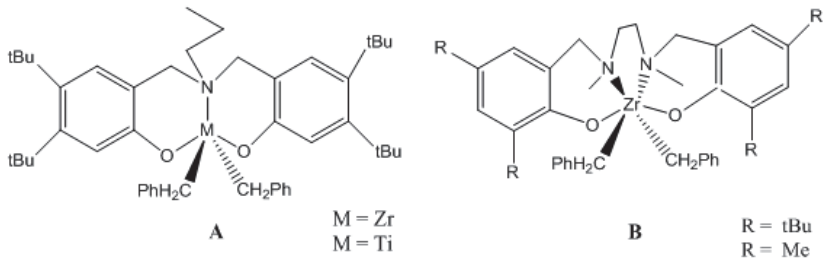

Figure 3. Examples of amine bis(phenolate) complexes

In the same period, Fujita and coworkers at Mitsui Chemicals[18] discovered that group 4 complexes supported phenoximine ligands (generic formula is given in Figure 4**)** are a remarkable class of catalysts for olefin polymerization.

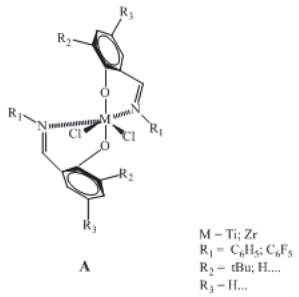

Figure 4. Generic formula of bis(phenoxyimine) catalyst precursor

The phenoxy-imine ligands have the advantageous properties of diversity and tenability. By changing the substituentes, R_1 to R_2 in Figure 4, it is possible to obtain catalyst which show very high activity in living fashion[3]. These catalysts are discussed more deeply in the next sections.

3. Investigation of a amine bisphenolate zirconium catalyst

The [ONNO] complexes, with general formula reported in Figure 5**,** were the first post-metallocene C_2-symmetrical system active for isospecific and living polymerization ofα-olefins.

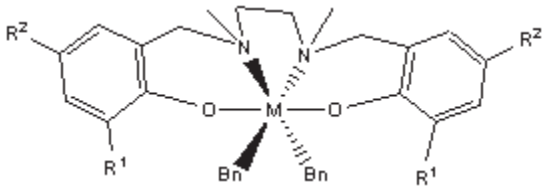

Figure 5. Generic formula of the [ONNO] catalyst system

The straightforward of synthesis of a variety of ligand precursors, and of the resulting metal complexes make this new family of catalysts a potential alternative to *ansa*-metallocene family. The [ONNO] systems was at first synthesized by Kol and coworkers[17], using as R^1=R^2= *t*Bu and M=Zr. The resulting [ONNO] catalysts showed a living polymerization of 1-hexene as already discussed above[17]. Later Busico and coworkers[19] polymerized propylene using Kol's octahedral [ONNO]-type zirconium based catalysts. They observed that depending on the steric hindrance at active metal, isotactic site-controlled or weakly syndiotactic chain-end-controlled polymers were obtained, in both cases via highly regioselective1,2 (primary) monomer insertion. They concluded that the complexes mimic the behavior of active Ti species on the surface of heterogeneous Ziegler-Natta.

It was also proposed[20, 21]that the control of propylene polymerization will be achieved by modification of ligand, in particular by installing bulky 1-adamantyl or cumyl(=α,α-dimethylbenzyl) group (complex **I** in Figure 6) substituentes at ortho-position. The PPs obtained with these complexes activated with $[PhNMe_2H][B(C_6F_5)_4]$/Al*i*Bu_3 showed a narrow molar mass distribution (PDI = 1.2-1.5)[20, 21]. As observed in previous studies, in case of propylene, the activity was quite low[19, 21]– less than 250 ($kgPP{\cdot}mol_{Zr}^{-1}{\cdot}h^{-1}{\cdot}[C_3H_6]^{-1}$)– indicative of a slowness of the catalyst toward propylene polymerization. Among the different co-catalyst used for activating the complex **I** in Figure 6 the boron-based activators gave essentially the same very low activity (10-20$kgPP{\cdot}mol_{Zr}^{-1}{\cdot}h^{-1}{\cdot}[C_3H_6]^{-1}$). A larger increase in productivity was observed when complex **I** in Figure 6 was activated using MAO and 2,6-di-tert-butylphenol.

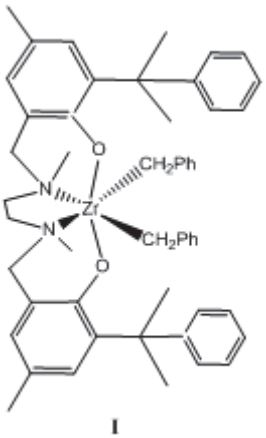

I

Figure 6. The Bis(cumyl)[ONNO]ZrBz_2 complex.

Complex **I** in Figure 6 was also be able to be used in the production of ethylene in controlled fashion when activated with MAO and 2,6-di-tert-butylphenol at 25°C up to 3 minute of polymerization (M_n = 30 kg·mol^{-1} PDI =1.5-1.8)[22]. This last characteristic makes this complex a good candidate for kinetic investigation in the QFR.

Bis(cumyl)[ONNO]ZrBz$_2$ complex activated with MAO/tBu_2-PhOH: a kinetic study.

The Bis(cumyl)[ONNO]ZrBz_2 was the object of a study carried out among different laboratories, in particular the studies on the structure and activation behavior[23-25] have been reported in literature. In particular, they showed that the activation of bis(phenoxy-amine)Zr-based is coupled with an isomerization and that the rate limiting step in propylene polymerization is the insertion of monomer due to a large negative $\Delta S^{\ddagger}$.

In next paragraphs the kinetic investigation of ethylene polymerization using Bis(cumyl)[ONNO]ZrBz_2/MAO/*t*Bu_2-PhOHcatalyst system carried out in collaboration with U-Naples laboratories is presented.

3.1 The kinetics of bis(cumyl)[ONNO]ZrBz_2 at low temperatures[a]

In U-Naples laboratory a series of ethylene polymerization experiments with increasing reaction time at three different temperatures (273, 261, 250 K) has been carried out[b]. The Bis(cumyl)[ONNO]ZrBz_2/MAO/*t*Bu_2-PhOH system was used for this series of tests, at [Al]/[Zr] ratio of 1.3×10^3, corresponding to maximum catalyst productivity, and the [*t*Bu_2-PhOH]/[MAO] ratio of0.9, which leads to an effective trapping of $AlMe_3$ present in

[a]The series of tests showed in paragraph 3.1 were carried out in the Laboratory of Stereospecific Polymerization, LSP, by Dr. Francesco Cutillo at University of Naples "Federico II" Italy.

[b]The ethylene polymerization runs were carried out in a 1 L graduated jacketed Pyrex reactor with magnetic stirring. The polymerization procedure was as follows. A *t*Bu_2-PhOH/MAO solution was added todry toluene directly into the reactor and kept in the glove-box at room temperature for 1 h. The reactor is then taken out of the glove-box, connected to the Schlenk manifold and the cylinder of ethylene, thermostated at the specific temperature, evacuated to remove nitrogen, and saturated with ethylene at the polymerization pressure. The polymerization is started by syringing in the catalyst solution through the silicone septum, and allowed to proceed at constant monomer pressure under vigorous magnetic agitation, so as to avoid mass transfer limitations in the diffusion from gas to liquid phase. During the reaction, at ca. 2 min intervals (4 min for run #3), aliquots of the reaction phase are sampled out of the bottom tap and quenched immediately with a double volume of methanol/HCl (aq, conc.) (95/5 v/v).

commercial MAO used in U-Naples laboratory. The results obtained are reported in Table 1.

Table 1. Ethylene polymerization using Bis(cumyl)[ONNO]ZrBz$_2$/MAO/*t*Bu$_2$-PhOH catalyst system at three different temperatures

Run[a]	[[ONNO]ZrBz$_2$] (μmol)	t (min)	Y (n_{C2H4}/n_{Zr})	M_n (kg·mol^{-1})	Pnx10^{-2}	PDI
		T = 273 K; [C_2H_4] = 0.27 mol·L^{-1}				
1.1	17.1	2.02	288	20.6	7.3	1.53
1.2	9.66	4.05	469	36.5	13	1.62
1.3	8.22	5.9	620	43.8	15.6	1.55
1.4	5.28	7.82	884	51	18.2	1.59
		T = 261 K; [C_2H_4] = 0.29 mol·L^{-1}				
2.1	18.89	3.57	219	16.3	5.8	1.41
2.2	7.28	5.58	431	24	8.5	1.47
2.3	7.97	7.62	532	30.9	11	1.49
2.4	3.55	9.58	603	39.9	14.2	1.53
		T = 250 K; [C_2H_4] = 0.31 mol·L^{-1}				
3.1	17.28	8.00	202	14.7	5.2	1.52
3.2	9.36	12.03	278	21.6	7.7	1.43
3.3	9.36	16.05	350	27.2	9.7	1.44
3.4	5.99	19.98	428	33.4	12	1.59

a.[*t*Bu$_2$-PhOH] =57.0 mmol; [MAO] = 58.5 mmol; in 750 mL of dry toluene

At all three temperatures the plot of yield as a function of time is linear, and the interpolating straight lines pass through the origin (Figure 7). This rules out appreciable catalyst induction and deactivation effects, which is a pre-condition for the applicability of Eqs (1) and (2) reported below:

$$\frac{1}{P_n} = \frac{1}{k_p\,[mon]t} + \frac{\sum_{i=1}^{n} k_{tr}\,[X]^i\,t}{k_p\,[mon]t} \qquad (1)$$

$$Y = k_p \frac{[M^*]}{[Zr]}[mon]t \qquad (2)$$

As a matter of fact, the plots of 1/P$_n$*vs* 1/*t* are also linear (Figure 8), in accordance with Eq (1).

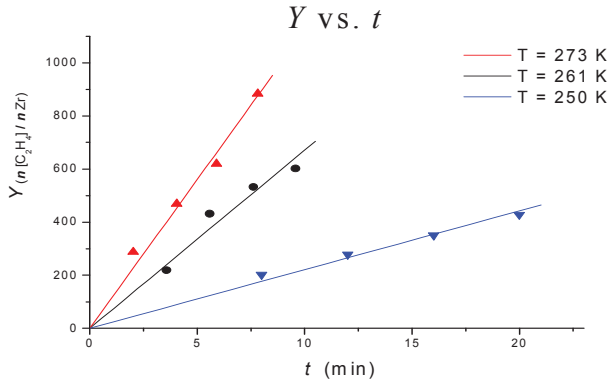

Figure 7. Plot of polymerization yield as function of time for Bis(cumyl)[ONNO]ZrBz$_2$/MAO/*t*Bu$_2$-PhOH catalyst system at three temperatures (273, 261, 250 K).

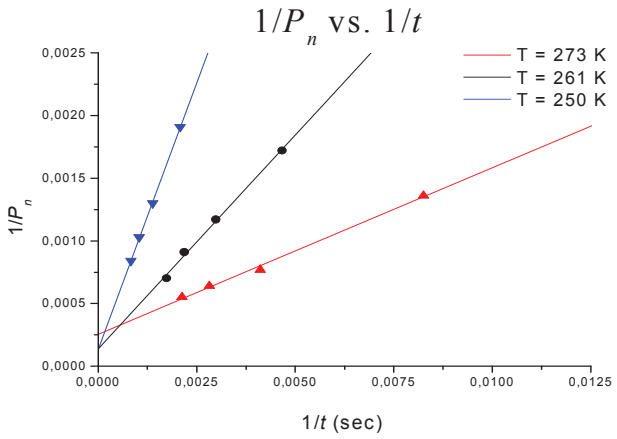

Figure 8. Plot of reciprocal of degree of polymerization as function of reciprocal of time for Bis(cumyl)[ONNO]ZrBz$_2$ /MAO/*t*Bu$_2$-PhOHcatalyst system at three temperatures

The best fit values of k_p, and [M*]/[Zr] obtained by linear interpolation of the three the three data sets of Table 1 using Eqs (1) and (2) are reported in Table 2.

Table 2. Best-fit value of main kinetic parameter for Bis(cumyl)[ONNO]ZrBz$_2$/MAO/*t*Bu$_2$-PhOH catalyst system at three temperatures.

T (K)	**k_p** (L·mol^{-1}·s^{-1})	**[M*]/[Zr]** (mol·mol$_{Zr}^{-1}$)
273	28 ± 1	0.25 ± 0.02
261	10 ± 0.4	0.39 ± 0.02
250	4 ± 0.06	0.32 ± 0.01

The k_p values can then be used to build an Eyring plot according to the well-known equation below:

$$\ln\left(\frac{k_p}{T}\right) = \frac{-\Delta H \ddagger}{RT} + \frac{\Delta S \ddagger}{R} + ln\frac{k_B}{h} \qquad (3)$$

Where is the $\Delta H^{\ddagger}$ enthalpy of activation; $\Delta S^{\ddagger}$ is the entropy of activation; $\mathbf{k_B}$ is the Boltzmann constant (5.76 x10^{-23}cal·K^{-1}); **h** is Planck constant (27.69 x10^{-34}cal·s); **R** is the gas constant (1.986 cal K^{-1}·mol^{-1}). **T** is the temperature in K.

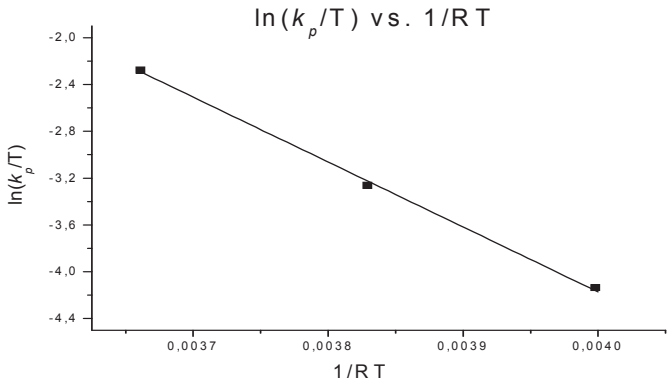

Figure 9. Eyring plot

As can be seen from Figure 9 the correlation is very good (R = 0.999), and the following best-fit values of the activation parameters are obtained:

$$\Delta H^{\ddagger} = 11.0 \pm 0.4 \text{ kcal mol}^{-1}; \quad \Delta S^{\ddagger} = -11.0 \pm 1.5 \text{ cal mol}^{-1}\text{ K}^{-1}$$

At higher temperatures, the investigation of the initial controlled regime required shorter reaction time which cannot easily be had led in a conventional reactor. In fact, at 25°C the bis(cumyl)[ONNO]ZrBz$_2$/MAO/*t*Bu$_2$-PhOH catalyst system polymerized ethylene in a living fashion for time shorter than 3 minutes finding a k_p= 127 L·mol^{-1}·s^{-1} (at 25°C and [C_2H_4] = 0.22 mol·L^{-1})[22]. Polymerization tests at higher temperatures such as 40°C and 60°C have been carried out in Lyon laboratory using the quenched flow reactor. The next session reports this study in order to compare the results obtained at low temperatures with results obtained at high temperatures.

3.2 The kinetics of bis(cumyl)[ONNO]ZrBz$_2$ at high temperatures.

As shown in the previous paragraph the polymerization of ethylene using the bis(cumyl)[ONNO]ZrBz$_2$/MAO/*t*Bu$_2$-PhOH catalyst system displays a controlled regime at low temperatures, even for reaction times of up to 20 min at T=-23°C. Furthermore, at higher temperatures and higher monomer concentrations the bis(cumyl)[ONNO]ZrBz$_2$/MAO/*t*Bu$_2$-PhOHcatalyst system polymerizes ethylene in controlled regime for reaction times on the order of seconds or fraction of seconds, thus the quenched flow reactor presented in this work is well-adapted to do a kinetic investigation of this catalyst system for temperatures higher than 25°C.A series of tests was performed in batch reactor before starting the kinetic investigation in order to find the best experimental conditions for the QFR. In particular a series of ethylene polymerizations was carried out at different *t*Bu$_2$-PhOH/Al ratios. Note that for this investigation the free tri-methyl aluminium (TMA) content in MAO was determined by NMR and found to be equal at 20 mol%.

The experimental protocol was as follows. A solution of *t*Bu$_2$-PhOH(2.4-5.6 mmol·L^{-1})in toluene was added to a stirred solution of MAO in toluene. After precontacting these components for 30 minutes at room temperature, the solution was introduced into thebatch reactor and pressurized with ethylene up to 5 bar$_{abs}$ ([C_2H_4]=0.34 mol·L^{-1}) at 60°C. The catalyst precursor was injected only when the solution of cocatalyst and phenol reached the suitable temperature (60°C). The polymerization reactions were carried our for 10 minutes and the results are reported in Table 3. The activity values found are in general one or two order of magnitude lower than activity found for metallocene catalysts such as $Cp^*_2ZrCl_2$.

Table 3. Ethylene polymerization using bis(cumyl)[ONNO]ZrBz$_2$/MA/*t*Bu$_2$-PhOH in batch reactor

Run[a]	*t*Bu$_2$-PhOH/Al	Y (g)	Activity (kgPE·mol$_{Zr}^{-1}$·h^{-1}·[C_2H_4]$^{-1}$)
ERC52_10	0.7	0.375	3.2x10^3
ERC27_10	0.5	1.568	13.6x10^3
ERC53_10	0.3	0.599	5.2x10^3

a.[bis(cumyl)[ONNO]ZrBz$_2$] = 8µmol·L^{-1}; Al/Zr = 1000 ; [C_2H_4] = 0.34mol·L^{-1} ; T = 60°C ; reaction time = 10 minutes; in 250 mL of toluene

Figure 10 shows that the maximum activity under these conditions was found for a *t*Bu$_2$-PhOH/Al ratio equal to approximately0.5.

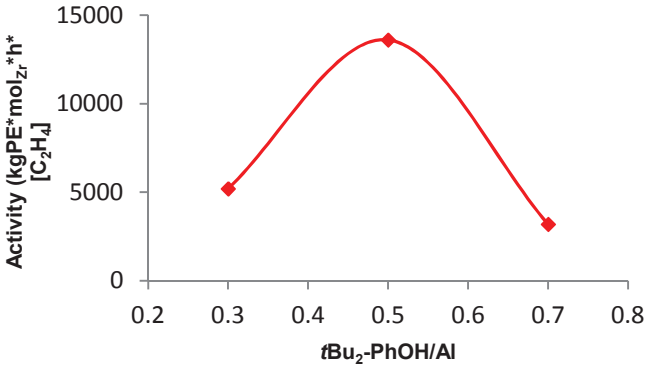

Figure 10. The dependence of activity from *t*Bu$_2$-PhOH/Al ratiofor bis(cumyl)[ONNO]ZrBz$_2$/MA/*t*Bu$_2$-PhOH catalyst system.

Note that these results are for an MAO with approximately 20% free TMA. In other batches with different levels of TMA it is to be expected that this ratio might be different from 0.5.

The results in Table 4 suggest that an Al/Zr ratio greater than 750 led to a reduction in the activity. For this reason we chose to add approximately 700 equivalents of aluminium to reaction moiety during the quenched flow experiments.

Table 4. Dependence of activity from Al/Zr ratio for bis(cumyl)[ONNO]ZrBz$_2$/MAO/*t*Bu$_2$-PhOH catalyst system in batch conditions at 60°C

Run[a]	Al/Zr	Y (g)	Activity (kgPE·mol$_{Zr}^{-1}$·h^{-1}·[C$_2$H$_4$]$^{-1}$)
ERC55_10	750	2.002	17.4x10^3
ERC27_10	1000	1.568	13.6x10^3
ERC56_10	1500	1.694	14.7x10^3

a.[bis(cumyl)[ONNO]ZrBz$_2$] = 8µmol·L^{-1}; *t*Bu$_2$-PhOH/Al = 0.5 ; [C$_2$H$_4$]=0.34mol·L^{-1} ; reaction time = 10 minutes; T = 60°C ; in 250 mL of toluene

The values of M_n found were on the order of 30 kg·mol^{-1}. As expected, the PDI found is on the order of 2.2 for test at 60°C and [C$_2$H$_4$] = 0.34 mol·L^{-1} since the catalyst system is not in the controlled regime for the experimental conditions chosen here.

3.2.1 Kinetics at 60°C using the quenched flow reactor.

As explained in previous paragraphs the bis(cumyl)[ONNO]ZrBz$_2$ complex showed a controlled behavior in batch reactor for temperatures below 0°C when activated by MAO/*t*Bu$_2$-PhOH. Increasing the polymerization temperature will reduce the time during which the catalyst polymerizes in a controlled regime for long reaction times. Thus the kinetic

investigation of bis(cumyl)[ONNO]ZrBz$_2$/MAO with the addition of phenol has been carried out using the quenched flow reactor. This catalyst complex was tested at two temperatures, 40°C and 60°C, keeping the same monomer concentration employed in tests performed in the laboratories at the University of Naples. The experimental protocol followed was as follows. Phenol (5mmol in 250 mL) was added to a stirred solution of toluene and MAO (10 mmol in 250 mL) as activator and to a second solution of toluene and MAO as scavenger (2 mmol in 250 mL of MAO and 1 mmol in 250 mL of phenol). The pre-contacting of the phenol and TMA was allowed to last for 30 minutes at room temperature, and then the two solutions added to the steel feed vessels of the QFR. After 15 minutes, when the temperature reached the set point, a solution of catalyst precursor (34 µmol·L^{-1}) in 10 mL toluene was filled in the steel reactor containing MAO as activator. The contact between the MAO/phenol and bis(cumyl)[ONNO]ZrBz$_2$ was maintained for an additional 15 minutes. In total 45 minutes of pre-contact between MAO and phenol has been performed, and a further 15 minutes of pre-contact between catalyst precursor and co-catalyst system. The solution containing MAO as scavenger was pressurized with ethylene while the solution containing MAO as activator was pressurized with argon. In order to obtain a 2 bar pressure drop in the reactor (to maintain the residence times) the upstream pressure was set to 10bar$_{abs}$ and downstream pressure was 8 bar$_{abs}$. All tests reported in Table 5 were performed at relatively long polymerization times, for a quenched flow device, using tube lengths from 2 to 4 meters.

Table 5. Ethylene polymerization using stopped flow reactor for bis(cumyl)[ONNO]ZrBz$_2$/MAO/*t*Bu$_2$-PhOH at 60°C

Run[a]	Time (s)	Yield (mg)	Activity[b]	M_n (kg·mol^{-1})	PDI	Y (mol·mol$_{Zr}^{-1}$)	n_{Chain}/n_{Zr}	Consumption of C_2H_4(%)
249	0.67	16	15.7x10^3	3.0	1.35	35.5	0.33	1.1
283	0. 72	17	15.5x10^3	3.1	1.37	37.8	0.34	1.3
284	0.75	18	15.8x10^3	3.1	1.38	40.1	0.36	1.4
287	1.05	25	15.6x10^3	4.1	1.41	55.5	0.37	1.9
286	1.32	32	15.7x10^3	6.0	1.27	69.8	0.33	3.1
285	1.39	37	17.6x10^3	6.6	1.39	80.9	0.34	2.7

a.[bis(cumyl)[ONNO]ZrBz$_2$] = 23.20-35.05 µmol·L^{-1}; Al/Zr = 700; *t*Bu$_2$-PhOH/Al = 0.5; T = 60°C; [C_2H_4] = 0.34 mol·L^{-1} in 557±59 mL toluene ; **b.**kgPE·mol$_{Zr}^{-1}$·h^{-1}·[C_2H_4]$^{-1}$

It can be seen from Table 5 that from run to run a constant activity is obtained with this catalyst system, and that the activity values are in good agreement with those found in the longer batch reactions at longer polymerization time. The fact that similar activities are observed for each run underlines also the good reproducibility of the polymerization tests in QFR. Furthermore, the yield and M_n both increased with time, and the PDI values are measurable lower than 2 (1.3-1.4). All of these observations are consistent with the fact that we are operating in a controlled regime.

The molar masses obtained are lower than that found at lower temperatures, but this should be due to short reaction time typical of the quenched flow reactor.

The plot of the reciprocal of degree of polymerization as function of the reciprocal of time (Figure 11) confirms that bis(cumyl)[ONNO]ZrBz$_2$/MAO/*t*Bu$_2$-PhOH catalyst system works in a controlled regime, and that it is possible to apply Eq. (1) for calculating the kinetic parameters of interest at this temperature.

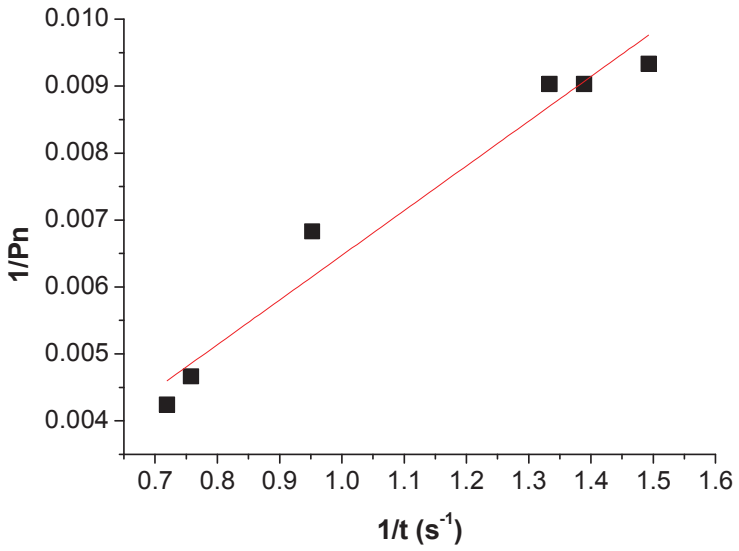

Figure 11. Plot of reciprocal of degree of polymerization vs. the reciprocal of time for bis(cumyl)[ONNO]ZrBz$_2$/MAO/*t*Bu$_2$-PhOH catalysts system at 60°C

By applying Eq. (2), it is possible to calculate [M*]/[Zr] value from plot of Y vs time in Figure 12. The best-fit values of the activation parameters are obtained and reported in Table 6.

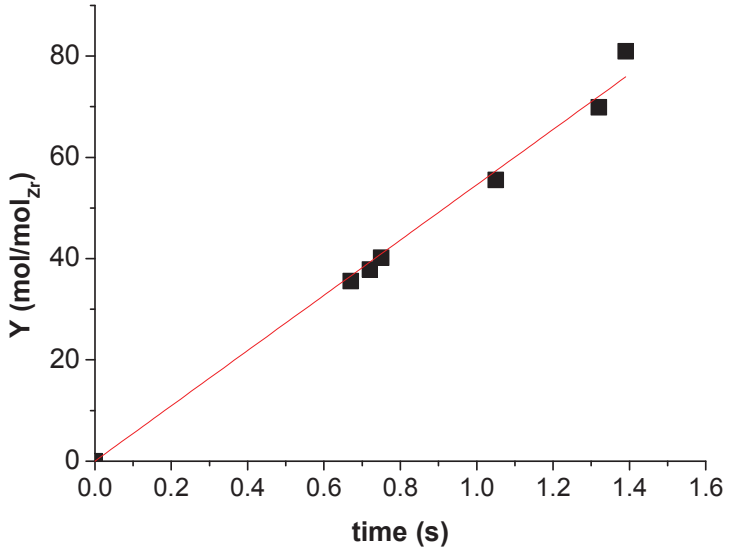

Figure 12. Plot of polymerization yield as function of time using bis(cumyl)[ONNO]ZrBz$_2$/MAO/*t*Bu$_2$-PhOH catalysts system at 60°C

Table 6. Best fit values for main kinetic parameters for bis(cumyl)[ONNO]ZrBz$_2$/MAO/*t*Bu$_2$-PhOH catalysts system at 60°C

T (K)	k_p ($L \cdot mol^{-1} \cdot s^{-1}$)	[M*]/[Zr] $mol \cdot mol_{Zr}^{-1}$
333	440 ± 13	0.36 ± 0.03

As expected the k_p value is higher than ones found at lower temperatures, however it is very interesting that the [M*]/[Zr] value found is the same as those obtained for the tests carried out in Naples at low temperature (250-273 K), meaning that temperature does not appear to influence the formation of active sites. If the activity = 137 $molPE \cdot mol_{Zr}^{-1} \cdot s^{-1} \cdot [C_2H_4]^{-1}$ of run ERC27_10 carried out in batch reactor is divided per the fraction of active site [M*]/[Zr] = 0.33 the k_p = 417 $L \cdot mol^{-1} \cdot s^{-1}$ is obtained, which is in agreement with result obtained in quenched flow time scale.

3.2.2 Kinetics at 40°C using the quenched flow reactor

The experimental procedure adopted was the same as the one explained in paragraph 3.3.1 for tests at 60°C. The only difference was in the pressure valuesset. In fact for keeping the same monomer concentration, 0.34 $mol \cdot L^{-1}$, the upstream pressure was set to 7.6 bar_{abs} and pressure

in downstream was set to 5.6 bar_{abs} in order to have ΔP = 2bar. The results obtained are reported in Table 7.

Table 7. Ethylene polymerization using bis(cumyl)[ONNO]$ZrBz_2$/MAO/tBu_2-PhOH catalysts system at 40°C in quenched flow reactor

Run[a]	time (s)	Yield (mg)	Activity[b]	M_n ($kg{\cdot}mol^{-1}$)	PDI	Y ($mol{\cdot}mol_{Zr}^{-1}$)	n_{chain}/n_{Zr}	Consumption of C_2H_4(%)
343	0.90	15	11.5 x10^3	2.6	1.16	35.1	0.37	0.38
346	0.91	15	11.1 x10^3	2.8	1.32	34.3	0.34	0.27
332	1.52	25	11.5 x10^3	4.7	1.14	59.3	0.35	0.58
344	1.67	27	11.5 x10^3	5.0	1.20	64.9	0.36	0.66
345	1.85	31	11.6 x10^3	5.2	1.16	72.9	0.39	0.71

a.[bis(cumyl)[ONNO]$ZrBz_2$] = 28.05-35.94 µmol·L^{-1}; Al/Zr = 700; *t*Bu_2-PhOH/Al = 0.5 ; T = 40°C; [C_2H_4] = 0.34 mol·L^{-1} in 530±42 mL of toluene ; **b**. kgPE·mol_{Zr}^{-1}·h^{-1}·[C_2H_4]$^{-1}$

As expected the activity found is slightly lower than that at 60°C, but the reproducibility is still very good. The ethylene consumption is very low, less than1% and again the monomer concentration can be considered as constant.

The molar masses increased with time, and the polydispersity index is on the order of 1.1-1.3; both observations are indicative of a controlled regime. Figure 13 shows the plot of $1/P_n$ vs. 1/t.

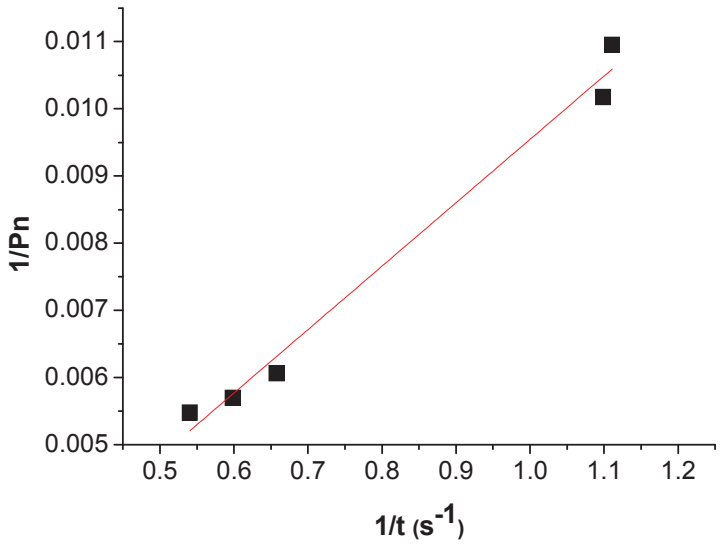

Figure 13. Plot of reciprocal of degree of polymerization as function of reciprocal of time using bis(cumyl)[ONNO]$ZrBz_2$/MAO/*t*Bu_2-PhOH catalyst system at 40°C

From the plot of polymerization yield in function of time (Figure 14), it is possible to calculate [M*]/[Zr] by applying equation (2).

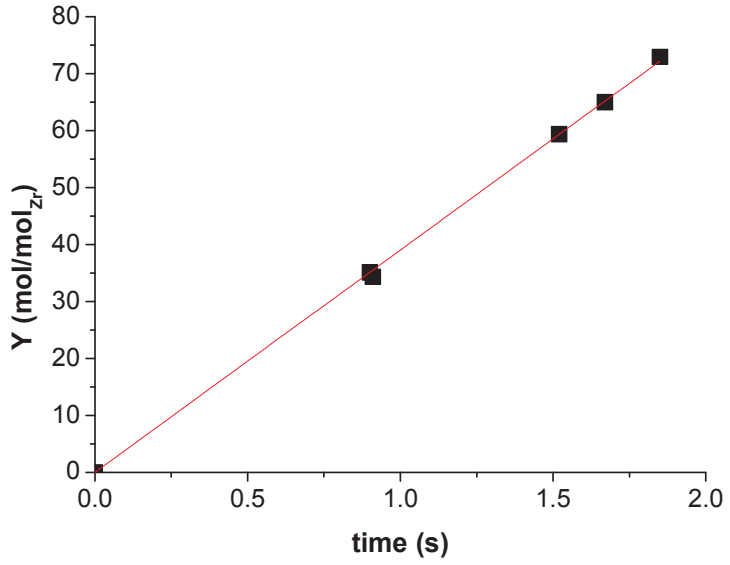

Figure 14. Plot of polymerization yield as function of time using the bis(cumyl)[ONNO]ZrBz$_2$/MAO/*t*Bu$_2$-PhOH catalyst system at 40°C

The best-fit values of the activation parameters obtained from Figures 13 and 14 are reported in Table 8.

Table 8. Best fit values for main kinetic parameters for bis(cumyl)[ONNO]ZrBz$_2$/MAO/tBu$_2$-PhOH catalysts system at 40°C

T (K)	**k_p** (L·mol^{-1}·s^{-1})	**[M*]/[Zr]** mol·mol$_{Zr}^{-1}$
313	312±21	0.36 ± 0.03

The results are in agreement with tests performed at 60°C since the same [M*]/[Zr]value was obtained which was also the same obtained at lower temperature. Evidently the activation of this catalyst does not depend on temperature.

3.3 Conclusions

The kinetic investigation of bis(cumyl)[ONNO]ZrBz$_2$/MAO/*t*Bu$_2$-PhOH catalyst system was the object of a collaboration between the two laboratories involved in DPI project #635. It is striking to find such good agreement between the polymerization tests carried out in different

reactors in different laboratories, under different experimental conditions, different batches of MAO. The studies presented here allow us to conclude that the active site concentration does not depend on the temperature, since the same value of [M*]/[Zr] was found in very large temperature range (from -23°C to 60°C).

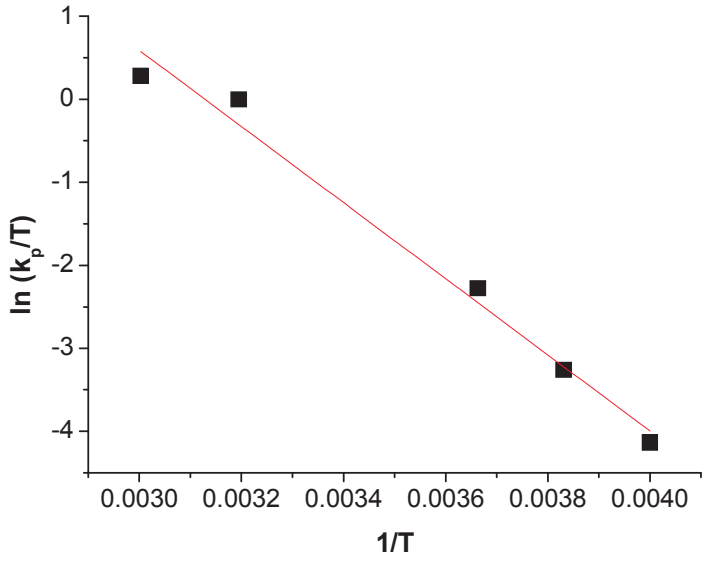

Figure 15. Eyring plot built with the addition of tests carried out in quenched flow reactor.

The kinetic results obtained in the QFR have been used to calculate new values of $\Delta H^{\ddagger}$ and $\Delta S^{\ddagger}$for Eyring plot, and the new fit can be seen in Figure 15. Fitting of the straight line allows us to calculate the following values using equation shown in section 3.2.

$$\mathbf{\Delta H^{\ddagger} = 8.8 \pm 0.6\ kcal \cdot mol^{-1}} \qquad \mathbf{\Delta S^{\ddagger} = -18 \pm 2\ cal \cdot mol^{-1} \cdot K^{-1}}$$

It is interesting to compare such values with the corresponding ones for the polymerization of propylene (results reported by Dr. F. Cutillo in the framwork of DPI project #635): $\Delta H^{\ddagger}$ = 5.2 ± 0.2 kcal·mol^{-1}**;** $\Delta S^{\ddagger}$ = -41.7 ± 0.8 cal·mol^{-1}·K^{-1}.

Note that using a model of bis(phenoxy-amine) catalyst[24, 25] it has been reported an intramolecular isomerization of cation OSIP cis(N,N)-cis(O,O) (species **C1** in Figure 16) ligand wrapped around Zr-center in distorced pyramidal configuration in cation OSIP trans(O,O)-cis(N,N)(species **C2** in Figure 16) with an octahedral configuration.

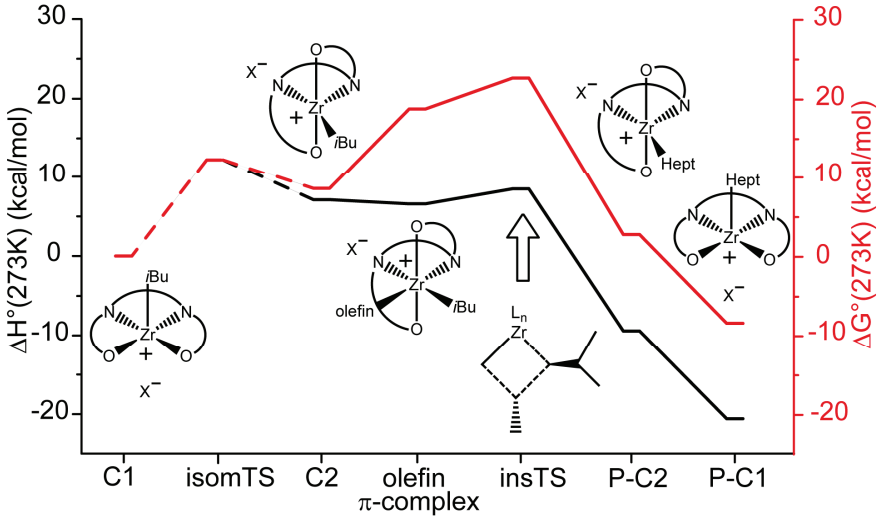

Figure 16. DFT-calculated propylene insertion profile for a model of bis(cumyl)[ONNO]ZrBz$_2$ derivates. *Reprinted with permission from*[25]*. Copyright (2010) American Chemical Society.*

The large negative $\Delta S^{\ddagger}$ calculated which is in good agrement with the experimetal results shows that the rate limiting step was the 1,2 propylene insertion[25].

In the case of ethylene polymerization, we showed that the chain propagation of ethylene is faster due to a smaller entropic term (only 8.8 cal·mol^{-1}·K^{-1}) the reason for this difference in the entropic term is not yet clear; possibly future DFT calculations could explain this behavior.

4.1 FI-based complexes as catalysts for olefin polymerization.

The post-metallocene catalysts have broadened the range of olefin-based materials accessible by transition metal based catalytic technology. Already in 60s at same time of investigation on metallocene made by Natta and Breslow, Taylor[26] examined the several phenoxy-azo and phenoxy-imine chelating compounds in combination with $TiCl_4$ in search of another soluble version of Ziegler catalysts. However this chemistry was not pursued any further. Only in late the 1990s it was discovered that salicylaldimine (phenoxy-imine) group can be used as a ligand for olefin polymerization catalysts with early transition metals[18]. The phenoxy-imine ligands (L^{FI}) can be synthesized by straightforward Schiff base condensation of amines and phenolic compounds bearing carbonyl groups, both of which can be purchased as commercially available chemicals or readily prepared from them. The design of phenoxy-imine ligands has resulted in the discovery of a number of highly active catalysts for polymerization of olefins. Further the activation of phenoxy-imine based complexes is similar to that of metallocene precursor indeed the activated form of bis(phenoxy-imine) group 4 metal was presumed to be a cationic alkyl species $[(L^{FI})_2M—R]^+$ and this presumption is supported by several NMR studies[27, 28]. In particular using the bis(phenoxy-imine) Ti complex shown in Figure 17, cationic methyl $[(L^{FI})_2M—Me]^+$ species was found as product of $[(L^{FI})_2MX_2]$/MAO from NMR experiments[28] similar to the active species formed by metallocene precursors as shown in chapter I.

Among the bis(phenoxy-imine) complexes, we have focused on Ti-complex **I**, and Zr- based complex **II** (Figure 17).

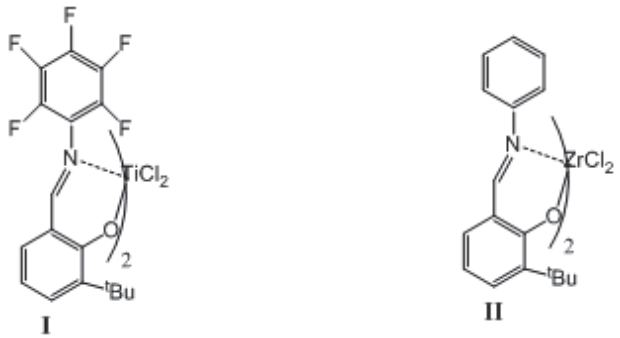

Figure 17. Bis(Phenoxy-imine) based complexes : <u>species I</u> [*N*-(3-*tert*-butylsalicylidene)-2,3,4,5,6 pentafluoroanilinato] titanium dichloride ; <u>species II</u> [*N*-(3-*tert*-butylsalicylidene)phenylaminato] zirconium dichloride

In fact, it has been shown that by using **I/MAO** it is possible to observe the living polymerization of ethylene[29,30] and propylene[31,32] at room temperature. The activity of $FITiCl_2$/MAO for ethylene polymerization[29, 30, 33] is high whereas in the case of propylene only moderate activities were found[31-33]. Further when complex **I** is activated with MAO a high syndiotactic polypropylene was found[32].

In regards to complex **II**, very high activities have been reported but the properties of the polymer (molar masses, microstructure) are highly depending from the activation system. **II**/MAO is highly active in the case of propylene polymerization but produces an atactic oligomer, while when the activator is $iBu_3Al/[Ph_3CB(C_6F_5)_4]$ system the product is highly isotactic[3].

In the case of ethylene polymerization, **II**/MAO shows higher activity than **II**/iBu$_3$Al/[Ph$_3$C][B(C$_6$F$_5$)$_4$](550 kgPE·mmol$_{Zr}^{-1}$·h^{-1} rather than 4 kgPE·mmol$_{Zr}^{-1}$·h^{-1} at 25°C and P = 1 bar[34]).When the complex **II** is activated with borate salts obtains polymers with higher molar masses than one obtained using MAO (M_n = 9000 g·mol^{-1} rather than M_v = 3830000 g·mol^{-1} at 25°C and P=1 bar[3, 34]). The same authors[34] found that when this complex is activated with MAO, the activity increases with temperature to reach a maximum at 40°C (587 kgPE·mol$_{Zr}^{-1}$·h^{-1} at P = 1 bar)[34]; above 40°C the activity decreased. The authors[3] suggest that the difference of behavior obtained with the two different activators could be due to the reduction of imine function of the ligand by iBu$_3$Al, or a contaminant Al-H species such as H(iBu)$_2$Alwhich is present in commercial iBu$_3$Al,as shown in Figure 18.

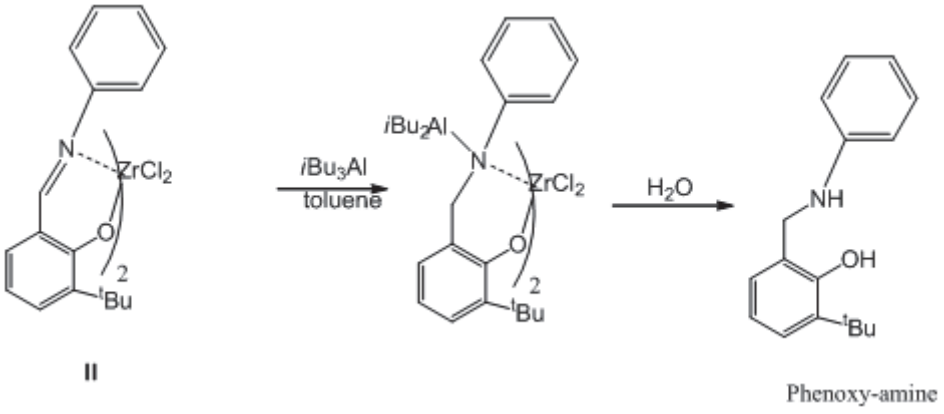

Figure 18: Possible reaction between II (complex II) and alkylating agent

The activity shown by the **II**/MAO catalyst system is comparable with a metallocene-based catalyst, making this catalyst a good candidate for a kinetic investigation in quenched flow reactor.

4.1 The investigation of complex [*N*-(3-*tert*-butylsalicylidene)phenylaminato] zirconium dichloride (II)

4.1.1 The II/MAO catalyst system

We investigated the kinetics of the [*N*-(3-*tert*-butylsalicylidene)phenylaminato] zirconium dichloride (**II**) complex, (see complex **II** in Figure 17) synthesized in our laboratory, according to Fujita[c] methods. As usual, before starting the investigation of the **II**/MAO catalyst system in the QFR, a test in glass batch reactor was performed in order to assess the best experimental conditions (see Table 9). We have performed a test at higher monomer concentration, 0.5 mol·L^{-1}, than that usually reported in literature.

Table 9. Ethylene polymerization using II/MAO catalyst system in batch reactor

Run[a]	Time (min)	Y (g)	Activity (kgPE·mol$_{Zr}^{-1}$·h^{-1}·[C_2H_4]$^{-1}$)	M_n (kg·mol^{-1})	PDI	n_{Chain}/n_{Zr}
ERC11_6	1	1.97	15x10^5	5	2.13	131

a. [**II**] = 0.6µmol·L^{-1}; Al/Zr = 2000; [C_2H_4] = 0.5mol·L^{-1}; T = 25°C in 250 mL of toluene;

The activity value is only slightly lower than those exhibited by metallocene catalysts such as Cp*$_2$ZrCl$_2$/MAO and FESBIZrCl$_2$/MAO catalyst systems under similar conditions (see previous chapter). It is possible that this could be due to different Al/Zr ratio employed during the reaction. In fact, all the tests reported in literature have been carried out at exceptionally high Al/Zr ratio from 6250 to 312500. As expected, $M_n$was quite low, with a typical Schultz-Flory distribution (PDI 2.13).

Table 10. Ethylene polymerization in quenched flow reactor using II/MAO catalyst system

Run[a]	Time (s)	Y (mg)	Activity (kgPE·mol$_{Zr}^{-1}$·h^{-1}·[C_2H_4]$^{-1}$)	M_n (kg·mol^{-1})	PDI	n_{Chain}/n_{Zr}	Consumption of C_2H_4 (%)
327	0.13	51	22 x10^5 1129[b]	5	1.8	8.1	1.2

a.[**II**] = 2.5µmol·L^{-1}; Al/Zr = 2000; [C_2H_4] = 0.5mol·L^{-1}; T=25°C in toluene; **b.** kgPE·mol$_{Zr}^{-1}$·h^{-1}

[c] For description of method see appendix B

The activity found using the quenched flow device (see Table 10) was a little bit higher (x 1.5) than the activity obtained in batch reactor, and it is of the same order of magnitude as the activities found for metallocene catalyst. Furthermore, even at shortest reaction time that we can accurately handle in quenched flow reactor at this pressure the reaction is out of controlled regime. In fact, not only the $M_n$value found is the same found at longer polymerization time with a Shultz-Flory value of PDI but the n_{chain}/n_{Zr} is 8.1 which means that even at this short reaction time the chain transfer reactions are very significant.

According to the conclusion reported in chapter III the II/MAO catalyst system is not suitable for quenched flow polymerization investigation.

4.1.2 The II/Alkylaluminium/$[PhNMe_2H][B(C_6F_5)_4]$catalyst system

A series of tests was carried out using borate salts as activators. Results from the reference batch polymerizations are shown in Table 11.

As reported in the literature[3] complex **II** when activated with iBu$_3$Al/[Ph$_3$C][B(C$_6$F$_5$)$_4$] produced a very high molar weight polyethylene (M_v=5.05x10^6 at 50°C and P = 1 bar), which suggests that transfer reactions are less significant with this catalyst. The activity measured is one to two orders of magnitude lower than that found with MAO (11kgPE·mmol$_{Zr}^{-1}$·h^{-1} rather than 496 kgPE·mmol$_{Zr}^{-1}$·h^{-1} at 50°C and 1 bar) at 50°C. The fact that the molar mass is very high makes this catalyst a good candidate for kinetic investigations.

The experimental procedure was as follow: a solution of borate salt $[PhNMe_2H][B(C_6F_5)_4]$in toluene was prepared and added to a toluene solution of alkylaluminium compounds (iBu$_3$Al and/or H(iBu)$_2$Al). Then the solution containing the co-catalyst was injected in the reactor and pressurized with ethylene. The catalyst solution was added to solution only when the co-catalyst solution reached the reaction temperature (about 10 minutes) via an injection module.

Table 11. Ethylene polymerization using II/Alkylaluminium/[PhNMe$_2$H][B(C$_6$F$_5$)$_4$] in batch reactor

Run[a]	*i*Bu$_3$Al (mmol·L^{-1})	H(*i*Bu)$_2$Al (mmol·L^{-1})	Time (min)	Y (g)	Activity	M$_n$ (kg·mol^{-1})	PDI	n$_{chain}$/n$_{Zr}$
ERC11_15	1	-	5	1.530	11.7x10^{5}[b] 91[c]	5	1.8	1530
ERC11_16	0.9	0.1	5	0.654	4.7x10^{5} [b] 39[c]	12	2.5	272
ERC11_14	-	1	5	0.233	1.7x10^{5} [b] 14[c]	140	1.5	8.3

a.[**II**] = 0.8 µmol·L^{-1}; [PhNMe$_2$H][B(C$_6$F$_5$)$_4$] = 1.6µmol·L^{-1}; Al/Zr = 1250; T = 50°C; [C$_2$H$_4$] = 0.08 mol·L^{-1}; in 250 mL of toluene ; **b.** kgPE·mol$_{Zr}^{-1}$·h^{-1}· [C$_2$H$_4$]$^{-1}$;**c**. kgPE·mol$_{Zr}^{-1}$·h^{-1}

Unlike the results reported in the literature with this same catalyst, run ERC11_15, which was carried out using the **II**/*i*Bu$_3$Al/[PhNMe$_2$H][B(C$_6$F$_5$)$_4$] catalyst system, gave an activity comparable to that obtained with **II**/MAO catalyst system. Furthermore, the average molar mass was only 5000 g·mol^{-1}, and GPC chromatogram showed a bimodal profile similar to the one in Figure 19. For run ERC11_15 the deconvolution of GPC chromatogram gave that more than 80% is formed by polymer with a low M$_n$ value, 3 kg·mol^{-1}, while less than 20% is represented by polymer with high M$_n$ value 61 kg·mol^{-1} (see Figure 19 and Table 12).

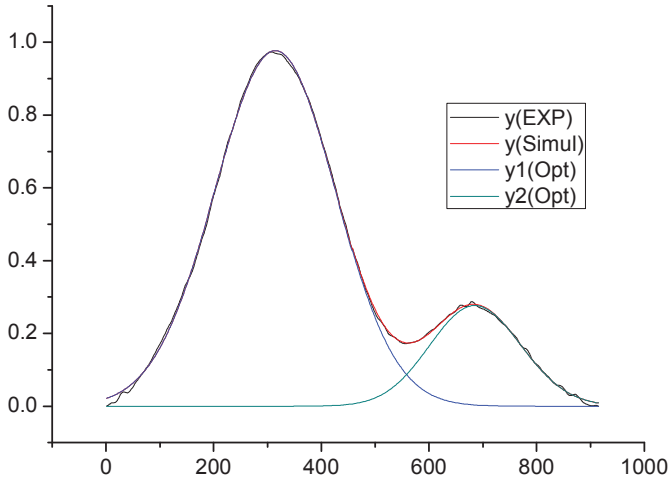

Figure 19. Deconvolution of run ERC11_15. The black curve is the original chromatogram, the green and blue curves are the two families of polymer and the red curve is the simulation curve which is the sum of green and blue curves.

The value found for M$_n$ is not in agreement with result reported in literature for this kind of system where much higher molar masses are obtained. Since it was assumed that the reduction of the imine function of the ligand could be due to presence of H(*i*Bu)$_2$Al present in

*i*Bu$_3$Al, run ERC11_16was carried out using a mixture of*i*Bu$_3$Aland H(*i*Bu)$_2$Al (9/1). In this case a polymer with a broad molar masses distribution was obtained. Using the deconvolution software[d] it was possible to separate the different polymer families. From deconvolution of run ERC11_16 (Table 10 Figure 20) it was observed that the 89% of polymer shows M_n of 9 kg·mol^{-1} and 11% of the polymer has M_n of 89 kg·mol^{-1}. Note this percentage of each fraction correspond to initial ratio of *i*Bu$_3$Al and H(*i*Bu)$_2$Al.

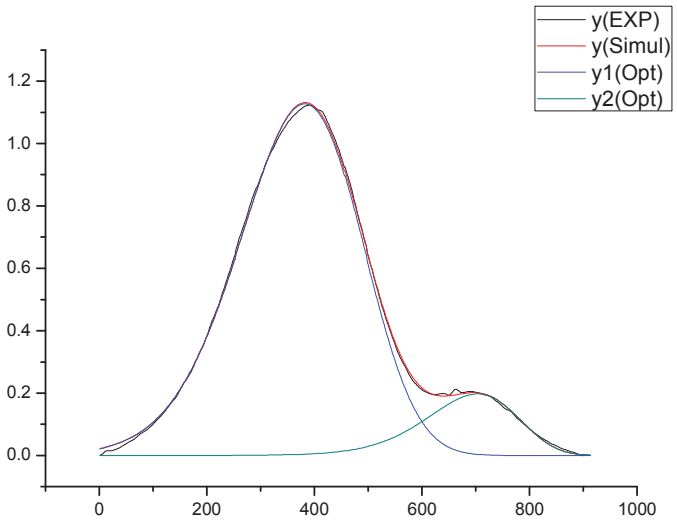

Figure 20. Deconvolution of run ERC11_16.The black curve is the original chromatogram, the green and blue curves are the two families of polymer and the red curve is the simulation curve which is the sum of green and blue curves.

Table12.Results of deconvolution for test ERC11_15 and ERC11_16

curve	%	M_n (kg·mol^{-1})	PDI	Yield (g)
		ERC11_15		
Y1(opt)	82.4	3200	1.94	1.260
Y2(opt)	17.6	61600	1.44	0.270
		ERC11_16		
Y1(opt)	88.5	9400	1.96	0.578
Y2(opt)	11.5	89100	1.36	0.075

Finally when **II** was activated by using only H(*i*Bu)$_2$Al as alkylating agent (run ERC11_14) a high value of average molar masses was found with a quite narrow molar masses distribution

[d] For more information on deconvolution software used for these tests see appendix A

for this time scale (see GPC profiles in Figure 21).Furthermore the activity value was lower than one order of magnitude than activity of test with *i*Bu_3Al.

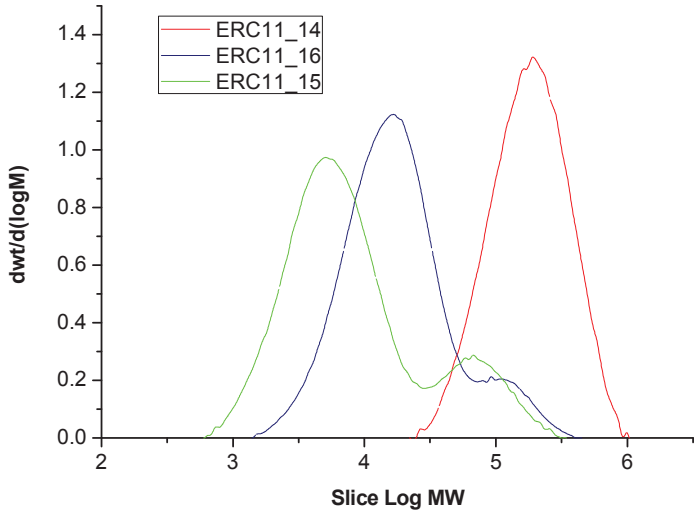

Figure 21. Overlapping of run ERC11_14 (red curve), ERC11_15 (green curve) and ERC11_16 (blue curve)

In summary, the catalyst **II**/MAO displayed high activity for ethylene polymerization. Surprisingly, the use of the combination of *i*Bu_3Al with borate salt as activators does not show the production of extremely high molar masses as reported in literature. A bimodal distribution was obtained which suggested the presence of two different active species. By using H(*i*$Bu)_2Al$ rather than *i*Bu_3Al a decrement of activity was observed and a polymer with monomodal MWD was obtained. However this molar mass was lower than expected. Due to the lack of time together with these unexpected results, quenched flow investigations were not performed with this catalyst, but could be put for further studies.

4.2 Kinetic investigation of the Bis[*N*-(3-*tert*-butylsalicylidene)-2,3,4,5,6 pentafluoroanilinato] titanium dichloride (I)

Phenoxy-imine (FI) Ti-based complexes typically show lower polymerization activities then analogous zirconium catalysts, but they are known for producing high molar mass polymers. However, reasonable activities can be obtained by modifying the ligands in an appropriate manner. In fact, the titanium FI complex bearing a pentafluorophenyl group (complex **I** in Figure 17) such as the bis[*N*-(3-*tert*-butylsalicylidene)-2,3,4,5,6 pentafluoroanilinato] titanium dichloride (**I**) shows an appreciable activity when activated with MAO and, perhaps more importantly in the context of this work, it also exhibits a living ethylene polymerization behaviour at temperatures up to 50°C with M_n = 424 kg·mol^{-1} and low polydispersity index (PDI = 1.13)[29]. In fact, this is one of first example of a polymerization catalyst that displays living behaviour for both ethylene and propylene polymerization. The authors suggest that the presence of *ortho*-F accounts for living polymerization by mitigating β-H transfer. In particular for ethylene-coordinated species, the transition state of the β-H transfer is probably disfavoured by the fact that the β-H is positively charged and is stabilized by negatively charged *ortho*-F, whereas the β-H should behave as a hydride in the β-H transfer process.

All these results make this complex a good catalyst precursor for kinetic investigation using quenched flow reactor. In an initial step, we synthesized the complex **I** using Fujita's method[e], and carried out a series of preliminary tests using in the same experimental conditions used in literature[29] in order to compare the results.

The complex **I** was used in the batch reactor using the following experimental procedure: a solution of MAO (5 mmol·L^{-1}) in toluene was prepared at room temperature and introduced in the reactor and pressurized with ethylene at pressure of 2 absolute bars. A Ti-complex solution (2 µmol·L^{-1}) was injected to start the polymerization when the solution reached the reaction temperature, through an injection module on the top of reactor. Since the complex **I** activated by MAO showed a living behaviour even in conventional conditions at short reaction times the reactions were carried for about 1 minute.

[e] For the description of method see appendix B

Table 13.Ethylene polymerization by using I/MAO catalyst system in batch reactor: comparison test

Run[a]	Time (min)	Y (g)	Activity $kgPE \cdot mol_{Ti}^{-1} \cdot h^{-1} \cdot [C_2H_4]^{-1}$	M_n ($kg \cdot mol^{-1}$)	PDI	n_{chain}/n_{Ti}
ERC11_3	1	0.198	$2.1x10^5$	408[b]	1.54	0.96

a.[**I**] = $2\mu mol \cdot L^{-1}$; Al/Ti = 2500; T = 25°C; $[C_2H_4] = 0.11 mol \cdot L^{-1}$; in 250 mL of toluene; **b.** GPC value obtained by using light scattering detector coupled with refractometer detector.

The activity value is about 30% lower than activity reported in literature (0.283 mg of PE obtained in the same conditions of run ERC11_13 which correspond to $3.1x10^5$ $kgPE \cdot mol_{Ti}^{-1} \cdot h^{-1} \cdot [C_2H_4]^{-1}$) and the M_n value found is comparable with M_n reported in literature (412 $kg \cdot mol^{-1}$) but the PDI is slightly higher than one reported in literature (1.1-1.3 vs 1.5)[29]. Nevertheless, the catalyst behaves in a manner similar to that reported in the literature, so we can now run QFR experiments at much higher monomer concentrations to understand the kinetics under different conditions. Since no studies of this catalysts system at elevated monomer pressure are reported in the literature, a series of polymerization tests were performed at higher ethylene concentration.

As usual, a series of tests was carried out in batch reactor in order to have reference data at longer reaction time, and find the best experimental conditions. Note that runs reported in Table 14 were performed in different reactors. Indeed, the upper pressure limit of conventional glass reactor is 4 bar_{rel}. Keeping the same monomer concentration for run at 55°C means working at 6.85 bars, for this reason this test was performed in steel batch reactor. The experimental procedure adopted was different according to reactor used. In glass batch reactor the catalyst solution was injected into MAO/toluene solution in which the ethylene was solubilized C_2H_4 via injection module on the top of the reactor. While in steel batch reactor a solution of MAO, toluene and complex **I** was injected in the reactor, and only when the temperature reached the suitable value was the solution pressurized with ethylene due to the absence of injection module on the top of reactor.

In the literature[29], this catalyst is activated using $2.5x10^3$ equivalents of MAO but according to tests reported in Table 14 the observed activity is still reasonably high at lower Al/Ti ratios. Thus tests performed in quenched flow reactor have been carried out at Al/Ti= 2000 as shown in the next paragraphs.

Table 14. Ethylene polymerization usingI/MAO in batch reactor at different temperature and Al/Ti ratios

run[a]	T (°C)	Time (min)	Y (g)	Activity ($kgPE \cdot mol_{Ti}^{-1} \cdot h^{-1} \cdot [C_2H_4]^{-1}$)	M_n[d] ($kg \cdot mol^{-1}$)	PDI
			Al/Ti = 2000			
ERC11_26	25	1.02	0.65	1.5 x10^5	727	1.8
ERC11_27[b]	40	1.02	0.71	1.8 x10^5	729	1.6
ERC11_25[c]	55	1.10	0.61	1.3 x10^5	636	2.3
			Al/Ti = 2500			
ERC11_19	25	1.60	1.40	2.1 x10^5	1150	1.4
ERC11_18[b]	40	1.00	0.96	2.6 x10^5	685	2.1

a.[**I**] = 2µmol·L^{-1}; [C_2H_4] = 0.5 mol·L^{-1} in 250 mL toluene; **b**. Tests carried out at [C_2H_4] = 0.44 mol·L^{-1}; **c**. Tests carried out in steel reactor; **d**. GPC obtained with light scattering detector coupled with refractometer detector.

It is interesting to observe the good agreement in term of activity between reaction ERC11_19 and ERC11_3 which were carried out under the same experimental conditions but at different monomer concentrations. Further temperature dependence with a maximum at 40°C was observed (see Figure 22).

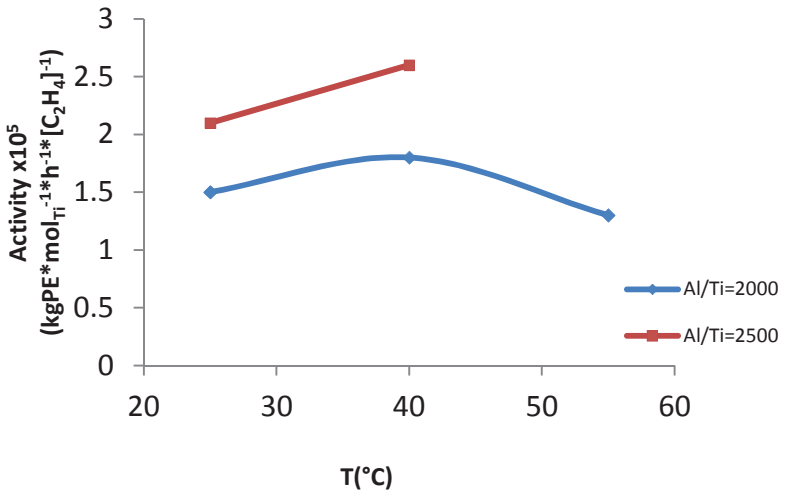

Figure 22. Dependence of activity from temperature at different Al/Ti ratios

As expected the molar masses found were very high. Since we have no standards in this range of molar masses we used the light scattering detector coupled with the refractometer detector for the measurement of the MWD in this case. Increasing the temperature leads to a broadening of the MWD, meaning that the temperature influences the chain transfer and termination reactions more strongly that it influences the propagation rate.

4.2.1 The kinetic investigation of I/MAO using quenched flow reactor at 25°C

The kinetic investigation using the quenched flow reactor was carried out using the following experimental protocol. One of the steel feed vessels of the QFR was filled with a solution of MAO (3-9mmol·L^{-1} in 250 mL). When the temperature reached the 25°C a solution of complex **I** in toluene was added to the same vessel and the reactor was pressurized with argon. The other feed vessel was filled with a solution of MAO in toluene as scavenger (1 mmol·L^{-1} in 250 mL). The reaction was begun once both the solutions have reached the desired temperature and pressure. For series of tests at 25°C the upstream pressure was set at 9 bar_{abs} in order to keep the monomer concentration at 0.5 mol·L^{-1} and the downstream pressure was set at 7 bar_{abs}. As explained in previous paragraph 2000 equivalents of MAO was used.

Table 15.Ethylene polymerization by using I/MAO catalyst system at 25°C

Run[a]	Time (s)	Y (mg)	Activity[b]	M_n (kg·mol^{-1})	PDI	n_{chain}/n_{Ti}	Y (mol·mol_{Ti}^{-1})	Consumption of C_2H_4(%)
323	0.13	6	1.7 x10^5	12	1.1	0.26	111	0.12
313	0.16	18	1.7 x10^5	15	1.1	0.25	134	0.47
324	0.38	15	1.4 x10^5	27	1.1	0.28	279	0.34
326	0.44	18	1.6 x10^5	33	1.1	0.29	345	0.47
325	0.63	25	1.5 x10^5	49	1.1	0.27	480	0.66

a.[**I**] = 3.83-10.6 µmol·L^{-1}; Al/Zr = 2000;T = 25°C; [C_2H_4] = 0.5 mol·L^{-1}; in 470±30 mL of toluene; **b.**kgPE·mol_{Ti}^{-1}·h^{-1}·$[C_2H_4]^{-1}$

The activity values observed are in agreement with the activity measured for the batch experiment ERC11_26. The n_{chain}/n_{Ti} is constant from test to test. This implies that the transfer

reactions are negligible which is also shown by the very narrow MWD (PDI = 1.1) together with the increasing of M_n according to polymerization time. The plot of polymerization yield as function of time is linear and the straight line pass through origin meaning that this catalyst system does not show an induction period.

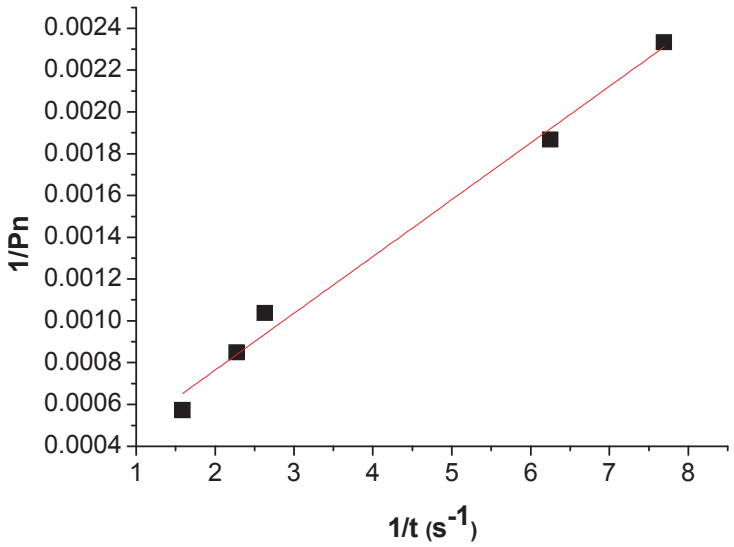

Figure 23. Plot of reciprocal of degree of polymerization vs reciprocal of time for I/MAO at 25°C

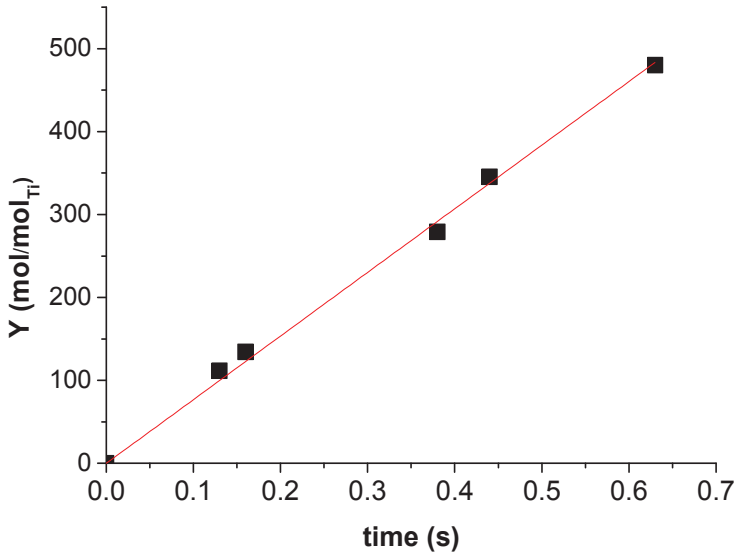

Figure 24. Polymer yield as function of time for I/MAO at 25°C

It is possible to calculate the value of k_p from plot in Figure 23 using equation (1), and [M*]/[Ti] from plot in Figure 24 by using Eq.(2). The results are reported in Table 16.

Table 16. Best fit for main kinetic parameters for I/MAO at 25°C

T (K)	**k_p** ($L \cdot mol^{-1} \cdot s^{-1}$)	**[M*]/[Ti]** $mol \cdot mol_{Ti}^{-1}$
298	$7.3 \pm 0.4 \times 10^3$	0.21 ± 0.01

The measured k_p found was one of magnitude higher than that found for bis(cumyl)[ONNO]$ZrBz_2$/MAO/*t*Bu_2-PhOH but lower than k_p measured for metallocene catalyst which are on the order of $10^5 L \cdot mol^{-1} \cdot s^{-1}$. It is interesting to remark that the value of [M*]/[Ti] obtained is in agreement with the average value of n_{chain}/n_{Ti}.

4.2.2 The kinetic investigation of I/MAO using quenched flow reactor at 40°C

In Table 23 the results of ethylene polymerization obtained using **I**/MAO at 40°C in quenched flow reactor are reported. The experimental protocol is the same employed for other series of tests, the only difference being that in order to maintain the ethylene concentration at 0.5 $mol \cdot L^{-1}$the upstream the pressure was set at 12.2 bar_{abs} and downstream pressure at 10.2 bar_{abs}. For this series of tests the activity was slightly higher than that obtained for the batch test, but the monomer consumption always remains lower than 1%. Unlike test at 25°C in which n_{chain}/n_{Ti} were constant test to test, for series at 40°C the n_{chain}/n_{Ti} grows with time, as does the PDI, meaning that some transfer reactions occur. However, as shown below, the polymerization is reasonably well-controlled at this time scale. Note that some GPC profiles (354, 355, 359) have required a deconvolution due to an issue with column: general broadening toward low M_n was observed for all the samples of the carousel (see appendix A).

Table 17. Ethylene polymerization using I/MAO catalyst system at 40°C in quenched flow reactor

test[a]	Time (s)	Y (mg)	Activity[b]	M_n ($kg \cdot mol^{-1}$)	PDI	n_{chain}/n_{Ti}	Y ($mol \cdot mol_{Ti}^{-1}$)	Consumption of C_2H_4(%)
359	0.15	12	3.1 x10^5	18 [c]	1.2	0.36	232	0.18
358	0.36	13	2.4 x10^5	41	1.1	0.29	429	0.16
357	0.39	15	2.4 x10^5	37	1.2	0.35	465	0.22
354	0.7	25	2.2 x10^5	51 [c]	1.1	0.42	769	0.33
356	0.76	35	2.8 x10^5	58	1.1	0.51	1068	0.58
355	1.12	41	2.2 x10^5	77 [c]	1.2	0.45	1273	0.63

a.[I] = 2.01-3.79 $\mu mol \cdot L^{-1}$; Al/Zr = 2000; T = 40°C; $[C_2H_4]$ = 0.5 $mol \cdot L^{-1}$; in 535±42 mL of toluene; **b**. $kgPE \cdot mol_{Ti}^{-1} \cdot h^{-1} \cdot [C_2H_4]^{-1}$ **c**. After decovolution (see appendix)

The best fit values are reported in Table 18.

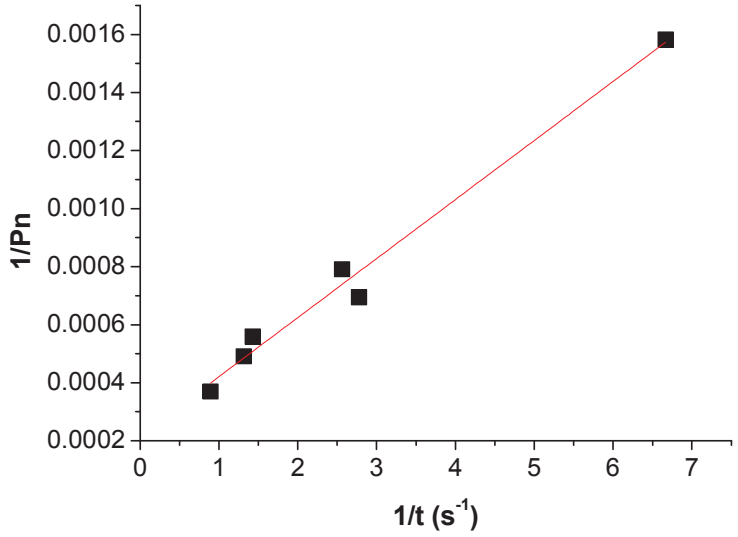

Figure 25. Reciprocal of degree of polymerization as function of reciprocal of time using I/MAO catalyst system at 40°C

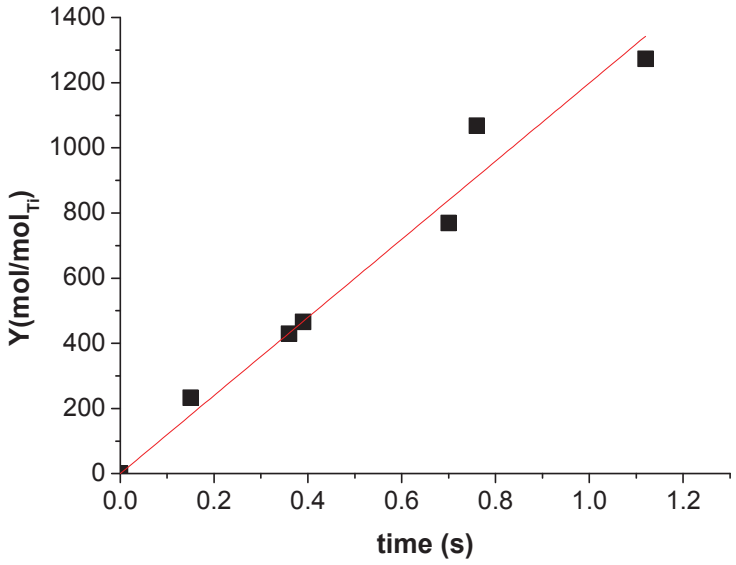

Figure 26. Dependence of polymerization yield from time using I/MAO at 40°C

Table18. Best fit values for I/MAO catalyst system at 40°C

T (K)	k_p ($L \cdot mol^{-1} \cdot s^{-1}$)	[M*]/[Ti] ($mol \cdot mol_{Ti}^{-1}$)
313	9.8±0.6 x10^3	0.24±0.03

As expected, the k_p value, reported in Table 18, is higher than one measured at 25°C, but the concentration of active sites is the same, meaning that an increment of the temperature of 15°C does not influence the activation of this catalyst system.

4.2.3 The kinetic investigation of I/MAO using quenched flow reactor at 55°C

In order to complete the kinetic investigation of **I**/MAO catalyst system a series of test has been carried out using the quenched flow reactor at 55°C. The experimental protocol used for these tests was the same adopted for tests at lower temperatures. However in order to maintain thesame monomer concentration of 0.5mol·L^{-1}, the upstream the pressure was set at 13.7 bar_{abs} and the downstream at 11.7 $bar_{abs.}$

Table 19.Ethylene polymerization using I/MAO at 55°C in QFR

run[a]	Time (s)	Y (mg)	Activity[b]	M_n ($kg \cdot mol^{-1}$)	PDI	n_{chain}/n_{Ti}	Y ($mol \cdot mol_{Ti}^{-1}$)	Consumption of C_2H_4 (%)
364	0.16	3	1.1×10^5	20	1.0	0.13	90	0.05
365	0.17	4	1.4×10^5	21	1.0	0.16	119	0.06
367	0.64	15	1.4×10^5	57	1.1	0.22	465	0.19
366	0.90	20	1.4×10^5	71	1.1	0.25	637	0.30

a.[**I**] = 2.08-2.51 $\mu mol \cdot L^{-1}$; Al/Zr = 2000; $[C_2H_4]$ = 0.5$mol \cdot L^{-1}$; T = 55°C ; toluene = 543±28 mL ;**b.**$kgPE \cdot mol_{Ti}^{-1} \cdot h^{-1} \cdot [C_2H_4]^{-1}$

A good agreement was observed between the activity obtained using the batch reactor (1.3 $kgPE \cdot mol_{Ti}^{-1} \cdot h^{-1} \cdot [C_2H_4]^{-1}$) and the activity obtained in QFR. However this activity was once again lower than that measured at 40°C. The fact that the activity is constant regardless of the polymerization time shows that the decrease in activity is not due to a deactivation of catalyst according to reaction time. The number of polymer chains produced per mol of titanium is constant from test to test, and the average value is 0.16, which is slightly lower than value found for series of test at 25°C and 40°C. Considering the linearity of M_n with time it was possible to calculate the main kinetic parameters using the plots in Figure 27 and Figure 28. The best fit results for this temperature have been reported in Table 20. As expected, considering the lower activity observed at 55°C than that at 40°C, [M*]/[Ti] decreased. However, surprisingly the k_p measured at 55°C is roughly the same than the one at 40°C.

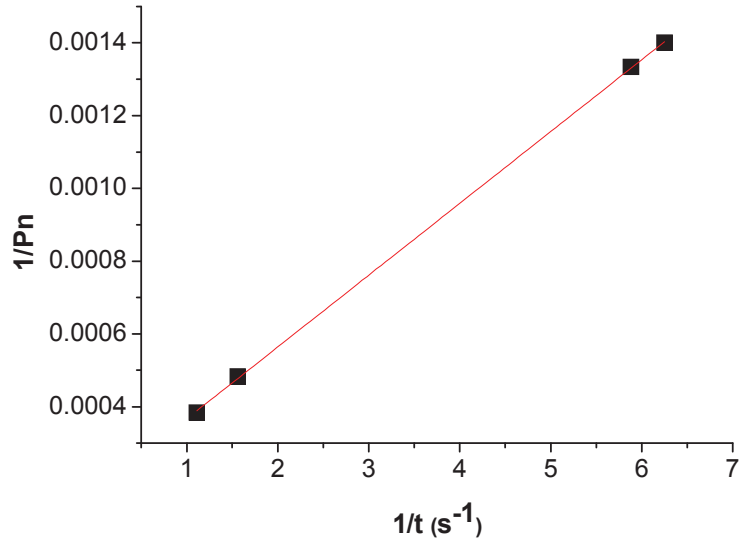

Figure 27. Reciprocal of degree of polymerization as function of reciprocal of time using I/MAO catalyst system at 55°C

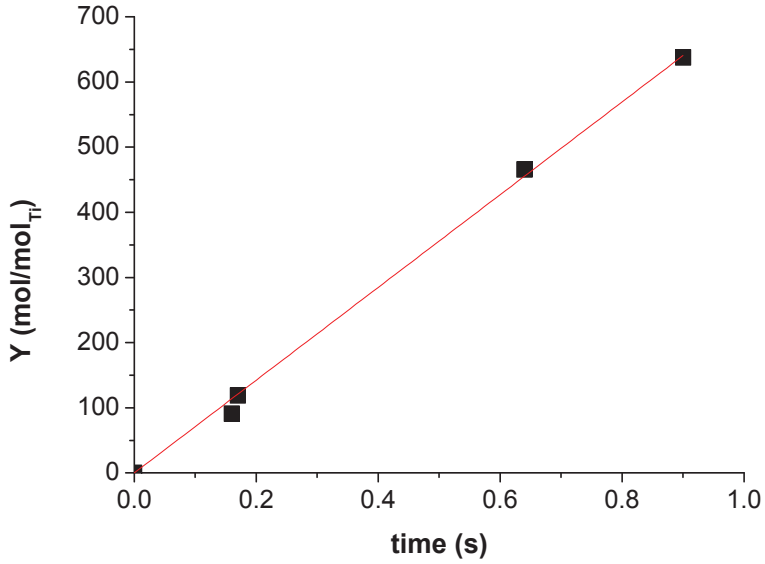

Figure 28. Dependence of polymerization yield from time using I/MAO at 55°C

Table 20. Best fit values for I/MAO catalyst system at 55°C

T (K)	k_p ($L \cdot mol^{-1} \cdot s^{-1}$)	[M*]/[Ti] ($mol \cdot mol_{Ti}^{-1}$)
328	$10.1 \pm 0.06 \times 10^3$	0.13 ± 0.01

4.3 Conclusions at the kinetic investigation of I/MAO in QFR

As for Bis(cumyl)[ONNO]ZrBz$_2$/MAO/*t*Bu$_2$-PhOHcatalyst system investigated in section II we have tried to build up an Eyring plot using data obtained at three temperatures (25°C to 55°C) in order to obtain the main activation parameters. As expected, from k_p values the data are not aligned which suggests that we have observed a changing in kinetic regime which is hard to explain.

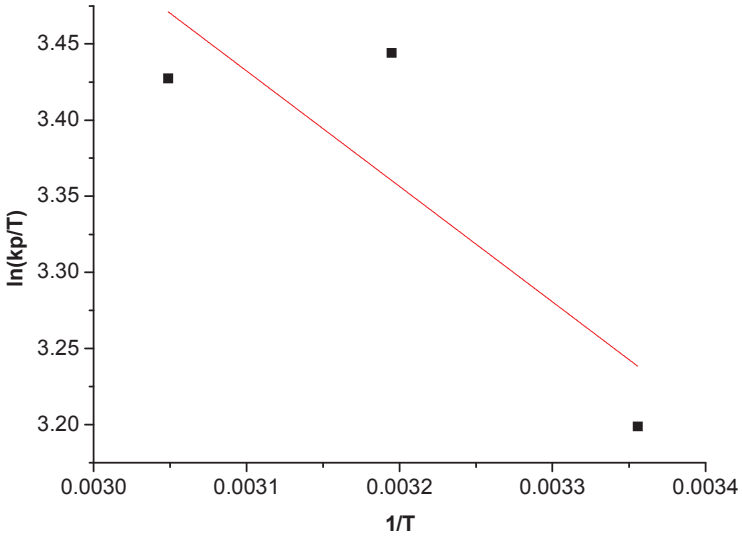

Figure 29. Eyring plot for I/MAO catalyst system

In literature it has been assumed that for the phenoxy-imine zirconium catalyst system the decrease in activity observed for temperature above 40°C was probably due to the decomposition of the active species because of the loss of the ligand(s)[3]. A similar temperature dependence of activity with a maximum at 40°C for **I**/MAO catalyst was observed in both batch and QF reactor with a exceptionally agreement in activity values, meaning that the phenomena which were occurred at short time scale could be the same at long reaction times. We could suppose that even for **I**/MAO catalyst system a loss of the ligand(s) might occur with a rise of temperature, which could decrease the number of active sites. However no deactivation was observed with polymerization time. This means that there is no decomposition of active species with polymerization time at 55°C.

Another explanation is the possible isomerization of the cationic species formed when **I** is activated by MAO. The bis[*N*-(3-*tert*-butylsalicylidene)-2,3,4,5,6 pentafluoroanilinato] titanium dichloride exists as single isomer[35] in a distorted octahedral geometry with trans-O, cis-N and cis-Cl arrangement[36] (see species **I** Figure 31) unlike the $FIZrCl_2$ which exists as mixture of 5 isomers at 75°C[35] (see Figure 30).

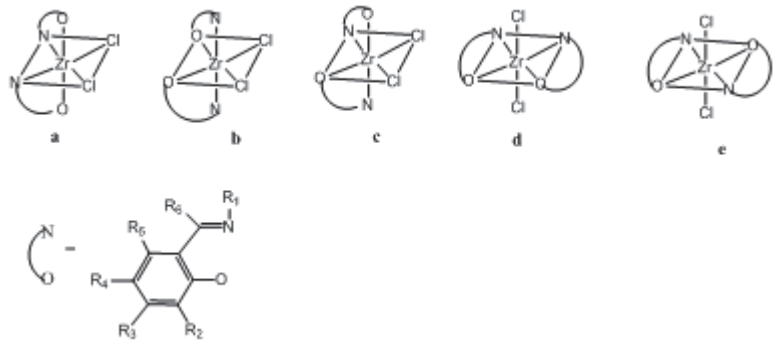

Figure 30. Possible isomers for a FIZr-based complex

When **I** is activated with MAO, this leads to active cationic species. Based on the existence of **I** as a single isomer[35] the species **A** is probably formed. When species **A** coordinates with ethylene, it is able to polymerize (species **A'** in Figure 31) [28].

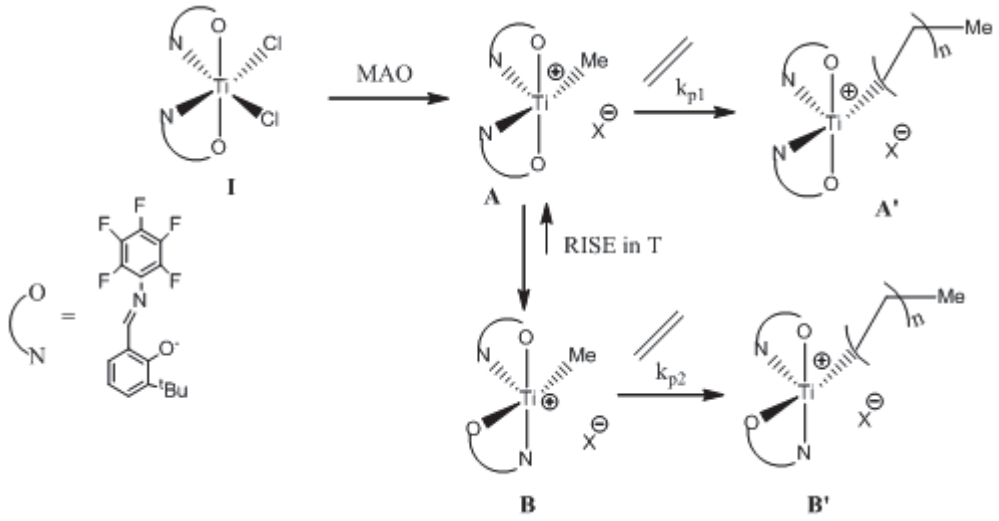

Figure 31. Proposed isomerization of the cationic species $[FITiMe]^+[X]^-$

We propose that by rising the temperature, the species **A** evolves by intramolecular isomerisation into a more stable structure such as species **B** (or similar isomers). This assumption might be confirmed by experimental investigation such as NMR studies or/and DFT calculation on the model of the excellent work reported by Ciancaleoni et al. on bis(phenoxy-amine)Zr-based complex.

References

1. Gibson, V. C.; Spitzmesser, S. K. *Chemical Reviews* **2002,** 103, (1), 283-316.
2. Ittel, S. D.; Johnson, L. K.; Brookhart, M. *Chemical Reviews* **2000,** 100, (4), 1169-1204.
3. Makio, H.; Kashiwa, N.; Fujita, T. *Advanced Synthesis & Catalysis* **2002,** 344, (5), 477-493.
4. Canich, J. A. M.; Turner, H. W. WO1991US09676 19911226 **1992**.
5. Chum, P. S.; Kao, C. I.; Knight, G. W. *Plastics Engineering* **1995,** 51, (6), 21-3.
6. van der Linden, A.; Schaverien, C. J.; Meijboom, N.; Ganter, C.; Orpen, A. G. *Journal of the American Chemical Society* **1995,** 117, (11), 3008-3021.
7. Sernetz, F. G.; Muelhaupt, R.; Fokken, S.; Okuda, J. *Macromolecules* **1997,** 30, (6), 1562-1569.
8. Fokken, S.; Spaniol, T. P.; Okuda, J.; Sernetz, F. G.; Muelhaupt, R. *Organometallics* **1997,** 16, (20), 4240-4242.
9. Froese, R. D. J.; Musaev, D. G.; Matsubara, T.; Morokuma, K. *Journal of the American Chemical Society* **1997,** 119, (31), 7190-7196.
10. Miyatake, T.; Mizunuma, K.; Kakugo, M. *Makromolekulare Chemie. Macromolecular Symposia* **1993,** 66, (1), 203-214.
11. Kakugo, M.; Miyatake, T.; Mizunuma, K.; Tominaga Keii and Kazuo, S., 36. Polymerization of Styrene and Copolymerization of Styrene with Olefin in the Presence of Soluble Ziegler-Natta Catalysts. In *Studies in Surface Science and Catalysis*, Elsevier: 1990; Vol. Volume 56, pp 517-529.
12. A. H. Male, N.; Thornton-Pett, M.; Bochmann, M. *Journal of the Chemical Society, Dalton Transactions* **1997**, (14), 2487-2494.
13. Horton, A. D.; de With, J.; van der Linden, A. J.; van de Weg, H. *Organometallics* **1996,** 15, (12), 2672-2674.
14. Scollard, J. D.; McConville, D. H.; Payne, N. C.; Vittal, J. J. *Macromolecules* **1996,** 29, (15), 5241-5243.
15. Scollard, J. D.; McConville, D. H.; Vittal, J. J.; Payne, N. C. *Journal of Molecular Catalysis A: Chemical* **1998,** 128, 201-214.
16. Tshuva, E. Y.; Versano, M.; Goldberg, I.; Kol, M.; Weitman, H.; Goldschmidt, Z. *Inorganic Chemistry Communications* **1999,** 2, (8), 371-373.
17. Tshuva, E. Y.; Goldberg, I.; Kol, M. *Journal of the American Chemical Society* **2000,** 122, (43), 10706-10707.
18. Fujita, T.; tohi, Y.; Mitani, M.; matsui, S.; Saito, J.; Nitabaru, M.; Sugi, M.; Makio, H.; Tsutsui, T. EP0874005 **1998**.
19. Busico, V.; Cipullo, R.; Ronca, S.; Budzelaar, P. H. M. *Macromolecular Rapid Communications* **2001,** 22, (17), 1405-1410.
20. Busico, V.; Cipullo, R.; Friederichs, N.; Ronca, S.; Togrou, M. *Macromolecules* **2003,** 36, (11), 3806-3808.
21. Busico, V.; Cipullo, R.; Friederichs, N.; Ronca, S.; Talarico, G.; Togrou, M.; Wang, B. *Macromolecules* **2004,** 37, (22), 8201-8203.
22. Cipullo, R.; Busico, V.; Fraldi, N.; Pellecchia, R.; Talarico, G. *Macromolecules* **2009,** 42, (12), 3869-3872.
23. Ciancaleoni, G.; Fraldi, N.; Budzelaar, P. H. M.; Busico, V.; Macchioni, A. *Organometallics* **2011,** 30, (11), 3096-3105.
24. Ciancaleoni, G.; Fraldi, N.; Budzelaar, P. H. M.; Busico, V.; Macchioni, A. *Dalton Transactions* **2009**, (41), 8824-8827.
25. Ciancaleoni, G.; Fraldi, N.; Budzelaar, P. H. M.; Busico, V.; Cipullo, R.; Macchioni, A. *Journal of the American Chemical Society* **2010,** 132, (39), 13651-13653.
26. Taylor, K. J. *Polymer* **1964,** 5, (0), 207-211.

27. Bryliakov, K. P.; Kravtsov, E. A.; Pennington, D. A.; Lancaster, S. J.; Bochmann, M.; Brintzinger, H. H.; Talsi, E. P. *Organometallics* **2005,** 24, (23), 5660-5664.
28. Makio, H.; Fujita, T. *Macromolecular Symposia* **2004,** 213, (1), 221-234.
29. Saito, J.; Mitani, M.; Mohri, J.; Yoshida, Y.; Matsui, S.; Ishii, S.; Kojoh, S.; Kashiwa, N.; Fujita, T. *Angewandte Chemie International Edition* **2001,** 40, (15), 2918-2920.
30. Mitani, M.; Mohri, J.; Yoshida, Y.; Saito, J.; Ishii, S.; Tsuru, K.; Matsui, S.; Furuyama, R.; Nakano, T.; Tanaka, H.; Kojoh, S.-i.; Matsugi, T.; Kashiwa, N.; Fujita, T. *Journal of the American Chemical Society* **2002,** 124, (13), 3327-3336.
31. Mitani, M.; Furuyama, R.; Mohri, J.; Saito, J.; Ishii, S.; Terao, H.; Kashiwa, N.; Fujita, T. *Journal of the American Chemical Society* **2002,** 124, (27), 7888-7889.
32. Saito, J.; Makoto Mitani; Mohri, J.; Ishii, S.; Yoshida, Y.; Matsugi, T.; Kojoh, S.-i.; Kashiwa, N.; Fujita, T. *Chemistry Letters* **2001,** 30, (6), 576-577.
33. Tian, J.; Hustad, P. D.; Coates, G. W. *Journal of the American Chemical Society* **2001,** 123, (21), 5134-5135.
34. Matsui, S.; Mitani, M.; Saito, J.; Tohi, Y.; Makio, H.; Matsukawa, N.; Takagi, Y.; Tsuru, K.; Nitabaru, M.; Nakano, T.; Tanaka, H.; Kashiwa, N.; Fujita, T. *Journal of the American Chemical Society* **2001,** 123, (28), 6847-6856.
35. Tohi, Y.; Nakano, T.; Makio, H.; Matsui, S.; Fujita, T.; Yamaguchi, T. *Macromolecular Chemistry and Physics* **2004,** 205, (9), 1179-1186.
36. Mitani, M.; Nakano, T.; Fujita, T. *Chemistry – A European Journal* **2003,** 9, (11), 2396-2403.

Conclusions and Perspectives

Conclusions and Perspectives

In this Ph.D. dissertation, we focused on the investigation of kinetic behavior of molecular catalysts for ethylene polymerization. The main objective was the measuring the fraction of active sites ([M*]/[M]) in order to obtained the real value of constant of rate propagation k_p using the relationship between the degree of polymerisation, P_n, and the concentration of active sites. In order to obtain a reliable value of [M*]/[M] it is necessary to work in the *transient controlled regime* where the chain transfer reactions, such as transfer to monomer or aluminum, and the chain transfer termination are negligible. The Quenched Flow technique allows performing polymerization times going from fraction of seconds to a few seconds, which is expected to be the range of validity of initial controlled regime for many olefin polymerization catalysts using the conventional polymerization conditions.

The initial phase of this work focused on the validation of the high-pressure-Quenched Flow technique. The device used for these studies was a classical Quenched Flow reactor able to work at high pressures (up to 16 bars) and high temperatures (up to 80°C) with the minimum of residence time of 80 ms. Since this reactor was originally devised for morphogenesis studies of $MgCl_2$-supported Ziegler Natta catalysts, it was not ideally configured for very precise studies such as the kinetic investigations. As shown in chapter II, we therefore made two major types of modifications: mechanical and technical such as the stabilization of flow rate and the use of very strong quencher for stopping immediately the reaction. At the end we were able to perform tests with satisfactory reproducibility, despite the delicacy of the technique.

Once we obtained a robust technique to follow the kinetic one of main objectives of this thesis was to investigate the influence of some experimental parameters such as the polymerization conditions and the co-catalyst in the activation of some of most important catalysts such as metallocene and post-metallocene catalysts in the first instants of ethylene polymerization.

In chapter III we have focused on the investigation of metallocene precursors such as the FESBIZrCl_2 complex. We have observed that when this catalyst precursor is activated by MAO the resulting complex is immediately active for ethylene polymerization and the results obtained are in agreement with results reported in literature and obtained with different

devices and lot of MAO, meaning that actually our facilities is able to give very reproducible and useful tests. However, it was difficult to operate in a controlled regime in time scale permitted by our QFR. Even in mild conditions (T = 25°C and P = 1.5 bar), the polymerization shows activities and molar masses distributions typical of a Shultz-Flory regime. On the other hand, by changing MAO by an activator obtained by combination of *i*Bu_3Al with $[HNMe_2Ph][B(C_6H_5)_4]$ provided a catalyst showing an induction period that lasts for at least 0.5 seconds. The same catalyst is highly active when investigated in batch reactor at longer polymerization times than that performed in our QFR.

The activation of $(CPh_2)CpFluZrCl_2$ complex was the object of a long part of this thesis in term of experiments performed. The metallocene complex was activated by MAO, MAO modified via the addition of *t*Bu_2-PhOH, and by the combination of *i*Bu_3Al with borate salt. In every case measurable polymerization activities were found in the batch reactor but, when the reaction occurs in time scale of Quenched Flow polymerization, an induction period was observed. The initial induction period was found to be longer than one second in the case of $(CPh_2)CpFluZrCl_2$/MAO and $(CPh_2)CpFluZrCl_2$/MAO/*t*Bu_2-PhOH catalysts system, and longer than 2 seconds in the case of $(CPh_2)CpFluZrCl_2$/Al*i*Bu_3/$[Me_2PhNH][B(C_6F_5)_4]$ catalyst system. In a conventional time scale this induction period is negligible but it becomes dramatic during the Quenched Flow experiments.

The $Cp^*_2ZrCl_2$/MAO catalyst system was the last metallocene-based catalyst that we have studied. In particular we have investigated the influence of temperature on the activation at first instant of polymerization. Only in mild condition of temperature and monomer concentration a kinetic description of catalyst system was possible giving a real value to k_p and [M*]/[M]. In fact, increasing the temperature from 25°C to 40°C and 60°C the polymerization in controlled regime was possible only for fraction of seconds.

In chapter IV the study of the influence of polymerization condition on activation was assessed for two major classes of post metallocene complexes.

To the best of our knowledge the study of bis(cumyl)[ONNO]$ZrBz_2$/MAO/*t*Bu_2-PhOH catalyst was one of first example of a kinetic investigation on a vast range of temperatures (-23°C to 60°C). For this catalyst system, the same value of [M*]/[Zr] was found not only in a very large range of T but also in two different laboratories using different reactors, under

different experimental conditions, and with different batches of MAO. Lastly, the main activation parameters such as $\Delta H^{\ddagger}$ and $\Delta S^{\ddagger}$ were calculated for this catalyst system using the value of k_p found at five temperatures.

The last kinetic investigation has been performed using a bis(phenoxy-imine)Ti-based catalyst activated with MAO. The use of Quenched Flow technique allow us to assess the main kinetic parameters such as k_p and [M*]/[M] for this catalyst system at high monomer concentration. In particular the values of k_p found allowed us to observe a change in kinetic regime which is hard to explain but to the best of our knowledge was an unique example of such behavior.

In summary, the main objective of this Ph.D. thesis was measuring the fraction of active sites concentration [M*]/[M] for ethylene polymerization catalysts. We have observed that even for very active catalysts, 30% is the maximum of metal centers that are active for all the catalyst that we have investigated. But the Quenched Flow is a very useful technique which also allowed us to observe some interesting phenomena which occurred in the first instant of polymerization. In some case we have observed a good agreement with results obtained at very short reaction times with that obtained in conventional conditions using batch reactor. This comparison allowed us to observe interesting phenomena such as in case of $Cp^*_2ZrCl_2$/MAO catalyst system which is much less active after a longer polymerization time. The reason of the decrease in activity is still unclear but either could be due to deactivation or a change in the catalyst structure after the formation of the first polymer chain. In conclusion the Quenched Flow technique has proved to be very representative of reaction system.

However, we must admit that the metallocene activation is very complicated process. Even though the QFR is a very useful and original technique our actual device is not suitable for all kind of catalyst systems as in the cases of FESBI$ZrCl_2$/*i*Bu_3Al/$[HNMe_2Ph][B(C_6H_5)_4]$ and catalyst based on $(CPh_2)CpFluZrCl_2$, where an induction period was detected, and in the case of catalyst system too fast for time scale of QFR. This allowed us to conclude that the lifetime of growing chain is shorter than the shortest reaction time that we can accurately handle, in the case of mostly active catalysts.

A new device will be designed in order to stretch the window of residence times from 10^1 ms to several seconds in order to offer us longer reaction times for skipping the induction period

showed by certain catalyst system, and also very short reaction times for investigation of very fast catalyst systems. A system of precise pump for regulation of flow could be allow us to obtain high amount of polymer, on the order of 10^2 mg, even for very short reaction times for further analysis, such as NMR, DSC, TGA, than SEC chromatography.

Appendix A

The molar mass distribution: definition, distributions, GPC chromatograms

1. Introduction

The molar mass distribution, MMD, given in Figure 1, is the main element to characterize a synthetic polymer, since influence the final material proprieties such as modulus, tensile strength etc.

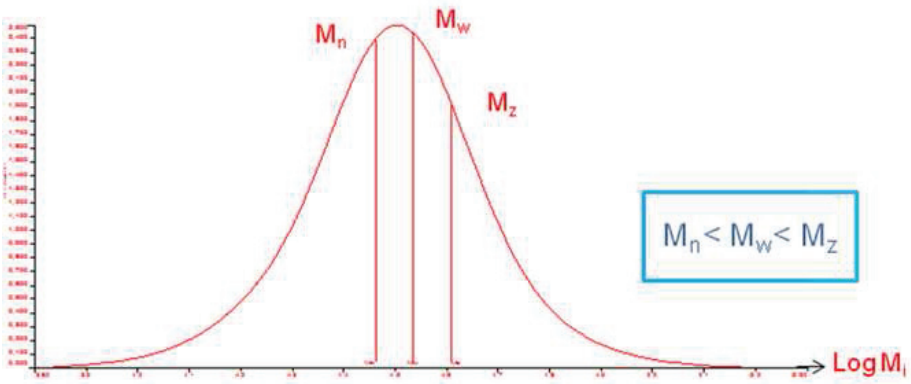

Figure 1. Molar mass distribution of macromolecules

The importance of MMD is connected to averages molar mass. Among many possible ways of reporting averages, three are commonly used: the *number average* M_n, *weight average* M_w and *viscosity average* M_v molar mass.

$$M_n = \frac{\sum M_i n_i}{\sum n_i} \qquad M_w = \frac{\sum M_i w_i}{\sum w_i} = \frac{\sum M_i^2 n_i}{\sum M_i n_i}$$

Where: M_i is the molar mass of macromolecules of *i* monomer unit;

n_i is the number of macromolecule of *i* monomer units;

w_i weight fraction of polymer with molar mass *i*.

The weight average M_n is probably the most useful, because it fairly accounts for the contributions of different sized chains to the overall behavior of the polymer, and correlates best with most of the physical properties of interest. But also the form and amplitude of MMD

provide a series of information such as the composition and chemical behavior of catalyst system that produced the polymer.

In general, in specific kinetic conditions, some homogeneous and heterogeneous catalyst systems produce polymer with well-defined MMD concerning both the form of distribution and polydispersity index $PDI = \frac{M_w}{M_n}$.

In particular for homogeneous catalyst it is possible to find two limit distribution:

1. *Schulz-Flory MMD* (most probable distribution): this MMD is relative to polymers produced by single-site catalyst system such as metallocene. The catalytic regime which produces a Schulz-Flory MMD is featured by a high rate of initiation (k_{in}) and a rate of termination (k_{tr}) or transfer constant during the time and lower than the rate of propagation ($k_{tr} \ll k_p$). In this case the polydispersity index is about 2. All deviations of these conditions determine a broadening of distribution.
2. *Poisson MMD* is generated by <u>living</u> single site catalysts (see chapter I for more details). The kinetic regime which produces a Poisson MMD is a living or controlled regime featured by a higher rate of initiation than propagation rate ($k_i \gg k_p$) and a rate of chain termination or transfer negligible ($k_{tr} \approx 0$) during the polymerization time. In this case the polydispersity index is about 1.

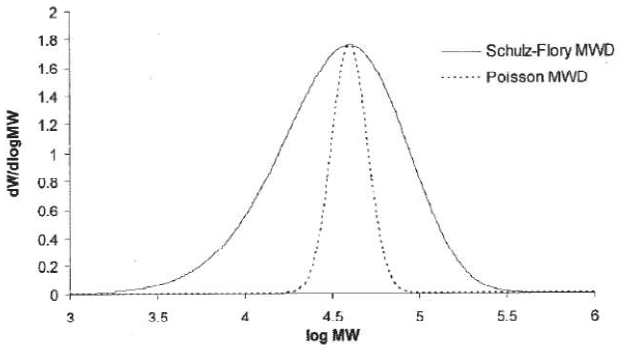

Figure 2. Overlapping Schulz-Flory MMD with Poisson MMD with the same max value.

Between this two limit situation it is possible to find other molar mass distributions which kinetically hard to characterize. A mathematical or quasi-quantitative interpretation could be given.

3. *Hybrid MMD*. It is a uni-modal distribution with a polydispersity index between 1 and 2. The polymer which showed this distribution is produced by metallocene catalysts which follow intermediate kinetic regimes.

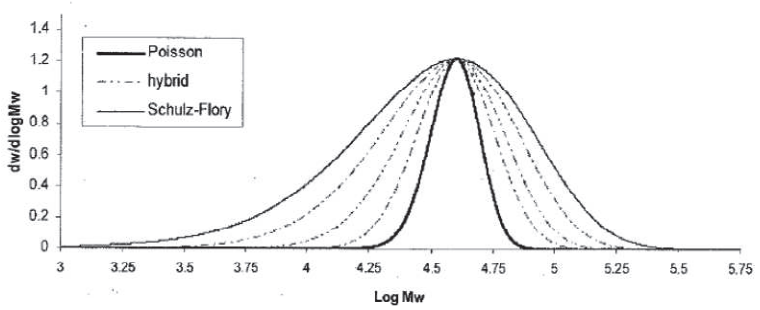

Figure 3. Overlapping Schulz-Flory MMD with Poisson MMD with the same max value

All these MMD are different from the broad or multimodal MMDs which are characterized by high PDI values in general higher than 2.5. Polymers with this MMD are produced by heterogeneous Ziegler-Natta catalysts, but in some case are observed also for polymers produced by homogeneous catalyst systems.

2. Size Exclusion Chromatography

The Size Exclusion Chromatography (SEC) also known as Gel Permeation Chromatography (GPC), allows to separate polymers with different molar masses and determinate the MMD. SEC is a separation technique based on the molecular size of the components. Separation is achieved by the differential exclusion from the pores of the packing material, of the sample molecules as they pass through a bed of porous particles (styrene-divinylbenzene copolymer). In general the smaller macromolecules contained in sample solution permeate the pores increasing the separation time.

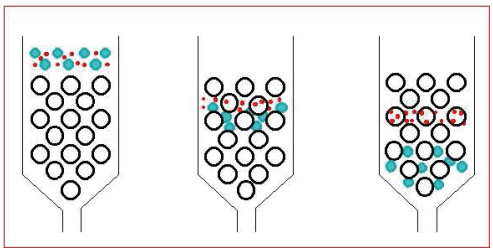

Figure 4. Principle of size exclusion chromatography; large macromolecules do not permeate the pores and they pass quickly through the porous packing; smaller macromolecules permeate the pores and they go out slower than bigger ones.

The separation occurs on discrimination of hydrodynamic volume, V_h, of macromolecules which is the spherical volume of single macromolecules including the solvent. This means that macromolecules are eluted at different times (different elution volumes V_{el}) depending from the length of polymer chain.

The **molar mass distributions** of the polymers showed in previous chapter were determined using an Alliance GPCV 2000 system by Waters. This SEC instrument is equipped with differential refractive index and multi-capillary viscosimetry detectors, and three PLgel Olexis columns in series designed specifically for high temperature applications. Analyses were performed at 150°C, with analytical grade 1,2,4-trichlorobenzene (TCB), stabilized with 2.6, di-*ter*-4-methylphenol, as mobile phase at a flow rate of 1 ml•min^{-1}. The polymer sample was dissolved in TCB (at concentration around 1 mg•ml^{-1}) and injected in the column.
For the determination of molar mass averages and molar mass distribution needs a calibration curve. For the PEs samples reported in this thesis two calibrations have been used.

Relative calibration: the calibration curve is given by logarithm of molar mass of standards vs the retention volume. In this case the standard is the same polymer type of sample which could be analyzed.

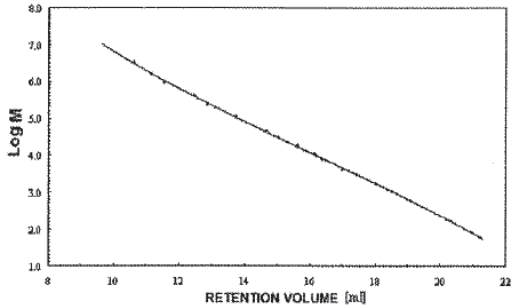

Figure 5. Relative calibration curve built with molar mass of narrow PE standards vs retention volume

For example a relative calibration curve built from PE molar mass standards is only valid for PE samples. A calibration with narrow polyethylene standards (supplied by Polymer Standards Service) covering the entire molar mass range of sample was used for determining the MWD of PE obtained using bis(cumyl)[ONNO]$ZrBz_2$, $FITiCl_2$ and $FIZrCl_2$ catalyst precursors.

Universal calibration: the calibration curve is built plotting Log (Mw*IV) vs retention volume where **IV is the intrinsic viscosity**.

A series of narrow polystyrene standards with certified molar mass and known concentration is used. From RI detector is possible to measure the retention volume while from viscosimeter detector it is possible to calculate the IV.

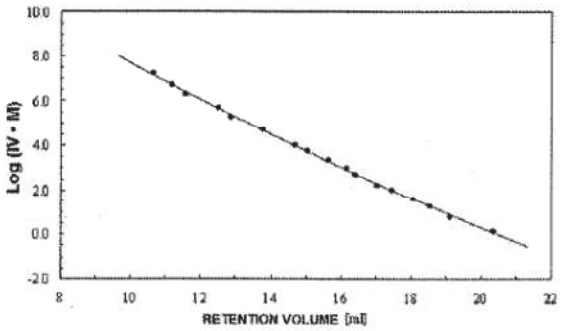

Figure 6: Universal calibration curve built with Log(Mw*IV) vs retention volume

Then, from calibration curve of Log(Mw*IV) vs retention volume (e.g. in Figure 6) it is possible to calculate the molar mass of unknown sample which has a determinate retention volume.

The retention volume is correlated to hydrodynamic volume which is proportional to the product of molar mass and intrinsic viscosity $Mw*IV = 5/2*N_A*V_h$ (where N_A is Avogadro's number).

For this thesis, the standard samples used are narrow polystyrenes standards supplied by Agilent Technologies while the unknown samples are the PEs samples. For the same elution time the two samples of different nature have the same V_h:

$$V_{hPE} = V_{hPS}$$

$$IV_{PE}Mw_{PE} = IV_{PS}Mw_{PS}$$

$$Mw_{PE} = \frac{IV_{PS} Mw_{PS}}{IV_{PE}}$$

Where IV_{PS} and Mw_{PS} are respectively the intrinsic viscosity of polystyrene, used for the calibration curve, and IV_{PE} and Mw_{PE} are relative to unknown sample of polyethylene (see Figure 7). The IV_{PE} is measured with the viscosimetry detector

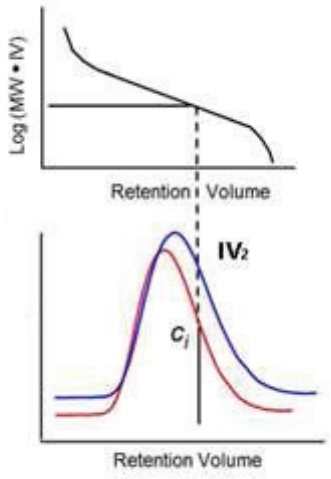

Figure 7. Molar mass determination using the universal calibration. The blue curve is given by viscosimeter detector and red one is obtained by using refractometer detector.

Calibration with narrow polystyrene standards (Polymer Standard Service) covering the entire molar mass range of sample was used for determining the MMD of PE obtained using FESBIZrCl$_2$ (CPh$_2$)CpFluZrCl$_2$ and Cp*$_2$ZrCl$_2$ catalyst precursors.

The MMD of PEs obtained using the batch reactor have been determinate using calibration with narrow polyethylene standards (Polymer Standard Service) covering the molar mass range of 350-128000 g*mol^{-1}. Samples with higher molar masses have been investigated by using the light scattering detector (low angle, 7°, and right angle 90°) coupled with refractometer detector. These samples have been analyzed in a Malvern Viscotek 350-A HT-GPC device.

3. Deconvolution

When a monodisperse sample is analyzed by chromatography it will appears as a peak more or less of Gaussian shape. The main reasons for the broadening of peaks are diffusion phenomena on the column and the detector which can be minimized but not completely avoided. Additional broadening of peaks can be due to high sample loads, interaction of sample with column packing and an imperfect chromatographic system. In general the experimental chromatogram cold be described by the function F(LogMw) which could be expressed as a convolution of other two functions W(LogMw) which is the shape function of a solute eluting at the mean elution volume and G(LogMw) the chromatogram corrected for band spreading.

$$F(\text{Log Mw}) = \int W(Log\ Mw) * G(Log\ Mw)$$

The analytical determination of G(LogMw) was object of several studies[1-4] and it should depend from diffusion phenomena, not-homogeneous or aging of column. In order to determine the "real" chromatogram is sometimes necessary to use deconvolution software as we did for some tests using $FITiCl_2$/MAO at 40°C (see chapter IV). For tests 354, 355 and 359 the GPC chromatogram showed a broadening on low molar masses. Since the reference peak also showed a broadening, this phenomenon is probably due to device problems. For this reason, the deconvolution has been carried out on these three tests. The software used is the *ShapeGPC software* created by prof. M. Vacatello, University of Naples "Federico II". The results before and after the deconvolution have been reported in table 1.

Table 1. Values of Mn and PDI before and after deconvolution

Test	Time (s)	before deconvolution		after deconvolution	
		M_n	PDI	M_n	PDI
354	0.7	27	1.8	51	1.16
355	1.12	62	1.3	77	1.22
359	0.15	10	1.7	18	1.2

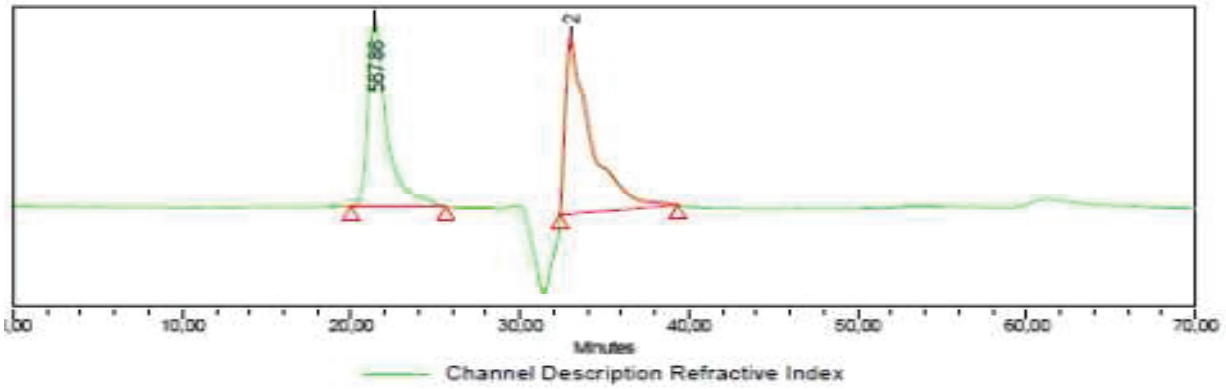

Figure 8. SEC profile of test 354

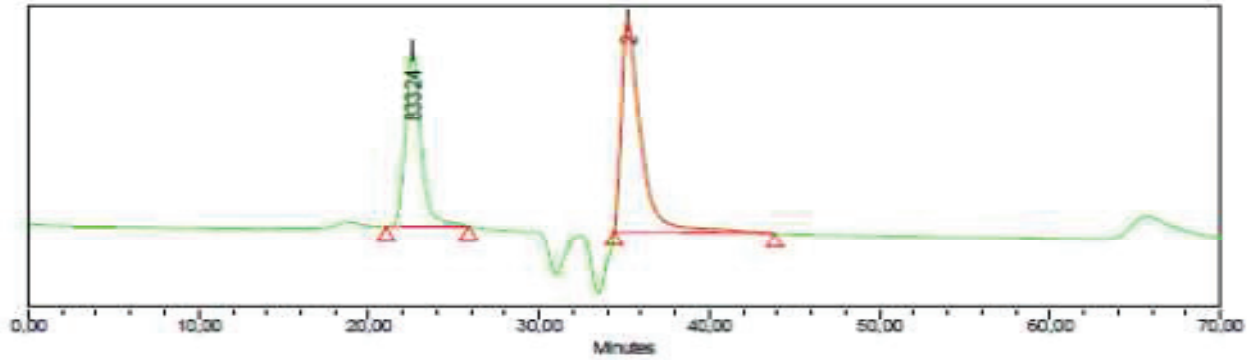

Figure 9. SEC profile of test 355

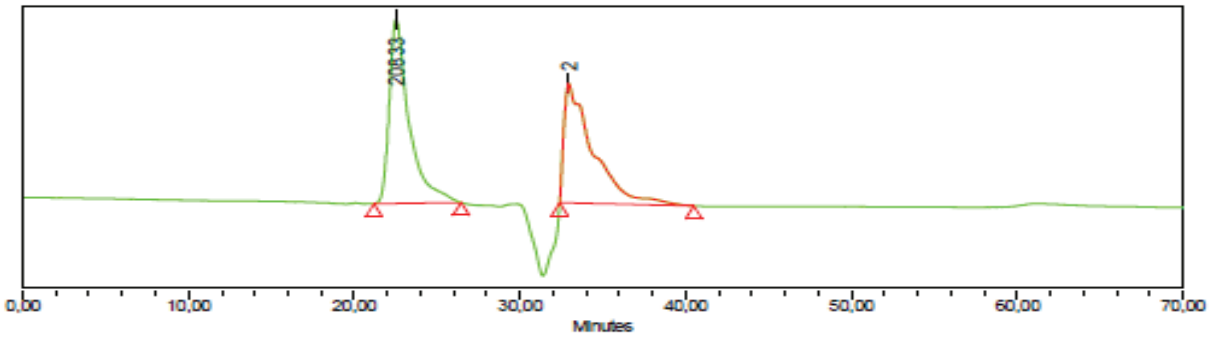

Figure 10. SEC profile of test 359

After the deconvolution a very narrow MMD has been found.

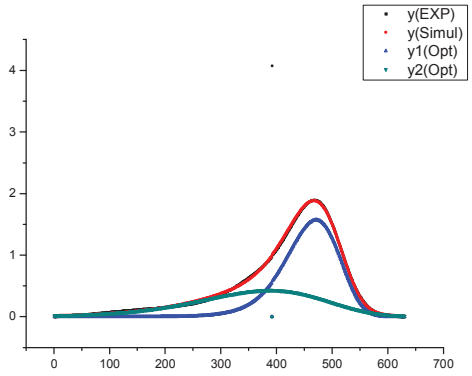

Figure 12. Deconvolution of test 359 : the black curve is the experimental curve, the blue one is the first family of polymer and the green one is the contribute of aging columns. The red curve is the simulation curve given by the sum of curve green and blue.

Table 2. Values of deconvolution for test 359

curve	%	M_n	PDI
Y1	61.7	18000	1.2
Y2	38.3	7000	1.9

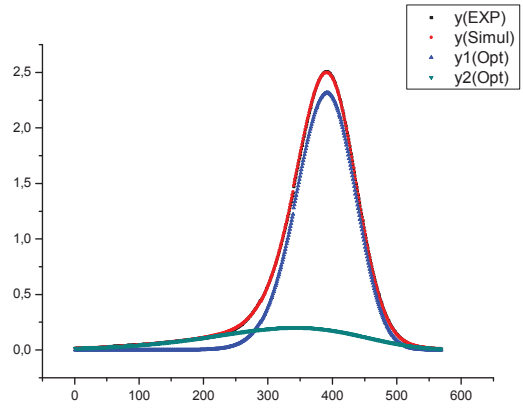

Figure 13. Deconvolution of test 355 : the black curve is the experimental curve, the blue one is the first family of polymer and the green one is the contribute of aging columns. The red curve is the simulation curve given by the sum of curve green and blue.

Table 3. Values of deconvolution for test 355

curve	%	M_n	PDI
Y1	82.4	77000	1.1
Y2	17.6	34000	1.9

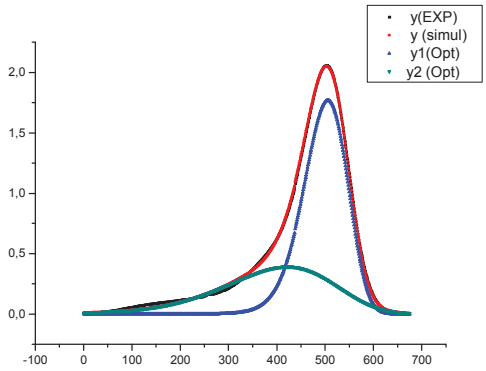

Figure 14. Deconvolution of test 354: the black curve is the experimental curve, the blue one is the first family of polymer and the green one is the contribute of aging columns. The red curve is the simulation curve given by the sum of curve green and blue.

Table 4. Values of deconvolution for test 354

curve	%	M_n	PDI
Y1	64.5	51000	1.16
Y2	35.5	18000	1.97

References

1. Tung, L. H. *Journal of Applied Polymer Science* **1966,** 10, (3), 375-385.
2. Tung, L. H.; Moore, J. C.; Knight, G. W. *Journal of Applied Polymer Science* **1966,** 10, (9), 1261-1270.
3. Hamielec, A. E. *Journal of Applied Polymer Science* **1970,** 14, (6), 1519-1529.
4. Ishige, T.; Lee, S. I.; Hamielec, A. E. *Journal of Applied Polymer Science* **1971,** 15, (7), 1607-1622.

Appendix B

Synthesis of phenoxyimine-based -Ti and –Zr based catalysts

1. Synthesis of N-(3-tert-Butylsalicylidene)-2,3,4,5,6-pentafluoroanilinato titanium dichloride

Synthesis of FI ligand

The $FITiCl_2$/MAO catalyst system has been synthesized according Fujita method[1].

To a stirred solution of 3-*tert*-Butylsalicylaldehyde (5.11 g; 2.8 mmol) in 15 ml of methanol, 2,3,4,5,6-pentafluoroaniline (6.45 g; 3.5 mmol) and 20 mg of p-toluenesulfonic acid, as catalysts, were added at room temperature. The resulting mixture was stirred at reflux for 4h, and concentration of the reaction mixture in vacuo afforded a crude imine compound shown in equation 1:

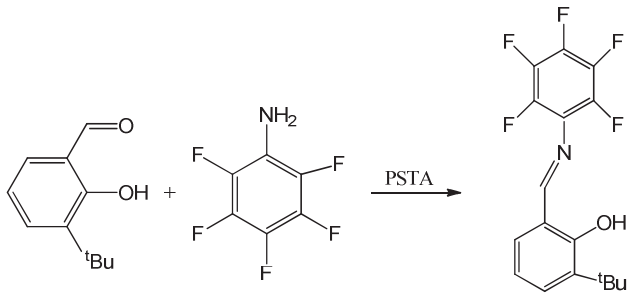

Purification by chromatography column on silica gel using n-hexane/AcOEt (10:0.5) as eluent gave N-(3-*tert*-Butylsalicylidene)-2,3,4,5,6-pentafluoroaniline (2.4 g; 0.007 mol) as yellow crystals in 25% yield. From ^{1}H NMR we have checked the purity of product.

^{1}H NMR ($CDCl_3$, 25°C): δ 1.46(s, 9H, tBu), 6.91(t, *J* = 7.8 Hz, 1H, aromatic-H), 7.23-7.26 (m, 1H, aromatic-H) 7.47 (dd, *J* = 7.7, 1.5 Hz, 1H, aromatic-H) 8.81(s, 1H, CH=N), 12.88 (s, 1H, OH).

Synthesis of $FITiCl_2$ Complex (I)

To a stirred solution of N-(3-*tert*-Butylsalicylidene)-2,3,4,5,6-pentafluoroaniline (2g; 6.8mmol) in dried diethyl ether (50 ml) was added n-butyllithium (1.6 $molL^{-1}$ in n-heptane, (4.25 ml; 6.8 mmol), dropwise over a 10-min period at -78°C (see equation 2). The solution was allowed to warm to room temperature and stirred for 2h

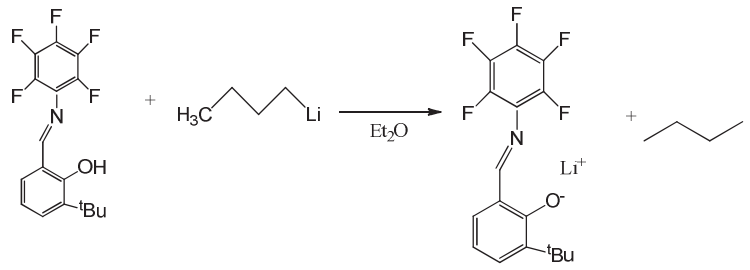

(2)

To the resulting solution was added dropwise over 10 min period solution of $TiCl_4$, (2.5 $molL^{-1}$ in n-heptane, 1.36 ml; 3.4mmol) in dried diethyl ether (50 ml) at -78°C. The mixture was allowed to warm to room temperature and stirred over night. Concentration of the reaction mixture in vacuo gave a crude product (see equation 3):

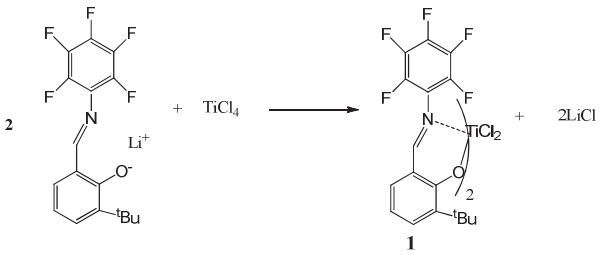

(3)

Dried CH_2Cl_2 (50 ml) was added to the crude product, and suspension was stirred for 15 min and then filtered. The solid residue (LiCl) was washed with dried CH_2Cl_2(30 mL x 3 times) and the combined organic filtrates were concentrated in vacuo to afford a brown solid. Diethyl ether (10 mL) and n-heptane (40 mL) were added to solid and suspension was stirred for 2h and then the product was filtered. The resulting solid was washed with n-hexane (20mL x 3 times) and dried to give complex **1** (0.5 g; 0.61 mol) as a reddish brown solid in 18% yield.

^{1}H NMR ($CDCl_3$, 25°C): δ 1.35(s, 18H, ^{t}Bu), 7.02(t, *J* = 7.6 Hz, 2H, aromatic-H), 7.29 (dd, *J* = 7.6, 1.6 Hz, 2H, aromatic-H) 7.64 (dd, *J* = 7.6, 1.6 Hz, 2H, aromatic-H) 8.22(s, 2H, CH=N), 1.21 (t, *J*=7.0Hz (CH_3CH_2)O) 3.48(q, *J*=7.0 Hz, (CH_3CH_2)O).

2. Synthesis of $FIZrCl_2$ N-(3-*tert*-Butylsalicylidene)anilinato zirconium dichloride

Synthesis of FI ligand

In order to accomplish the investigation of $FIZrCl_2$/MAO catalyst system, the phenoxy-imine based complex has been synthesized according to Fujita method[2].

To a stirred solution of 3-*tert*-Butylsalicylaldehyde (2.6g; 0.015mol) in 25 ml of ethanol, aniline (1.4g; 0.015mol) and 20 mg of p-toluenesulfonic acid, as catalysts, were added at room temperature. The resulting mixture was stirred at reflux for 3h, and concentration of the reaction mixture in vacuo afforded a crude imine compound shown in equation 1:

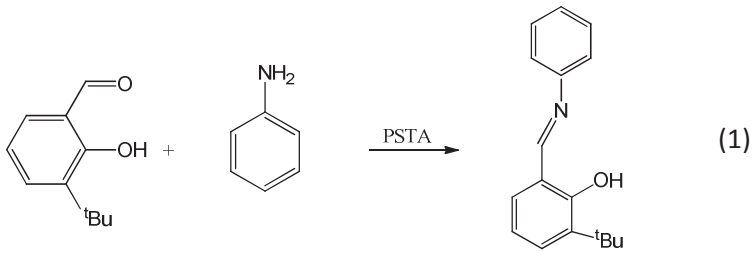

(1)

Purification by chromatography column on silica gel using n-hexane/AcOEt (10:0.5) as eluent gave N-(3-*tert*-Butylsalicylidene)anilinato (3.1g; 0.012mol) as orange oil in 80 % yield. From ^{1}H NMR we have checked the purity of product.

^{1}H NMR ($CDCl_3$, 25°C): δ 1.47(s, 9H, tBu), 6.82-7.48(m, 8H, aromatic-H), 8.64(s, 1H, CH=N), 13.95 (s, 1H, OH).

Synthesis of $FIZrCl_2$ Complex (II)

To a stirred solution of N-(3-*tert*-Butylsalicylidene)anilinato (3.1g; 12.23 mmol) in dried diethyl ether (50 ml) was added n-butyllithium, 1.6 $molL^{-1}$ in n-heptane, (7.95 ml; 12.73 mmol), dropwise over a 10 min period at -78°C (see equation 2). The solution was allowed to warm to room temperature and stirred for 2h

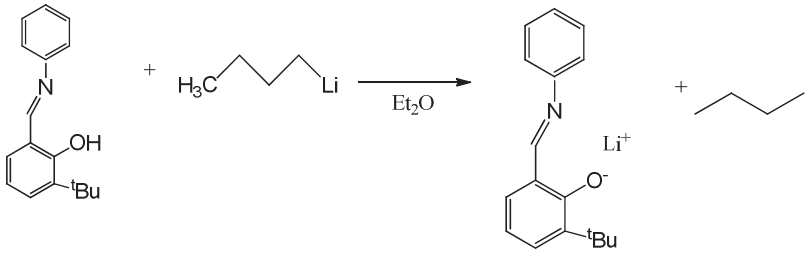

(2)

To the resulting solution was added dropwise over 10 min period solution of $ZrCl_4 \cdot 2THF$(1:2) (2.3 g; 6.11 mmol) in dried tetrahydrofuran, THF, (50 ml) at 0°C. The mixture was allowed to warm to room temperature and stirred over night. Concentration of the reaction mixture in vacuo gave a crude product (see equation 3):

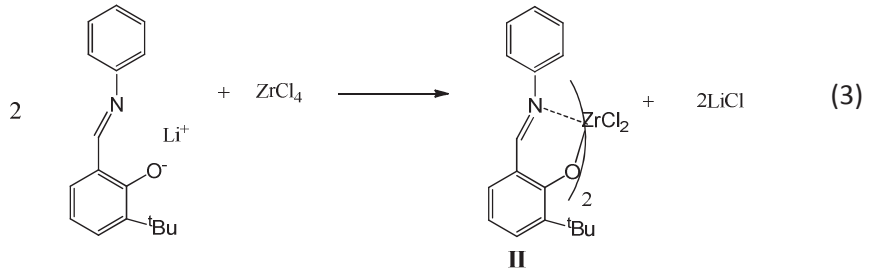

(3)

Dried dichloromethane, CH_2Cl_2, (50 ml) was added to the crude product, and suspension was stirred for 15 min and then filtered. The solid residue (LiCl) was washed with dried CH_2Cl_2(30 mL x 3 times) and the combined organic filtrates were concentrated in vacuo to afford a yellow solid. The solid was recrystallized from a dichloromethane/diethyl ether (1:4) solution at -18°C to give the complex **I** (2.5 g; 3.73 mmol) as a yellow solid in 61% yield.

^{1}H NMR ($CDCl_3$, 25°C): δ 1.33-1.59(m, 18H, ^{t}Bu), 6.78-7.42(m, 16H, aromatic-H), 8.12(s, 2H, CH=N).

References

1. Mitani, M.; Mohri, J.; Yoshida, Y.; Saito, J.; Ishii, S.; Tsuru, K.; Matsui, S.; Furuyama, R.; Nakano, T.; Tanaka, H.; Kojoh, S.; Matsugi, T.; Kashiwa, N.; Fujita, T. *Journal of the American Chemical Society* **2002,** 124, (13), 3327-3336.
2. Matsui, S.; Mitani, M.; Saito, J.; Tohi, Y.; Makio, H.; Matsukawa, N.; Takagi, Y.; Tsuru, K.; Nitabaru, M.; Nakano, T.; Tanaka, H.; Kashiwa, N.; Fujita, T. *Journal of the American Chemical Society* **2001,** 123, (28), 6847-6856.

Appendix C

Determination of « free » TMA in commercial MAO.

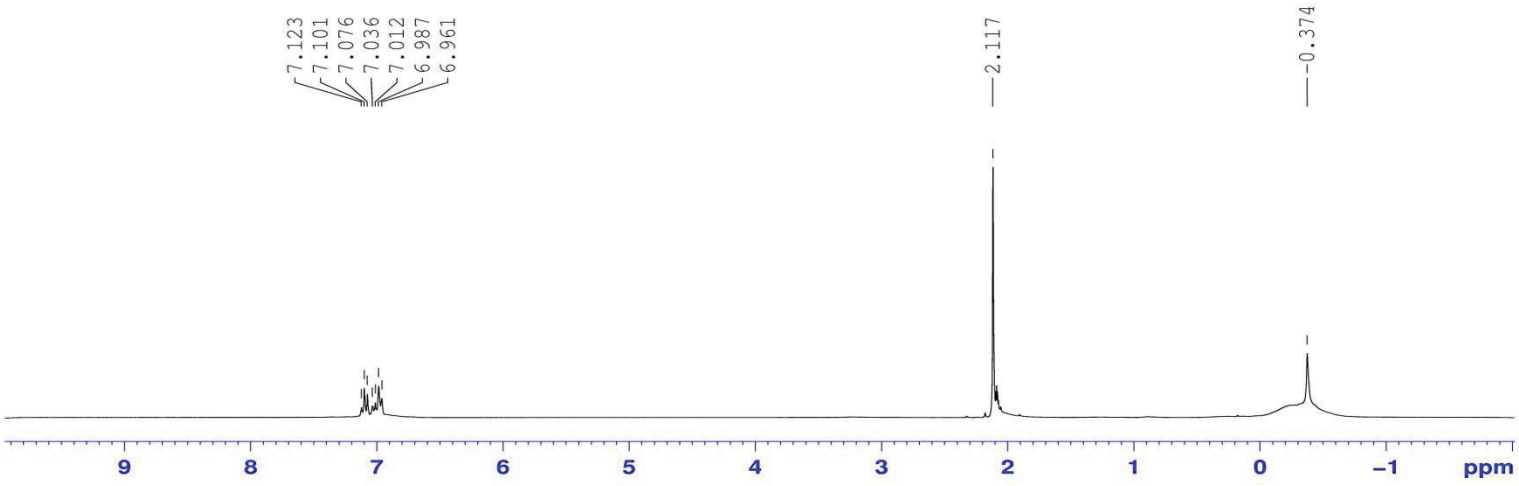

MAO supplied by Sigma Aldrich, ^{1}H NMR in toluene-d8.

TMA = 3.00/3 = 1

MAO = (3.75+1.95)/1.5 = 3.8

TMA = 1/(3.8+1) = 0.21